

“Determining mode of action and optimum use of phytochemicals as food preservatives”

Ryan Sweet, Bsc. Hons.

PhD Thesis,

University of East Anglia (UEA),

Quadram Institute Bioscience (QIB),

Primary Supervisor: Dr. Mark Webber,

Date of Submission: 22.08.22

"This copy of the thesis has been supplied on condition that anyone who consults it is understood to recognise that its copyright rests with the author and that use of any information derived therefrom must be in accordance with current UK Copyright Law. In addition, any quotation or extract must include full attribution."

Abstract:

Antimicrobial resistance and the lack of novel antimicrobials are urgent global issues. New compounds with direct antimicrobial action or synergy with current antimicrobials are sorely needed. This thesis attempts to define the potential and mode of action (MOA) of one alternative, novel antimicrobial compound source: phytochemicals. These structurally diverse compounds may be suitable solutions to the above issues. There is a large but contradictory evidence base for the antimicrobial activity of many phytochemicals within the literature. I compared a phytochemical panel using a standardised, OD-based assay to identify antimicrobial activity, followed by quantitative assays, against four foodborne pathogens. From this data, caffeic acid, thymol and a commercial phytochemical preservative substitute (the Prosur NATPRE T-10+ mix) were identified as holding antimicrobial promise. Mutant selection revealed thymol could select for tolerant mutants of *Salmonella enterica*, *Staphylococcus aureus* and *Pseudomonas aeruginosa* at a rate akin to classic antibiotics. Genome sequencing of the mutants and a thymol-challenged *Salmonella enterica* TraDIS-Xpress library revealed SNPs and key loci for thymol resistance to be heavily associated with efflux and other envelope functions. Transmission electron microscopy of a thymol-selected *Salmonella enterica* mutant and its parental strain revealed a damaged morphology of the parental strain under thymol exposure, while the mutant possessed a more rounded morphology under control conditions and was unaffected by thymol challenge. This evidence brings support for an envelope-targeting primary MOA for the inhibitory nature of thymol. A food challenge test was undertaken to determine the *in situ* efficacy of thymol within a vegetarian burger model, where it exerted an antimicrobial effect against inoculated *Salmonella enterica*. Together this work shows phytochemicals can have potent antimicrobial activity with potential for application as preservatives. The cell membrane seems to be a key target for phytochemicals but resistance due to efflux may be an issue for their wider usage.

Access Condition and Agreement

Each deposit in UEA Digital Repository is protected by copyright and other intellectual property rights, and duplication or sale of all or part of any of the Data Collections is not permitted, except that material may be duplicated by you for your research use or for educational purposes in electronic or print form. You must obtain permission from the copyright holder, usually the author, for any other use. Exceptions only apply where a deposit may be explicitly provided under a stated licence, such as a Creative Commons licence or Open Government licence.

Electronic or print copies may not be offered, whether for sale or otherwise to anyone, unless explicitly stated under a Creative Commons or Open Government license. Unauthorised reproduction, editing or reformatting for resale purposes is explicitly prohibited (except where approved by the copyright holder themselves) and UEA reserves the right to take immediate 'take down' action on behalf of the copyright and/or rights holder if this Access condition of the UEA Digital Repository is breached. Any material in this database has been supplied on the understanding that it is copyright material and that no quotation from the material may be published without proper acknowledgement.

Contents-

- [Title \(pg. 1\).](#)
- [Abstract, \(pg. 2\).](#)
- [Figure List \(pg. 8-10\).](#)
- [Table List \(pg. 11-12\).](#)
- [List of abbreviations \(pg. 13-14\).](#)
- [**Chapter 1: Introduction \(pg. 15-59\).**](#)
- [1.0.0 Food poisoning and Its' Impact \(pg. 16-19\).](#)
- [1.1.0 Food Preservatives As Antimicrobials: Sodium Nitrite \(pg. 19-23\).](#)
- [1.2.0 Antibiotics; the Golden Age of Discovery \(pg. 23-27\).](#)
- [1.3.0 Antimicrobial Resistance; Mechanisms of AMR, AMR Transfer and Impact \(pg. 28-35\).](#)
- [1.3.1 Alteration/Protection of Antibiotic Targets \(pg. 28-29\).](#)
- [1.3.2 Antibiotic Inactivating Enzymes \(pg. 29\).](#)
- [1.3.3 Efflux of Antibiotic Molecules \(pg. 30-31\).](#)
- [1.3.4 Selection of Resistance \(pg. 31-33\).](#)
- [1.3.5 Antimicrobials/Nitrite Substitutes and Synergy \(pg. 33-35\).](#)
- [1.4.0 Phytochemicals; Polyphenol Classes and Structures \(pg. 35-50\).](#)
- [1.4.1 Phytochemicals; Phenolic Acids \(pg. 41-42\).](#)
- [1.4.2 Phytochemicals; Terpenes \(pg. 43-44\).](#)
- [1.4.3 Phytochemicals; Flavonoids \(pg. 45-46\).](#)
- [1.4.4 Flavonoids; Flavanones \(pg. 47-48\).](#)
- [1.4.5 Flavonoids; Flavonols and Flavanols \(pg. 49-50\).](#)
- [1.5.0 Phytochemicals; Known Antimicrobial Activity and Mechanisms of Action \(pg. 51-54\).](#)
- [1.5.1 Cellular Membrane/Wall Disruption \(pg. 51-52\).](#)
- [1.5.2 Binding and Disruption of Enzyme Activity \(pg. 52\).](#)

- [1.5.3 Efflux Pump Inactivation, Potentiation Capacity and Synergy \(pg. 53-54\).](#)
- [1.5.4 Unresolved Questions Relating to Phytochemicals Potential As Antimicrobial Substitutes \(pg. 54\).](#)
- [1.6.0 Organisms \(pg. 54-59\).](#)
- [1.6.1 *Listeria monocytogenes* \(pg. 54-55\).](#)
- [1.6.2 *Pseudomonas aeruginosa* \(pg. 55-57\).](#)
- [1.6.3 *Salmonella enterica* serovar Typhimurium \(pg. 57-58\).](#)
- [1.6.4 *Staphylococcus aureus* \(pg. 58-59\).](#)
- [1.7.0 Project Aims \(pg. 59\).](#)
- [**Chapter 2: Materials & methods \(pg. 60-96\).**](#)
- [2.1.1 Bacterial Strains \(pg. 61\).](#)
- [2.1.2 Phenotypic Identification of Bacterial Strains \(pg. 63\).](#)
- [2.1.3 Storage of Bacterial Strains \(pg. 63\).](#)
- [2.1.4 Broth Cultures \(pg. 63-64\).](#)
- [2.1.5 Preparation/Standardisation of Inocula \(pg. 64\).](#)
- [2.1.6 Viable Counts \(pg. 65-66\).](#)
- [2.2.0 Chemicals \(pg. 66\).](#)
- [2.2.1 Sourcing of Phytochemicals \(pg. 66-67\).](#)
- [2.2.2 Solubilisation and Storage of Phytochemical Stock Solutions \(pg. 68\).](#)
- [2.2.3 Sourcing, Solubilisation and Storage of Chemicals and Reagents \(pg. 68-71\).](#)
- [2.3.0 Semi-High Throughput Phytochemical Activity Screening Assays \(pg. 72-75\).](#)
- [2.3.1 Growth Inhibition Assays \(pg. 74-75\).](#)
- [2.3.2 Antimicrobial Potentiation Assays \(pg. 75\).](#)
- [2.4.0 Growth Curves After Phytochemical Exposure \(pg. 76-77\).](#)
- [2.5.0 Drug Accumulation Assays \(pg. 77-83\).](#)
- [2.5.1 *S. aureus* and *L. monocytogenes* Positive Control Optimisations \(pg. 81-82\).](#)

- [2.5.2 *S. aureus* and *L. monocytogenes* Ethidium Bromide Fluorescence Indicator Optimisations \(pg. 82-83\).](#)
- [2.6.0 Antimicrobial Susceptibility Determination Experiments \(pg. 83-85\).](#)
- [2.6.1 Microdilution Broth Minimum Inhibiting Concentration \(MIC\) Experiments \(pg. 83-84\).](#)
- [2.6.2 Microdilution Agar Minimum Inhibiting Concentration \(MIC\) Experiments \(pg. 84-85\).](#)
- [2.7.0 Mutant Selection Using Phytochemical-laced Agar \(pg. 85-86\).](#)
- [2.8.0 Crystal Violet Biofilm Staining Assays \(pg. 86-87\).](#)
- [2.9.0 Congo Red Plate Biofilm Phenotyping \(pg. 88\).](#)
- [2.10.0 Bacterial DNA Extraction, Quantification and Sequencing \(pg. 88-90\).](#)
- [2.10.1 DNA Extraction, Quantification and Sequencing of Phytochemical-selected Mutants \(pg. 89-90\).](#)
- [2.10.2 DNA Extraction, Quantification and Sequencing of Thymol-Challenged *S. enterica* TraDIS-Xpress Mutants \(pg. 90\).](#)
- [2.11.0 *S. enterica* TraDIS-Xpress Library Thymol Challenge \(pg. 91\).](#)
- [2.12.0 Transmission Electron Microscopy \(TEM\) \(pg. 91-92\).](#)
- [2.13.0 Food Challenge Testing \(FCT\) \(pg. 92-96\).](#)
- [2.13.1 *S. enterica* Cold Temperature Optimisations \(pg. 94-95\).](#)
- [2.13.2 *S. enterica* Enumeration Validations in Food Matrix Model \(pg. 95-96\).](#)
- [**Chapter 3: Selection of antimicrobial compounds for further investigation \(pg. 97-139\).**](#)
- [3.1.0 Chapter Introduction \(pg. 98\).](#)
- [3.2.0 Results \(pg. 99-132\).](#)
- [3.2.1 Rational Selection of Phytochemical Compounds \(pg. 99-103\).](#)
- [3.2.2 Identifying Compounds Potent Antimicrobial Phytochemicals and Narrowing the Selection Panel \(pg. 104-109\).](#)

- [3.2.3 Identifying Compounds With Ability to Potentiate Antibiotics \(pg. 110-115\).](#)
- [3.2.4 Thymol, and Other Compounds, Significantly Alter the Growth Kinetics of the Tested Foodborne Pathogens \(pg. 116-122\).](#)
- [3.2.5 Dose-Dependant Effects Were Observed For Some Compounds, Including the Prosur NATPRE T-10+ \(pg. 123-125\).](#)
- [3.2.6 Caffeic Acid, Amongst Other Compounds, Increases the Drug Accumulation In Tested Pathogens \(pg. 126-132\).](#)
- [3.3.0 Chapter Discussion \(pg. 133-139\).](#)
- [**Chapter 4: Selection & characterisation of thymol-tolerant mutant strains \(pg. 140-165\).**](#)
 - [4.1.0 Chapter Introduction \(pg. 141\).](#)
 - [4.2.0 Results \(pg. 142-162\).](#)
 - [4.2.1 Identifying Appropriate Phytochemical Compounds For Use in Mutant Selection Experiments \(pg. 142-143\).](#)
 - [4.2.2 Thymol Retains the Capacity To Select for Candidate Resistant Mutants \(pg. 144-145\).](#)
 - [4.2.3 Thymol-selected Candidate Mutants Display Tolerant, Not Resistant, Phenotypes \(pg. 146-147\).](#)
 - [4.2.4 Thymol-tolerant Mutants Across Bacterial Species Carry Single Nucleotide Polymorphisms Within Efflux Pump Operons \(pg. 148-152\).](#)
 - [4.2.5 Thymol-tolerant Mutants Present Increased MICs for Clasically Effluxed Antibiotics \(pg. 153-154\).](#)
 - [4.2.6 Thymol-tolerant Mutants Grow Better Under Thymol Stress \(pg. 155-156\).](#)
 - [4.2.7 Thymol-tolerant Mutants Display A Decreased Drug Accumulation \(pg. 157-158\).](#)
 - [4.2.8 Thymol-tolerant Mutants Present Decreased Capacities to Form Biofilms \(pg. 159-160\).](#)
 - [4.2.9 Colony Morphologies of Thymol-tolerant Mutants \(pg. 161-162\).](#)
 - [4.3.0 Chapter Discussion \(pg. 163-165\).](#)

- **Chapter 5: A whole genome functional screen identifies various cell envelope genes in determining *S. enterica* sensitivity to thymol (pg. 166-186).**
 - **5.1.0 Chapter Introduction (pg. 167).**
 - **5.2.0 Results (pg. 168-182).**
 - **5.2.1 Identifying Appropriate Thymol Concentrations For Use in *S. enterica* TraDIS-Xpress Library Challenge (pg. 168-169).**
 - **5.2.2 *S. enterica* Mutants Deficient in Efflux and Envelope-associated Gene Expression Are More Vulnerable To Thymol Challenge (pg. 170-177).**
 - **5.2.3 Thymol Exhibits Envelope-damaging Effects (pg 178-182).**
 - **5.3.0 Chapter Discussion (pg. 183-186).**
- **Chapter 6: Food challenge testing of thymol as a preservative (pg. 187-200).**
 - **6.1.0 Chapter Introduction (pg. 188).**
 - **6.2.0 Results (pg. 189-197).**
 - **6.2.1 Selection of 10°C As An Appropriate Chilled Incubation Temperature for *S. enterica* (pg. 189-190).**
 - **6.2.2 Validation of CFU Enumeration Method in the Food Matrix Model (pg. 191-193).**
 - **6.2.3 Thymol Retains Antimicrobial Capacity in An *In Situ* Food Model (pg. 194-197).**
 - **6.3.0 Chapter Discussion (pg. 198-200).**
- **Chapter 7: Final discussion & acknowledgements (pg. 201-204).**
 - **7.1.0 Final Discussion (pg. 202-203).**
 - **7.2.0 Acknowledgements (pg. 204).**
- **Chapter 8: References (pg. 205-225).**
- **Chapter 9: Appendix (pg. 226-257).**

Figure List

Figure 1.1: *Diagram summarising the chemical reactions of nitrite, pg. 21*

Figure 1.2: *Phytochemical class structure: the phenolic acids, pg. 42*

Figure 1.3: *Phytochemical class structure: the monoterpenes, pg. 44*

Figure 1.4: *Phytochemical class structure: the core flavonoid chemical structure, pg. 46*

Figure 1.5: *Phytochemical class structure: the flavanones, pg. 48*

Figure 1.6: *Phytochemical class structure: the flavonols and flavanols, pg. 50*

Figure 2.1: *The semi-high throughput screening assays 96-well microtitre plate layout, pg. 73*

Figure 2.2: *The drug accumulation assay layout, pg. 79*

Figure 3.1: *OD_(600nm) measurements for the S. enterica cultures challenged with various concentrations of the selected phytochemicals, pg. 106*

Figure 3.2: *OD_(600nm) measurements for the P. aeruginosa cultures challenged with various concentrations of the selected phytochemicals, pg. 107*

Figure 3.3: *OD_(600nm) measurements for the S. aureus cultures challenged with various concentrations of the selected phytochemicals, pg. 108*

Figure 3.4: *OD_(600nm) measurements for the L. monocytogenes cultures challenged with various concentrations of the selected phytochemicals, pg. 109*

Figure 3.5: *Impact of phytochemicals as potentiators of chloramphenicol based on OD(600nm) measurements for S. enterica cultures, pg. 112*

Figure 3.6: *Impact of phytochemicals as potentiators of chloramphenicol based on OD(600nm) measurements for P. aeruginosa cultures, pg. 113*

Figure 3.7: *Impact of phytochemicals as potentiators of chloramphenicol based on OD(600nm) measurements for S. aureus cultures, pg. 114*

Figure 3.8: *Impact of phytochemicals as potentiators of chloramphenicol based on OD(600nm) measurements for L. monocytogenes cultures, pg. 115*

Figure 3.9: *Growth curves for the tested pathogens challenged with 0.5mg/ml of the various phytochemicals, pg. 118*

Figure 3.10: *Growth curves for two pathogens challenged with 0.5mg/ml and 0.05mg/ml of vanillin and the Prosur NATPRE T-10+ mix, pg. 124*

Figure 3.11: *Exemplar resazurin accumulation assays for S. enterica challenged with 0.5mg/ml of various phytochemicals, pg. 128*

Figure 4.1: Growth of the thymol-selected pathogenic strains compared to their parental strains on thymol-laced agar, pg. 147

Figure 4.2: 3D tertiary protein structure of the RamR protein and its two subunits, pg. 152

Figure 4.3: Thymol-tolerant mutant growth curves, pg. 156

Figure 4.4: Thymol-tolerant mutant drug accumulation assays, pg. 158

Figure 4.5: Thymol-tolerant mutant crystal violet biofilm assays, pg. 160

Figure 4.6: Congo red staining of the parental and mutant strains, pg. 162

Figure 5.1: Photographic evidence for the culture turbidity of *S. enterica* exposed to a thymol concentration range, pg. 169

Figure 5.2: Artemis plots for the *S. enterica* TraDIS-Xpress library surrounding the *acrAB* operon on the 14028S reference genome, pg. 175

Figure 5.3: Artemis plots for the *S. enterica* TraDIS-Xpress library surrounding the *tolC* operon on the 14028S reference genome, pg. 176

Figure 5.4: Artemis plots for the *S. enterica* TraDIS-Xpress library surrounding the *ompA* operon on the 14028S reference genome, pg. 177

Figure 5.5: Exemplar TEM images of the *S. enterica* parental strain under various experimental conditions, pg. 180

Figure 5.6: Exemplar TEM images of the *S. enterica* mutant strain #2 under various experimental conditions, pg. 181

Figure 6.1: *S. enterica* temperature optimisation growth curves, pg. 190

Figure 6.2: Recovery of *S. enterica* from the vegetarian burger model, pg. 192

Figure 6.3: *S. enterica* growth on XLD agar supplemented with fluconazole, pg. 193

Figure 6.4: Preparation of the vegetarian food model samples, pg. 195

Figure 6.5: Results from the FCT, pg. 196

Figure 6.6: Physical appearance of the FCT vegetarian food samples, pg. 197

Figure 9.3.1: Growth curves for *S. enterica* challenged with 0.5mg/ml of various phytochemicals, pg. 235

Figure 9.3.2: Growth curves for *P. aeruginosa* challenged with 0.5mg/ml of various phytochemicals, pg. 236

Figure 9.3.3: Growth curves for *S. aureus* challenged with 0.5mg/ml of various phytochemicals, pg. 237

Figure 9.3.4: Growth curves for *L. monocytogenes* challenged with 0.5mg/ml of various phytochemicals, pg. 238

Figure 9.3.5: Growth curves for *S. enterica* challenged with 0.05mg/ml of various phytochemicals, pg. 239

Figure 9.3.6: Growth curves for *P. aeruginosa* challenged with 0.05mg/ml of various phytochemicals, pg. 240

Figure 9.3.7: Growth curves for *S. aureus* challenged with 0.05mg/ml of various phytochemicals, pg. 241

Figure 9.3.8: Growth curves for *L. monocytogenes* challenged with 0.05mg/ml of various phytochemicals, pg. 242

Figure 9.3.9: Resazurin accumulation assays for *S. enterica* challenged with 0.5mg/ml of various phytochemicals, pg. 247

Figure 9.3.10: Resazurin accumulation assays for *P. aeruginosa* challenged with 0.5mg/ml of various phytochemicals, pg. 248

Figure 9.3.11: EtBr accumulation assays for *S. aureus* challenged with 0.5mg/ml of various phytochemicals, pg. 249

Figure 9.3.12: EtBr accumulation assays for *L. monocytogenes* challenged with 0.5mg/ml of various phytochemicals, pg. 250

Figure 9.4.1: Growth curves for *S. aureus* parental and selected thymol-tolerant mutant strains challenged with 0.25mg/ml of thymol, pg. 252

Table List

Table 1.1: Summary of antibiotic classes, pg. 25-26

Table 1.2: Polyphenol classes, structures and exemplar compounds, pg. 37-40

Table 2.1: Bacterial strains used within this thesis, pg. 62

Table 2.2: Summary of phytochemicals utilised within this thesis, pg. 67

Table 2.3: Summary of chemicals and reagents utilised within this thesis, pg. 69-71

Table 2.4: Experimental conditions and constituent reagents of the drug accumulation assays, pg. 80

Table 3.1: The phytochemical classes, structures and rationale for a compounds inclusion within the panel, pg. 101-103

Table 3.2: Summary of growth velocity impacts after challenging the Gram-negative pathogens with various phytochemicals at 0.5mg/ml concentrations, pg. 119

Table 3.3: Summary of growth velocity impacts after challenging the Gram-positive pathogens with various phytochemicals at 0.5mg/ml concentrations, pg. 120

Table 3.4: Summary of impacts on the final growth achieved after challenging Gram-negative pathogens with various phytochemicals at 0.5mg/ml concentrations, pg. 121

Table 3.5: Summary of impacts on the final growth achieved after challenging Gram-positive pathogens with various phytochemicals at 0.5mg/ml concentrations, pg. 122

Table 3.6: Summary of growth curves challenging the Gram-positive pathogens with various phytochemicals at 0.05mg/ml, pg. 125

Table 3.7: Summary of resazurin accumulation assays challenging the Gram-negative pathogens with various phytochemicals at 0.5mg/ml concentrations, pg. 129

Table 3.8: Summary of resazurin accumulation assays challenging the Gram-positive pathogens with various phytochemicals at 0.5mg/ml concentrations, pg. 130

Table 3.9: Summary of the resazurin accumulation assays challenging the Gram-negative pathogens with various phytochemicals at 0.5mg/ml concentrations, pg. 131

Table 3.10: Summary of the resazurin accumulation assays challenging the Gram-positive pathogens with various phytochemicals at 0.5mg/ml concentrations, pg. 132

Table 4.1: Phytochemical MICs (mg/ml) for high density inocula of each tested pathogen, pg. 143

Table 4.2: Mutation frequencies of the tested pathogens against the selected phytochemicals, pg. 145

Table 4.3: Unique SNPs found within the sequenced thymol-tolerant mutant strains, pg. 151

Table 4.4: Antibiotic MIC fold changes for the selected pathogenic strains, pg. 154

Table 5.1: Identified loci of the sequenced surviving mutants from the thymol-challenged *S. enterica* TraDIS-Xpress library, pg. 173-174

Table 5.2: Analytical metrics generated from the Figure 5.5-5.6 TEM images, pg. 182

Table 9.3.1: Summary of results of the semi-high throughput inhibitive assays against the Gram-negative species, pg. 227-228

Table 9.3.2: Summary of results of the semi-high throughput inhibitive assays against the Gram-positive species, pg. 229-230

Table 9.3.3: Summary of results of the semi-high throughput inhibitive assays against the Gram-negative species, pg. 231-232

Table 9.3.4: Summary of results of the semi-high throughput inhibitive assays against the Gram-positive species, pg. 233-234

Table 9.3.5: Summary of the growth velocity impacts after challenging the Gram-negative pathogens with various phytochemicals at 0.05mg/ml concentrations, pg. 243

Table 9.3.6: Summary of the growth velocity impacts after challenging the Gram-positive pathogens with various phytochemicals at 0.05mg/ml concentrations, pg. 244

Table 9.3.7: Summary of the impacts on the final growth achieved after challenging the Gram-negative pathogens with various phytochemicals, pg. 245

Table 9.3.8: Summary of the impacts on the final growth achieved after challenging the Gram-positive pathogens with various phytochemicals, pg. 246

Table 9.4.1: Antibiotic MIC changes for selected pathogenic strains, pg. 251

Table 9.4.2: Summary of the growth velocity impacts after challenging the thymol-tolerant mutants with thymol at 0.25mg/ml concentrations, pg. 253

Table 9.4.3: Summary of the impacts on the final growth achieved after challenging the thymol-tolerant mutants with thymol at 0.25mg/ml concentrations, pg. 254

Table 9.4.4: Summary of the drug accumulation assays utilising thymol-tolerant mutant strains of *S. enterica*, *S. aureus* and *P. aeruginosa*, pg. 255

Table 9.4.5: Summary of the drug accumulation assays utilising thymol-tolerant mutant strains of *S. enterica*, *S. aureus* and *P. aeruginosa*, pg. 256

Table 9.4.6: Summary of the $OD_{(595nm)}$ measurements from the crystal violet assays using the thymol-tolerant mutant strains, pg. 257

List of abbreviations

ANOVA- Analysis of variance,
AMR- Antimicrobial resistance,
BHI- Brain-heart infusion,
CCCP- Carbonyl cyanide 3-chlorophenylhydrazone,
CDC- Centre for Disease Control,
CFU- Colony forming units,
DALY- Disability adjusted life year,
DMSO- Dimethyl sulfoxide,
EtBr- Ethidium bromide,
ET- exfoliative toxin,
FCT- Food challenge test,
GRAS- Generally recognised as safe,
Hrs- Hours,
LB(-NaCl)- Luria-Bertani (- without NaCl),
LPS- Lipopolysaccharide,
LSD Test- Least significant differences test,
MAP- Modified atmospheric packaging,
MRSA- Methicillin-resistant *S. aureus*,
MFS- Major facilitator superfamily,
MH- Mueller-Hinton,
MIC- Minimum inhibitory concentration(s),
Mins- Minutes,
MOA- Mechanism of action,
MSSA- Methicillin-susceptible *S. aureus*,
NO- Nitric oxide,
PABN- Phenylalanine-arginine β -naphthylamide,
PBPs- Penicillin binding proteins,
RND- Resistance nodulation division,
ROI- Region of interest,
SE- *Staphylococcal* enterotoxin,
SNP- Single nucleotide polymorphism(s),
SPI- Soy protein isolate,

TEM- Transmission electron microscopy,

UK- United Kingdom,

US / USA- United States / United States of America,

WHO- World Health Organisation,

WWI / WWII- World War I / World War II

Chapter 1: Introduction

“A journey of a thousand miles begins with a single step.” - Chinese proverb

Introduction-

1.0.0 food poisoning and its impact

Bacterial infections transmitted through foodborne means are one of the most common forms of infectious diseases as the gastrointestinal tract offers an easily accessible and viable environment for bacterial pathogens which have adapted to the hosts innate, natural gastrointestinal defences (stomach acid, bile salts, innate immune cells such as Peyer's Patches, protective mucus and commensal microbiota layer etc.). To give an idea of the impact of foodborne disease, the World Health Organisation (WHO) have estimated that there were 600 million cases of foodborne illness, and 420,000 deaths from such, in 2010 alone^[1]. Of foodborne disease cases, diarrhoea (a common symptom of food poisoning) causes approximately 1.3 million deaths in infants <5 years of age per annum around the globe, particularly in developing countries^[2].

Some of the most common bacterial foodborne pathogens include *Campylobacter jejuni*, *Escherichia coli*, *Listeria monocytogenes*, *Salmonella enterica*, *Staphylococcus aureus* and, less commonly but particularly prevalent in dairy products, *Pseudomonas* species such as *P. aeruginosa*. The severity of infections varies from usually self-limiting as in the case of *C. jejuni* to potentially serious and life-threatening *L. monocytogenes* infections, especially to vulnerable patients like the immunocompromised, pregnant women and the elderly.

This latter bacterium has the highest hospitalisation rates (91%)^[3] of foodborne pathogens, with an equally alarming rate of mortality. The European Food Safety Authority counted 2161 confirmed human listeriosis cases in 2014^[4], with an approximate mortality rate at 15-30%^[5]; involving mainly pregnant women and their foetuses with abortion, septicaemia, meningitis and neonatal death^[4] all common symptoms of this deadly foodborne disease. Some studies put the global mortality rate as high as 34% with *L. monocytogenes* being the leading fatal foodborne pathogen of the USA^[5]. In the 1990's the Centre for Disease Control (CDC) estimated that 1700 cases occurred per annum in the USA, with 450 adult and 100 postnatal deaths resulting from such^[5, 6]. A more recent study published a US-focused disability adjusted life year (DALY) estimate of 8800 for this micro-organism alone^[7]. While this may be an aged estimate, what is definitive is that the

incidence of listeriosis is on the rise globally^[8].

Campylobacter are Gram-negative, micro-aerophilic and spiral-shaped bacteria with numerous species (of particular note, *C. jejuni*) comprising the genus^[9]. As the producers of pathogenic cytolethal distending toxins (CdtA etc.) with a natural animal reservoir comprising wild and farmed birds, including chickens^[9], *C. jejuni* has been estimated as the second most common cause of foodborne diarrhoeal diseases in the USA, infecting 1.3 million individuals per annum^[10]. In contrast to the lethal *L. monocytogenes*, *C. jejuni* infection is generally self-limiting in its' severity although it is widespread, commonly identified in raw chicken meat, and is held responsible for 8.4% of all global diarrhoeal cases^[10]. *C. jejuni* foodborne disease translates to a human impact of approximately 22,500 DALYs^[7] in the UK specifically, alongside a rare chance of inducing Guillain-Barré syndrome at a rate ~20 in 100,000 individuals^[7].

Salmonella enterica is another major foodborne pathogen which can cause serious disease, specifically serovars of the subspecies *enterica*^[11]. As is typical of foodborne pathogens, *Salmonella* is transmitted by the ingestion of water or food commonly contaminated by the faeces of another infected host^[12], causing an often severe form of gastroenteritis. This pathogen is a major issue in both developed and developing countries, where it is one of the major causes of foodborne illness and diarrheal disease, with a climbing rate of incidence^[13]. The CDC estimated last decade that there were 40,000 reported cases with 400 deaths in the US alone^[14], with a DALY impact of approximately 32,900^[7]. The real number of cases may possibly be up to 30-fold higher due to the lack of reporting for milder, self-limiting cases^[14]. In the EU Salmonellosis is also a major issue; recent estimates place *Salmonella* as the second most frequent cause of foodborne disease, with over half of foodborne illness cases being caused by this pathogen^[15]. Focusing on a larger perspective, for the year 2017 it is estimated that there were 95.1 million cases of *Salmonella* foodborne disease globally, associated with 3.1 million DALYs and 50,771 fatalities^[15]. A gross impact on human life.

Food poisoning by *Staphylococcus aureus* (also known as Staphylococcal food poisoning) is another very common foodborne intoxication^[16] that impacts the economic potential of many households^[17, 18]. Approximately less than 0.1% of foodborne *S. aureus* cases result in death^[17], with hospitalisation being rare and usually restricted to vulnerable populations

such as infants, the elderly *et al*^[19]. While Staphylococcal food poisoning may not generally be severe the isolation of methicillin-resistant strains of *S. aureus* (MRSA) from livestock is concerning considering the food poisoning affects humans and is not readily apparent by causing gastrointestinal disease in the animals themselves^[19]. Additionally, *S. aureus* food poisoning has been reported from a broad range of contaminated food products; beef, pork, poultry, salads and dairy products^[20], making it a common if not life-threatening infection. However, the lethality of this opportunistic pathogen when attacking a human host from routes other than foodborne ingestion should not be underestimated. The mortality rates of non-foodborne *S. aureus* infections, such as bacteraemia for example, have been estimated to be between 15-60%^[21]. Estimates from the last decade place the incidence rates of *S. aureus* food poisoning at 241,000 cases per annum (within the USA), with an economic cost of \$167,597,860, although this number is potentially lower than the reality as there is the very real possibility of under-reporting of this condition^[22].

When *P. aeruginosa* was first identified as a common cause of Gram-negative bacteraemia, effective antibiotics were unavailable and thus the mortality rate amongst infected patients was staggering; approximately 90%. At present, this mortality rate has dropped however it is still disturbingly high. One study has found that, in a 123-patient cohort, the 30-day mortality was nearly 28% in patients who received effective antimicrobial therapy immediately. This mortality increased to 43.4% in patients who received delayed antimicrobial treatment^[23], highlighting this organism's importance as a lethal infection, one which should not be side-lined. Other studies have estimated the *P. aeruginosa* mortality rate at up to 60% in nosocomial pneumonia and ventilator-associated infections^[24]. Although fewer studies have identified the incidence rates for *P. aeruginosa*-induced foodborne illness, many studies have identified this bacterium within a wide range of foodstuffs, including meats (where *Pseudomonas* species contribute to the odours, flavours and discolouration associated with spoilage)^[25]. *P. aeruginosa* was found to be the most common bacterial pathogen identified from ready-to-eat Indian street food, with ~25% of samosa samples testing positive for the presence of this micro-organism^[26], suggesting an important role if not in foodborne illness then the large economic costs linked to food spoilage.

Overall, foodborne diseases affect approximately one in ten people annually^[27]. The impact of food poisoning due to bacterial pathogens is clearly extensive, however, this

burden is controlled by various effective mechanisms to combat the dangers of foodborne pathogens.

1.1.0 Food preservatives as antimicrobials: sodium nitrite

To prevent food spoilage and subsequent infections humans have, for thousands of years, implemented various processes designed to extend the “shelf-life” of foods; smoking, salting, drying and fermenting are all prime examples of these processes. The use of salts as food preservatives is an ancient tradition^[28], however it was not until the close of the 19th Century that it was discovered that contaminating nitrate (as saltpetre) is converted to nitrite by commensal, nitrate-reducing bacteria^[29] present in the applied brine solutions and meat surfaces. It is this chemical species that is responsible for the curing effects of saltpetre as nitrate is reduced *in situ* and released as reactive nitrite during and after the curing process.

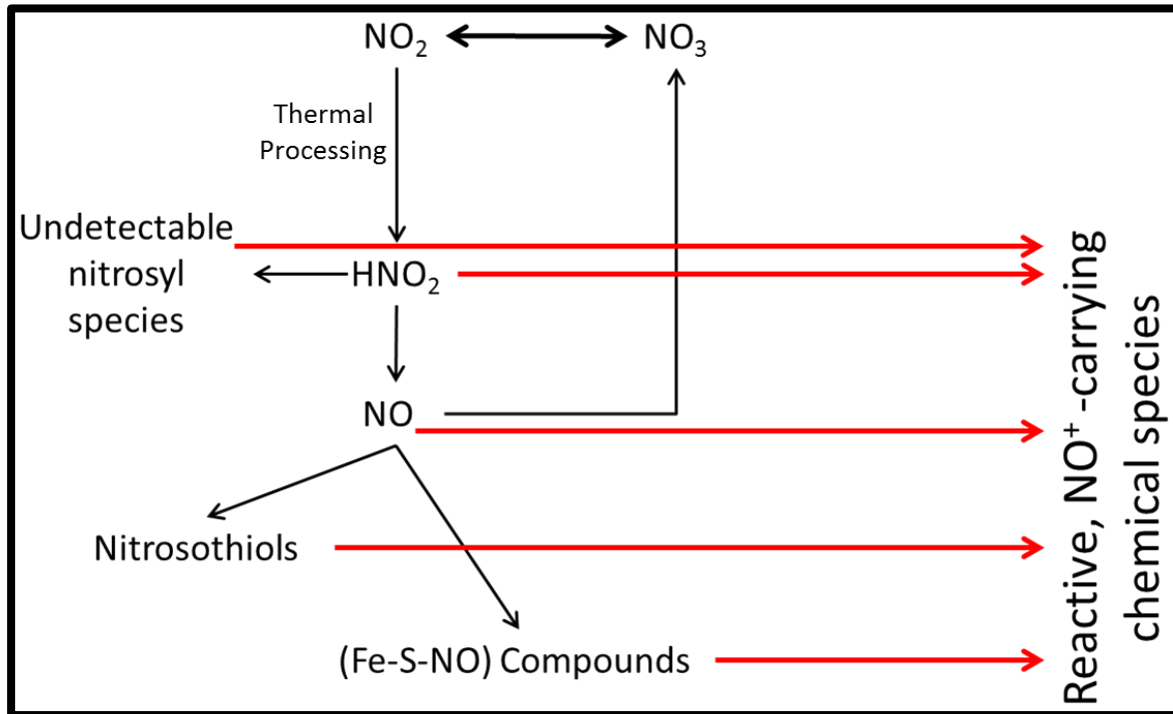
Nitrite is particularly effective at inhibiting the growth of *Clostridium botulinum* (a fortunately rare yet lethal foodborne pathogen that causes the paralysing intoxication known as “botulism”), in addition to other Gram-positive and toxin-producing bacterial species^[30] in meats cured with relatively small quantities of sodium/potassium nitrite salts^[31]. More recent studies have displayed nitrite’s effectiveness at inhibiting the growth of more common foodborne pathogens such as *E. coli* O157:H7, *Salmonella enterica* Typhimurium, *L. monocytogenes* and *S. aureus*^[32].

As a food preservative nitrite is thought to target the outgrowth of germinating spores, their subsequent growth and various key pathways of vegetative bacterial cells^[33-35], however the nitrite anion is not directly responsible for the strong inhibitory effects attributed to it^[36]. As a highly reactive chemical species nitrite can be converted to a variety of related compounds including nitrous acid, nitric oxide (NO), iron-sulphur-nitrosyl (Fe-S-NO) compounds and again, nitrate^[29, 32, 33, 37], which then acts as a reservoir for further nitrite release due to the nature of chemical equilibria (See **Figure 1.1**). Previous studies have shown that these products of decomposition are more effective inhibitors of bacterial growth than nitrite itself with the shared nitrosonium (NO⁺) group being

suggested as the responsible reactive species for the preservative effects observed^[30, 38], although the detection thresholds of analytical technology^[30, 37] have made describing a primary inhibitory MOA of nitrite difficult.

Like most acids, nitrous acid is a reactive chemical species that can deaminate amino groups within peptides and nucleotides^[37, 39]. This behaviour naturally damages the proteins/DNA of contaminating bacterial species and hence may contribute to the inhibitory effect of nitrite. However, during the 1960's emerging evidence subsequently discounted nitrous acid as the main inhibitory mechanism of nitrite, with the highly reactive NO being suggested instead^[40]. NO and the miscellaneous nitrosyl species derived from it also behave in a similar manner; to such an extent that the deamination of lysine residues has previously been suggested as a viable experimental marker for nitrite exposure to the proteins of meat samples^[37, 40, 41]. Nitrosothiols are produced from the nitrosylation of thiol moieties by NO and NO-derived species^[42]; these sulphur-containing groups may be associated with cysteine residues or the iron-sulphur clusters of a range of eukaryotic and prokaryotic enzymes. Nitrosothiols and NO have been shown to promote the breaking of DNA strands after reacting with superoxide (in the case of NO) and H₂O₂ (with nitrosothiols)^[37-39]. **(Kroncke K.D. et al 1994)**^[43] also showed that NO can attack zinc-finger DNA-binding proteins in a similar manner, potentially disrupting the gene regulation of inhibited cells^[37]. Alternatively, nitrite's inhibitory effects on the growth of bacteria may be due to the species' strong affinity for binding and chelating metal ions, inhibiting the formation of necessary metallo-proteins^[37, 41, 44].

Figure 1.1: Diagram summarising the chemical reactions of nitrite



Chemical reactions underpinning nitrite's food preservative usage. Note the presence of nitrosothiols *et al* may increase the risk of developing oesophageal and gastrointestinal cancers.

In addition to its antimicrobial preservative action nitrite also contributes heavily to the characteristic pink colour of cured meats^[31, 40] via a chemical chain reaction^[45] resulting in the formation of nitrosylmyoglobin, which is itself thermally transformed into the pink “cured pigment” nitrosyl-hemochrome during heat treatment^[46]. Nitrite also adds to the flavour of cured meat products by acting as an antioxidant, inhibiting the lipid oxidation that otherwise results in the development of a “warmed-over” taste^[40]. Nitrite possesses strong anti-oxidant activity, with various MOA^[47] proposed such as the stabilisation of unsaturated lipids within the cellular membranes of meat tissues, direct interactions with free, non-haem iron and a third paradigm postulating the sequestering of iron to inhibit its catalysing lipid oxidation^[46, 48, 49].

Nitrite is used widely in the curing of meats: certain fish, poultry and pork products such as hams, bacons and European sausages are prime examples. The addition of nitrite to these products during manufacture can take various forms; from traditional submersion in curing brines, dry curing (massaging the preservative mixture onto exposed surfaces followed by a set aging period to allow full penetration of the meat), addition by mixing the nitrite salts in with the product’s seasoning or direct injections of a nitrite-containing brine or meat slurry into the product, commonly followed by a slow tumbling process to achieve an even distribution throughout before subsequent heat treatments^[50]. The legal maximum limits of nitrate and nitrite that can be added to meat products is a balanced trade-off between the microbiological safety of the product in question and the minimisation of the health risks posed by excessive nitrate/nitrite intake. Within the EU the legal residual limit is presently 150mg/kg of meat^[50, 51].

Legislative limits on the usage of nitrite as a food preservative are necessary as nitrite is certainly not without its complicating issues^[52]. Excessive nitrite intake has been previously correlated with certain forms of cancer; the Henan province of China for example possessed an abnormally high incidence of oesophageal cancer prior to the new millennium. This was linked to the area’s high contamination of nitrite/nitrate in the local water supply, which works its way into the local traditional diet of pickled vegetables and other foodstuffs^[37]. One branch of nitrite-derived compounds, the N-nitroso compounds, including the nitrosamines, are known potent carcinogens that can be produced by the reaction of nitrite with secondary or tertiary amines^[40, 50, 53, 54]. This nitrosation can be

catalysed by thermal methods (i.e. the heat treatments many cured meat products undergo during manufacture and/or consumers cooking their purchases) and endogenously by the acidic conditions of the upper gastrointestinal tract^[40].

1.2.0 Antibiotics; the golden age of discovery

While antimicrobial food preservatives have been utilised by humanity for millennia to protect our food supplies, in the face of infectious diseases it is only relatively recently that we have gained the knowledge and skills to manipulate other antimicrobial compounds to combat the infections and diseases that are caused by the wide plethora of viruses, protozoa, fungi and bacteria that inhabit our world. Over the centuries infections have decimated millions of people in epidemics and pandemics worldwide, with just one example being the Black Death, caused by the bacterium *Yersinia pestis*, that wiped out 30-50% of Europe's populations between 1347 and 1351^[55]. During this period, like much of humanity's history, there was a lack of scientific knowledge to aid in combating, curing and reducing the spread of infectious diseases; chief being the identification of the microscopic arbiters of disease with the invention of the first effective microscope^[56].

Many early medical practices were ineffective, superstitious and most often barbaric and damaging in themselves^[57]. This vulnerability to infection was the status quo even up until the beginning of World War II (WWII), with far more fatalities in WWI being attributed to infectious diseases associated with the reduced hygiene and wounds of war than any bullet or bomb. This changed dramatically with the discovery of penicillin by Fleming in 1928 (although not commercially available until the 1940s) and sulphonamides just three years earlier^[58, 59]. To give a measure of the effectiveness of both these antibiotics, the mortality rates from limb wounds alone decreased by 5.6% down to 2.1% between WWI and the beginning stages of WWII^[60, 61]. The discoveries of sulphonamides and penicillin in 1937 and 1928, respectively, were the first of many exciting antimicrobial compound discoveries to be made in the next few decades to come. This heralded in what would be termed the "golden age of antibiotic discovery". Beginning in the early 1940s and lasting until around the mid-1980s, a broad range of antibiotic classes were discovered in rapid succession; mostly fermentation products found from screening soil-living bacteria for natural products as a low-throughput but effective *modus operandi*. With the discovery, development and commercialisation of such natural products antibiotics became available

therapeutically to treat once-epidemic and terminal diseases; cholera, syphilis, tuberculosis and typhoid fever stopped being the death sentences they once were for millions of people and became easily treated with a short and simple course of antibiotics^[57, 62, 63].

However from the 1980s to the early 2000s the discovery of novel antibiotic classes, and the approval of new antibiotics, dropped by 90%^[64]. Nevertheless, the golden age of antibiotic discovery gave rise to eight antibiotic classes, each comprising multiple structurally analogous compounds which share a common MOA for their antibacterial effects. A summary table of the different classes, with a brief description of their MOA and example compounds can be found in **Table 1.1**.

Table 1.1: Summary of antibiotic classes.

Antibiotic class	MOA	Example compounds/synonyms	References
Sulphonamides	PABA-structural analogues; competitive antagonists of Folic Acid synthesis pathways ^[65, 66]	Sulfamerazine, Sulfamethoxazole	(Wu Q. et al 2018) ^[67]
β -Lactams	Inhibitors of Penicillin Binding Proteins that cross-link the peptidoglycan cell wall, leading to cellular lysis ^[68]	Ampicillin, Penicillin G, Amoxicillin, Carbapenem, Cephalosporin	(Bush K. et al 2016) ^[69]
Chloramphenicol	Bacteriostatic, inhibits peptidyl transferase activity of the bacterial ribosome by preventing elongation of the nascent protein chain ^[70-72]	Chloromycetin, Chlornitromycyin, Levomycetin	National Center for Biotechnology Information. PubChem Compound Database ^[73]
Tetracyclines	Reversibly binds to the 30S bacterial ribosomal subunit, preventing attachment of the aminoacyl-tRNA required for protein synthesis ^[74, 75]	Chlortetracycline, Methacycline, Doxycycline, Tigecycline	(Grossman T.H. 2016) ^[76]
Aminoglycosides	Binds to 30S bacterial ribosomal subunit, causing a misread of the genetic code. Subsequently leads to interruption of protein synthesis ^[77, 78]	Kanamycin, Tobramycin, Neomycin	(Jana S. and Deb J.K. 2006) ^[79] (McKeating K.S. et al 2016) ^[80]
Macrolides	Inhibition of bacterial protein synthesis. Similar to Chloramphenicols, ^[81, 82]	Erythromycin, Tylosin A, Josamycin,	(Weisblum B., et al 1969) ^[83] (Arsic B. et al 2018) ^[84]
Quinolones	Converts gyrases and topoisomerase IV into toxic	Nalidixic Acid, Ciprofloxacin,	(Naeem A. et al 2016) ^[87]

	enzymes that degrade the bacterial chromosome ^[85, 86]	Voreloxin,	
Streptogramins	Inhibit the bacterial 23S rRNA of the 50S bacterial ribosomal subunit. Individually, bacteriostatic. Used synergistically, are bactericidal. ^[72]	Dalfopristin, Quinupristin	(Harms J.M. et al 2004)^[88]

A brief overview of the various antibiotic classes discovered during the Golden Age of Antibiotic Discovery, with described MOA and example compounds attached.

Since the early 2000's, a few other classes of antibiotic have also been discovered and approved for use; namely the oxazolidinones, lipopeptides, mutilins, fidaxomicin and diarylquinolones. Many antibiotic classes were discovered from bacteria themselves, with many of those found within the golden age of antibiotic discovery being from species within the soil-dwelling *Actinomycetes* genus^[63]. Thanks to numerous studies we know that bacterial production of antimicrobial compounds is the result of a millennia-long biological arms race between competing microbial species inhabiting the same or proximate ecological niches^[89]. **(Kommineni S. et al 2015)**^[90] found, for example, that commensal bacteria within the gastrointestinal tract (a microbial-dense and relatively nutrient-limited environment) can influence niche competition by the production of antimicrobial bacteriocin to eliminate competitors. **(Patin N.V. et al 2016)**^[91] found in a separate study two *Streptomyces* species that had developed different strategies for niche competition, despite being genetically closely related and found within the same environment. *S. tropica* utilises nutrient depletion of the environment to starve competitors while *S. arenicola* utilises antibiotic production early in its' growth cycle to compete effectively within the species' shared marine sediment environment. These and other studies^[90-92] suggest that antibiotic production is an effective mechanism for bacteria to minimise niche overlap and competition, a natural advantage and tool for survival. As a response to this biological arms race it is thus no surprise that many bacterial species have developed, over the millennia of competitive antibiotic exposure, intrinsic and transferable resistances to these antimicrobial compounds; there is much evidence from metagenomics and functional genomic studies for example that support the idea of antimicrobial resistance (AMR) being an ancient phenomenon^[93]. In fact; Sir Alexander Flemming himself observed resistant bacterial colonies to his newly-discovered penicillin and warned of the dangers of antibiotic overuse and growing antimicrobial resistance within his Nobel acceptance speech after his discovery; stating that "...there is the danger that the ignorant man may easily underdose himself and by exposing his microbes to non-lethal quantities of the drug make them resistant."^[94].

1.3.0 AMR: mechanisms of AMR, AMR transfer and impact

AMR can be achieved by various methods and means; of which the various strategies are detailed below^[95-97].

1.3.1 Alteration/protection of antibiotic targets

The targets of antibiotics, be they cell wall precursors, ribosomes, essential enzymes or metabolic pathways, can be altered so that the antibiotic's specific molecular target is altered to no longer be present, disguised or shielded from attack. This can be achieved through point mutations in the organisms' genes encoding the antibiotic target or commonly through the gain of horizontally transferred genes encoding enzymes that chemically modify the target, nullifying the antibiotic's MOA and rendering the organism resistant^[95, 98, 99].

Some examples of this target alteration include common fluoroquinolone resistances where mutations in DNA gyrase and/or topoisomerase IV genes, specifically in the fluoroquinolone-resistance-determining-region of the GyrA subunit and ParE/GrlB subunits of the two respective enzymes, result in the loss of binding of fluoroquinolone-type antibiotics^[95, 100]. Another example can be demonstrated by the resistances displayed by *E. coli* and *Streptococcus pneumoniae* to trimethoprim, which targets and inhibits the dihydrofolate reductase enzyme that converts the metabolite dihydrofolic acid to tetrahydrofolic acid in the folate synthesis pathway. Resistance can occur by chromosomal point mutations in the dihydropteroate synthase enzymes making up the pathway, or through plasmid-mediated acquisition of antibiotic resistant enzyme variants^[95, 101]. A final and classic example of altered antibiotic targets as a resistance mechanism is the gain of resistant penicillin binding proteins (PBPs), enzymes that facilitate the synthesis of cell wall peptidoglycan by the transpeptidation of peptidoglycan precursors. β -lactam antibiotics are competitive antagonists of their target PBPs and prevent the enzyme's normal function, leading to a lack of newly synthesised peptidoglycan and the eventual lysis of the affected cell as the wall structural integrity is compromised. The gain of resistant PBPs with

lower affinities for β -lactam antibiotics, such as PBP2 and PBP2a, is common in Gram-positive organisms such as *S. aureus*^[95, 102].

1.3.2 Antibiotic inactivating enzymes

Another common mechanism of antibiotic resistance is the use of enzymes which modify or degrade the antibiotic itself, rather than modify the antibiotic target, to nullify its' effects. There are many examples of such enzymes; a classic being the production of periplasmic β -lactamases (e.g.; penicillinases by *Staphylococcus* species) to degrade β -lactam antibiotics like penicillin^[95].

Resistance-enabling enzymes have a variety of MOAs as varied as their antibiotic targets, including: the hydrolytic cleaving of antibiotic molecules, the transfer of chemical moieties to reduce the antibiotics affinity for its target or its efficacy and the complex use of redox reactions to neutralise the antibiotic threat to the resistant organism.

Hydrolysing enzymes commonly cleave amide and ester bonds present within a specific antibiotics molecular structure, rendering the antibiotic ineffective and thus conferring antibiotic resistance. A classic example of a hydrolytic enzyme is the production of β -lactamases (mentioned above), which hydrolyses and cleaves the β -lactam ring of penicillin and other β -lactam antibiotics^[103].

Enzymes that mediate the transfer of chemical groups on the structural backbone of antibiotic molecules are common, taking advantage of the wide array of chemical groups and reactions available in biochemistry. Transferases are common resistance enzymes that can give resistance to aminoglycosides, macrolides, chloramphenicol and others by the substituting of phosphoryl, adenylyl or acetyl groups onto the fringes of an antibiotic's structural scaffold. These altered antibiotic molecules are impaired in their function, be that in their target binding or mechanistic capacities^[104]. *S. enterica* has been reported to encode and produce acetyltransferases that neutralise aminoglycosides, while *E. coli* strains have been found that produce erythromycin resistance-associated esterases (e.g. the *ere* gene), and macrolide phosphotransferases (e.g. the *mph* gene)^[105, 106].

1.3.3 Efflux of antibiotic molecules

Another mechanism of AMR is the expulsion of antibiotics from the bacterial cell before their intracellular concentration can rise to a sufficient level for their bacteriostatic or bactericidal effects. This is accomplished via efflux pump systems found within all trees of life (prokaryotes, archaea and eukaryotes)^[107]. These systems are both ancient and common, with efflux pump systems consisting of as much as 10% of many bacterial species encoded transporters^[107]. One of their main functions includes the efflux of toxic elements out of the cell such as heavy metals, solvents, bile salts and detergents etc. Efflux pump systems are intricately regulated and can respond to alterations in the intracellular concentrations of their substrates (e.g.; studies have shown that the gene expression of *P. aeruginosa* efflux pumps increases in the presence of increasing concentrations of heavy metals). These transporter systems are also vital in many bacterial species virulence/pathogenicity for the secretion of toxins, curli, and other effector proteins/products^[107].

A defining characteristic of efflux pumps is the wide range of structurally different compounds that any one system can recognise, bind and eject from the cell as opposed to many other transporter systems that are very substrate-specific^[107, 108]. While intrinsic antimicrobial tolerance of a cell can be determined by the extrusion of antibiotic molecules via the energy-dependant process that is efflux, resistance can be conferred by mutations that increase the expression levels of native efflux pumps or that alter the binding capacities of the substrate-recognition domains of the system. This latter may increase the affinity of the mutated pump system for its antimicrobial substrates. By either of these two routes the intracellular concentration of the antimicrobial substrate is drastically lowered to a point where its effects are void^[107-109]. There are five main families of efflux pumps, however it is the Major Facilitator Superfamily (MFS) and Resistance Nodulation Division (RND) families that have been most studied in association with AMR (particularly in Gram-negative bacteria)^[107, 109].

Examples of the RND family include the AcrAB-TolC efflux pump system found in *E. coli* (and all *Enterobacteriaceae*) and the MexAB-OprM system of *P. aeruginosa*. RND efflux pump systems are involved in the transport of lipophilic molecules, toxic divalent cations and antimicrobial compounds. These pumps are mainly found within Gram-negative

bacteria and form tripartite systems spanning the inner membrane, periplasm and outer membrane of the cell. Two pump system-specific proteins (e.g.; AcrB and AcrA) respectively form a pore through the inner membrane and a scaffold that attaches and guides substrates towards and through a non-specific protein pore (e.g.; TolC) which is embedded in the outer membrane^[107-109]. In Gram-positive bacteria AMR is conferred primarily by the MFS family; an example of which is the NorA pump encoded by *S. aureus*^[108, 109]. The MexAB-OprM pump system contributes to *P. aeruginosa* β -lactam resistance and to this species' resistance to novobiocin. The AcrAB-TolC pump of *S. enterica* and *E. coli* on the other hand are examples of pump systems gifting AMR to a range of antibiotics; tetracycline, quinolones, chloramphenicol and triclosan for example^[109].

1.3.4 Selection of resistance

Exposure of a bacterial population to an antibiotic acts as an evolutionary pressure that, if the prescribed course does not wipe out the whole population, can select for survival of a resistant sub-population. A resistant sub-population may carry genetic mutations conferring/enhancing one of the AMR phenotypes discussed above, rendering the antibiotic treatment ineffective and allowing the newly resistant sub-population to expand and double.

Compounding the increased exposure of bacteria to antibiotics is the ease in which certain AMR phenotypes may be transferred from bacterium to bacterium, both within and across species. AMR may spread throughout bacterial populations via mobile genetic elements; namely resistance plasmids and transposon or integron cassettes^[110] which harbour the resistance genes and, sometimes, genetic clusters that confer resistance to multiple antibiotics in one vector. This transmission of genetic elements is termed horizontal gene transfer and plays a key role in the developing global crisis of AMR as mobile elements can rapidly spread resistance phenotypes, enhancing existing and enabling new epidemics swifter than the rate of genetic mutation experienced within single, independent bacterial populations^[111-113]. The transfer of AMR genes is not only an issue within pathogenic bacterial populations but in commensal, non-pathogenic species too^[114]. **(Schmidt V. et al 2018)**^[115] found that multidrug resistant *E. coli* carried in the gastrointestinal tracts of canines may act as reservoirs for the transmission of resistance genes to the environment

and less benign bacterial species; pathogens of dogs and humans for example. **(Schmidt V. et al 2018)**^[115] concluded that “systemic antimicrobial therapy selects for AMR Gram-negative bacteria, so increased use compounds AMR issues...”.

The critical impact of AMR pathogens on human health and life are palpable; as the novel antibiotic pipeline dries up and the incidence of AMR steadily increases to globally-threatening proportions, recent research has revealed that frontline antimicrobials are becoming less and less effective against enteric pathogens^[63, 114]. The severe consequences of such are elegantly summed up by **(Cosgrove S.E. et al 2003)**^[21] who, after combining the data from 31 cohort studies, found there was a significant increase in the mortality rates associated with methicillin-resistant *S. aureus* (MRSA) bacteraemia when compared to comparable infections caused by methicillin-susceptible *S. aureus* (MSSA). Infection with MRSA was also found to significantly raise the lengths of hospital stay; MRSA in surgical wounds also increased the post-operative mortality rate by 3.3 fold and the medical charges associated with all of this significantly increased by approximately \$7000. In addition, the study found that MRSA infection in children increased the duration of fevers by nearly 3.5 days, and the overall time spent in hospital by 1.8 days^[21]. The human incidences and impact of AMR *Salmonella* has been growing over the last few decades, with a steady rise of multi-drug resistant strains being identified within Europe and North America^[116]. The AMR status of a *Salmonella* infection has been linked in Denmark with an up to 10.3 times higher mortality rate^[117]; coupled with the CDCs estimated case numbers of 100,000 AMR nontyphoidal *Salmonella* infections annually in the US alone it is no wonder that the WHO has listed AMR nontyphoidal *Salmonella* as a global health concern^[118]. A significant association between the AMR profiles of numerous pathogens (including *S. aureus*, enterococci, Gram-negative bacteria) and an increase in the mortality rates, length of time spent in hospital care and the overall cost of healthcare has also been found. The presence of an AMR-phenotype increased the healthcare cost by ~\$6000-\$30,000; a gross amount at an individual patient level and even more so when put into a national or global perspective^[21]. Other studies^[119-122] have corroborated the worse outcomes for infection with resistant AMR infections vs susceptible ones; patients with AMR bloodstream infections were found to be 2.5 times more likely to die within the first 30 days after infection for example. In 2003, the US Office of Technology Assessment estimated the national cost of AMR to be ~\$4 billion per annum^[121] while more recent estimates from the World Health Organisation place the economic burden of AMR

infections closer to US\$21-34 billion with more than 8 million extra days spent in hospital care^[122]; all vastly larger than the money spent on, and the days spent in, care for antimicrobial-susceptible infections.

1.3.5 Antimicrobial/nitrite substitutes and synergists

With all the above as context, and as ongoing research has revealed the extent and risks of nitrite usage as a food preservative, it comes as no surprise that food manufacturers are under pressure to develop natural and 'milder' antimicrobial substitutes that still maintain the high safety margin presently attained^[123, 124].

Plants and fungi have been suggested as a source of alternative food preservatives and much time has been invested into their research. Mushrooms have been studied as a nitrite substitute and certain species have shown remarkable anti-botulinal capabilities^[125], in parallel to the research on the general antibacterial properties of common herbs and spices including clove, nutmeg and sage^[126]. Waste products from other industrial processes may be utilised to aid in the reduction of nitrite, for example citrus wastewater (a by-product of fibre-extraction from oranges) has been shown to increase the shelf-life of sausages^[127]. Other studies^[128] have displayed the antimicrobial effectiveness of berry and fruit juices (such as sea buckthorn and quince) when added to food samples, highlighting their potential as antimicrobial agents applicable within the food industry. Indeed, many plant and fruit extracts are also excellent antioxidant agents that may help delay the onset of organoleptic decay via oxidation of the cellular lipids in meat foodstuffs. This two-pronged functionality of antimicrobial and antioxidant action is promising for nitrite substitutes, as nitrite is presently used for both purposes.

Essential oils (plant produced volatile mixtures of organic compounds) have been added to foods to manipulate and improve their flavours already; however, their antimicrobial properties also suggest them as decent candidates to replace nitrite as a chemical food preservative. Essential oils such as those from the plant species *Laurus nobilis* and *Myrtus communis* have already been shown to reduce the burden of foodborne pathogens when added directly to food products or as bioactive components in the foods packaging materials^[129]. This is an especially tempting solution for minimally processed foods when combined with the products' typically mild heat treatments. Oregano essential oil has

been shown to inhibit the growth of *E. coli*, *S. enterica* and *Listeria* species when added to the packaging films of spiked salads^[129]. Following the trend of adding antimicrobial plant extracts to packaging films, **(Khalid S. et al 2018)**^[130] showed that ground and dried pomegranate rind powder also enacted reasonable antimicrobial activity against *S. aureus* cultures when incorporated into polycaprolactone films. The main issue with the use of a single essential oil as a food preservative is their pungent taste and smell when used in concentrations high enough to enact their main constituent's antimicrobial effects^[131]. A solution to this has been proposed; the coupling of two or more essential oils or antimicrobials to enact a synergistic antimicrobial effect at individual concentrations lower than that required to impact the foodstuff's organoleptic qualities negatively^[131]. This method has been shown to be viable, at least, as a prime component of oregano essential oil, carvacrol, when combined with the typical food bacteriocin nisin was able to eliminate *L. monocytogenes* contaminating ready-to-eat carrots^[129]. The powerful antioxidant and antimicrobial properties of plants and fruits, specifically their phytochemical components, make them attractive natural preservative substitutes for the food industry^[132].

Plant and fruit extracts have also been intensively studied for their potential as antimicrobial therapeutics, with a particular focus being on their capacity to synergise with presently used antibiotics to overcome the AMR often found within pathogenic strains^[133]. One study has suggested that curcuminoids, compounds found naturally in ginger, and green tea gallic catechins could be prime candidates to co-administer with antibiotics as part of combinatorial antimicrobial therapy^[134] while another^[135] has observed synergism between tested tea extracts and penicillin G against the methicillin and penicillinase resistant *S. aureus* strain ATCC 25923. This synergy is thought to be effective due to the plant/fruit extract modifying the pathogens behaviour; affecting such aspects as motility, surface adhesion, biofilm formation and virulence factor production/secretion. This then potentiates the action of an antibiotic to which the bacterial strain would otherwise be resistant to. **(Maisuria V.B. et al 2015)**^[89] tested concentrated maple syrup extracts and found that they could potentiate the effects of ciprofloxacin in both planktonic cultures and biofilm-associated cells; possibly by permeabilising the bacterial membrane, inhibiting efflux pump systems and downregulating multidrug resistance-associated genes. Evidence presented within their study showed a significant reduction in the transport of ethidium bromide (EtBr) across the bacterial membrane; an indicator that there was a decrease in efflux pump activity. With their data and previous reports reinforcing the potential for

plant extracts to synergise with synthetic antibiotic drugs (e.g.; erythromycin or vancomycin), (Maisuria V.B. et al 2015)^[89] concluded that a synergism-based antibiotic therapeutic approach could be a promising paradigm to maintain the efficacy of current antibiotic treatments, as well as “preventing the emergence of resistant mutant strains during antibiotic treatment”^[89].

The main chemical components of all the plant-based substitutes detailed thus far are classified as phytochemicals, and for most of them, more specifically as “polyphenols”; a structurally diverse group of organic molecules that will be described below.

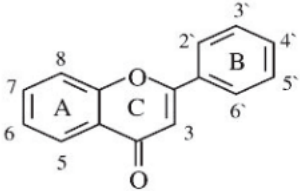
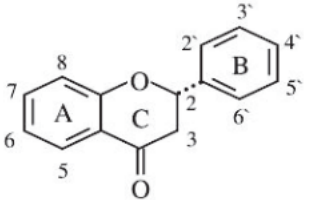
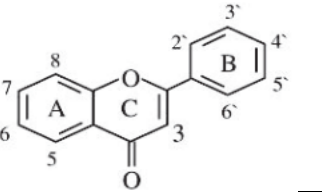
1.4.0 Phytochemicals; polyphenol classes and structures

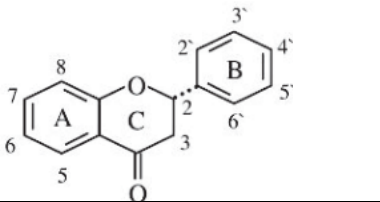
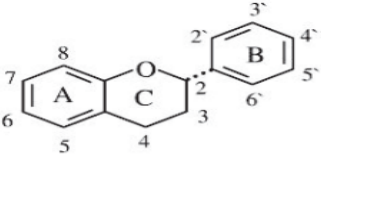
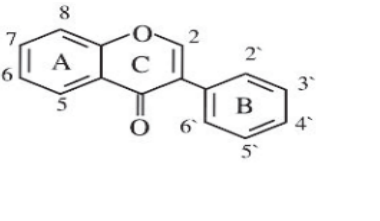
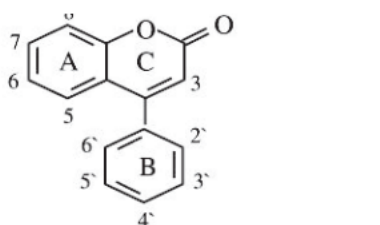
Polyphenols are organic phytochemical molecules consisting of one or more phenolic rings decorated with hydroxyl groups and a multitude of other chemical moieties^[132, 136-139]. Synthesised from phenylalanine (or tyrosine)^[132] by plant species, polyphenols are classed as secondary metabolites; that is they serve a number of physiological functions unrelated to the primary growth and maturation of the plants that produce them^[132]. Examples of these secondary functions include pigmentation for flowers, as olfactory attractors for pollinating insects, promoters for the growth of commensal bacterial species, as an antimicrobial defence against invading plant pathogens and as a defence against herbivores due to their ability to bind to and precipitate salivary proteins^[138, 140, 141].

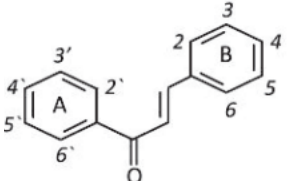
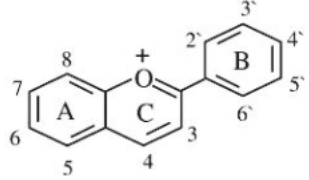
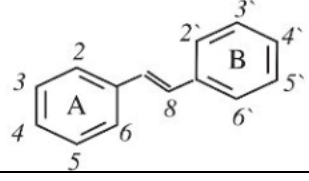
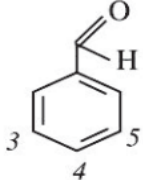
The term polyphenol encompasses a vast array of structures based on the aforementioned decorated (poly)phenolic ring structure; these polyhydroxylated phytochemicals are so structurally diverse that approximately 8,000 compounds have already been isolated and described from plants^[140]. Their structural diversity stems from alterations in the aglycone ring (the phenolic ring without the attachment of glycosidic moieties; a common addition to increase the solubility of these compounds *in vivo* aqueous conditions), the overall redox state of the molecule, as well as the degree of hydroxylation and derivatisation in the presence or absence of alkyl, carboxylic or alcoholic groups^[142]. While a list of major structural classes is detailed in **Table 1.2**, some of the more relevant classes that shall be

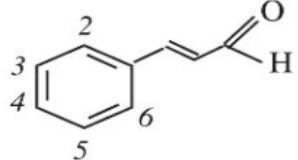
the focus here include the phenolic acids, phenolic terpenes and the flavonoid classes of flavanones and flavanols.

Table 1.2: Polyphenol classes, structure and example compounds.

Structural class	Structure	Example compounds
Flavone		Apigenin, Luteolin,
Flavanone		Hesperetin, Naringenin,
Flavonol		Quercetin, Kaempferol, Galangin,

<p>Flavanonol</p>		<p>Taxifolin, Fustin,</p>
<p>Flavan-3-ol</p>		<p>(+)-Catechin, (-)-Epicatechin,</p>
<p>Isoflavone</p>		<p>Genistein, Daidzein, Daidzin,</p>
<p>Neoflavonoid</p>		<p>Dalbergin, Calophyllolide,</p>

<p>Chalcone</p>		<p>Flavokawain A, Flavokawain B,</p>
<p>Anthocyanidin</p>		<p>Cyanidin, Peonidin, Cyanin,</p>
<p>Stilbenoid</p>		<p><i>Trans</i>-Resveratrol, Cajanotone,</p>
<p>Phenolic Acid- Benzoic Acid</p>	 <p><i>C6 – C1</i></p>	<p>Gallic Acid, Ellagic Acid,</p>

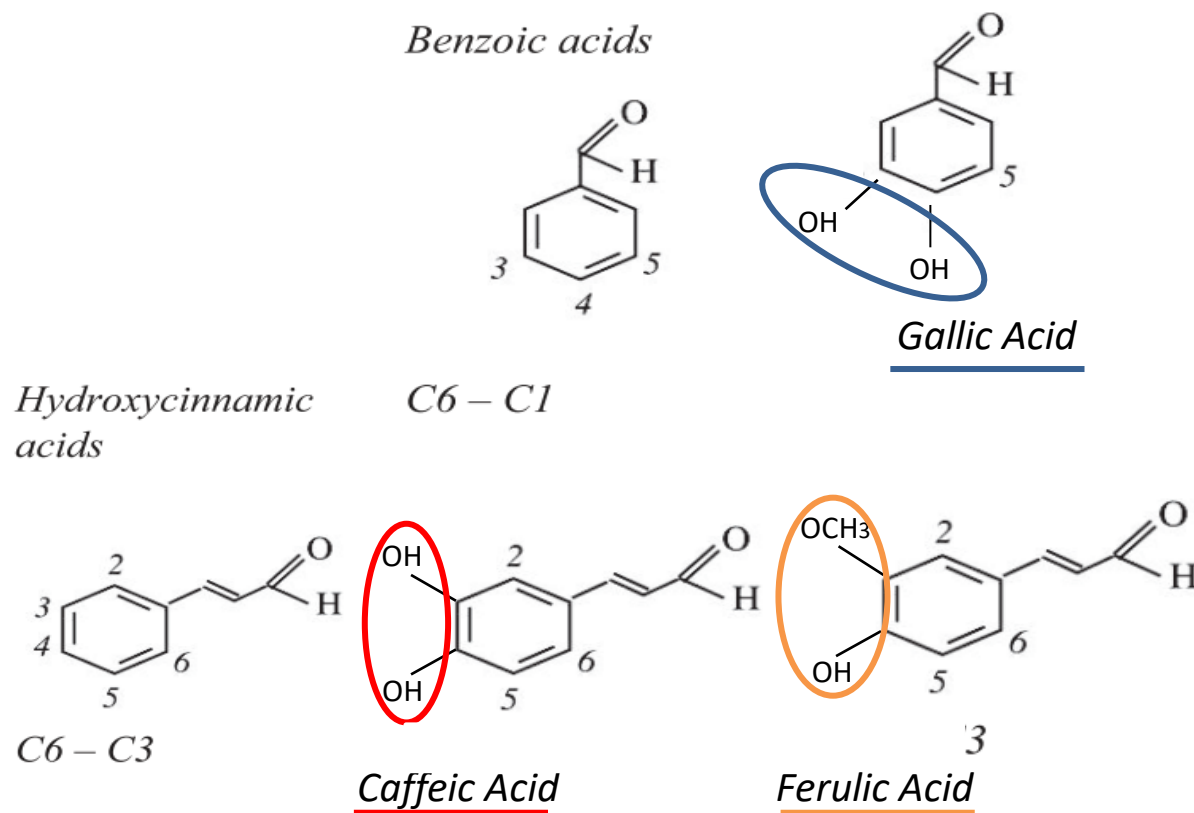
Phenolic Acid – Hydroxycinnamic Acid	 <i>C6 – C3</i>	Caffeic Acid, Ferulic Acid,
---	---	--------------------------------

A brief overview of the many polyphenol classes and structures that have been identified, and a few example compounds of each one. Table adapted from (Papuc C. et al 2017)^[132].

1.4.1 Phenolic acids

Phenolic acids are some of the most structurally simplistic phytochemicals that display bioactivity. They consist of a single phenolic ring (as shown in **Figure 1.2**) and are derived from either benzoic acid (bestowing a C6-C1 backbone to the molecule) or hydroxycinnamic acid (giving a C6-C3 backbone)^[132]. Examples of these highly oxidised molecules include the hydroxycinnamic acids caffeic, ferulic and cinnamic acid (see **Figure 1.2**)^[136, 138, 140]. The degree of hydroxylation of phenolic acids is thought to be responsible for their microbial toxicity, with the suggested MOA including essential enzyme inhibition by these oxidised compounds through reactions with sulfhydryl groups or nonspecific phenol-protein interactions^[143].

Figure 1.2: Phytochemical class structure; the phenolic acids.



Exhibits the general structure of phenolic acid molecules with the benzoic acid precursor on the top-left, the hydroxycinnamic acid precursor on the bottom-left and example molecules to the right of each. The distinguishing groups for each molecule are highlighted. Figure adapted from (Papuc C. et al 2017)^[132].

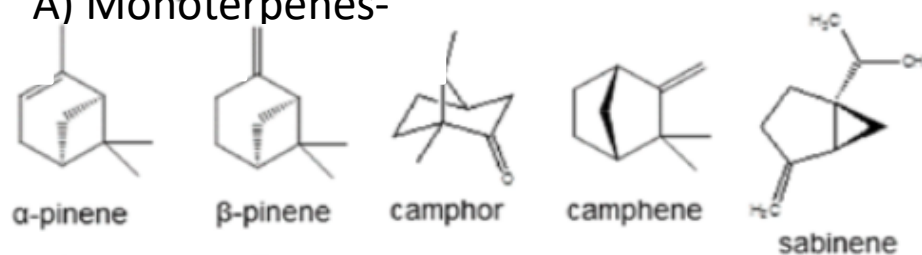
1.4.2 Terpenes

Terpenes, while not technically polyphenols as they are based on an isoprene structure, are still an important class of molecules that are abundant in the essential oil fractions of many herbs and plants. Sharing a common synthesis origin with fatty acids (being synthesised from acetate units, although differing from fatty acids in their extensive branching and cyclisation), terpenes have been shown to display antimicrobial activity against a range of bacterial species^[143]. The terpene general chemical structure is C₁₀H₁₆, and they are produced as diterpenes (C₂₀), triterpenes (C₃₀) or tetraterpenes (C₄₀)^[144]. They may also be modified via aromatisation and are thus termed “phenolic terpenes” or “terpenoid phenols”^[145] (See **Figure 1.3**).

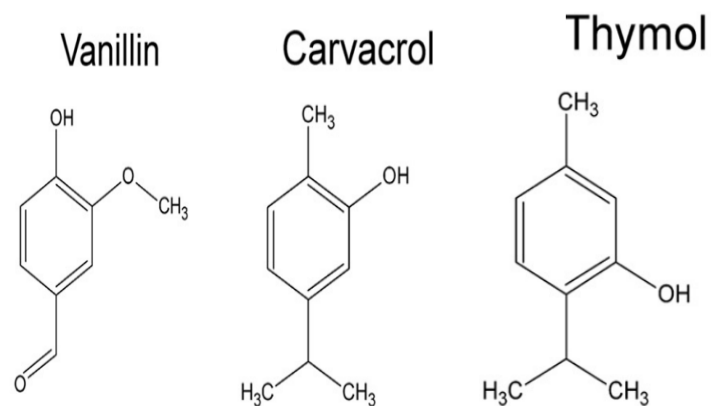
Examples of phenolic terpenes include carvacrol (a key component of oregano essential oil) and the monoterpenoid phenol thymol, both of which show antimicrobial activity against *S. aureus*, *P. aeruginosa* and *Salmonella* species^[146]. It has been observed that carvacrol exhibits a higher antimicrobial effect on Gram-positive bacteria such as *L. monocytogenes* rather than Gram-negative species like *E. coli*, possibly due to the phenolic terpene’s propensity to attack the cellular membrane, which is more easily accessible in the former^[147]. Thymol has also been shown to reduce AMR in drug-resistant pathogens, on top of its potent antioxidant capabilities. Its MOA of inhibition has been suggested to be the disruption of bacterial membranes, via disintegration of the membrane’s integrity and protein interactions^[148, 149].

Figure 1.3: Phytochemical class structure; the monoterpenes.

A) Monoterpenes-



B) Phenolic Terpenes-



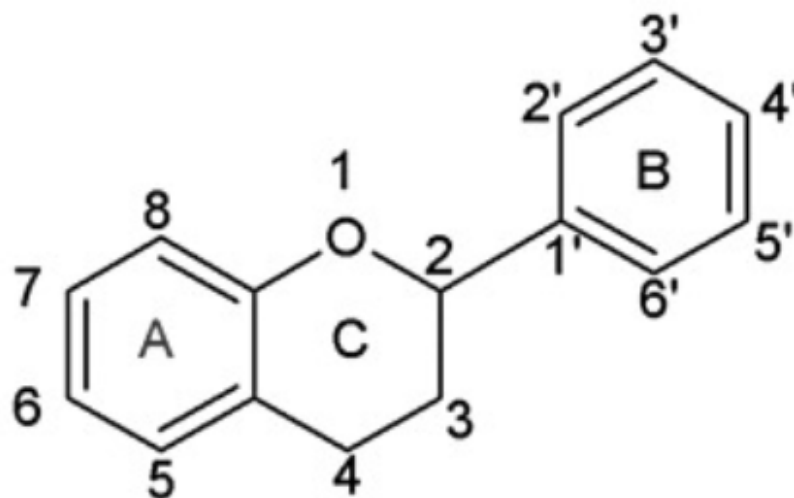
a) displays the various structures of cyclised monoterpenes, highlighting the variation that can be found within their branching/side groups.

b) presents the structures of a select few phenolic terpenes. Figure adapted from (Rao A. et al 2010)^[146] and (Cho K. et al 2017)^[144].

1.4.3 Flavonoids

With a backbone consisting of a 15-carbon structure organised into two benzene rings linked via a heterocyclic pyrane ring (see **Figure 1.4**), flavonoids are the major family of polyphenols, made up of many differing classes. These flavonoid classes are categorised based on their level of oxidation and substitution patterns of the C-ring (see **Figure 1.4**). Modifications of the A and B rings, however, define individual compounds within a class^[132, 138]. Again, a full list detailing the various classes can be seen in **Table 1.2**, but special attention is given to the following classes- the flavanones and flavanols.

Figure 1.4: Phytochemical class structure; the core flavonoid chemical structure.



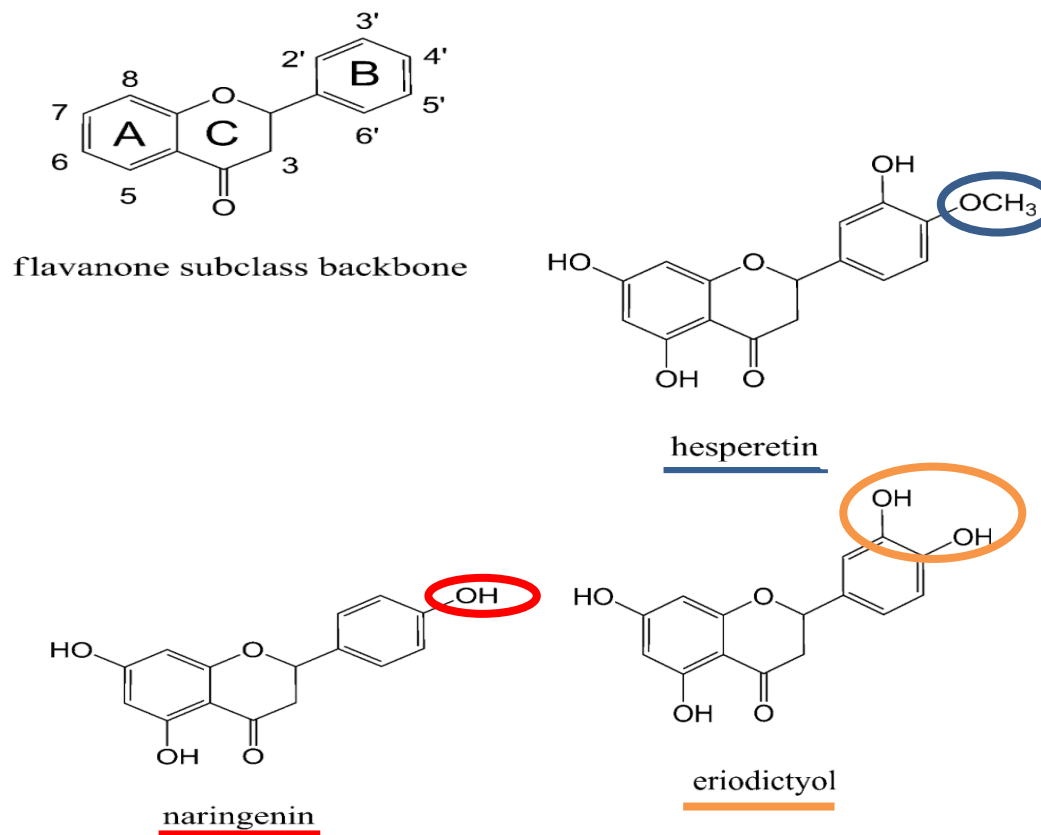
Displays a very basic overview of the polyphenolic backbone of flavonoid molecules. The C-ring, a pyrane ring, is formed during the conjugation of the A and B rings, and is formed from 5-carbon molecules as opposed to the other rings' 6-carbon structures. Figure adapted from **(Panche A.N. et al 2016)^[150]**.

1.4.4 Flavonoids; flavanones

The basic structure of flavanones can be seen in **Figure 1.5**; this flavonoid class is very common within citrus fruits, with different compounds being present in unique ratios within the fruit pulp, seeds and peel^[151]. Flavanones such as naringenin, eriodictyol and hesperetin are typically produced in their diglycosidic format, which increases the compounds solubility and bestows the characteristic taste of citrus fruits^[141, 152].

Flavanones (and flavones) lack a hydroxyl group at position 3 in their structures (see **Figure 1.5**) which reduces their antioxidant capacity, however the double bond present at the 2'-3' position makes the molecule a more reactive compound overall, potentially contributing to their antimicrobial efficacies^[152]. Naringenin, in addition to another flavanone sophoraflavanone G, have both been shown to exhibit antibacterial activity against MRSA strains, an intriguing characteristic; one which tempts further investigation^[141].

Figure 1.5: Phytochemical class structure; the flavanones.



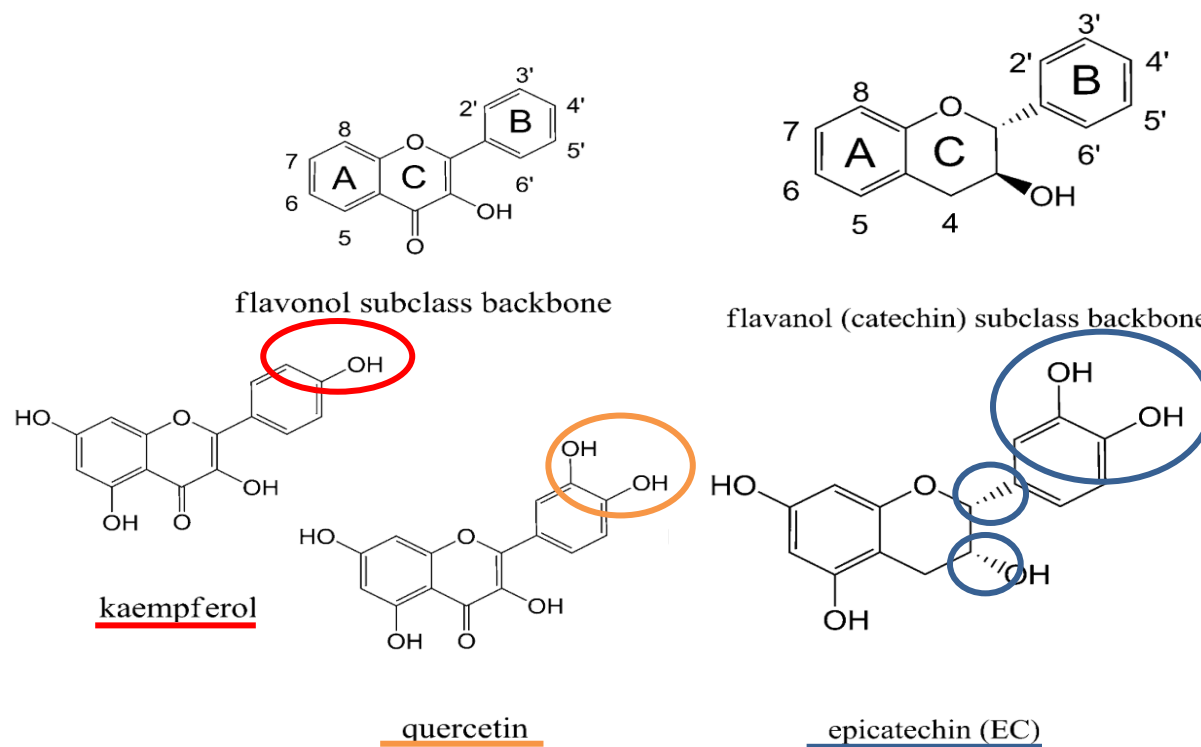
The general structure of flavanone molecules are shown on the top-left with the A, C and B rings annotated, and example molecules on the right and lower half of the Figure. The “trademark” groups (or lack thereof) for each molecule have been highlighted. Figure adapted from (Gorniak I. et al 2018)^[141].

1.4.5 Flavonoids; flavonols and flavanols

Flavonols (including the sub-category of molecules called flavanols, or alternatively “catechins”)^[141] are phenolic structures bearing a carbonyl group, with the addition of a 3-hydroxyl group^[143], such as can be seen in **Figure 1.6**. There is a fine line between a flavone and a flavanol; it is simply the extra hydroxyl group which distinguishes the two^[148].

Examples of flavonols include quercetin, kaempferol and for flavanols; all of the diverse epicatechin derivatives that can be found^[141].

Figure 1.6: Phytochemical class structure; the flavonols and flavanols.



The general structure of flavonol and flavanol molecules on the top-left and right with the A, C and B rings annotated. Example molecules are displayed on the lower half of the figure. The distinguishing groups (or lack thereof) for each molecule have been highlighted. Figure adapted from (Gorniak I. et al 2018)^[141].

1.5.0 Phytochemicals; known antimicrobial activities and MOA

The amphipathic attributes (the presence of both hydrophilic and hydrophobic moieties within the same molecule) of flavonoids play a key role in their antimicrobial properties. This is in addition to their anti-oxidative nature, potential to scavenge free radicals and chelate metal ions removing them from essential metallo-enzymes, bacterial metabolism inhibition, inhibition of nucleic acid synthesis and membrane disruption^[148, 153].

Phytochemicals have been intensely studied to understand their MOA's in respect to their antimicrobial activities, and many studies have highlighted evidence for the various mechanisms presently discussed.

1.5.1 Cellular membrane/wall disruption

Many studies have suggested cell membrane/wall disruption as the antimicrobial MOA of phytochemicals, particularly for catechin phytochemicals found in tea^[154]. Flavonoids, particularly flavonols and flavones, have had their antimicrobial activity attributed to their capacity to interact and complex with extracellular and soluble proteins, as well as being able to penetrate and complex with bacterial cell walls to disrupt their synthesis. This mechanism of antimicrobial attack overall disrupts the regular integrity of the cell membrane/wall, leading to lysis and cell death^[143, 155].

Phytochemicals have also been shown to perforate and decrease the fluidity of the cell membrane, complementing the compound interactions with ion channels that stud the bacterial cell surface; further disrupting the regular function of the cytoplasmic membrane^[142, 156]. As evidence for this MOA; using liposomal models to imitate the cellular membrane it has been shown that kaempferol interacts with the polar head groups of lipids and 6, 8-diprenyleriodictyol was found to inhibit and lyse *S. aureus* cultures via depolarization of the cellular membrane (as well as inhibiting DNA, RNA and protein synthesis)^[153]. Researchers have suggested that it is the presence of hydroxyl groups on the phenolic backbone that elicit these observed interactions and are responsible for this inhibitory MOA^[139]. Further evidence suggests that flavonoids interact with the lipid bilayer

by two mechanisms, depending on the flavonoid in question. Non-polar flavonoids insert into the hydrophobic interior of the membrane, disrupting its' stable function, and the more hydrophilic flavonoid compounds (such as kaempferol) tend to form hydrogen bonds with the polar head groups of the lipids, which also leads to structural and functional compromise^[141].

1.5.2 Binding and disruption of enzymatic activity

Another suggested MOA for the antimicrobial properties of phytochemicals is their interaction with key bacterial enzymes. Catechins have been observed to inhibit *S. aureus* glucosyltransferases *in vitro*^[143] and the underlying MOA is thought to be due to a phytochemicals capacity to form strong ligand complexes with the metal cations present in the catalytic sites of many essential enzymes. Phosphatases are a prime example of these metalloenzymes, and their disruption can lead to the metabolic collapse of bacterial cells^[142].

Researchers have suggested that the inhibitory MOA for galangin is the interaction and modification of the topoisomerase IV enzyme. 6, 8-diprenyleriodictyol behaves in a similar way to inhibit the synthesis of proteins, RNA and DNA synthesis in strains of *S. aureus* and another compound, jaceosidin, at as little as 100 μ M was also found to disrupt the activity of the *E. coli* enzyme FabI^[153]; an enzyme involved in the essential type 2 fatty acid metabolic synthesis pathway.

Further work with isoflavones and flavan-3-ols has implied that they bind and inhibit the topoisomerase IV as well as the dihydrofolate reductase enzymes. This further reinforces the importance of enzyme disruption as a MOA of phytochemical antimicrobial activity. Other studies have implied that phytochemicals may also interfere with the normal activity of NADH-cytochrome C reductase and the cell wall synthesis enzymes FabG, FabI and FabZ. Disruption of the Fab enzymes blocks the ligation of the D-ala-D-ala cell wall precursors, causing cell wall breaches and eventually cellular lysis due to osmotic pressure and leakage of cytoplasmic components^[157].

1.5.3 Efflux pump inactivation, potentiation capacity and significance

Another suggested phytochemical MOA is the inhibition of bacterial efflux pumps and ion channels; sensitive components that can represent targets for flavonoid interactions. Phytochemicals may interact with efflux pumps and porins to block their translocation cavities, preventing the ejection of substrates from the cell, or they may competitively inhibit the substrate binding domains of efflux pumps to achieve a similar effect^[142].

Phytochemical inhibition of efflux pumps represents two important roles; the first obviously being the inhibition of pumps to secrete products and generally the inhibition of regular bacterial homeostasis itself. The second, and arguably more interesting role, is the capacity for phytochemicals to potentiate (that is, to synergistically boost the efficacy of) presently used antimicrobials which have a reduced efficacy due to AMR. Many microorganisms nullify the effects of antibiotics, biocides and food antimicrobials by ejecting the compounds out of the cell before they can enact their inhibitory actions; if however an antimicrobial was given in conjunction with a phytochemical possessing known efflux pump inhibitive activity the pathogens AMR may be reduced to a level so that the antimicrobial regains its efficacy to a practically effective level. This holds significance for the pharmaceutical and food-processing industries as phytochemicals and essential oils, on the whole being designated as GRAS (generally recognised as safe) food additives^[129], may be easily incorporated into present food products or antimicrobial therapies.

Several phytochemicals have already had efflux pump inhibition described to them; chalcones for example have been shown to be active against MRSA via inhibition of their efflux pumps. Kaempferol (at a concentration of 31.25µg/ml) and genistein were both noted as efflux pump inhibitors of the NorA pump found in *S. aureus*. Baicalein can also reverse ciprofloxacin resistance in MRSA, and it has been suggested that this is due to inhibition of the NorA pump. Synthetic hybrid compounds such as naringenin-ethylidene-ciprofloxacin can also covalently bind to efflux pumps to overcome bacterial AMR^[153].

(Fujita M. et al 2005)^[158] used baicalein to restore the efficacy of tetracycline against *E. coli* strains, finding the compound inhibited the tetracycline efflux pump, TetK.

Epigallocatechin-3-gallate was also found to inhibit the same efflux pump; as well as the MexAB-OprM pump of *P. aeruginosa*^[141]. The isoflavone daidzein has been found to

potentiate the effects of carbenicillin and levofloxacin against the AcrAB-TolC RND efflux pump of *E. coli* and the MexAB-OprM efflux pump of *P. aeruginosa*.

1.5.4 Unresolved questions relating to phytochemicals' potential as antimicrobial substitutes.

Whilst phytochemicals have potential as antimicrobials, there are still many gaps in our present knowledge of phytochemicals and their antimicrobial activities. For example, what is their main MOA for bacterial inhibition, and does this change depending on the bacterial species and compound in question? As has been previously discussed, many studies have suggested different mechanisms and evidence for such, for a single compound, giving rise to confusion within the literature. A large knowledge gap remains in that few studies have combined the study of inhibitive action, MOA and the genetic basis of bacterial susceptibility to phytochemicals.

1.6.0 Organisms

This study focussed on four foodborne pathogens chosen as they are relevant to the industrial partner of this project, in addition to representing both Gram-positive and Gram-negative micro-organisms typically found within environments associated with food production.

1.6.1 *Listeria monocytogenes*

This Gram-positive, catalase-positive, facultative anaerobic bacillus is mainly transmitted to human hosts by ingestion of contaminated foodstuffs^[3, 5] due to its ubiquitous presence in the environment as a plant saprophyte, making it very likely to then be transferred to raw food materials. It is well-suited to survival in soil, food processing and storage environments, in addition to the cytosol of eukaryotic cells where it causes severe invasive disease (listeriosis)^[159, 160]. The adaptability of this pathogen makes it a real challenge in the food industry; *L. monocytogenes* is particularly an issue in chilled ready-to-eat products such as sliced meats and cheeses due to its' psychotropic growth range (minimum growth

temperature recorded at -0.4°C)^[161], where it is also motile with peritrichous flagella, allowing it to multiply within refrigerators and cold-rooms to infectious doses^[3, 162].

L. monocytogenes ability to grow in biofilms is also a major issue for the food processing industry, where the micro-organism can effectively hide from cleaning regimes in harbourage sites that protect the biofilm such as inappropriately designed equipment/premises and damaged materials. Pockets of recurring *L. monocytogenes* can still be found in these sites despite routine cleaning and disinfection, allowing for re-contamination of foodstuffs^[163, 164]. (Pan Y. et al 2006)^[165] found that after exposing an *L. monocytogenes* food-processing model, where biofilms were grown on stainless steel and Teflon “coupons”, to simulated processing regimes the bacteria eventually adapted to the stressed conditions and proliferated within biofilms. Cells which were removed from the biofilms were again sensitive to the peroxide sanitiser used, suggesting that the resistance of the species to the sanitizing regimes may be due to the extracellular, polymeric components of the biofilm and not an innate mechanism of the cells themselves^[165]. This study highlights the importance of *L. monocytogenes* biofilm formation in the contamination of food-processing environments, and also helps explain why individual food-processing plants may harbour established and persisting strains despite the best efforts to eradicate them, sometimes for years^[160, 164].

1.6.2 *Pseudomonas aeruginosa*

P. aeruginosa is a flagellated Gram-negative, facultative anaerobic mesophile able to survive in a range of environments due to its large coding capacity that allows for an enhanced metabolic adaptability^[166-169]. It has a ubiquitous habitat, being found in water, soil, flora, fauna including humans, and is an opportunistic pathogen commonly causing respiratory disease in nosocomial settings with cystic fibrosis patients, the immunocompromised and in burn victims where its potent biofilm capacity allows it to form persistent infections^[166]. Due to its far-reaching presence in nature, it has also been known as a causative agent of foodborne disease, albeit less commonly than other bacterial pathogens^[170, 171].

Pseudomonas hardy nature is aided by its minimal nutritional requirements and its innate AMR to many antimicrobial compounds^[167]. *P. aeruginosa* is notorious for its wide range of

AMR and isolates are commonly resistant to: ciprofloxacin, novobiocin, tetracycline, β -lactams and chloramphenicol^[166, 172, 173].

Arguably the largest contributor to *P. aeruginosa* AMR is the intrinsic lack of permeability in the cellular outer membrane. The permeability of the *P. aeruginosa* outer membrane is approximately 12-100-fold lower than that of *E. coli*, making it more difficult for antibiotics such as quinolones and β -lactams to penetrate the cell to enact their antimicrobial effect. The outer membrane of many Gram-negative bacterial species is studded with numerous outer membrane pores (Opr), proteins that facilitate or retard the passage of molecules across the membrane and *P. aeruginosa* is no different. However, the main non-specific porin of *P. aeruginosa* is OprF which has a high permeability for nutrients and saccharides, but not for most antibiotics. Many *P. aeruginosa* Oprs are at any one time in a closed state, and often associated with efflux pump systems when they are open. This opportunistic pathogen encodes 12 RND family efflux pumps, four of which contribute to *P. aeruginosa*'s AMR. One of these four systems is made up by the efflux pump proteins MexA and MexB, in conjunction with OprM, that pumps β -lactam and quinolone antibiotics out of the bacterial cell before their critical threshold concentration can be reached. MexXY, in combination again with OprM, is another efflux pump system that has a high affinity for aminoglycosides. Efflux pumps and the intrinsically restricted nature of the *P. aeruginosa* outer membrane contribute greatly to the AMR of this micro-organism, and reinforcing this is the fact that many clinical isolates of *P. aeruginosa* overexpress the organism's native efflux pumps^[166].

P. aeruginosa potent biofilm capabilities also contribute strongly to the micro-organisms AMR, as well as the tough persistence of *P. aeruginosa* in pulmonary, urinary or burn infections and contaminations^[174]. Cells of this species ensconced in a biofilm, formed mainly of secreted alginate and extracellular polysaccharide, can persist for an extended period due to the mechanical, immunological and antimicrobial protection that the extracellular matrix confers. Inorganic components such as kaolin and calcium carbonate contribute to the biocidal resistance of biofilm-associated *P. aeruginosa*. Bacterial cells are also protected from dehydration and nutrient-starvation as the biofilm matrix has a large hydration sphere that can retain water (and with it, nutrients) multiple times its own mass. *P. aeruginosa* biofilm capabilities place it as a major cause of biofilm infections, infections that are steadily becoming more tolerant to antibiotic treatment^[174-176].

These factors all together make *P. aeruginosa* a difficult organism to deal with in infections and also within food^[177-179], and the food processing industry, as biofilm-associated cells persist on processing equipment and processing plant environments. Studies have found that *Pseudomonas* species are some of the most common, psychrotrophic spoilage microorganisms in aerobically-stored foods with high water content and natural pH^[177]. As such, *Pseudomonas* species including *P. aeruginosa* are commonly detected within dairy-processing environments and can persist in and on equipment, milking lines and storage tanks even after cleaning-in-place practices have been applied. From here, *Pseudomonas* can cause spoilage of pasteurised milk during cold storage^[180]. Fish meat is also vulnerable to *Pseudomonas aeruginosa* contamination^[181, 182] causing devastating financial consequences with productivity, economic losses and risks to human health^[183] including gastroenteritis^[181, 182] if the contamination is not detected before shipment of products to the public^[184, 185].

1.6.3 *Salmonella enterica* serovar Typhimurium

S. enterica is a flagellated Gram-negative, non-spore forming facultative anaerobic bacilli; many strains of which can ferment lactose, producing hydrogen sulphite and the enzyme catalase^[14, 186]. While there are only two species in the *Salmonella* genus, *Salmonella enterica* (hence simply referred to as “*Salmonella*”) is comprised of six subspecies with a plethora of serovars.

Salmonella strains can display resistance to many drugs, including aminoglycosides, quinolones, β -lactams, chloramphenicol, folate pathway inhibitors, streptomycin and tetracycline and trimethoprim^[187-189]. Bolstering *Salmonella* AMR is its strong ability to form biofilms, mainly comprised of cellulose, curli and thin aggregative fimbriae; it was one of the first foodborne pathogens to be reported to form biofilms in environments associated with the food industry^[190]. *Salmonella* is a cause for concern in the meat industry, particularly beef (due to the shorter cooking times that steaks and burgers are generally subjected to) and pork products where it can easily result in human infection, and in seafood processing^[191, 192]. Biofilm formation on processing equipment poses a risk of contaminating the foodstuffs being prepared/processed, and their persistence can be a tough issue to solve. One study (**Corcoran M. et al 2014**)^[193] found that from a range of

tested cleaning agents commonly used in the food industry, none fully eradicated a mature *Salmonella* biofilm even after 90 minutes of contact time. (Corcoran M. et al 2014)^[193] concluded that “the difficulty of eradication of established *Salmonella* biofilms serves to emphasize the priority of preventing access of *Salmonella* to post-cook areas of food production facilities”. *Salmonella*' persistence when growing in a biofilm is made more serious as this organism can readily attach and form biofilms to materials commonly used in the food processing industry: stainless steel, glass, polyurethane, Teflon, wood and rubber^[192]. (Stepanovic S. et al 2004)^[194] found that a growth medium made to imitate the nutrient-levels encountered in food industry environments (i.e.; nutrient limited) encouraged the growth of *Salmonella* in biofilms.

1.6.4 *Staphylococcus aureus*

S. aureus is a Gram-positive, immobile mesophile typically growing as clusters of facultative anaerobic cocci; it can be distinguished from other *Staphylococcus* species based on the gold pigmentation of its colonies when grown on specific selective media^[195-197]. While usually a commensal organism on the skin and mucosa, particularly that of the nasal passages, *S. aureus* can behave as an opportunistic pathogen due to the wide variety of excreted proteins and toxins that it may produce. The evolutionary purpose of these secreted toxins is thought to be for the conversion of host tissues into accessible nutrients for bacterial growth; some examples include the *staphylococcal* enterotoxins (SEA, SEB etc.) and the exfoliative toxins ETA and ETB. *S. aureus* has long been associated with food poisoning in the form of a self-limiting gastroenteritis, called *staphylococcal* food poisoning, characterised by vomiting with or without diarrhoea. *Staphylococcal* food poisoning is often caused by the ingestion of pre-formed enterotoxins produced by *S. aureus* contaminating foodstuffs and while sufficient cooking can eliminate the bacterium, the enterotoxins are thermally stable and left intact to enact their cytotoxic effects on the gastrointestinal system when ingested^[198].

Compounding the pathogenicity of this organism, *S. aureus* strains have been found with resistances to numerous antibiotics; possibly the most infamous being that of MRSA. Resistance to β -lactam antibiotics was first discovered in the mid-1940s (not long after the discovery of penicillin itself), mediated by a plasmid-encoded penicillinase that hydrolyses the β -lactam ring of the antibiotic. Another method of methicillin resistance in *S. aureus* is

the encoding and expression of *fmtA*, a PBP with a low affinity for methicillin, rendering the antibiotic ineffective against selected strains. The first report of a specifically methicillin-resistant *S. aureus* strain was in 1961; highlighting again the fact that AMR is not a novel phenomenon, however this organism is gathering resistances to more antibiotics as time passes^[199, 200].

S. aureus is also capable of producing and multiplying within biofilms on both biotic and abiotic surfaces; a severe issue for medical devices implanted into the body, disrupted tissues such as burns, lacerations, and food processing equipment^[201]. As this microorganism is very adaptable to a range of environments, it is capable of attaching to contact surfaces and/or food products themselves. Even the smallest residues of organic matter, if left on improperly washed equipment, can act as nuclei for attachment and persistent biofilm formation; this is of course a serious hygienic risk that can lead to economic losses thanks to spoilage of the contaminated foodstuff^[16, 192]. Studies have tested the biofilm-forming capacity of *S. aureus* strains under conditions relevant for the food-processing industry. **(Rode T.M. et al 2007)**^[16] found that a combination of sodium chloride and glucose enhanced biofilm formation and that suboptimal growth temperatures also encouraged biofilm formation. This is concerning, for example, in the meat processing industry where sodium chloride is commonly used as an antimicrobial hurdle, glucose and other sugars may be used to kick-start fermentable starter cultures or to balance flavours and many meat processing plants are cooled to fairly low temperatures to reduce the rate of organoleptic decay of their raw materials^[16]. *S. aureus* biofilms growing on food processing equipment are also up to 100-fold more tolerant of cleaning disinfectants than their planktonic counterparts, making *S. aureus* contamination that much more difficult to eradicate in the food processing industry^[202].

1.7.0 Project aims

- To assemble and screen a phytochemical panel, to identify and compare antimicrobial activity on a standardised baseline.
- To study the MOA and potential for resistance development for selected phytochemical compounds,
- To test the efficacy of chosen phytochemicals within an *in situ* experimental model system.

Chapter 2: Materials & methods

“Man is a tool-using animal. Without tools he is nothing, with tools he is all.”- Thomas Carlyle, *Sartor Resartus*,
Bk.1, Ch.5, 1834

2.1.1 Bacterial strains

Four foodborne pathogens were selected for study in this project. These were chosen as priority organisms for food safety and spoilage relevant to the industrial partner, and to represent Gram-positive and Gram-negative species. These species were *L. monocytogenes*, *S. aureus*, *P. aeruginosa* and *S. enterica* Typhimurium (*S. enterica*). The full details of all bacterial strains used in this body of work are displayed in **Table 2.1**.

Table 2.1: Bacterial strains used within this thesis.

Bacterial strain	Laboratory reference number	Notes	Source
<i>S. enterica</i> serovar Typhimurium	14028S	Commonly used reference strain	Webber group
<i>S. aureus</i>	NCTC 8532	Commonly used reference strain	Webber group
<i>P. aeruginosa</i>	PA14	Commonly used reference strain	Webber group
<i>L. monocytogenes</i>	LM014, ATCC43256	Commonly used reference strain, originally isolated from soft cheese	Narbad group
<i>S. enterica</i> serovar Typhimurium TraDIS-Xpress Library	14028S: <i>lacI</i>	Created within Webber group by Dr. Emma Holden ^[203]	Webber group

Strain, laboratory reference number and brief details surrounding the food pathogens utilised in this thesis.

2.1.2 Phenotypic identification of strains

Strains were plated for single colonies and visually checked for morphologies typical of the expected species. If multiple or unexpected morphologies were present, strains were plated on selective media (high sodium chloride Luria-Bertani, LB, agar for *S. aureus*, XLD agar for *S. enterica* etc.) and single colonies were picked, cultured (as described in **Section 2.1.4**) and re-plated until a uniform colony morphology was achieved. Sequencing was performed to confirm the presence of the expected species in severe cases of doubt.

2.1.3 Storage of strains

Bacterial cryo-bead stocks were made by immersing Protect Micro-organism Preservation System ceramic cryo-beads (Technical Service Consultants Ltd., Heywood, UK) in 1ml of overnight culture (prepared as described in **Section 2.1.4**) and inverting the tube 2-5 times before pipetting off the liquid culture. Cryo-bead stocks were then stored in a freezer box in a freezer (Liebherr MedLine, Oxon, UK) at -20°C ($\pm 1^\circ\text{C}$). This was performed either under a lit R&L Enterprises 13mm natural gas Bunsen burner (Fisher Scientific, Leicestershire, UK) or using a BioMAT2-S2 Class II microbiological safety cabinet (Contained Air Solutions, Manchester, UK).

Alternatively, long-term bacterial stocks were made by resuspending 1ml of centrifuged overnight culture in 40% glycerol, stored in a New Brunswick Ultra-Low Temperature U725-G Innova freezer (Eppendorf, Hamburg, Germany) at -80°C ($\pm 1^\circ\text{C}$).

2.1.4 Broth cultures

In all cases and experiments requiring liquid broth cultures; using a sterile, 10 μl inoculation loop (ThermoFisher-Scientific, Cambridge, UK) one bead from the bacterial cryo-bead stocks, or scoop from the glycerol stocks (prepared as described in **Section 2.1.3**), was used to inoculate 5ml of sterile growth medium contained within a glass universal. This was performed under sterile conditions within a Class II microbiological safety cabinet, or under a lit Bunsen burner. The inoculated broth was then incubated aerobically at 37°C ($\pm 1^\circ\text{C}$), for 16 hours, in an Innova 4400 brand incubator shaker (New Brunswick Scientific,

St. Albans, UK) set at ~200rpm. *S. enterica*, *S. aureus* and *P. aeruginosa* strains were inoculated into LB broth (Fisher Scientific BioReagents, Loughborough, UK), while *L. monocytogenes* strains were instead grown at 37°C (±1°C), ~200rpm in Brain-Heart Infusion (BHI) Broth (Oxoid, Basingstoke, UK).

2.1.5 Preparation/standardisation of inocula

In experiments where a standardised inoculum was required bacterial cultures (produced as described in **Section 2.1.4**) were adjusted via optical density measurements at a wavelength of 600nm ($OD_{(600nm)}$). Using a suitable pipette (Gilson, Middleton, USA) within a Class II microbiological safety cabinet or under a lit Bunsen burner, 100µl of the bacterial culture was diluted with 900µl of PBS (Sigma-Aldrich, Gillingham, UK) in a semi-micro acrylic 1.6ml cuvette (Sarstedt Ltd., Leicester, UK) and the $OD_{(600nm)}$ was measured using a Jenway 7200 Visible Spectrophotometer (Cole-Parmer, Stone, UK). Multiplying the measured value by a factor of 10, we received the $OD_{(600nm)}$ of the undiluted bacterial culture. Using this as the *C1* value in the following formula an $OD_{(600nm)}$ -adjusted inoculum could be created by diluting an aliquot (*V1*) of the undiluted bacterial culture in a total volume of dilutant (*V2*).

$$C1 \times V1 = C2 \times V2$$
$$V1 = \frac{C2 \times V2}{C1}$$

Due to health and safety protocols concerning the handling of *L. monocytogenes* for the purposes of measuring the $OD_{(600nm)}$, bacterial cultures of this organism were instead diluted (20µl in 180µl) in the wells of a Greiner 96-well polypropylene microtitre plate (Sigma-Aldrich, Gillingham, UK), sealed using an optically clear adhesive seal sheet (ThermoFisher Scientific, Cambridge, UK) and the $OD_{(600nm)}$ measured using a FLUOstar Omega plate reader (BMG Labtech, Bucks, UK).

Typically, all $OD_{(600nm)}$ -adjusted inocula were contained in 15ml or 50ml Corning centrifuge tubes (Sigma-Aldrich, Gillingham, UK) and stored at approximately 4°C on ice until use.

2.1.6 Viable counts

All work was carried out under sterile conditions within a Class II microbiological safety cabinet, or under a lit Bunsen burner.

Viable counts of bacterial populations were utilised for multiple purposes within this body of work. Firstly, to determine the cell densities of OD_(600nm)-adjusted inocula, where the inoculum was serially diluted (100µl of the inoculum for the first dilution and 100µl of each previous dilution for subsequent dilutions in the series within 900µl of sterile PBS contained in 1ml microtubes (Axygen, Gillingham, UK), using a sterile TipOne pipette tip (Starlabs Ltd., Milton Keynes, UK) and thoroughly mixing via inversion for each dilution. After this, 100µl from each of the dilution series were pipetted in triplicate and spread using an L-shaped sterile spreader (Starlabs Ltd., Milton Keynes, UK) onto species-appropriate growth medium agar (LB agar for *S. enterica*, *S. aureus* and *P. aeruginosa* strains, BHI agar for *L. monocytogenes*) contained in circular, triple-vent petri dishes (ThermoFisher Scientific, Cambridge, UK). The agar plates were then placed upside down in an EN120 static incubator (Nüve, Ankara, Turkey) set at 37°C (±1°C) for an overnight incubation (~16 hours) before enumeration, and calculation, of the cell densities in colony forming units (CFU) of the original OD_(600nm)-adjusted inocula.

Secondly, viable counts were used as a quantifiable measure of bacterial growth after phytochemical exposure (please see **Section 2.4.0** for full experimental details). For these experiments 20µl aliquots of the sample cultures were taken at appropriate time points and, using a pipette with sterile unfiltered tips, serially diluted down the columns of a 96-well microtitre plate pre-filled with 180µl of sterile PBS. Then, using an mLINE multichannel pipette (Sartorius AG, Göttingen, Germany), 5µl samples of the serial dilutions were pipetted starting from the highest dilution onto species-appropriate growth medium agar (LB agar for *S. enterica*, *S. aureus* and *P. aeruginosa* strains, BHI agar for *L. monocytogenes*) contained in three square petri dishes (ThermoFisher Scientific, Cambridge, UK) for technical replicates and left for a minimum of 10 minutes to dry. When there were too many sample conditions to fit onto a single square petri dish using the multichannel pipette, additional petri dishes were also used to accommodate the additional samples. The agar plates were then placed upside down in a static incubator set at 37°C (±1°C) for an overnight incubation (~16 hours) before enumeration and calculation

of the CFU of the sample cultures over time as an indicator of the growth of the sample cultures.

2.2.0 Chemicals

All chemical reagents and tested phytochemicals with their uses, storage conditions and sources are listed in the following section.

2.2.1 Sourcing of phytochemicals

The majority of phytochemicals were initially selected from a library of compounds, aided by Dr. Paul Kroon (Quadram Institute, Norwich) who advised on assembly of the panel. Only one polyphenol mixture, the Prosur NATPRE T-10+ mix, was sourced from this projects Nestlé industrial supervisor. **Table 2.2** displays the full list of phytochemicals used.

Table 2.2: Summary of phytochemicals utilised within this thesis.

Phytochemical	Classification/sub family	Synonym	Source	Storage
Caffeic acid	Phenolic acids, hydroxycinnamic acids	3, 4-dihydroxycinnamic Acid	Merck, Gillingham, UK	Room temperature
Cinnamic acid	Phenolic acids, hydroxycinnamic acids	<i>Trans</i> -cinnamic acid	Merck, Gillingham, UK	Room temperature
Eriodictyol	Flavonoids, flavanones	5, 7, 3', 4'-tetrahydroxyflavanone	Extrasynthese, Genay, France	4°C
Ferulic acid	Phenolic acids, hydroxycinnamic acids	3-methoxy-4-hydroxycinnamic acid	Merck, Gillingham, UK	Room temperature
Hesperidin	Flavonoids, flavanones	Hesperetin 7-O-rutinoside	Merck, Gillingham, UK	4°C
Kaempferol	Flavonoids, flavonols	3, 5, 7, 4'-tetrahydroxyflavone	Merck, Gillingham, UK	4°C
Naringenin	Flavonoids, flavanones	5, 7, 4'-trihydroxyflavanone	Merck, Gillingham, UK	4°C
Naringin	Flavonoids, flavanones	Naringenin 7-O-neohesperidoside	Merck, Gillingham, UK	4°C
Prosur NATPRE T-10+	Commercial polyphenol mixture	N/A	Prosur, provided by Nestlé	Room temperature, away from direct light within a Duran bottle sealed with parafilm
Quercetin	Flavonoids, flavonols	3, 5, 7, 3', 4'-pentahydroxyflavone	Merck, Gillingham, UK	4°C
Rutin	Flavonoids, flavonols	Quercetin-3 β -D-rutinoside	Merck, Gillingham, UK	4°C
Thymol	Terpenes, phenolic terpenes	6-isopropyl-3-methylphenol	Merck, Gillingham, UK	Room temperature
Vanillic acid	Phenolic acids, hydroxybenzoic acids	4-hydroxy-3-methoxybenzoic Acid	Merck, Gillingham, UK	Room temperature
Vanillin	Hydroxybenzaldehydes	4-hydroxy-3-methoxy-benzoic aldehyde	Merck, Gillingham, UK	Room temperature

Phytochemicals listed with chemical classification, synonym, purchasing source and storage conditions utilised within this thesis.

2.2.2 Solubilisation and storage of phytochemical stock solutions

All phytochemical powders/crystals described in **Section 2.2.1** were dissolved at room temperature in 100% DMSO (Sigma-Aldrich, Gillingham, UK), vortexed and stored at 4°C. Phytochemical master stocks were made at 5mg/ml or 50mg/ml concentrations, depending on the experiment performed, and thawed on the day of use within a static incubator set at 27°C ($\pm 1^\circ\text{C}$). Phytochemical master stocks were made fresh at least once a month. All work was carried out under sterile conditions within a Class II microbiological safety cabinet, or under a lit Bunsen burner.

2.2.3 Sourcing, solubilisation and storage of chemicals and reagents

Table 2.3 displays the various chemicals and reagents used throughout this body of work. All sources, solubilisation methods and storage procedures for each individual chemical reagent are included.

Table 2.3: Summary of chemicals and reagents utilised within this thesis.

Chemical/reagent	Use	Source	Solubilisation	Storage
Dimethyl sulfoxide	To solubilise phytochemical compounds	Merck, Gillingham, UK	Liquid solvent itself	Room temperature
Phenyl-arginine β-naphthylamide (PAβN)	Known efflux pump inhibitor (EPI)	Merck, Gillingham, UK	Powder, dissolved in PBS	-20°C
Carbonyl cyanide 3-chlorophenylhydrazone (CCCP)	Known efflux pump inhibitor (EPI)	Merck, Gillingham, UK	Powder, dissolved in PBS	-20°C
Phosphate buffered saline (PBS)	To solubilise reagents, dilute bacterial cultures and act as a negative control	Merck, Gillingham, UK	Tablet, dissolved in sterile H ₂ O	Room temperature
Bioguard disinfectant	Disinfection agent used to clean work surfaces/spillages	Biochem, Northampton, UK	Purchased as liquid	Room temperature
Ethanol, 100%	Multiple uses; disinfection, use as a negative control, solubilising other reagents	VWR Chemicals, Lutterworth, UK	Liquid solvent itself	Room temperature
Resazurin	Fluorescent drug accumulation assay indicator	Merck, Gillingham, UK	Powder, dissolved in water	-20°C
Ethidium bromide (EtBr)	Fluorescent drug accumulation assay indicator	Merck, Gillingham, UK	Powder, dissolved in water	-20°C
Tetracycline	Antibiotic	Merck, Gillingham, UK	Powder, dissolved in water	4°C
Chloramphenicol	Antibiotic	Merck, Gillingham, UK	Powder, dissolved in 70% Ethanol	4°C

Kanamycin monosulphate	Antibiotic	Merck, Gillingham, UK	Powder, dissolved in water	4°C
Ampicillin trihydrate	Antibiotic	Merck, Gillingham, UK	Powder, dissolved in water	4°C
Piperacillin sodium salt	Antibiotic	Merck, Gillingham, UK	Powder, dissolved in water	4°C
Nalidixic acid	Antibiotic	Merck, Gillingham, UK	Powder, dissolved in 70% ethanol	4°C
Ciprofloxacin	Antibiotic	Merck, Gillingham, UK	Powder, dissolved in 70% ethanol	4°C
Congo red	Biofilm stain	Merck, Gillingham, UK	Powder, dissolved in water	4°C
Crystal violet	Biofilm stain	Merck, Gillingham, UK	Powder, dissolved in	4°C
25% Glutaraldehyde	TEM fixate	Agar Scientific, Stansted, UK	Liquid solvent itself	4°C
Sodium cacodylate	TEM fixate	Agar Scientific, Stansted, UK	25% Glutaraldehyde and H ₂ O	4°C
Tris-EDTA	DNA extraction buffer	Merck, Gillingham, UK	Liquid solvent itself	Room temperature
Lysozyme, 50mg/ml	Enzyme to lyse cells for DNA extraction	Merck, Gillingham, UK	Tris-EDTA Buffer	-20°C
RNAse A, 20mg/ml	Enzyme used to degrade RNA in DNA extraction	Merck, Gillingham, UK	Tris-EDTA Buffer	4°C
SDS	Reagent to lyse cells for DNA extraction	Merck, Gillingham, UK	Liquid solvent itself	Room temperature
Proteinase K, 50mg/ml	Enzyme to degrade proteins for DNA extraction	Merck, Gillingham, UK	Tris-EDTA Buffer	-20°C
KAPA SPRI Beads	Used to extract/concentrate DNA samples	Roche Diagnostics Ltd., Pleasanton, USA	Pre-suspended	4°C
Tris-Cl	DNA elution buffer	Merck, Gillingham, UK	Liquid solvent itself	Room temperature

Qubit ds DNA HS reagent	Qubit DNA quantification buffer component	Invitrogen, Thermo Fisher Scientific, Loughborough, UK	Liquid solvent itself	4°C
Quanti-iT dsDNA HS buffer	Qubit DNA quantification buffer component	Invitrogen, Thermo Fisher Scientific, Loughborough, UK	Liquid solvent itself	4°C
Qubit DNA HS 10ng/μl and 0ng/μl standards	Qubit DNA standards for DNA quantification	Invitrogen, Thermo Fisher Scientific, Loughborough, UK	Purchased as liquid, in TE buffer	4°C

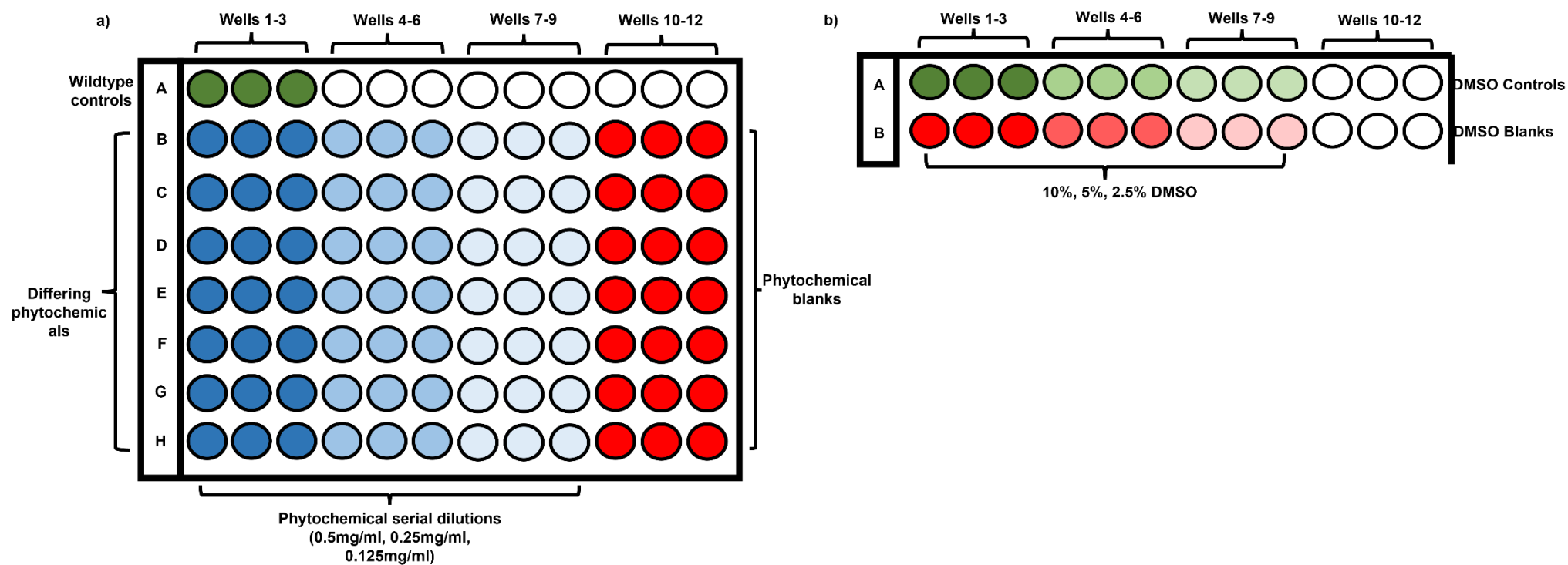
Chemicals and reagents listed with usage, purchasing source, solubilisation and storage conditions utilised within this thesis.

2.3.0 Semi-high-throughput phytochemical activity screening assays

A semi-high throughput phytochemical screening assay was designed to screen a range of phytochemicals and to identify potentially bioactive compounds for further, more quantitative, experimentation. All work was carried out under sterile conditions within a Class II microbiological safety cabinet, or under a lit Bunsen burner. Experiments were performed with three technical replicates per sample, for four biological replicates altogether.

An overnight bacterial culture of the selected micro-organism (*S. enterica*, *S. aureus*, *P. aeruginosa*, *L. monocytogenes*) was set up as described in **Section 2.1.4**. The day after the overnight incubation, four 96-well microtitre plates were filled using a suitable pipette and tips with 100µl x2-concentration growth medium (LB for *S. enterica*, *S. aureus*, *P. aeruginosa*, BHI for *L. monocytogenes*). Using 1mg/ml phytochemical working stocks (prepared by combining 2ml of the 5mg/ml phytochemical master stocks, see **Section 2.2.2**, with 8ml of sterile ultra-pure H₂O), 100µl was pipetted into the first three wells of a row, as well as the last three (wells 1-3, and 10-12). Then, 100µl was serially diluted in triplicate through wells 1-3 to wells 7-9 to produce a phytochemical concentration range of 0.5mg/ml, 0.25mg/ml and 0.125mg/ml across each row of the 96-well microtitre plates (see **Figure 2.1** for a pictorial representation of the 96-well microtitre plates layout).

Figure 2.1: The semi-high throughput screening assay's 96-well microtitre plate layout.



Layout of the semi-high throughput screening assays 96-well microtitre plates. Panel **a)** depicts the layout for phytochemical samples and blanks. **b)** depicts the layout for solvent vehicle (DMSO) controls and blanks due to a lack of room for all replicates on the first plate.

From wells 7-12, 100µl was removed so that the total volume in each well was 100µl. To account for and compare the various concentrations of DMSO (10%, 5% and 2.5%) which would be present in the serially diluted phytochemical samples, a separate 96-well microtitre plate was used to set up two rows using a 20% DMSO stock and the serial dilution method across wells 1-3 to wells 7-9 described above in this present section. Wildtype controls were produced by mixing 100µl of x2-concentration growth medium with 100µl of sterile, ultra-pure H₂O. From this point, the steps for the semi-high throughput inhibitive screening assays (using two 96-well microtitre plates) and potentiative screening assays (using two 96-well microtitre plates) differ and are described separately in the following **Sections 2.3.1** and **2.3.2**.

2.3.1 Growth inhibition assays

To identify growth inhibition, the plate set up described above was used (**Section 2.3.0**). A StarTub reagent reservoir (Starlabs Ltd., Milton Keynes, UK) and multichannel pipette was used to add 50µl of sterile H₂O to every well of two 96-well microtitre plates. Using the method described in **Section 2.1.5**, an OD_(600nm)-adjusted inoculum was prepared to an OD_(600nm) of 0.01 (~10⁷ CFU/ml, for ~10⁵ CFU/well) with sterile growth medium and kept at 4°C on ice until required. To each well (barring 10-12 which acted as the blank conditions for each corresponding inoculated sample) 50µl of the OD_(600nm)-adjusted inoculum was added. To maintain an equal volume in all wells 50µl of sterile, ultra-pure H₂O was then added to the blank conditions, including the DMSO blank controls row (see **Figure 2.1** of **Section 2.3.0**). The total volume in each well was thus 200µl.

The 96-well microtitre plates were then sealed with a paper, gas-permeable seal sheet (ThermoFisher Scientific, Cambridge, UK), and placed inside a static incubator set at 37°C (±1°C) for an overnight incubation of 16 hours. The morning after, the gas-permeable seal was replaced with a transparent adhesive seal and the OD_(600nm) of the cultures was measured using a FLUOstar Omega plate reader. By comparing the OD_(600nm) measurements of the DMSO controls to their respective phytochemical concentration samples, the inhibitive effect of the phytochemical compounds against the microbial growth of the tested micro-organisms could be determined and disentangled from the effect of their carrying solvent. Statistical analysis via a 1-way repeated measures ANOVA test, with the inclusion of Fisher's least significant differences (LSD) test was performed

using the GraphPad software package version 8.0 to distinguish statistically significant results.

2.3.2 Antimicrobial potentiation assays

Following the plate setup with phytochemicals (**Section 2.3.0**) a positive control was added in triplicate using wells A4-6 of the potentiative assay 96-well microtitre plates, with the addition of 50µl of a 1.024mg/ml working stock of Phenyl-Arginine β-naphthylamide (PAβN), a known efflux pump inhibitor. Afterwards, 50µl of a chloramphenicol solution (8µg/ml working stock concentration, for a 2µg/ml final concentration) was added to every well of two 96-well microtitre plates. Using the method described in **Section 2.1.5**, an OD_(600nm)-adjusted inoculum was prepared to an OD_(600nm) of 0.01 (~10⁷ CFU/ml, for ~10⁵ CFU/well) with sterile growth medium, and kept at 4°C on ice until required. To each well, barring wells 10-12 which acted as the blank conditions for each corresponding inoculated sample, 50µl of the OD_(600nm)-adjusted inoculum was added utilising a sterile reagent reservoir and a multichannel pipette. To maintain an equal volume in all wells 50µl of sterile, ultra-pure H₂O was then added to the blank conditions. The total volume in each well was 200µl.

The 96-well microtitre plates were then sealed with a gas-permeable seal and placed inside a static incubator set at 37°C (±1°C) for an overnight incubation of 16 hours. The morning after, the gas-permeable seal was replaced with a transparent adhesive seal and the OD_(600nm) of the cultures was measured using the FLUOstar Omega plate reader. By comparing the OD_(600nm) measurements of the DMSO controls to their respective phytochemical-concentration samples, the potentiative effect of the tested phytochemical compounds to synergise and enable the antimicrobial effect of the sub-lethal chloramphenicol concentration could be determined and disentangled from the effect of their carrying solvent. Statistical analysis via a 1-way repeated measures ANOVA test, with the inclusion of Fisher's LSD test was performed using the GraphPad software package version 8.0 to distinguish statistically significant results.

2.4.0 Growth curves after phytochemical exposure

To identify the impact of phytochemicals on bacterial viability over time, CFU measures were made to generate growth curves. This was used for a selection of compounds after the semi-high throughput inhibition assays (**Sections 2.3.0-2.3.2**). Measuring the viability of the challenged micro-organisms is more labour intensive but provides a more detailed observation of the dynamics of phytochemical interaction, allowing for bacteriostatic vs bactericidal activity to be identified over time. Experiments were performed with three technical replicates per sample, for three biological replicates altogether.

Overnight bacterial cultures were set up in triplicate as described in **Section 2.1.4**. On the same day, using a sterile reagent reservoir and multichannel pipette, six 96-well microtitre plates were filled with 180µl sterile PBS per well, sealed with a transparent adhesive seal and placed into a fridge at 4°C until required for serial dilutions. The day after, x12 glass universals containing 5ml of growth medium suitable for the tested micro-organism (LB for *S. enterica*, *S. aureus*, *P. aeruginosa* and BHI for *L. monocytogenes*) were set up, and using a suitable pipette and sterile tips, 0.3ml of growth medium was removed from each of the vessels. To one glass universal 50µl of 100% DMSO (for a final DMSO concentration of 1%) was added to form the solvent vehicle control sample, while 50µl of sterile PBS was added to two glass universals to form the negative and wildtype control samples. To three of the remaining nine glass universals, 50µl of a 50mg/ml phytochemical master stock (prepared as described in **Section 2.2.2**) was added for a final phytochemical concentration of 0.5mg/ml; in this way three phytochemicals could be tested with triplicate biological replicates against one micro-organism per experimental run.

An OD_(600nm)-adjusted inoculum was prepared to an OD_(600nm) of 0.01 (~10⁷ CFU/ml) using each of the three overnight bacterial cultures (as described in **Section 2.1.5**). Then, 250µl of the first OD_(600nm)-adjusted inoculum was added to the wildtype and solvent controls and the first biological replicate of each phytochemical sample, for a starting cell density of ~10⁵ CFU/ml. This action was repeated so that the second OD_(600nm)-adjusted inoculum was used to inoculate the second biological replicate of each phytochemical sample, and so on

with the third inoculum until all vessels were inoculated. The negative control was inoculated with 250µl of sterile PBS.

The sample cultures were then immediately sampled, processed for viable CFU enumeration (as described in the latter half of **Section 2.1.6**) and placed into a shaking incubator set at 37°C ($\pm 1^\circ\text{C}$). This process was repeated so that a viable CFU count for the following time points was gathered: T0hrs, T1hrs, T2hrs, T4hrs, T8hrs and T16hrs. For each sample and for each time point tested, the log of the average value of the technical and biological replicates was then plotted on a line graph to determine the growth behaviour of the tested micro-organisms when challenged with 0.05mg/ml and 0.5mg/ml of the selected phytochemicals. Growth velocity and endpoint state CFU/ml values were calculated for each data set and statistical analysis via a 1-way repeated measures ANOVA test, with the inclusion of Fisher's LSD test was performed using the GraphPad software package version 8.0 to distinguish statistically significant results.

2.5.0 Drug accumulation assays

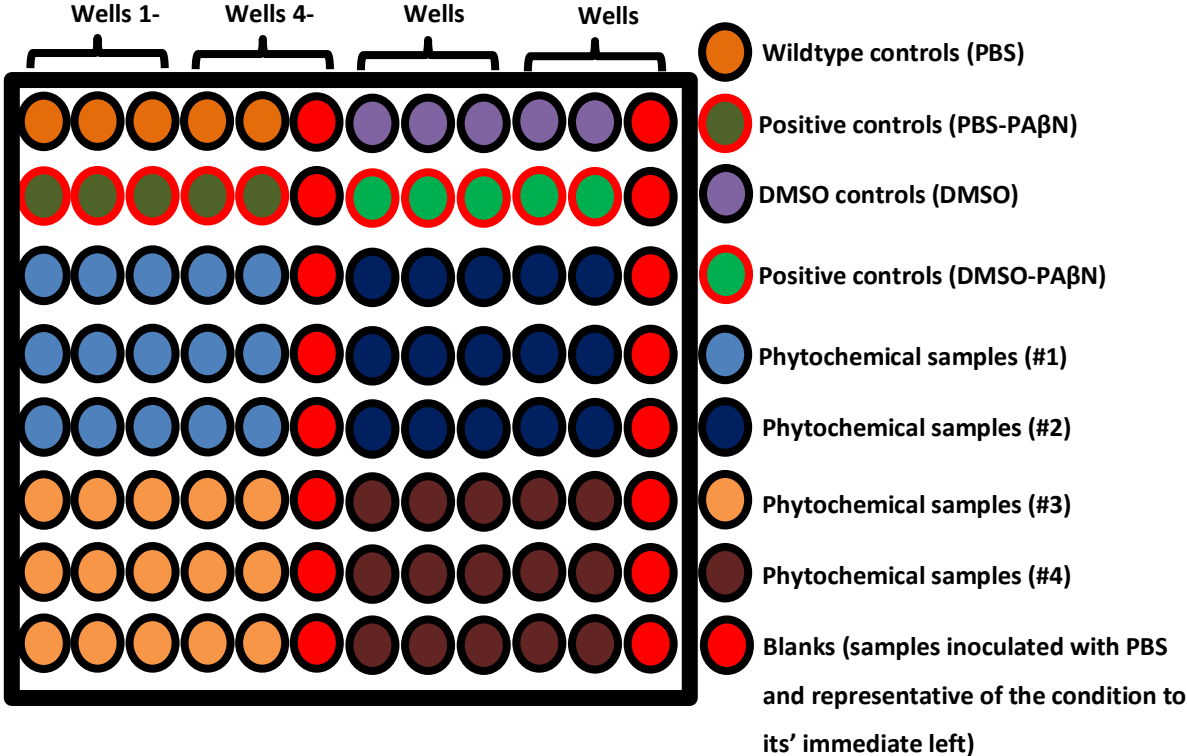
The drug accumulation assays were performed to further investigate the potentiative effect of the selected phytochemicals and to identify increased accumulation of extraneous molecules usually excluded from the cell due to the bacterial membrane's integrity and/or the action of efflux pumps. Experiments were performed with five technical replicates per sample, for three biological replicates altogether.

Overnight bacterial cultures of the selected micro-organism (*S. enterica*, *S. aureus*, *P. aeruginosa*, *L. monocytogenes*) were set up in triplicate (as described in **Section 2.1.4**). The day after the overnight incubation the three bacterial cultures were used to inoculate (via a 50µl inoculum) two glass universals containing 5ml of species-appropriate growth medium (LB for *S. enterica*, *S. aureus*, *P. aeruginosa* and BHI for *L. monocytogenes*), for a total of six fresh cultures (or x12 for *L. monocytogenes* due to the variability of its growth). These x6-12 fresh bacterial cultures were then incubated in a shaking incubator set at 37°C ($\pm 1^\circ\text{C}$) until four had reached the exponential phase of their growth, indicated by an $\text{OD}_{(600\text{nm})}$ within the range of 0.2-0.5 (taking approximately 1.5hrs for *S. enterica* and *P. aeruginosa*, 2 hours for *S. aureus* and *L. monocytogenes*, measured as described in **Section 2.1.5**). Once four bacterial cultures had reached an $\text{OD}_{(600\text{nm})}$ reading within the 0.2-0.5

range, the cultures were transferred to 50ml corning centrifuge tubes and centrifuged using a Heraeus Multifuge 3SR+ centrifuge (ThermoFisher Scientific, Cambridge, UK) pre-cooled to 4°C, at 4075rcf for 20 minutes (3220rcf, 25 minutes for *L. monocytogenes*). After the resulting supernatant was pipetted off the cell pellets, the pellets were resuspended in sterile PBS and normalised to the lowest of the four OD_(600nm) measurements recorded.

While the exponential phase cultures were being centrifuged, a 96-well microtitre plate was set up as presently described. The layout of the assay plate is represented in **Figure 2.2**, and the constituents for each experimental condition is displayed in **Table 2.4**. To ensure that the assay reagents did not interact prematurely, 2µl of 50mg/ml phytochemical stock or control substitute (100% DMSO or 100% PBS) was pipetted directly into the bottom of the sample wells, as well as the 5µl of PAβN (5mg/ml working stock concentration), used in these experiments as a positive control. The 5µl of resazurin (400µg/ml working stock concentration) was pipetted onto the side of the sample well, where it clung due to the droplet's surface tension. Using four sterile reagent reservoirs and a multichannel pipette, the last solutions to be added to each well were the 193µl of OD_(600nm)-adjusted inocula (one for the controls, three for three biological replicates of each phytochemical tested) or PBS, making the total volume of each well up 200µl (or 205µl, a negligible increase, in the case of the positive controls). This sequence of steps was performed to prevent the bacterial cells interacting with reagents before the 96-well microtitre plate could be sealed and measured.

Figure 2.2: The drug accumulation assays layout.



Pictorial presentation of the drug accumulation assay's 96-well microtitre plate layout.

Table 2.4: Experimental conditions and constituent reagents of the drug accumulation assays.

Sample type	Reagent/solution	Volume (μl)	Final concentration
Wildtype control (PBS)	Resazurin (400μg/ml)	5	10μg/ml
	PBS (100%)	2	1%
	OD _(600nm) -Adjusted Inoculum	193	-
Positive control (PBS-PAβN)	Resazurin (400μg/ml)	5	10μg/ml
	PBS (100%)	2	1%
	PAβN (5mg/ml)	5	0.125mg/ml
	OD _(600nm) -Adjusted Inoculum	193	-
DMSO control (DMSO)	Resazurin (400μg/ml)	5	10μg/ml
	DMSO (100%)	2	1%
	OD _(600nm) -Adjusted Inoculum	193	-
Positive control (DMSO-PAβN)	Resazurin (400μg/ml)	5	10μg/ml
	DMSO (100%)	2	1%
	PAβN (5mg/ml)	5	0.125mg/ml
	OD _(600nm) -Adjusted Inoculum	193	-
Phytochemical samples	Resazurin (400μg/ml)	5	10μg/ml
	50mg/ml Polyphenol Stock (100% DMSO)	2	0.5mg/ml
	OD _(600nm) -Adjusted Inoculum	193	-
Blanks	Resazurin (400μg/ml)	5	10μg/ml
	PBS / DMSO (100%) / 50mg/ml Polyphenol Stock (100% DMSO)	2	1% / 1% / 0.5mg/ml
	PBS (100%)	193	1%

Describes the reagents and volumes used in each experimental condition presented in **Figure 2.2**.

Once all wells were inoculated a transparent, gas-permeable adhesive plate seal (ThermoFisher Scientific, Cambridge, UK) was placed on top of the 96-well microtitre plate and placed without delay into the FLUOstar Omega Plate Reader. The OD_(600nm) and fluorescence readings (excitation at 544nm, emission at 590nm for resazurin) of the assay plate were measured every three minutes overnight and the data was subsequently trimmed to an appropriate time-point for the calculation of accumulation velocities and steady state fluorescence metric values. OD_(600nm) values were checked for consistency between the experimental conditions, and found to satisfaction. Statistical analysis via a 1-way repeated measures ANOVA test, with the inclusion of Fisher's LSD test was performed using the GraphPad software package version 8.0 to distinguish statistically significant metric results.

2.5.1 *S. aureus* and *L. monocytogenes* positive control optimisation

The known efflux pump inhibitor PaβN is specific for RND-type family efflux pumps and in practice does have a limited range of other efflux systems found in Gram-negative species. This spectrum of activity does not include efflux pumps encoded by *S. aureus* and *L. monocytogenes* strains, where RND pumps are not present. Due to this, PAβN was not an appropriate efflux pump inhibitor for the use of *S. aureus* in these experiments. Carbonyl cyanide 3-chlorophenylhydrazone (CCCP), a known membrane protonophore with the capacity to dissipate the bacterial membrane's electro-chemical potential and disrupt the activity of MFS-type efflux pumps, was tested instead. With this in mind 5µl of a 0.08mg/ml CCCP working stock was used, for a final concentration of 2µg/ml per well, replacing the 5µl of a 5mg/ml PAβN working stock within the positive controls (as described in **Section 2.5.0**) of the *S. aureus* drug accumulation assays. All other sample constituents remained the same as described in **Section 2.5.2**.

For *L. monocytogenes*, consistent results using a CCCP positive control were difficult to obtain and thus a dead cell control with no active efflux was used instead. The dead cell control was created as follows; an overnight culture of *L. monocytogenes* (grown as outlined in **Section 2.1.3**) was transferred to a 50ml corning centrifuge tube and centrifuged at 4075rcf, for 25 minutes at 4°C in a Heraeus Multifuge 3SR+ centrifuge. The resulting pellet was resuspended in 5ml 70% ethanol and allowed to incubate at room

temperature for at least 1 hour; this lysed cell suspension was then added via pipette as the inoculum in the dead cell control sample wells, along with ethidium bromide (EtBr, detailed in **Section 2.5.2**) and PBS or DMSO solvent as required (as described in **Section 2.5.0**). The use of this control was possible due to the use of EtBr as a fluorescence indicator molecule in the experiments with this micro-organism (detailed further in **Section 2.5.2**), which fluoresces when allowed to intercalate with DNA. The dead cell control, consisting largely of lysed cells, provided an abundance of free DNA for the EtBr to interact with, producing a rapid fluorescence accumulation in the plate reader that would confirm the validity of the equipment and methodology used to detect a rapid increased in fluorescence.

2.5.2 *S. aureus* and *L. monocytogenes* EtBr fluorescence indicator optimisation

The use of resazurin as a fluorescent indicator of drug accumulation is based on the fact that, after chemical reduction via the intracellular metabolism of viable bacterial cells, it is converted into the fluorescent compound resorufin^[204]. If the integrity of the bacterial membrane is compromised or efflux is inhibited there is an increased uptake of resazurin, leading to an increased production of resorufin, which can then be detected and measured. However, it was found through optimising experiments that *S. aureus* and *L. monocytogenes* metabolised resazurin at too rapid a rate to capture a clear fluorescence accumulation curve.

In this case, EtBr was used as an alternative fluorescent indicator of drug accumulation. The fluorescence of EtBr in the presence of bacterial cells is predicated on the conformational changes that EtBr undergoes after binding to deoxyribonucleic acids within the bacterial cytoplasm, enabling a metabolism-independent fluorescent measurement as an indication of drug accumulation. The utilisation of EtBr also brings the additional benefit of having an emission wavelength of 355nm, different to that of resazurin.

Therefore, in the *S. aureus* and *L. monocytogenes* drug accumulation assays 20µl of a 100µM EtBr working stock, for a final concentration of 10µM per well, was used to replace the 5µl of resazurin (400µg/ml working stock) in all sample wells as described in **Section 2.5.0**. To accommodate for this increased volume, the volume of the OD_(600nm)-adjusted

inoculum or PBS added to the sample and blank wells respectively was dropped to 178µl. While preparing the 96-well microtitre plates, the EtBr was also added directly to the bottom of the wells while the tested phytochemicals, DMSO or PBS was pipetted onto the side of the well to retard their interactions with the EtBr prior to completing the assay preparation. With the exceptions of the use of EtBr described here and the use of CCCP/dead cell controls as a positive control in **Section 2.5.1**, all sample constituents and procedural steps remained the same as that detailed in **Section 2.5.0**.

2.6.0 Antimicrobial susceptibility determination experiments

2.6.1 Microdilution broth minimum inhibitory concentration (MIC) experiments

Microdilution broth MIC experiments were performed to quantify the MICs of specific compounds (antibiotics or phytochemicals) against the pathogenic panel examined in this project. Experiments were performed with three technical replicates per sample, for two biological replicates altogether.

Overnight bacterial cultures of the selected micro-organisms (*S. enterica*, *S. aureus*, *P. aeruginosa*, *L. monocytogenes*) were set up (as described in **Section 2.1.4**) in duplicate, in Mueller-Hinton (MH) broth. The day after, a suitable multi-channel pipette and sterile reagent reservoir were used to add 100µl of MH broth to columns 2-12 of a sterile 96-well microtitre plate. Using a single-channel pipette 100µl of a compound working stock, prepared in MH broth, for the highest concentration to be tested was added to columns 1, 2 and 12. Wells within column 2 of the 96-well microtitre plate were then serially diluted (100µl) up until column 11, when 100µl was removed from both columns 11 and 12. Next, the overnight bacterial cultures of the selected micro-organisms were diluted 1:10 in PBS (100µl:900µl) within 1ml microtubes and 250µl of this dilution was added to 4.75ml of sterile MH-B creating a suitable set of inocula for the assay. Again, using a multi-channel pipette and sterile reagent reservoirs, 50µl of each inoculum was added to columns 1-11 within the appropriate rows of the 96-well microtitre plate, according to a recorded plate map, followed by 50µl of PBS to column 12. Finally, 50µl of sterile MH broth was added to

all wells to make the final volume in each up to 200µl and the plate was sealed using a suitable, gas-permeable paper plate seal. The assay plate was then incubated overnight at 37°C in a static incubator before being visually observed for culture turbidity the following morning. As the micro-organisms were tested in biological duplicate, the lowest compound concentration across the two without a turbid culture was deemed to be the MIC of the tested compound against the selected micro-organism.

2.6.2 Microdilution agar MIC Experiments

Microdilution agar MIC experiments were also used to confirm the MICs of phytochemicals before mutant selecting laced-agar plating (using serially diluted agar plates) and to test resistant mutants isolated during mutant selection (detailed in **Section 2.7.0**). Experiments were performed with three technical replicates per sample, for two biological replicates altogether.

Overnight bacterial cultures of the selected candidate mutant strains and their paternal counterparts (*S. enterica*, *S. aureus*, *P. aeruginosa* and *L. monocytogenes*) were set up (as described in **Section 2.1.4**) in duplicate, in MH broth. The day after, a JB Nova water bath (Grant Instruments Ltd, Cambridge, UK) was heated to 70°C and a rack of 50ml centrifuge tubes was placed within it alongside a 500ml Duran bottle filled with 250ml MH Agar, melted prior using a 950 watt Micro Chef ST44 microwave oven (Proline, UK). Once the centrifuge tubes had warmed up these were then taken out of the water bath along with the MH agar, and 25ml aliquots of the agar was separated into the centrifuge tubes. An appropriate volume of a 1g/ml phytochemical master stock was added by pipette to one centrifuge tube to provide double the highest phytochemical concentration tested within the dilution series. This tube was then inverted three times to thoroughly mix its' contents, before pouring all of the molten agar into another centrifuge tube. This 50ml of molten MH agar was then inverted again, 25ml poured into the next centrifuge tube and this process repeated until the phytochemical dilution series had been completed. Each centrifuge tube containing 25ml of molten phytochemical-laced MH agar was then poured into a sterile, square petri dish measuring 100mmx100mm and allowed to set and dry for ~10 minutes. Two separate square petri dishes were also filled with 25ml of molten MH agar to provide non-supplemented agar plates for inoculation controls.

The duplicate overnight bacterial cultures of the selected candidate mutant strains and their paternal counterparts were removed from the static incubator and diluted 1:100 in PBS (10 μ l:990 μ l) within 1ml microtubes. Of these culture dilutions, 150 μ l was added via pipette to the wells of a 96-well plate according to a recorded plate map. Using a sterile replicate-plating tool ~1 μ l of each culture dilution was simultaneously transferred from the 96-well microtitre plate and the tool's prongs pressed gently onto each agar plate. In this way, a range of phytochemical concentrations were tested against many mutant candidate strains and their paternal counterparts, as a comparison, at once. Non-supplemented agar plates provided controls, inoculated at the start and end, to ensure the inoculation process was consistent. All agar plates were then incubated overnight in a static incubator set to 37°C and observed for colony growth the following morning. As the micro-organisms were tested in biological duplicates, the lowest phytochemical concentration without colony growth between the two was deemed to be the MIC against the candidate mutant strains.

2.7.0 Mutant selection using phytochemical-laced agar

Phytochemical-laced agar plates were used to quantify the mutation frequency of the pathogens against selected phytochemicals at MIC and 2xMIC (determined by experiments as described in **Section 2.6.0**). Experiments were performed with three technical replicates per sample, for one biological replicate altogether.

Overnight bacterial cultures of the selected micro-organism (*S. enterica*, *S. aureus*, *P. aeruginosa* and *L. monocytogenes*) were set up (as described in **Section 2.1.4**), in MH broth. The day after, a second overnight culture consisting of 50ml MH broth contained within an Erlenmeyer flask was inoculated using 100 μ l of the previous night's culture. This second culture was incubated overnight at 37°C in a shaking incubator set to ~200rpm and subsequently used from this point on.

The following day, five 500ml Duran bottles containing 250ml sterile MH agar were melted using a microwave oven and cooled to 70°C within a pre-heated water bath. Once the Duran bottles had reached a comfortable temperature to handle, each was supplemented as will be detailed and swirled to thoroughly mix their contents before ~20ml was poured into individual sterile Petri dishes and allowed to set.

For each experiment, five sets of plates were produced: one for the MIC of the phytochemical being tested, one at 2xMIC. Then, two sets of controls containing no phytochemical but the solvent vehicle control (DMSO) at comparable concentrations to that used in the phytochemical plate preparation. For each set of plates, different inocula were applied of each pathogen. Overnight cultures were concentrated via centrifugation (as previously described for cultures), diluted in sterile PBS, and 100µl corresponding to 10^9 , 10^8 , 10^7 and 10^6 CFU applied. In addition, the overnight culture of the tested micro-organism was also serially diluted 1:10 (100µl:900µl) using sterile PBS within 1ml microtubes and 100µl of three appropriate dilutions were plated in triplicate using a sterile, L-shaped spreader on DMSO-containing plates. These plates provided a viable count to help calculate the mutation frequency of the bacterium in question cultured on the phytochemical-laced agar plates. After overnight incubation the DMSO-agar plates were counted, the viable count was calculated in CFU/ml, and the experimental plates were inspected for colony growth. Colony numbers were recorded for each experimental condition and inoculum used, with individual colonies being picked at random using a sterile toothpick and subsequently cultured (as described in **Section 2.1.4**) in MH broth. These mutant cultures were then centrifuged (4075rcf, for 20 mins) the next day, and the pellet processed for glycerol stock storage as set out in **Section 2.1.3** for future use and sequencing. Agar plates that did not show any signs of colony growth were incubated for a further 24 hours and re-examined afterwards. The mutation frequency of the tested micro-organism against each phytochemical concentration was calculated as below:

$$\text{Average Mutation Frequency} = \frac{[\text{Average CFU/ml for each inoculum}]}{\text{Corresponding DMSO Viable Count (CFU/ml)}}$$

The mutation frequencies were calculated separately for the phytochemical MICs and 2xMICs.

2.8.0 Crystal violet biofilm staining assays

Due to the genomic sequencing (**Section 2.10.0**) of the thymol-tolerant mutants, selected from the phytochemical-laced agar plating experiments (see **Section 2.7.0**), revealing single nucleotide polymorphisms (SNPs) within efflux-associated pathways the following experiment was performed. As defined within the literature many AMR pathogens displaying modified efflux phenotypes also present a lower capacity to form biofilms; crystal violet assays were performed to quantify and compare the parental and mutant

strains' biofilm capacities via $OD_{(590nm)}$ measurements. Experiments were performed with three technical replicates per sample, for four biological replicates altogether.

Overnight bacterial cultures of the parent and mutant micro-organisms (*S. enterica*, *S. aureus* and *P. aeruginosa*) were set up (as described in **Section 2.1.4**). The day after, 50 μ l of the overnight cultures were added via pipette to 5ml of LB without NaCl (LB-NaCl) broth within a glass universal to produce culture dilution A. Culture dilution A was then pipetted (50 μ l) into a fresh glass universal of 5ml LB-NaCl, creating culture dilution B. The wells of a sterile 96-well microtitre plate were then filled in triplicate with 100 μ l of culture dilution B and 100 μ l of sterile LB-NaCl. Alternative wells were also filled with 100 μ l of culture dilution B and 100 μ l of LB-NaCl supplemented (using 50 μ l of a 50mg/ml thymol master stock in 5ml of LB-NaCl) to give a final concentration of 0.25mg/ml thymol per well, or 50 μ l of 100% DMSO for a comparable solvent control. Once the 96-well microtitre plate had been inoculated in this way, the plate was then sealed with a gas-permeable paper seal and incubated statically at 30°C for 48 hours.

After the 48 hour incubation the microtitre plate(s) were removed from the incubator, unsealed and the culture poured into a plastic tray placed into a sink and filled with Bioguard disinfectant (Bioguard Hygiene, Northampton, UK). A gentle stream of water was used to flush the wells of the 96-well microtitre plate, which was subsequently placed upside-down to dry on a sheet of blue roll for five minutes. Using a multichannel pipette and reservoir, 200 μ l of 0.1-1% crystal violet (Merck, Gillingham, UK) solution was pipetted into the wells of the 96-well microtitre plate and left to stain for 10 minutes. After this time the crystal violet solution was removed from each well via pipette and a gentle stream of water was poured over the 96-well microtitre plate, poured into the Bioguard disinfectant and left upside-down to dry on a sheet of blue roll for five minutes. Then, 200 μ l of 70% ethanol was pipetted into each well of the 96-well microtitre plate and left to incubate for 10 minutes before the plate was sealed with a transparent adhesive seal and the $OD_{(590nm)}$ measured using a FLUOstar Omega plate reader. The data points, in triplicate, for each tested condition were statistically analysed via a 1-way repeated measures ANOVA test, with the inclusion of Fisher's LSD test, using the GraphPad software package version 8.0 to distinguish statistically significant results.

2.9.0 Congo red plate biofilm phenotyping

Again, following on from the genomic sequencing (**Section 2.10.0**) of the thymol-tolerant mutants selected from the phytochemical-laced agar plating experiments (see **Section 2.7.0**), the following experiment was performed to capture visual observations of the biofilm morphologies presented by the parental and mutant strains. Congo red stain (Merck, Gillingham, UK) was selected as a visual indicator of biofilm matrix production as this diazo textile dye stains the amyloid appendages curli, in addition to other polysaccharides constituting the bacterial biofilm matrix^[205]. All work was carried out under sterile conditions within a Class II microbiological safety cabinet, or under a lit Bunsen burner. Experiments were performed with three technical replicates per sample, for two biological replicates altogether.

Overnight bacterial cultures of the parental and selected mutant micro-organisms (*S. enterica*, *S. aureus* and *P. aeruginosa*) were set up in triplicate (as described in **Section 2.1.4**). The following day 1ml of a 10mg/ml congo red working stock was pipetted into 250ml of LB-NaCl agar pre-melted via a microwave oven, giving a final congo red concentration of 40µg/ml. The molten agar was then swirled to ensure thorough mixing before being poured into sterile, square petri dishes. The agar plates were left to dry for approximately 30 minutes while the overnight cultures of the parental and mutant strains were serially diluted in triplicate, 20µl into 180µl of sterile PBS, within a sterile 96-well microtitre plate. Using a multichannel pipette 10µl of the serially diluted cultures were then spotted onto the dried LB-NaCl congo red agar plates and left to dry for another 20 minutes. The inoculated agar plates were then incubated at 30°C for 48 hours before being observed for biofilm growth and photographed. Representative colonies were then gathered, judged on a qualitative, visual basis and presented.

2.10.0 Bacterial DNA extraction, quantification, and sequencing

Extraction of DNA was used to isolate the genetic material from bacterial strains. This was done to sequence mutant strains and highlight genetic pathways affected by

phytochemicals, and to gain insight into the bacterial mechanisms of resistance/MOA. Two methods were implemented, depending on the experimental context.

2.10.1 DNA extraction, quantification and sequencing of phytochemical-selected mutants

For the thymol-tolerant bacterial mutants selected as described in **Section 2.7.0**, the following method was used. Overnight bacterial cultures of the selected micro-organism (*S. enterica*, *S. aureus*, *P. aeruginosa* and *L. monocytogenes*) were set up as described in **Section 2.1.4**. The next day, 1ml of the overnight cultures was transferred to a sterile 1ml microtube and centrifuged at 959rcf for 25mins. The supernatant was then removed, and the tubes pulse-spun to fully sediment the bacterial growth. Afterwards, 100µl of lysing buffer (consisting of 5µg/ml lysozyme and 98µg/ml RNase A suspended in Tris-EDTA buffer at pH 8) was added to each bacterial pellet. This suspension was then transferred via pipette to a fresh 1ml microtube and placed into a ThermoMixer C (Eppendorf, Hamburg, Germany) set to 37°C, 1600rpm for 25mins. Next, 10µl of lysing additive (comprising of 1mg/ml proteinase K, 1mg/ml RNase A, 5% SDS and Tris-EDTA buffer at pH 8) was added to the suspension via pipette before the samples were placed back into the ThermoMixer C, set to 65°C, 1600rpm for 15mins. After this time period, the samples were briefly centrifuged to pellet cellular debris, and 100µl of the resulting supernatant was transferred to lo-bind PCR microtubes (Invitrogen, Thermo Fisher Scientific, Loughborough, UK), incubated at room temperature for a further five minutes. Via pipette, 50µl of KAPA SPRI beads (Roche Diagnostics Ltd., Pleasanton, USA) was added to each sample, gently resuspended, and incubated at room temperature for five minutes. After this, the samples were centrifuged at 959rcf for 25mins, and the supernatant removed. Then, 100µl of freshly made 80% EtOH was ran over the pelleted beads and gently resuspended via pipette. The samples were centrifuged (959rcf for 25mins), the supernatant removed; this 80% EtOH wash was repeated another two times. After the third 80% EtOH wash the samples were air-dried for 15 mins before 50µl of 10mM Tris-Cl (Merck, Gillingham, UK) was added to the KAPA SPRI beads, resuspended via pipette, and left to incubate for five minutes at room temperature. The samples were then centrifuged (959rcf for 25mins) before the supernatant was collected in fresh microtubes, the KAPA SPRI beads being discarded.

For the quantification of the extracted DNA samples, a Qubit working buffer stock was created by adding the Qubit dsDNA HS reagent to the Quanti-iT dsDNA HS buffer (Invitrogen, Thermo Fisher Scientific, Loughborough, UK) in a ratio of 1:200. This working buffer stock was added, 200 μ l via pipette, to lo-bind PCR microtubes for each sample to be quantified and an additional two tubes for the DNA standards. To create the DNA standards, 10 μ l of the Qubit DNA HS 10ng/ μ l standard (Invitrogen, Thermo Fisher Scientific, Loughborough, UK) was added to one tube and 10 μ l of the Qubit DNA HS 0ng/ μ l standard was added to the second. Of the DNA samples, 1-20 μ l was added to the Qubit working buffer microtubes and the DNA concentration was measured using the Qubit 4 Fluorometer system (Invitrogen, Thermo Fisher Scientific, Loughborough, UK), HS dsDNA programme. DNA samples diluted down to 5ng/ μ l were subsequently submitted to the QIB Core Sequencing department (Mr. Dave Baker) for Illumina sequencing. Raw IRIDA FASTQ files were received from Mr. Dave Baker, after quality control checks, and processed through the Galaxy platform Snippy bioinformatical pipeline alongside the parental strain's reference genome. In this way single nucleotide polymorphisms (SNPs) were identified, visualised in the Artemis software then cross-referenced with the literature and Basic Local Alignment Search Tool (BLAST) searches of the highlighted loci's nucleotide and amino acid sequences.

2.10.2 DNA extraction, quantification and sequencing of thymol-challenged *S. enterica* TraDIS-Xpress mutants

For the thymol-challenged *S. enterica* TraDIS-Xpress library described in **Section 2.11.0**, an alternative DNA extraction method performed by Dr. Mohammed Yasir utilising the Zymo *Quick-DNA Fungal/Bacterial* 96 Kit, catalogue no. D6006 (Zymo, Irvine, USA) was implemented. DNA concentrations were quantified via the Qubit 4 Fluorometer system as described above in the latter half of **Section 2.10.1**; samples were sequenced via Illumina sequencing and analysed via the AlbaTraDIS software (Dr. Keith Turner) before data were handed over to the author. From the resulting gene list, significant loci were identified via filtering by *q* value (≥ 0.00001) and Log₂FC value (± 2). Highlighted genes were then cross-referenced with the existing literature for their potential association in the mechanisms of thymol resistance/susceptibility.

2.11.0 *S. enterica* TraDIS-Xpress library thymol challenge

To further study the genetics involved in thymol susceptibility (see **Section 2.7.0**), an *S. enterica* Typhimurium (ATCC 14028S:*lacI*) TraDIS-Xpress library was exposed to a concentration range of this monoterpenoid phenol. Experiments were performed with two technical replicates per sample, for one biological replicate altogether.

First, a suitable thymol concentration to add to the dense TraDIS-Xpress library inoculum was identified using the microdilution broth MIC experiment methodology outlined in **Section 2.6.1**, with the modification of utilising an *S. enterica* inoculum at approximately $\sim 10^7$ CFU/ml. However, when the following methodology was attempted using the identified thymol concentration of 0.125mg/ml, in addition to 0.25mg/ml and 1mg/ml, no surviving mutants could be rescued for DNA extraction and sequencing. Therefore, a lower thymol range was utilised with four glass universals containing 5ml of sterile LB being set up, in duplicate, as follows; solvent control (with 6.25 μ l DMSO added via pipette), 0.125mg/ml thymol (with 12.5 μ l of a 50mg/ml thymol stock added), 0.0625mg/ml thymol (with 6.25 μ l of a 50mg/ml thymol stock added) and 0.03125mg/ml thymol (with 3.125 μ l of a 50mg/ml thymol stock added). Another set of glass universals were set up in the same manner, with the 5 μ l addition of a 1M IPTG stock for a final inducing concentration of 1mM IPTG. The OD_(600nm) of a pre-made *Salmonella* STM51 TraDIS-Xpress library aliquot was measured as described in **Section 2.1.5** and 1 μ l was inoculated via pipette into each glass universal. The inoculated cultures were then transferred to a shaking incubator, set to 37°C and ~ 200 rpm, for 24 hours prior to being centrifuged in 50ml centrifuge tubes (4075rcf for 35mins), and the resulting pellets placed in a freezer set to -20°C until a DNA extraction was performed (see **Section 2.10.2**).

2.12.0 Transmission electron microscopy (TEM)

TEM was implemented to visualise alterations to the bacterial surface as well as any additional morphological, cytoplasmic, effects resulting from thymol exposure. Experiments were performed with one technical replicate per sample, for two biological replicates altogether.

Overnight bacterial cultures of the *S. enterica* parental strain and the thymol-selected mutant strain #2 were set up (as described in **Section 2.1.4**). The next day two Erlenmeyer flasks filled with 200ml sterile LB were then inoculated, via pipette, using 1ml of the overnight cultures. The Erlenmeyer flasks were then placed into a shaking incubator, set to 37°C and ~200rpm, overnight. After this incubation, the 200ml cultures were separated into five 30ml aliquots within 50ml centrifuge tubes. The culture aliquots were then treated with the following supplementary solutions to create the following conditions: negative control (with the addition of 0.15ml PBS), solvent control (0.15ml 100% DMSO), 0.25mg/ml thymol (0.075ml of a 100mg/ml thymol stock), 0.5mg/ml thymol (0.15ml of a 100mg/ml thymol stock) and 1mg/ml thymol (0.3ml of a 100mg/ml thymol stock). The samples were then allowed to incubate at room temperature for two hours, before centrifugation (4075rcf for 20 minutes) to pellet the cells. The pellets were resuspended in 10ml PBS, lightly vortexed and then pelleted again via centrifugation (4075rcf for 20 minutes). After this, the sample pellets were covered with 1ml of PBS and processed by Ms. Kathryn Gotts and Dr. Catherine Booth of the QIB Bioimaging Core Facility for fixing and imaging. Resulting images were parsed to identify representative examples of the bacterial morphologies. Five individual cells, randomly selected, were analysed via the ImageJ version 1.53r software (National Institutes of Health, Maryland, USA). The analysed region of interest (ROI) was isolated to the surface of the selected cells across two TEM images. Mean gray values (the sum of the gray values of all the pixels within the ROI, divided by the number of pixels) and circularity values (indicating the degree to which the ROI is approaching a perfect circle. Values closer to 1.0 indicate a perfect circle, values closer to 0.0 indicate a more elongated cell shape) were measured. Mean gray values were labelled as average cytoplasmic density values in the corresponding table, as this was the intended inference. Numerical values were displayed to two decimal places and a statistical analysis via a 1-way repeated measures ANOVA test, with the inclusion of Fisher's LSD test was performed using the GraphPad software package version 8.0 to distinguish statistically significant results.

2.13.0 Food challenge testing (FCT)

To determine the *in situ* efficacy of thymol as an alternative food preservative (with the Prosur NATPRE T-10+ mix included as a current food industry comparable standard), a

food challenge test (FCT) utilising a vegetarian burger product (Linda McCartney vegetarian ¼lb burgers, Linda McCartney Foods, UK) was implemented. This particular food matrix was chosen due to the lack of food preservatives in its formulation, the lack of scientific literature on the use of thymol within vegetarian meat substitutes, in addition to being a readily available food product. All work (excluding the vacuum packing) was carried out under sterile conditions within a Class II microbiological safety cabinet, or under a lit Bunsen burner. Experiment was performed with three technical replicates plated per sample, for one biological replicate, altogether.

Two days before the experimental set up a 5ml overnight culture of *S. enterica* was made as laid out in **Section 2.1.4**. The next day, 1ml of this culture was transferred via pipette to inoculate a 500ml Erlenmeyer flask containing 100ml of sterile LB. This Erlenmeyer flask was placed into a shaking incubator, set to 37°C and ~200rpm, overnight. The food matrix to be used was purchased in a supermarket (ASDA, Norwich, UK) 3-5 days prior to use and stored at -20°C until required. The day before the experimental set up, 5kg of the product was thawed overnight at 4°C, to ensure an easy manipulation within the lab.

The next day, using a balance (Portable Scale, Sartorius, Göttingen, Germany), sterilised spoons, scissors and plastic containers cleaned and air-dried prior to use with 70% EtOH, the food matrix was separated into 1kg portions. Using these five 1kg portions the following experimental conditions were created by addition of the supplementary solutions and thorough manual mixing for 10 minutes: positive control (100ml sterile PBS), negative control (100ml PBS, to be left uninoculated), solvent control (100ml of 100% DMSO), 1% thymol (100ml of 100mg/ml thymol stock) and 1% Prosur NATPRE T-10+ (100ml of 100mg/ml Prosur NATPRE T-10+ mix stock). Once an experimental batch was thoroughly mixed, 10g portions were then measured via scales and spooned into separate vacuum pouches (180x300mm 90µm pouches, The Vacuum Pouch Company Ltd., Bury, UK) before being placed on ice. Those experimental conditions to be inoculated then had 5µl of an inoculum (created via the centrifugation of the 100ml *S. enterica* Erlenmeyer flask culture at 3220rcf for 25mins, resuspended in 10ml of sterile PBS) spotted in triplicate randomly across the surface of the food sample before once again being placed on ice. Vacuum pouch samples were then vacuum packed using a vacuum packing machine (15 second cycle, Buffalo Chamber, model no. GF439-02, Buffalo, UK) and stored as soon as possible in a fridge set to 10°C (see **Section 2.13.1**).

On the day of the experimental set up three samples from each condition were removed from the fridge, with one sample being photographed to record the visual appearance of the food matrices. All samples were then stomached for two minutes on the high setting with 10ml sterile PBS in strainer bags (Stomacher 80 Biomaster strainer bags, Seward, West Sussex, UK) and a stomacher machine (Stomacher 400 Lab system, Seward, West Sussex, UK), before as much filtrate as possible could be drawn off via an ErgoOne FAST pipette controller (Starlabs Ltd., Milton Keynes, UK) and 10ml Sterilin pipette (ThermoFisher-Scientific, Cambridge, UK). From this point, the inoculum and samples were enumerated as described in **Section 2.1.6**, with the substitution of LB agar for XLD agar supplemented with 10µg/ml fluconazole (Merck Life Sciences Ltd., UK). This modification was applied to ensure the elimination of fungal contaminants growing on the plates and to select specifically for *S. enterica* colonies, both ensuring a more accurate enumeration (see **Section 2.13.2**).

For 30 days after this initial set up one random sample from each experimental condition was photographed daily, before being placed back into the -10°C fridge, and three were enumerated in this way every three days. No sample was photographed more than once. The collected enumerations, in triplicate, for each tested condition were presented in graphical format, where the area under the curve (AUC) for each sample condition biological replicate was calculated. These AUC values were then statistically analysed via a 1-way repeated measures ANOVA test, with the inclusion of Fisher's LSD test was performed using the GraphPad software package version 8.0 to distinguish statistically significant results.

2.13.1 *S. enterica* cold temperature optimisation

Prior to the FCT (**Section 2.13.0**) to investigate the *in situ* efficacy of thymol as an alternative food preservative a suitable temperature to reflect the chilled conditions within the food industry, while still allowing for the detectable growth of *S. enterica*, required optimisation. Experiments were performed with three technical replicates per sample, for three biological replicates altogether.

An overnight bacterial culture of *S. enterica* was set up (as described in **Section 2.1.4**). Glass universals containing 5ml of sterile LB were placed, in triplicate, to acclimatise in a cold room set to 5°C, a fridge set to 10°C, on a room temperature bench, and within a 37°C shaking incubator set to ~200rpm. The following day, the OD_(600nm) of the overnight culture was adjusted to 0.01 (as described in **Section 2.1.5**), 250µl was removed from each of the glass universals and 250µl of the adjusted inoculum was added via pipette. A 20µl sample was used to enumerate the fresh cultures immediately, as described in **Section 2.1.6**, before placing the glass universals back at their respective temperatures (5°C, 10°C, room temperature and 37°C). The *S. enterica* cultures were then enumerated in this way once daily for three days, with the data being plotted in the GraphPad v.8 statistical software package. A statistical analysis was deemed unnecessary as the cultures did not grow during the three-day time period at 5°C but growth was observed at 10°C.

2.13.2 *S. enterica* enumeration validation in food matrix model

Prior to the FCT (**Section 2.13.0**) to investigate the *in situ* efficacy of thymol as an alternative food preservative the enumeration method outlined in **Section 2.1.6** required validating for use within the food matrix chosen. Experiments were performed with three technical replicates per sample, for three biological replicates altogether.

An overnight bacterial culture of *S. enterica* was set up (as described in **Section 2.1.4**), while a vegetarian burger was allowed to thaw at 4°C overnight. The next day, the vegetarian burger was separated into eight 10g portions via scales, sterile scissors and spoons into sterile square petri dishes. The OD_(600nm) of the overnight culture was then adjusted to 0.5 (as described in **Section 2.1.5**) with PBS, and 5µl of this inoculum was spotted three times across the surface of six of the food matrix samples. The final two burger samples were inoculated with an equal volume of sterile PBS to form a pair of negative controls. One negative control and three inoculated samples were then sealed shut with parafilm and placed into a static incubator set at 37°C for a three-day incubation. The remaining four samples were each stomached with 10ml PBS in strainer bags for two minutes on the high setting of a stomacher machine. A 20µl aliquot of the resulting filtrates was then enumerated (along with a 20µl sample of the inoculum) as outlined in **Section 2.1.6**. This stomaching and enumerating process was repeated for the incubated food matrix samples after three days.

First attempts were hindered by the presence of fungal growth obscuring the bacterial colonies and thus the LB agar plates were substituted for XLD agar supplemented with 10µg/ml fluconazole which, after repeating the procedure outlined here, enabled for an accurate and reliable enumeration, comparable with the inoculum, of the food matrix samples.

Chapter 3: Selection of antimicrobial compounds for further investigation

“All...are equal, but some...are more equal than others.”-

George Orwell, *Animal Farm*, 1945

3.1 Chapter introduction

There are multiple reports of phytochemicals that exhibit anti-microbial activities^[139, 143, 206] but for the majority a primary inhibitory MOA is unknown, although multiple possibilities have been proposed^[132], (see **Section 1.5**).

The aim of the work presented in this chapter was to test a panel of phytochemicals for antibacterial activity and use this data to select a compound trio for further mechanistic studies.

A panel of suitable compounds were selected for bioactivity-based assessment based on several criteria including previous reports of antimicrobial activity, availability of compounds for study, diversity of chemical structure and existing use in a commercially available phytochemical-based antimicrobial product (Prosur). The selected compounds were then tested in (i) a high throughput assay to identify growth inhibition (based on fixed time-point changes in culture OD_(600nm)), repeated with and without chloramphenicol challenge to identify possible antibiotic potentiation), (ii) viability assays to allow quantification of CFU/ml values, and (iii) drug accumulation assays, using *S. enterica* Ser. Typhimurium, *S. aureus*, *L. monocytogenes* and *P. aeruginosa*.

Hypotheses:

- 1.** Phytochemicals will display differing levels of directly inhibitive and potentiative antimicrobial activity, and non-glycosylated compounds will display more potent antimicrobial properties than glycosylated chemical structures.
- 2.** Selected phytochemicals will increase membrane permeability and therefore drug accumulation by tested bacteria.

3.2 Results

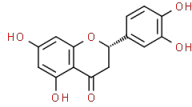
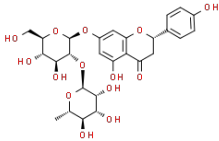
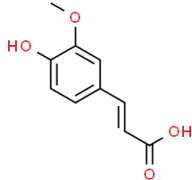
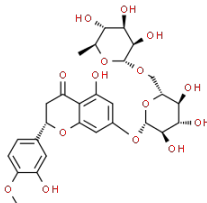
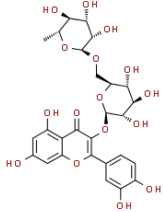
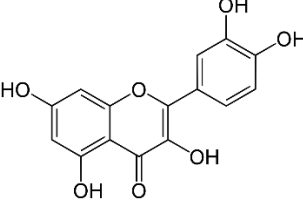
3.2.1 Rationally selecting phytochemical compounds

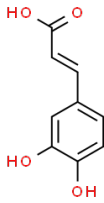
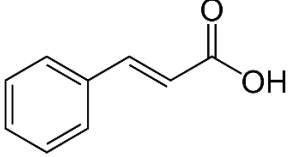
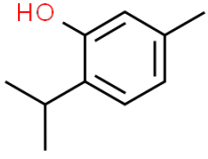
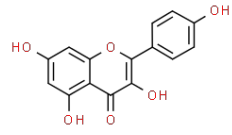
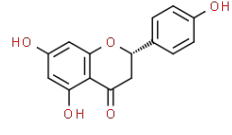
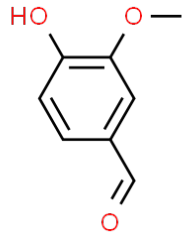
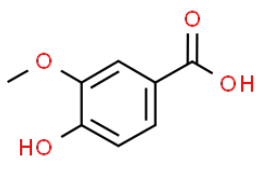
The first step in identifying a primary inhibitory MOA for phytochemical alternatives to current food preservatives was selecting a suitable panel of compounds to investigate. Although there is a plethora of evidence within the literature to support the antimicrobial activity of phytochemicals, discrepancies between recorded active concentrations, employed methodologies and the sheer diversity of phytochemical structures makes selecting a single compound to focus upon difficult. A panel of 13 phytochemical compounds and one commercially available phytochemical mixture (presently used as a preservative within the food industry) were selected for subsequent experimentation using a semi-high throughput assay to screen for antimicrobial activity based on measurements of growth (by optical density). These were chosen to represent a diverse structural range and to include distinct chemical structures whilst including compounds previously suggested to be antimicrobial. **Table 3.1** shows the phytochemicals selected for the initial screening assays (see **Section 2.3.0-2.3.2**). Many phytochemicals can be expensive to synthesize/purify and purchase; an approach balancing selection of compounds that were readily available (in the laboratory or reasonably priced) with previous reports of bioactivity within the literature was considered in the selection process.

Quercetin, hesperidin, caffeic acid and kaempferol were included due to previous reports of antimicrobial activity and their relatively cheap costs. Vanillin and thymol were chosen based on their present use within the food industry, albeit for non-preservative functions including as flavouring additives. The Prosur NATPRE T-10+ mix was included in the phytochemical panel due to industrial collaborations with this project, while also acting as a convenient standard for alternative phytochemical preservatives currently used in the food industry. Eriodictyol, ferulic acid and naringenin were included in this panel due to mass spectrometric analysis of the Prosur NATPRE T-10+ mix identifying these three compounds as being the main phytochemical constituents of the product (Dr. Paul Needs, QIB, unpublished data). Naringin and rutin were selected due to being glycosylated versions of naringenin and quercetin, respectively, thus their comparative activity was of

interest. Cinnamic acid provided a further representative of the phenolic acid classes of phytochemical, while vanillic acid was selected due to its structural similarities to vanillin. In this way, a final panel of 13 phytochemical compounds and one commercial phytochemical mixture was chosen for the initial stages of screening to identify a compound for the work of this project. Each compound was tested against *S. enterica*, *S. aureus*, *P. aeruginosa* and *L. monocytogenes* cultures to identify bioactivity.

Table 3.1: The phytochemical classes, structures, and rationale for a compound's inclusion within the panel.

Phytochemical	Class	Structure	Selection rationale
Prosur NATPRE T-10+	Phytochemical mixture	Eriodictyol*, Ferulic Acid*, Naringenin*	Industrially relevant
Eriodictyol	Flavanone		Antimicrobial, industrially relevant
Naringin	Flavanone-7-O-rutinoside		Glycosidic derivative of naringenin
Ferulic acid	Hydroxycinnamic acid		Antimicrobial, industrially relevant
Hesperidin	Flavanone rutinoside		Antimicrobial, readily available**
Rutin	Flavonol-3-O-rutinoside		Glycosidic conjugate of quercetin
Quercetin	Flavonol		Antimicrobial, readily available**

Caffeic acid	Hydroxycinnamic acid		Antimicrobial, readily available**, representative of hydroxycinnamic acid class
Cinnamic acid	Cinnamic acid		Alternative representative of phenolic acids
Thymol	Monoterpenoid phenol		Antimicrobial, readily available**, representative of essential oil components
Kaempferol	Flavonol		Antimicrobial, readily available**
Naringenin	Flavanone		Antimicrobial, industrially relevant
Vanillin	Phenolic aldehyde		Readily available**, already accepted for industrial use
Vanillic acid	Dihydroxybenzoic acid		Readily available**, included to compare against vanillin

*The Prosur NATPRE T-10+ mix is composed of numerous phytochemicals, although the major constituents were identified as denoted. **Readily available as defined by a balance of expense against published antimicrobial activity.

3.2.2 Identifying comparatively potent antimicrobial phytochemicals and narrowing the selected panel

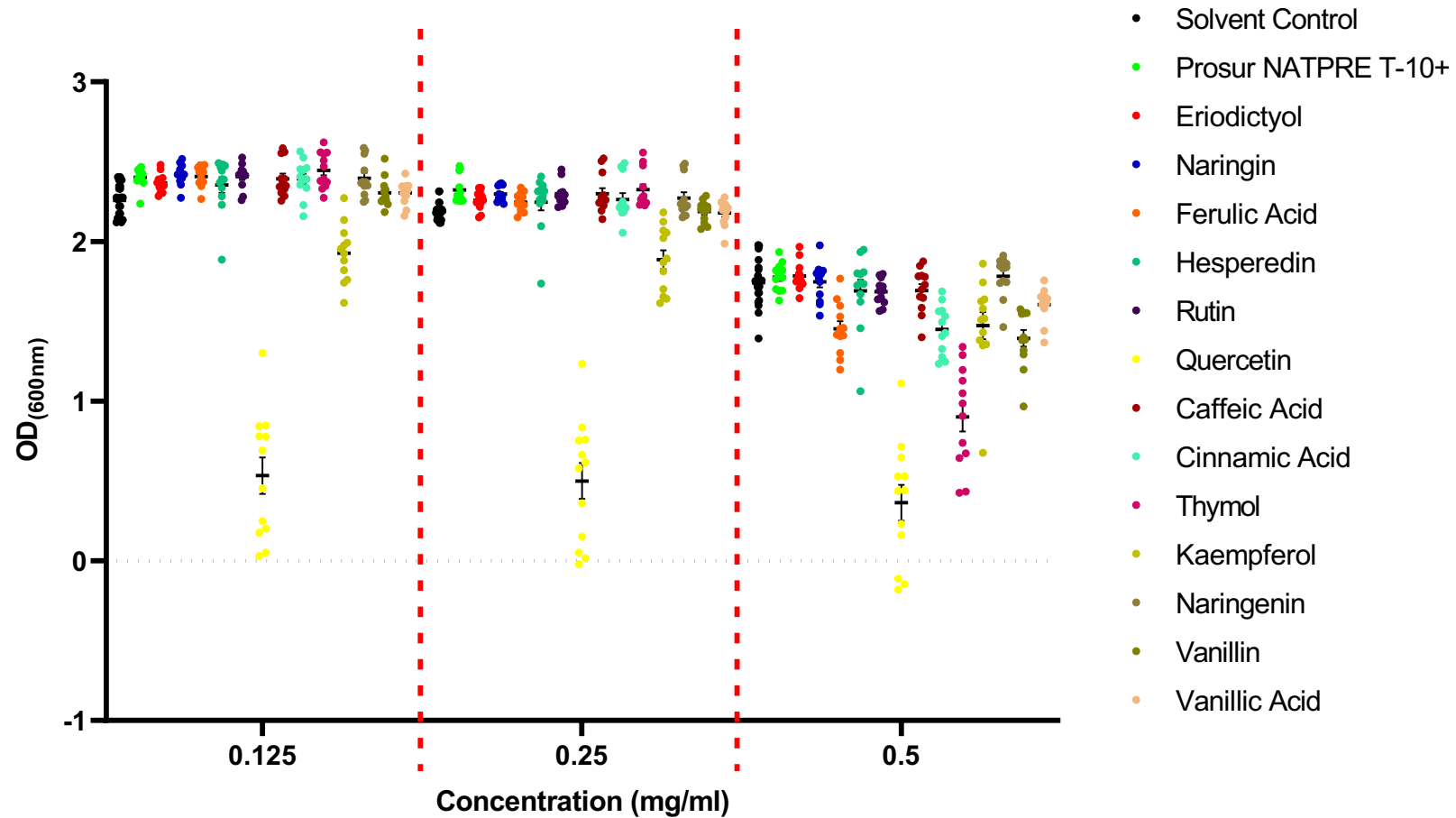
To directly compare the antimicrobial activity of the selected phytochemicals a semi-high throughput inhibition screening assay (see **Section 2.3.0-2.3.1**) was used, the results of which are displayed in **Figures 3.1-3.4** Full data sets discussed throughout this section are available in the **Appendix, Section 9.3**.

Of the phytochemical panel (as detailed above in **Section 2.2.0/3.2.1**), hesperidin, rutin, vanillic acid, caffeic acid, and naringin induced no statistically significant reduction in $OD_{(600nm)}$ measurements against any of the four tested pathogens. Cinnamic acid at 0.5mg/ml significantly reduced the $OD_{(600nm)}$ of growing *S. enterica* cultures by 17.61% and *P. aeruginosa* cultures by 20.18% when compared to the control. Quercetin and kaempferol, being highly pigmented yellow compounds, were difficult to statistically analyse due to having intrinsically high optical density values at 600nm, although they did display some level of $OD_{(600nm)}$ reduction within these experiments. The flavanone eriodictyol was demonstrated to reduce the $OD_{(600nm)}$ achieved by *S. aureus* by 86.87% (at 0.5mg/ml, see **Figure 3.3**) and *L. monocytogenes* cultures by 12.31%. In comparison, naringenin exposure resulted in a 92.80%, 89.53% and 8.94% reduction at 0.5mg/ml, 0.25mg/ml and 0.125mg/ml respectively in the growth of *S. aureus* cultures; suggesting a more potent antimicrobial effect of this compound against this species. The phenolic aldehyde vanillin exerted an inhibitive effect against *S. enterica* and *P. aeruginosa* cultures measured at a respective 20.80% and 27.81% reduction in $OD_{(600nm)}$ when compared to control conditions. Thymol was a particularly potent inhibitor of *S. enterica* (48.82% $OD_{(600nm)}$ reduction), *P. aeruginosa* (20.18%) and *L. monocytogenes* (23.35%) when compared against the control conditions

Many of the phytochemicals showed no inhibitive effect and in fact were seen to be significantly inducing, albeit slightly, $OD_{(600nm)}$ measurements of the challenged cultures. While the full list may be viewed in the **Appendix, Section 9.3**, examples of note include ferulic and vanillic acid both at 0.25mg/ml challenging *S. aureus* cultures (**Figure 3.3**) with a respective $OD_{(600nm)}$ increase of 14.62% and 13.84%, respectively, when compared to control cultures. These results are potentially significant in themselves, as it may suggest a microbial capacity to resist or even utilise certain phytochemical compounds.

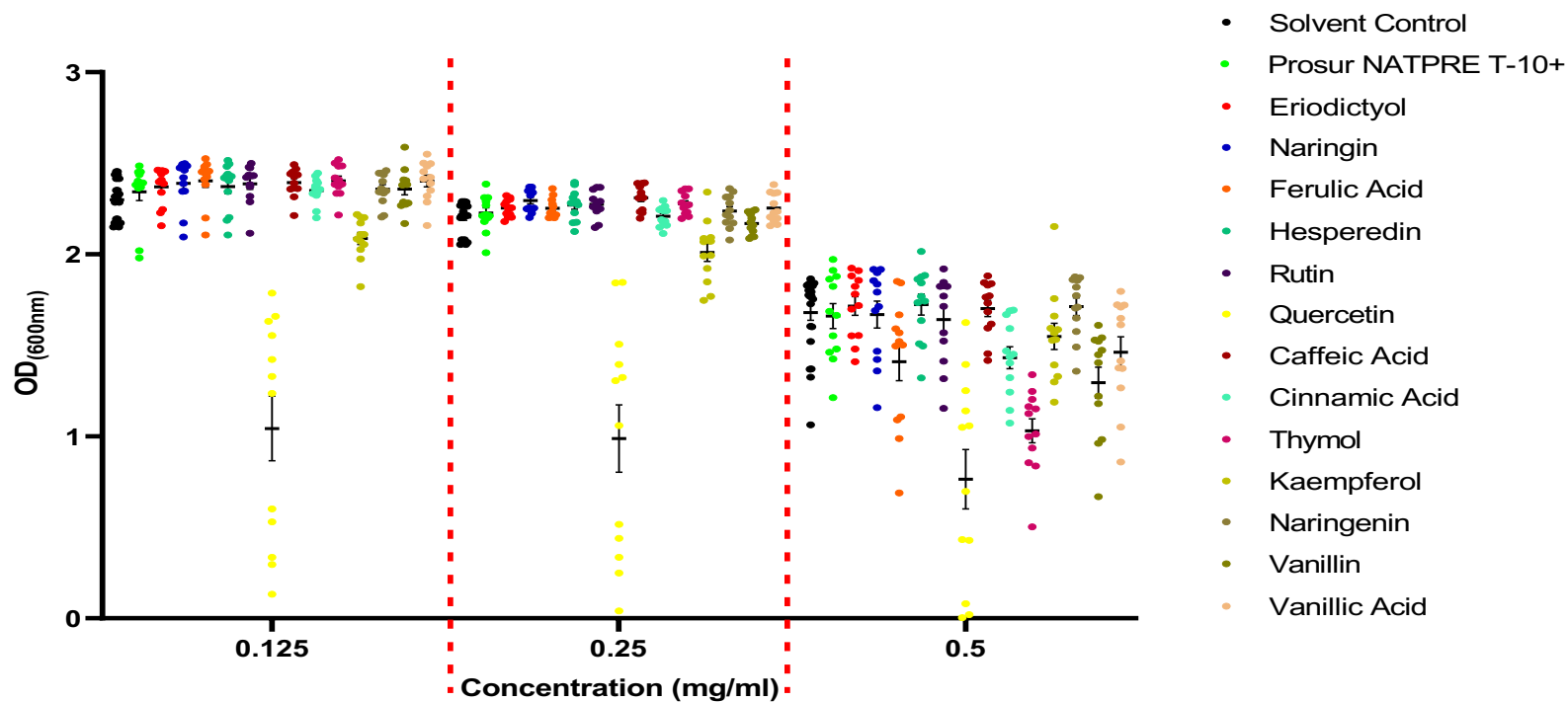
From these data and the contextual literature (**Section 3.6.0**), the following compounds were selected for further quantification of their more potent, direct antimicrobial properties: eriodictyol, naringenin and thymol.

Figure 3.1: OD_(600nm) measurements for *S. enterica* cultures challenged with various concentrations of selected phytochemicals.



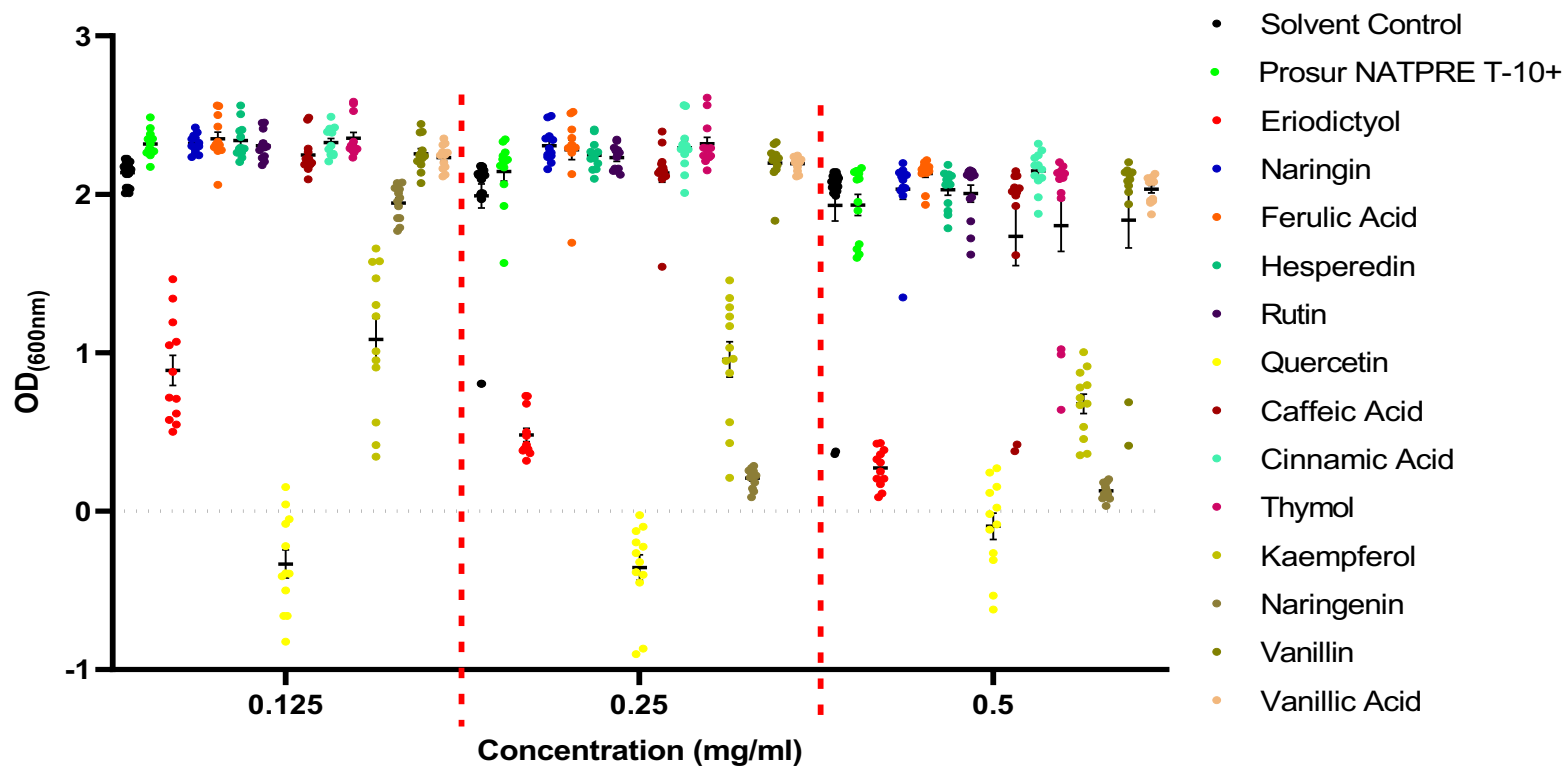
Data points show the final OD achieved after 16hrs of incubation of four biological replicates, with three technical replicates each. Horizontal bars show the mean for each set. Dashed line shows OD from media alone. Statistical analysis was performed using the GraphPad software v.8, using a 1-way repeated measures ANOVA Test with Fischer's LSD test.

Figure 3.2: OD_(600nm) measurements for *P. aeruginosa* cultures challenged with various concentrations of selected phytochemicals.



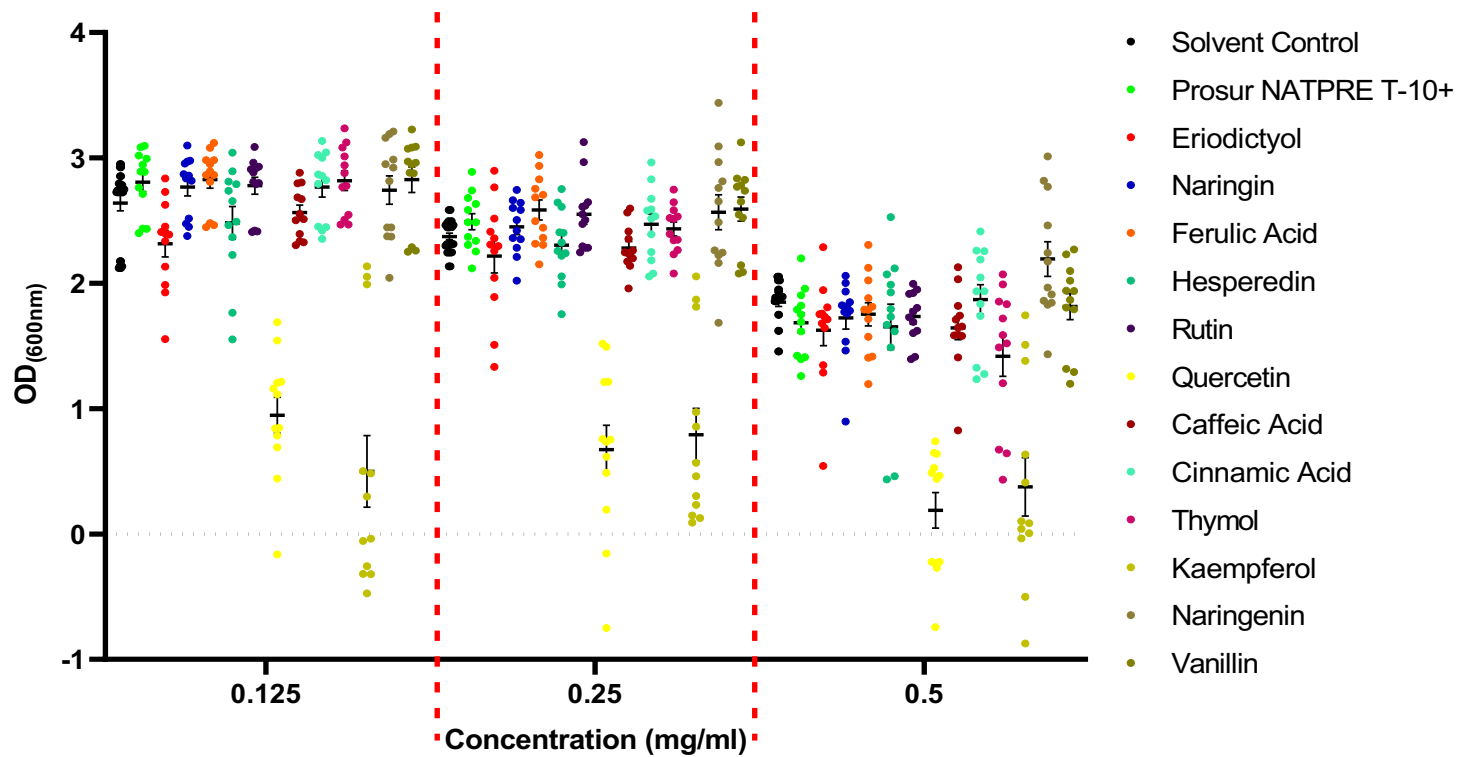
Data points show the final OD achieved after 16hrs of incubation of four biological replicates, with three technical replicates each. Horizontal bars show the mean for each set. Dashed line shows OD from media alone. Statistical analysis was performed using the GraphPad software v.8, using a 1-way repeated measures ANOVA Test with Fischer's LSD test.

Figure 3.3: OD_(600nm) measurements for *S. aureus* cultures challenged with various concentrations of selected phytochemicals.



Data points show the final OD achieved after 16hrs of incubation of four biological replicates, with three technical replicates each. Horizontal bars show the mean for each set. Dashed line shows OD from media alone. Statistical analysis was performed using the GraphPad software v.8, using a 1-way repeated measures ANOVA Test with Fischer's LSD test.

Figure 3.4: $OD_{(600nm)}$ measurements for *L. monocytogenes* cultures challenged with various concentrations of selected phytochemicals.



Data points show the final OD achieved after 16hrs of incubation of four biological replicates, with three technical replicates each. Horizontal bars show the mean for each set. Dashed line shows OD from media alone. Statistical analysis was performed using the GraphPad software v.8, using a 1-way repeated measures ANOVA Test with Fischer's LSD test.

3.2.3 Identifying compounds with ability to potentiate antibiotics

To identify and compare potentiative/synergistic activity of the selected phytochemicals, a semi-high throughput potentiation screening assay was implemented, the results of which are displayed in **Figures 3.5-3.8**. Tested bacterial cultures were coupled with a sub-lethal concentration of chloramphenicol, which a potentiating phytochemical would synergise with to provide a significant decrease in the measured $OD_{(600nm)}$. Percentage values discussed throughout this section are available in the **Appendix, Section 9.3**. Of the phytochemical panel (as detailed above in **Section 2.2.0**), all compounds at 0.125mg/ml displayed potentiative activity alongside a sub-lethal concentration of chloramphenicol to some degree (the exceptions being quercetin and kaempferol due to their high pigmentation skewing the subsequent statistical analysis) against growing cultures of *S. enterica*, *S. aureus* and *P. aeruginosa*. Of particular note; 0.25mg/ml of the Prosur NATPRE T-10+ mix significantly reduced the $OD_{(600nm)}$ of *S. enterica*, *P. aeruginosa* and *S. aureus* (**Figures 3.5-3.7**) cultures by 19.11%, 18.42% and 85.50% respectively, when compared to the control conditions. Eriodictyol at 0.25mg/ml reduced the $OD_{(600nm)}$ measurements of *S. enterica* and *P. aeruginosa* by a statistically significant average of ~14%, however the potentiative activity of this compound against *S. aureus* was more pronounced with a 90.59% reduction. Naringenin displayed similar behaviour at the same concentration, with an average reduction by ~14% of *S. enterica* and *P. aeruginosa* cultures, but a larger reduction of 77.29% in the $OD_{(600nm)}$ of growing *S. aureus* cultures, a more potent effect on this particular pathogen.

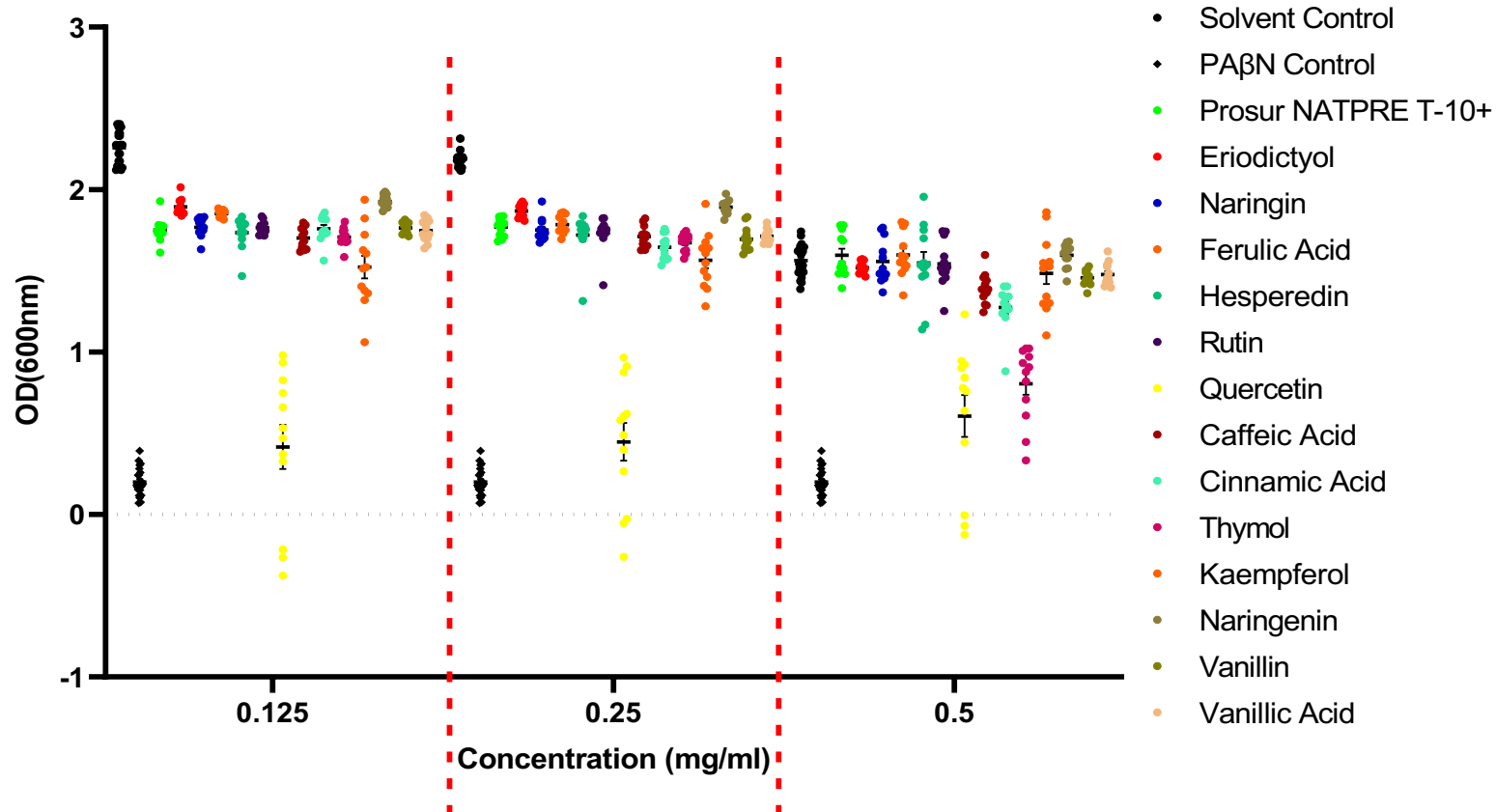
Ferulic acid at 0.25mg/ml exhibited a weaker, yet consistently significant, potentiative activity against three species with an average $OD_{(600nm)}$ reduction of ~16% (see **Figure 3.5-3.8** for the $OD_{(600nm)}$ decrease in the challenged *S. aureus* cultures). On the other hand, 0.25mg/ml caffeic acid reduced the $OD_{(600nm)}$ of growing *S. enterica* cultures by 21.72%, *P. aeruginosa* by 18.87% and *S. aureus* by 97.85%. Cinnamic acid was unusual in the tested panel in that it only affected the Gram-negative bacteria, *S. enterica* and *P. aeruginosa*, by 24.78% and 13.02%

respectively. Vanillin exerted potentiative effects in a similar range for *S. enterica* (23.50%), *P. aeruginosa* (17.60%) and *S. aureus* (19.45%) at a concentration of 0.25mg/ml, whereas vanillic acid significantly reduced the OD_(600nm) measurements of these bacteria by 21.67%, 16.24%, 18.69%. Thymol at 0.25mg/ml reduced the OD_(600nm) of growing *S. enterica* cultures significantly by 23.50%, *P. aeruginosa* by 17.60% and *S. aureus* by 19.45%.

Of the 14 phytochemical compounds tested, only one significantly increased the OD_(600nm), and by inference the growth, of a tested culture supplemented with sub-lethal chloramphenicol in these experiments. At a concentration of 0.5mg/ml, rutin significantly increased the OD_(600nm) of *L. monocytogenes* cultures by 11.89%.

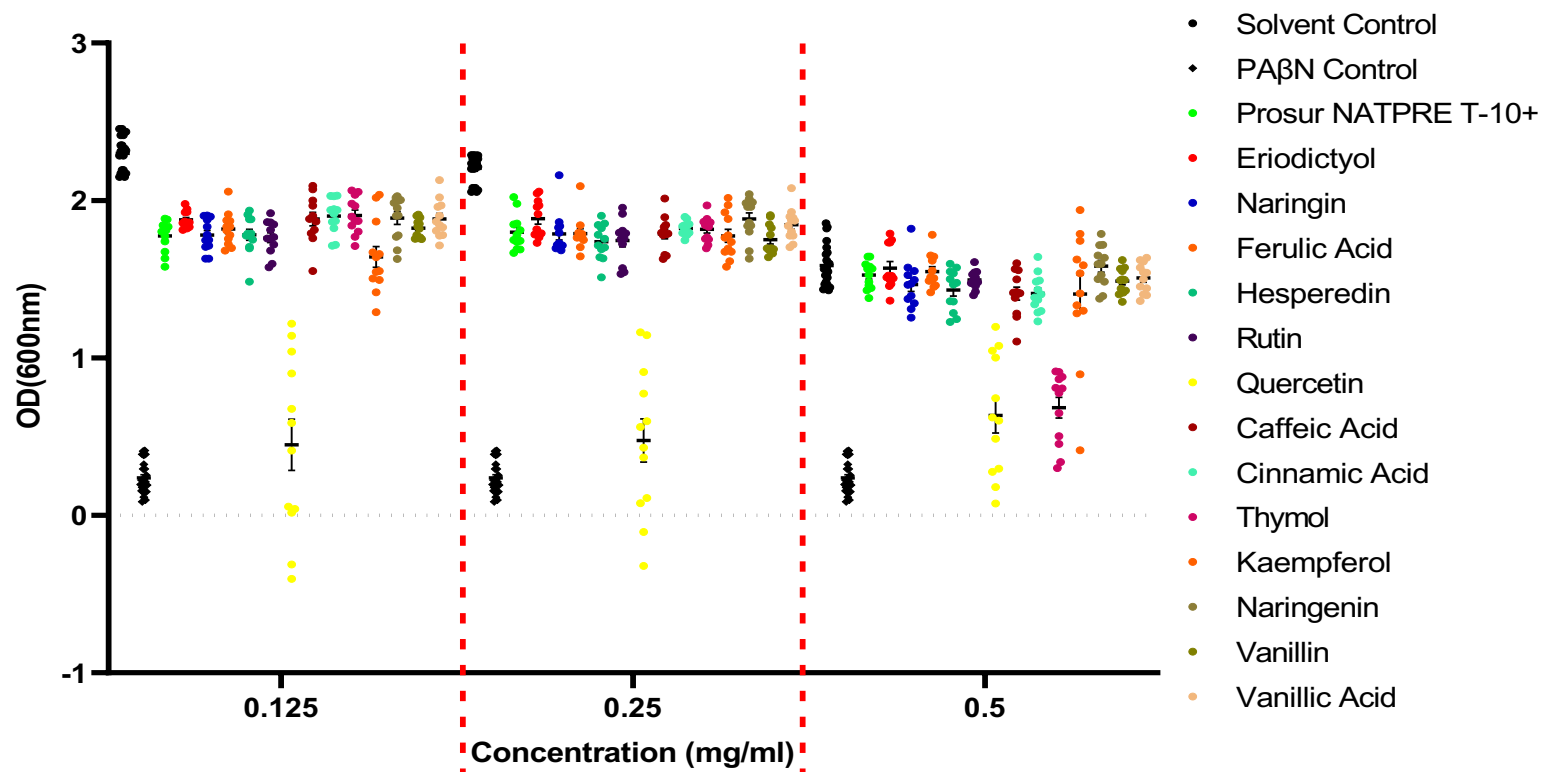
From these data, the following compounds were chosen for further investigation, based on their capacity to potentiate other antimicrobial compounds: caffeic acid, ferulic acid, quercetin and kaempferol and vanillin (based on the data presented here and this compounds present acceptance for use within the food industry). The Prosur NATPRE T-10+ mix was also taken forward due to its potentiative efficacy demonstrated in these semi-high throughput assays, in addition to its industrial relevance for this project and its advantages as a standard for current, industrially accepted, food preservative alternatives.

Figure 3.5: Impact of phytochemicals as potentiators of chloramphenicol based on OD_(600nm) measurements for *S. enterica* cultures.



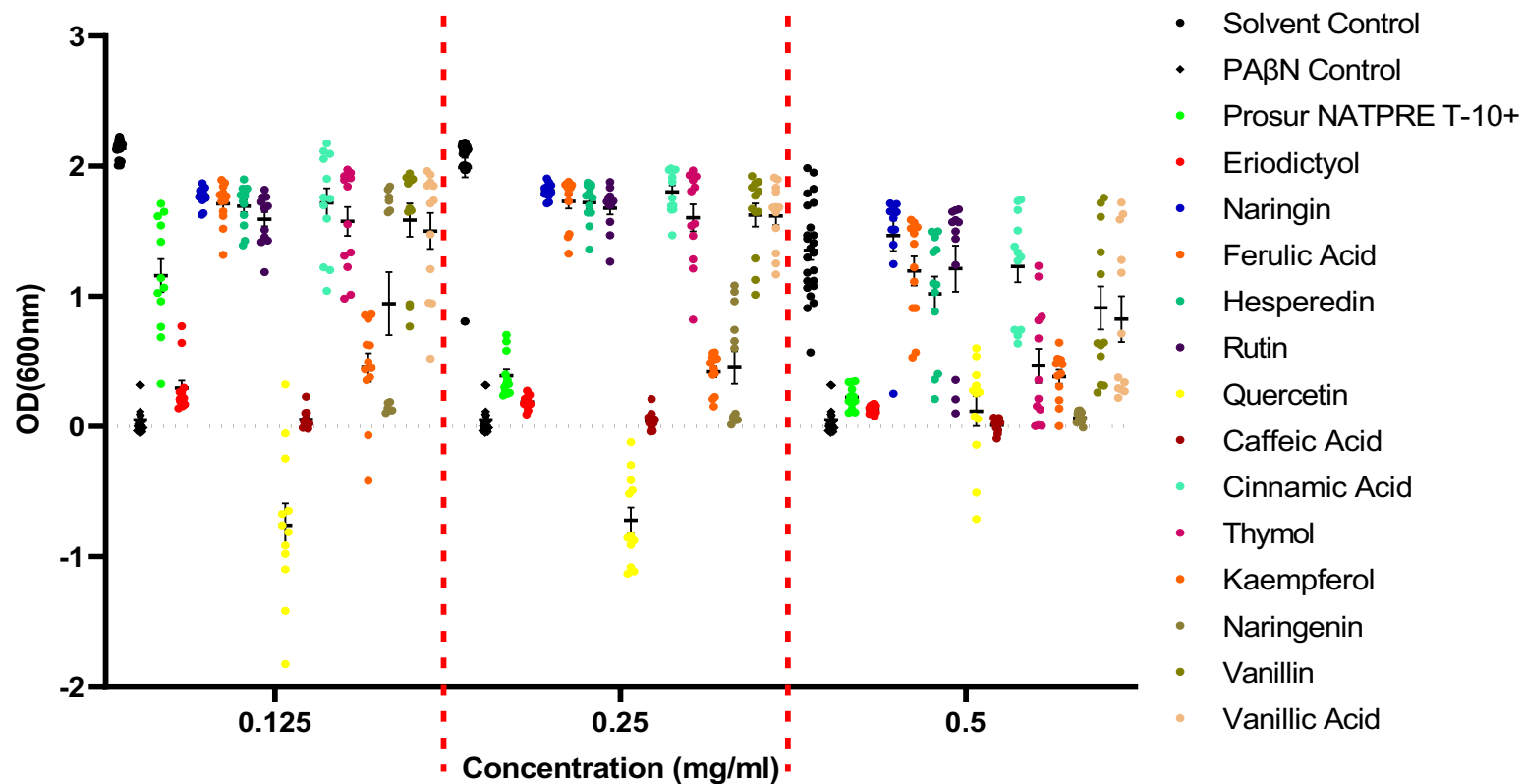
Data points show the final OD achieved after 16hrs of incubation of four biological replicates, with three technical replicates each. PABN was used as a control known efflux inhibitor which will potentiate the activity of chloramphenicol (present at 0.25 X MIC in all conditions). Horizontal bars show the mean for each set. Dashed line shows OD from media alone. Statistical analysis was performed using the GraphPad software v.8, using a 1-way repeated measures ANOVA Test with Fischer's LSD test.

Figure 3.6: Impact of phytochemicals as potentiators of chloramphenicol based on OD_(600nm) measurements for *P. aeruginosa* cultures.



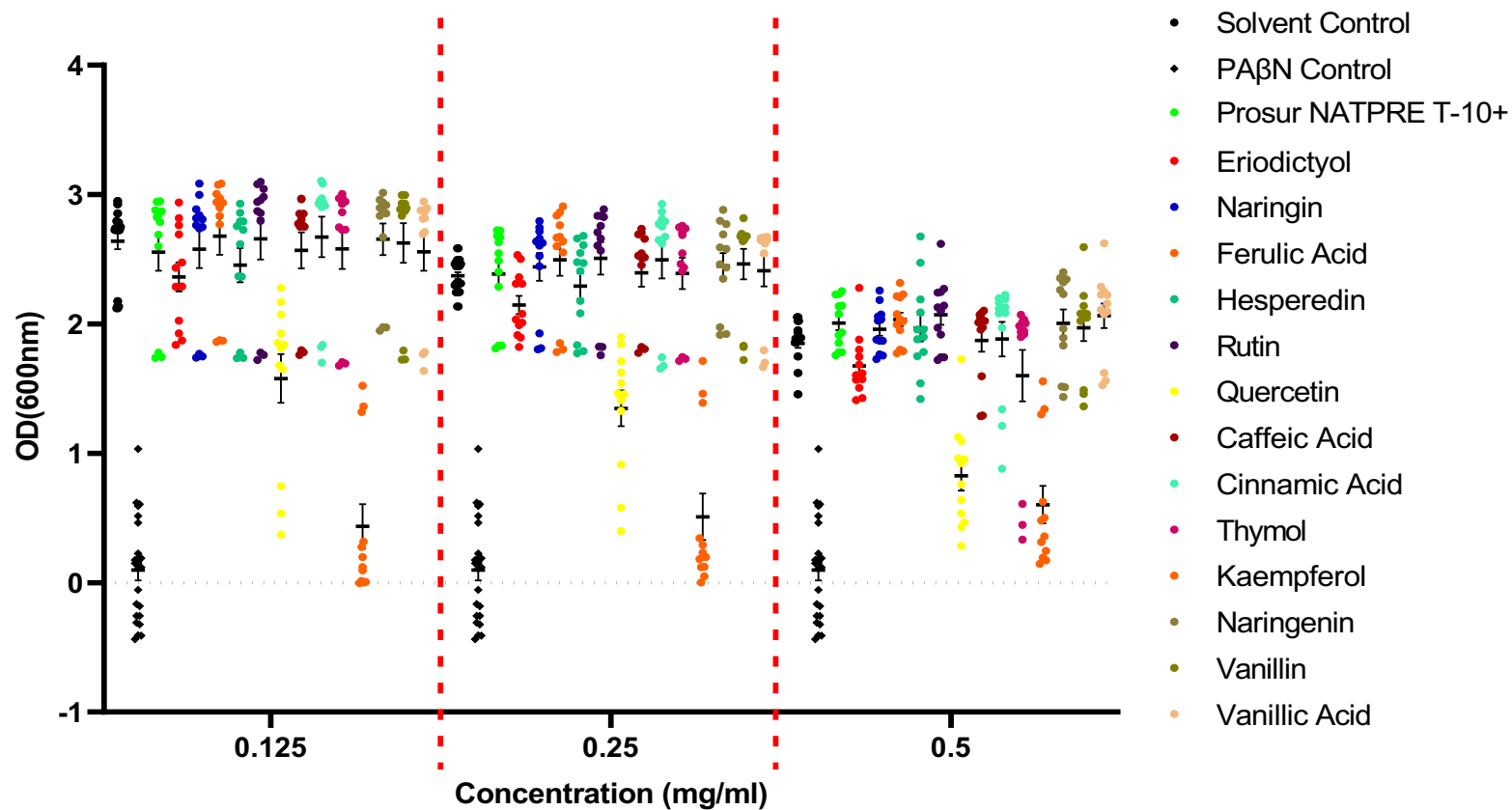
Data points show the final OD achieved after 16hrs of incubation of four biological replicates, with three technical replicates each. PABN was used as a control known efflux inhibitor which will potentiate the activity of chloramphenicol (present at 0.25 X MIC in all conditions). Horizontal bars show the mean for each set. Dashed line shows OD from media alone. Statistical analysis was performed using the GraphPad software v.8, using a 1-way repeated measures ANOVA Test with Fischer's LSD test.

Figure 3.7: Impact of phytochemicals as potentiators of chloramphenicol based on OD_(600nm) measurements for *S. aureus* cultures.



Data points show the final OD achieved after 16hrs of incubation of four biological replicates, with three technical replicates each. PABN was used as a control known efflux inhibitor which will potentiate the activity of chloramphenicol (present at 0.25 X MIC in all conditions). Horizontal bars show the mean for each set. Dashed line shows OD from media alone. Statistical analysis was performed using the GraphPad software v.8, using a 1-way repeated measures ANOVA Test with Fischer's LSD test.

Figure 3.8: Impact of phytochemicals as potentiators of chloramphenicol based on OD_(600nm) measurements for *L. monocytogenes* cultures.



Data points show the final OD achieved after 16hrs of incubation of four biological replicates, with three technical replicates each. PABN was used as a control known efflux inhibitor which will potentiate the activity of chloramphenicol (present at 0.25 X MIC in all conditions). Horizontal bars show the mean for each set. Dashed line shows OD from media alone. Statistical analysis was performed using the GraphPad software v.8, using a 1-way repeated measures ANOVA Test with Fischer's LSD test.

3.2.4 Thymol, and other compounds, significantly alter the growth kinetics of the tested foodborne pathogens

For a more detailed understanding of the direct antimicrobial activity highlighted in the semi-high throughput inhibition screening assays, and to determine whether compounds were bactericidal or bacteriostatic, viable CFUs were recorded from samples challenged with selected phytochemicals over time and used to calculate impacts on growth velocity and final population size.

The results of these experiments, utilising 0.5mg/ml concentrations of the eight selected phytochemicals and Prosur NATPRE T-10+ mix (see **Section 2.4.0**), are shown in **Tables 3.2-3.5**, and exemplar graphs of the experiments in **Figure 3.9**. Full data be found in the **Appendix, Section 9.3**. Confirming the semi-high throughput assays, eight of the nine selected compounds exerted significant inhibition on the growth kinetics of the tested pathogens. The Prosur NATPRE T-10+ mix significantly reduced the final CFU/ml of *L. monocytogenes* cultures by 38.79% when compared to the relevant control (**Table 3.5**). However, the Prosur NATPRE T-10+ mix did not significantly inhibit the growth of any other tested pathogen in these experiments (see **Figure 3.9**). Meanwhile it can be seen from the data in **Table 3.7** and **Table 3.5** that eriodictyol significantly decreased the growth velocity and final CFU/ml of *S. aureus* by 84.68% and 44.11% and *L. monocytogenes* (61.24% and 35.31%, respectively). **Figures 3.9c-d** depict these effects. The flavonol quercetin significantly decreased the growth velocities of growing *S. aureus* (by 69.82%) and *L. monocytogenes* (by 40.30%) cultures by a moderate degree within these growth curve experiments. Similarly, kaempferol significantly reduced the growth velocity of *S. aureus* cultures within the same range, by 56.89% (**Figure 3.3c**).

Caffeic acid exerted an even more potent effect with a decrease in the growth velocity of *S. aureus* cultures by 79.08% (**Table 3.5** and **Figure 3.9c**) and a reduction in the final CFU/ml of the cultures by 26.01%, when compared to the relevant control. The growth of *L. monocytogenes* was also affected by caffeic acid, evidenced by a significant decrease in the growth velocity by 21.57% and the endpoint state by 35.83%, in cultures of this micro-organism.

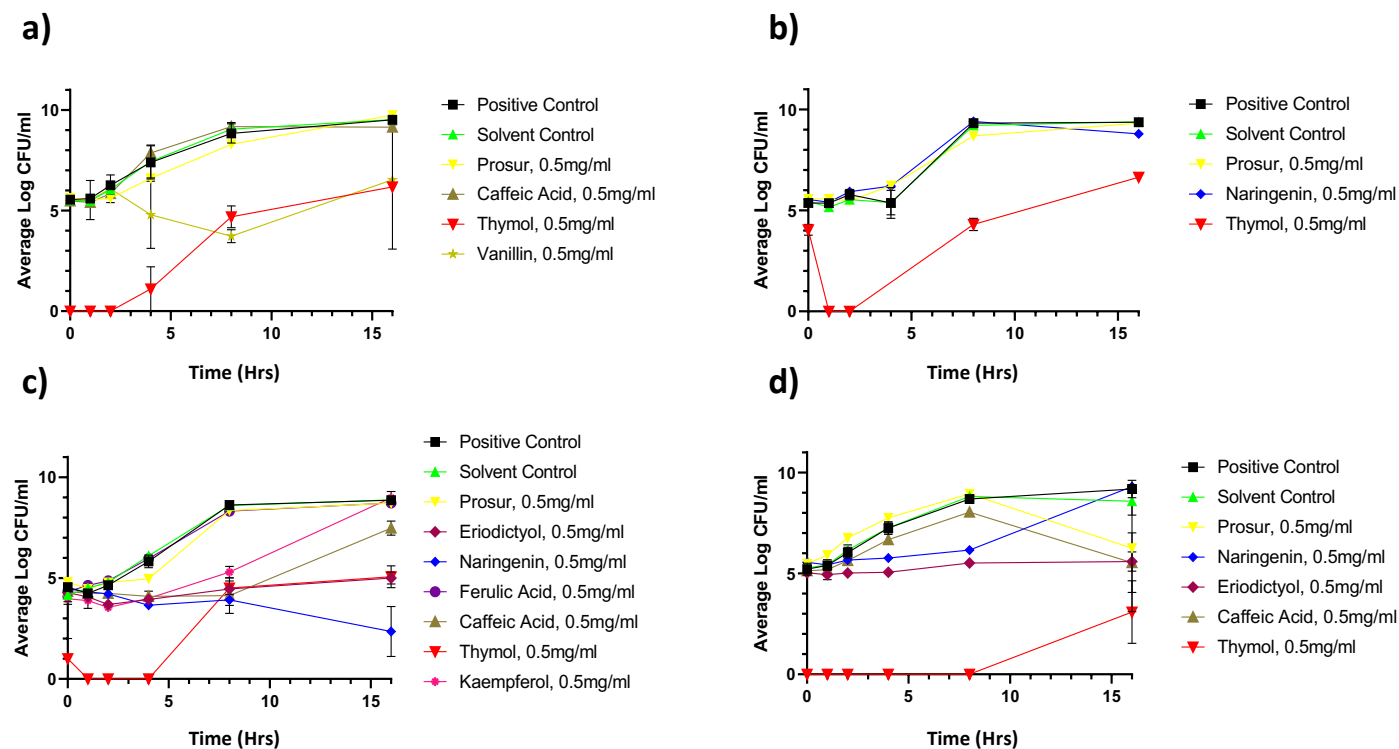
The flavanone naringenin showed statistically significant activity against all four tested pathogens (**Tables 3.2-3.5, Figures 3.9a-d**). Growing cultures of *S. enterica* challenged with

naringenin exhibited a reduced growth velocity by 57.44% and 46.24% in their final CFU/ml. Cultures of *S. aureus* were affected with a 98.07% reduced growth velocity, and a 43.19% decreased final CFU/ml. The Gram-positive *L. monocytogenes* cultures were reduced in both growth kinetic metrics by naringenin challenge, with a 48.04% reduction in growth velocity and a 70.16% reduction in the final CFU/ml.

Thymol exerted the most consistent and potent inhibitive activity across the tested pathogens (**Tables 3.2-3.5** and **Figures 3.9a-d**); with decreased growth velocities for *S. enterica* (70.20% reduction), *S. aureus* (75.88% reduction), *P. aeruginosa* (87.59% reduction) and *L. monocytogenes* (>99% reduction). Decreased final CFU/ml values were also seen for *S. enterica* (66.78% reduction), *S. aureus* (43.19% reduction), *P. aeruginosa* (29.47% reduction) and *L. monocytogenes* (70.16% reduction) as compared to the appropriate controls.

Overall, the selected phytochemicals were more effective at inhibiting the growth of the Gram-positive bacteria (*S. aureus* and *L. monocytogenes*), than the tested Gram-negative pathogens. From these data thymol was selected as the most consistently active compound with direct antimicrobial activity to be taken forward for further investigation into the bacterial responses elicited upon phytochemical challenge.

Figure 3.9: Growth curves for the tested pathogens challenged with 0.5mg/ml of various phytochemicals.



Panel **a)** *S. enterica*, **b)** *P. aeruginosa*, **c)** *S. aureus* and panel **d)** *L. monocytogenes* growth curves. Experiments were repeated with three biological replicates (three technical replicates each) over an incubation period of 16 hours. Points show the average value for each point and errors bars indicate the standard error of the mean.

Table 3.2: Summary of growth velocity impacts after challenging the Gram-negative pathogens with various phytochemicals at 0.5mg/ml concentrations.

Gram-negative pathogens growth curve average growth velocities (%)						
Phytochemical (0.5mg/ml)	<i>S. enterica</i>			<i>P. aeruginosa</i>		
	Normalised growth velocity (CFU/ml/min)	SEM (\pm)	<i>p</i> value	Normalised growth velocity (CFU/ml/min)	SEM (\pm)	<i>p</i> value
Solvent control	100	0.08	-	100	0.73	-
Prosur	98.20	0.08	0.8981	102.86	0.07	0.8000
Eriodictyol	79.10	1.00	0.1385	114.09	0.07	0.2135
Ferulic acid	75.89	0.96	0.0883	89.87	0.99	0.3705
Quercetin	89.37	0.75	0.4486	106.83	0.04	0.5446
Caffeic acid	96.50	0.08	0.8026	96.08	0.70	0.7281
Thymol	29.80	0.27	<0.0001	12.41	0.32	<0.0001
Kaempferol	104.51	0.06	0.7482	112.78	0.07	0.2584
Naringenin	42.56	1.12	<0.0001	114.99	0.07	0.1859
Vanillin	85.28	0.72	0.2952	98.66	0.06	0.9053

Data presented are the average values as percentages of the controls for the calculated growth velocity (CFU/ml/min) metric. Experiments were repeated with three biological replicates (three technical replicates each) over an incubation period of 16 hours. Values presented at 2 decimal places. Statistical analysis was performed using the GraphPad software v.8, using a 1-way repeated measures ANOVA Test with Fischer's LSD test. Values in bold were statistically, significantly, different to the relevant control.

Table 3.3: Summary of growth velocity impacts after challenging the Gram-positive pathogens with various phytochemicals at 0.5mg/ml concentrations.

Gram-positive pathogens growth curve average growth velocities (%)						
Phytochemical (0.5mg/ml)	<i>S. aureus</i>			<i>L. monocytogenes</i>		
	Normalised growth velocity (CFU/ml/min)	SEM (\pm)	<i>p</i> value	Normalised growth velocity (CFU/ml/min)	SEM (\pm)	<i>p</i> value
Solvent control	100	0.08	-	100	0.08	-
Prosur	85.48	0.63	0.1563	102.31	0.06	0.7756
Eriodictyol	15.32	0.29	<0.0001	38.76	0.31	<0.0001
Ferulic acid	86.26	0.64	0.1793	101.51	0.07	0.8530
Quercetin	30.18	0.36	<0.0001	59.70	0.91	<0.0001
Caffeic acid	20.92	0.44	<0.0001	78.43	0.60	0.0086
Thymol	24.12	0.36	<0.0001	0	0.00	<0.0001
Kaempferol	43.11	0.17	<0.0001	86.41	0.04	0.0940
Naringenin	1.93	0.11	<0.0001	51.96	0.17	<0.0001
Vanillin	81.96	0.61	0.0791	84.94	0.65	0.0638

Data presented are the average values as percentages of the controls for the calculated growth velocity (CFU/ml/min) metric. Experiments were repeated with three biological replicates (three technical replicates each) over an incubation period of 16 hours. Values presented at 2 decimal places. Statistical analysis was performed using the GraphPad software v.8, using a 1-way repeated measures ANOVA Test with Fischer's LSD test. Values in bold were statistically, significantly, different to the relevant control.

Table 3.4: Summary of impacts on final growth achieved after challenging Gram-negative pathogens with various phytochemicals at 0.5mg/ml concentrations.

Gram-negative pathogens growth curve average endpoint states (%)						
Phytochemical (0.5mg/ml)	<i>S. enterica</i>			<i>P. aeruginosa</i>		
	Normalised endpoint state (CFU/ml)	SEM (\pm)	<i>p value</i>	Normalised endpoint state (CFU/ml)	SEM (\pm)	<i>p value</i>
<u>Solvent control</u>	100	1.07	-	100	0.06	-
<u>Prosur</u>	114.48	0.06	0.2964	88.45	1.04	0.2687
<u>Eriodictyol</u>	86.45	1.08	0.3283	101.77	0.08=	0.8647
<u>Ferulic acid</u>	107.90	0.08	0.5678	99.85	0.08=	0.9886
<u>Quercetin</u>	115.10	0.04	0.2762	101.78	0.03=	0.8636
<u>Caffeic acid</u>	84.63	1.36	0.2679	98.32	0.06	0.8723
<u>Thymol</u>	33.22	0.76	<0.0001	70.53	0.12	0.0057
<u>Kaempferol</u>	113.03	0.10	0.3469	97.92	0.11	0.8417
<u>Naringenin</u>	53.76	1.44	0.0012	53.77	1.59	<0.0001
<u>Vanillin</u>	112.25	0.03	0.3764	87.32	1.02	0.2249

Data presented are the average values as percentages of the controls for the calculated endpoint state (CFU/ml) metric at the end of the 16 hour incubation period. Experiments were repeated with three biological replicates (three technical replicates each) over an incubation period of 16 hours. Values presented at 2 decimal places. Statistical analysis was performed using the GraphPad software v.8, using a 1-way repeated measures ANOVA Test with Fischer's LSD test. Values in bold were statistically, significantly, different to the relevant control.

Table 3.5: Summary of impacts on final growth achieved afters challenging Gram-positive pathogens with various phytochemicals.

Gram-positive pathogens growth curve average endpoint states (%)						
Phytochemical (0.5mg/ml)	<i>S. aureus</i>			<i>L. monocytogenes</i>		
	Normalised endpoint state (CFU/ml)	SEM (\pm)	<i>p</i> value	Normalised endpoint state (CFU/ml)	SEM (\pm)	<i>p</i> value
<u>Solvent control</u>	100	0.05	-	100	0.12	-
<u>Prosur</u>	97.78	0.09	0.7720	61.21	1.35	<0.0001
<u>Eriodictyol</u>	55.89	0.18	<0.0001	64.69	0.26	<0.0001
<u>Ferulic acid</u>	97.96	0.06	0.7904	104.53	0.03	0.5754
<u>Quercetin</u>	85.21	0.95	0.0559	98.17	0.11	0.8206
<u>Caffeic acid</u>	73.99	0.84	0.0010	64.17	0.73	<0.0001
<u>Thymol</u>	56.81	0.27	<0.0001	29.84	0.81	<0.0001
<u>Kaempferol</u>	100.77	0.16	0.9194	102.77	0.05	0.7321
<u>Naringenin</u>	19.76	0.70	<0.0001	55.79	0.60	<0.0001
<u>Vanillin</u>	90.00	0.20	0.1934	102.92	0.03	0.7183

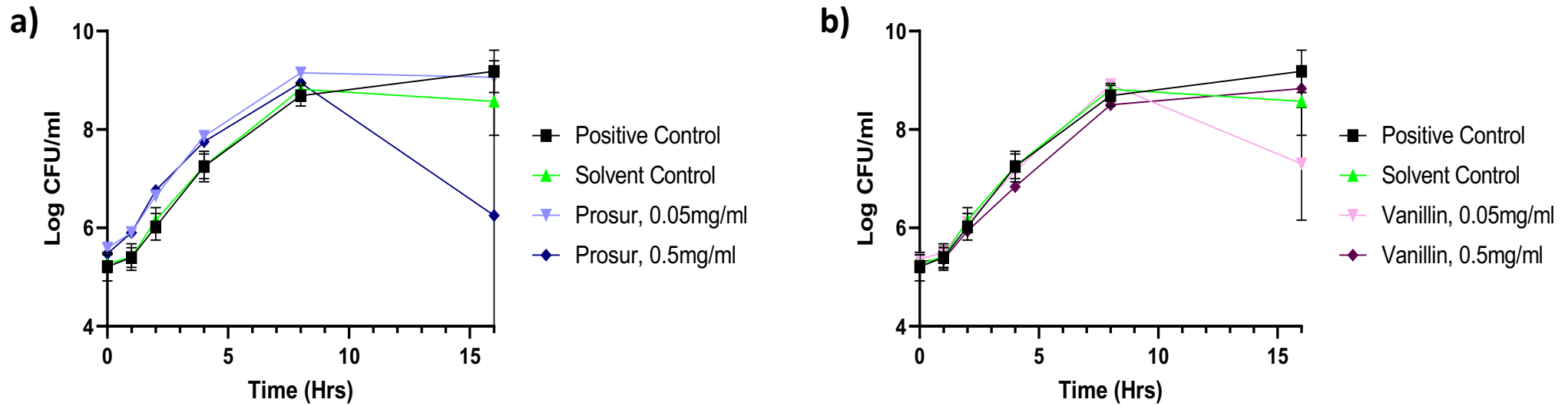
Data presented are the average values as percentages of the controls for the calculated endpoint state (CFU/ml) metric at the end of the 16 hour incubation period. Experiments were repeated with three biological replicates (three technical replicates each) over an incubation period of 16 hours. Values presented at 2 decimal places. Statistical analysis was performed using the GraphPad software v.8, using a 1-way repeated measures ANOVA Test with Fischer's LSD test. Values in bold were statistically, significantly, different to the relevant control.

3.2.5 Dose-dependent effects were observed for some compounds, including the Prosur NATPRE T-10+ mix

To determine the input of different doses, viability experiments were repeated with a 10-fold lower dose of each compound. The results are displayed in **Table 3.6** and **Figure 3.10** with full data in the **Appendix, Section 9.3**.

The Prosur NATPRE T-10+ mix at 0.5mg/ml was able to significantly reduce the endpoint achieved by *L. monocytogenes* cultures by 38.79% (see **Section 3.2.4, Table 3.5, Figure 3.10a**), but no effect was observed at the lower concentration (**Table 3.6**). The phenolic aldehyde vanillin, on the other hand, exhibited significant effects at 0.05mg/ml on the growth kinetics of *S. aureus* (with 25.17% and 24.41% reductions in the growth velocity and final CFU/ml, respectively), *P. aeruginosa* (a 22.35% decrease) and a reduced final CFU/ml of *L. monocytogenes* cultures by 15.42% when compared to the relevant controls. These effects were not apparent at a concentration of 0.5mg/ml (see **Figure 3.10b**). These results indicate a dose-dependent effect on the inhibitive activity of, at least certain, phytochemical compounds.

Figure 3.10: Growth curves for two pathogens challenged with 0.5 and 0.05mg/ml of vanillin and the Prosur NATPRE T-10+ mix.



Panel a) *L. monocytogenes* growth curves challenged with 0.05mg/ml and 0.5mg/ml Prosur NATPRE T-10+ mix, b) *L. monocytogenes* growth curves challenged with 0.05mg/ml and 0.5mg/ml vanillin. Experiments were repeated with three biological replicates (three technical replicates each) over an incubation period of 16 hours. Points show the average value for each point and errors bars indicate the standard error of the mean.

Table 3.6: Summary of growth curves challenging the Gram-positive pathogens with various phytochemicals at 0.05mg/ml.

Gram-positive pathogens growth curve endpoint states (%)						
Phytochemical (0.05mg/ml)	<i>S. aureus</i>			<i>L. monocytogenes</i>		
	Normalised Endpoint State (vCFU/ml)	SEM (\pm)	<i>p</i> value	Normalised Endpoint State (vCFU/ml)	SEM (\pm)	<i>p</i> value
Solvent Control	100	0.22	-	100	0.12	-
Prosur	103.83	0.14	0.7205	105.73	0.03	0.4484
Eriodictyol	68.26	1.29	0.0038	99.64	0.14	0.9623
Ferulic Acid	101.26	0.08	0.9069	104.34	0.07	0.5657
Quercetin	106.52	0.03	0.5427	54.06	1.17	<0.0001
Caffeic Acid	107.36	0.03	0.4916	44.85	1.15	<0.0001
Thymol	25.86	1.15	<0.0001	99.63	0.06	0.9601
Kaempferol	102.30	0.21	0.8297	106.39	0.04	0.3983
Naringenin	22.61	0.80	<0.0001	102.74	0.03	0.7159
Vanillin	75.59	0.86	0.0246	84.58	0.56	0.0435

Data presented are the average values as percentages of the controls for the calculated endpoint state metric (CFU/ml) metric at the end of the 16 hour incubation period. Experiments were repeated with three biological replicates (three technical replicates each) over an incubation period of 16 hours. Values presented at 2 decimal places. Statistical analysis was performed using the GraphPad software v.8, using a 1-way repeated measures ANOVA Test with Fischer's LSD test. Note the significant *p* values obtained for the use of vanillin against *L. monocytogenes* at 0.05mg/ml, not observed at 0.5mg/ml. Values in bold were statistically, significantly, different to the relevant control.

3.2.6 Caffeic acid, amongst other compounds, increases the drug accumulation in tested pathogens

Following on from the semi-high throughput potentiation assays, drug accumulation assays were used to further assess the tested phytochemicals potentiative capacity. Resazurin was used as a model fluorescent drug for *S. enterica* and *P. aeruginosa*, while EtBr was used for *S. aureus* and *L. monocytogenes*. This is shown in **Tables 3.7-3.10** and **Figure 3.11** and in the **Appendix, Section 9.3**.

Six of the nine tested compounds exerted a significant increase in the tested pathogens fluorescent substrate accumulation kinetics. Quercetin and kaempferol, being highly pigmented compounds, were found to be unsuitable for these assays due to the high level of background noise within the measured fluorescence readings when these compounds were present. Eriodictyol, however, significantly increased the fluorescence accumulation velocity of tested *L. monocytogenes* cultures by 167.68% when compared to the relevant controls (**Table 3.8**). Naringenin increased the fluorescence accumulation velocity of *S. enterica* cultures by 17.93%; meanwhile ferulic acid exerted a 29.14% increase in drug accumulation for the same pathogen (**Table 3.8, Figure 3.11**). In addition to these observed effects, ferulic acid induced a statistically significant 86.53% increase in the fluorescence accumulation velocity, and a 150.17% increase in the steady state fluorescence, of *P. aeruginosa* cultures.

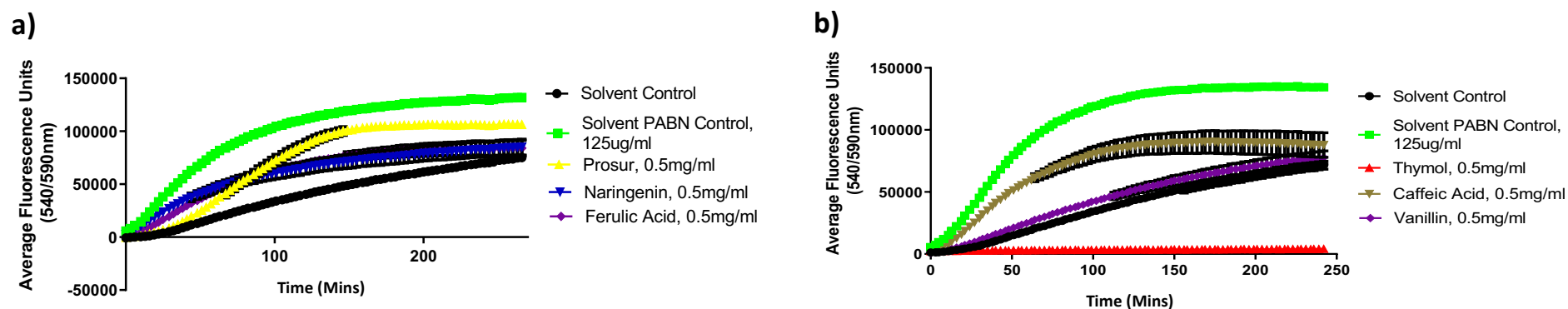
Vanillin was only significantly effective at increasing the steady state fluorescence of one pathogen, *P. aeruginosa*, by 71.61%. Similarly, caffeic acid only significantly increased the fluorescence accumulation velocity of *S. enterica* cultures, by 40.80%, when compared to the relevant controls; this is displayed in **Figure 3.11b**. The Prosur NATPRE T-10+ mix was particularly potent at increasing the drug accumulation of the tested pathogens. This phytochemical mixture increased the fluorescent drug accumulation velocities of *S. enterica* and *P. aeruginosa* cultures by 69.80% and 200.56%, respectively, while *P. aeruginosa* and *L. monocytogenes* cultures challenged with the Prosur NATPRE T-10+ mix exhibited an increased steady state fluorescence of 218.34% and 709.83% respectively, when compared to the relevant controls (**Figure 3.11a**).

Multiple phytochemicals induced significant decreases in the drug accumulation for some species. Examples from **Tables 3.7-3.10** include the Prosur NATPRE T-10+ mix against *S.*

aureus (with a 47.54% fluorescence accumulation velocity decrease), *L. monocytogenes* (a decrease of 72.46% in the same metric) and a 23.01% decrease in the steady state fluorescence of tested *S. enterica* cultures. Caffeic acid exhibited a similar influence on *S. enterica* and *S. aureus* with decreases in their steady state fluorescence metric of 46.30% and 92.28%, respectively, in addition to an 86.90% decrease in the fluorescence accumulation velocity in *S. aureus* cultures. Naringenin in comparison decreased the steady state fluorescence of *S. aureus* (79.54%) and the fluorescence accumulation velocities of *S. aureus* and *P. aeruginosa* by 83.31% and 83.37%, respectively.

From these data caffeic acid was selected as a representative compound with potential as a synergistic agent to be taken forward for further investigation into the bacterial responses elicited upon phytochemical challenge. The Prosur NATPRE T-10+ mix was also selected as a candidate for further study due to its potency within these drug accumulation assays, as well as its relevance as a current industrial standard for alternative food preservatives.

Figure 3.11: Exemplar resazurin accumulation assays for *S. enterica* challenged with 0.5mg/ml of various phytochemicals.



Panel a) *S. enterica* resazurin accumulation assays challenged with 0.5mg/ml of ferulic acid, naringenin and the Prosur NATPRE T-10+ mix. b) *S. enterica* resazurin accumulation assays challenged with 0.5mg/ml of thymol, caffeic acid and vanillin. PaβN is a positive control known to increase drug accumulation. Experiments were repeated with three biological replicates (five technical replicates each) over an incubation period of 16 hours, then trimmed to an appropriate timescale where the accumulation curves begun to plateau.

Table 3.7: Summary of resazurin accumulation assays challenging the Gram-negative pathogens with various phytochemicals at 0.5mg/ml concentrations.

Gram-negative pathogens average resazurin accumulation velocities (%)						
Phytochemical (0.5mg/ml)	<i>S. enterica</i>			<i>P. aeruginosa</i>		
	Normalised fluorescence accumulation velocity (Fluorescence Units/min)	SEM (\pm)	<i>p</i> value	Normalised fluorescence accumulation velocity (Fluorescence Units/min)	SEM (\pm)	<i>p</i> value
Solvent control	100	12.28	-	100	14.55	-
Positive control	197.30	5.95	<0.0001	506.62	30.74	<0.0001
Prosur	169.80	15.57	<0.0001	300.56	37.47	<0.0001
Eriodictyol	108.53	4.03	0.3430	24.96	2.73	0.0449
Ferulic acid	129.14	26.82	0.0014	186.53	3.56	0.0210
Quercetin	2.23	N/D	N/D	-282.52	N/D	N/D
Caffeic acid	140.80	47.14	<0.0001	108.54	3.41	0.8184
Thymol	2.36	0.43	<0.0001	4.18	0.21	0.0108
Kaempferol	108.91	18.82	0.3218	57.33	10.80	0.2521
Naringenin	117.93	30.66	0.0473	16.63	2.84	0.0261
Vanillin	104.80	25.57	0.5938	84.21	2.65	0.6713

Data presented are the average values as percentages of the controls for the calculated fluorescence accumulation velocity (Fluorescence units/min) metric. Experiments were repeated with three biological replicates (five technical replicates each) over an incubation period of 16 hours, trimmed to an appropriate timescale where the accumulation curves begun to plateau. Values presented at 2 decimal places. Statistical analysis was performed using the GraphPad software v.8, using a 1-way repeated measures ANOVA Test with Fischer's LSD test. Values in bold were statistically, significantly, different to the relevant control.

Table 3.8: Summary of EtBr accumulation assays challenging the Gram-positive pathogens with various phytochemicals at 0.5mg/ml concentrations.

Gram-positive pathogens average EtBr accumulation velocities (%)						
Phytochemical (0.5mg/ml)	<i>S. aureus</i>			<i>L. monocytogenes</i>		
	Normalised fluorescence accumulation velocity (Fluorescence Units/min)	SEM (\pm)	<i>p value</i>	Normalised fluorescence accumulation velocity (Fluorescence Units/min)	SEM (\pm)	<i>p value</i>
Solvent control	100	97.15	-	100	12.02	-
Positive control	95.34	61.60	0.7157	565.91	64.85	<0.0001
Prosur	52.46	36.82	0.0003	-27.54	8.23	0.0310
Eriodictyol	62.45	80.66	0.0038	267.68	50.83	0.0048
Ferulic acid	12.96	5.768	<0.0001	57.69	2.36	0.4713
Quercetin	7.20	6.64	N/D	8.72	12.84	N/D
Caffeic acid	13.10	3.10	<0.0001	-10.70	9.43	0.0608
Thymol	-34.90	16.69	<0.0001	89.11	18.20	0.8528
Kaempferol	14.01	10.41	<0.0001	48.06	13.63	0.3768
Naringenin	16.69	9.03	<0.0001	-5.39	8.68	0.0740
Vanillin	1.38	1.48	<0.0001	5.02	0.55	0.1071

Data presented are the average values as percentages of the controls for the calculated fluorescence accumulation velocity (Fluorescence units/min) metric. Experiments were repeated with three biological replicates (five technical replicates each) over an incubation period of 16 hours, trimmed to an appropriate timescale where the accumulation curves begun to plateau. Values presented at 2 decimal places. Statistical analysis was performed using the GraphPad software v.8, using a 1-way repeated measures ANOVA Test with Fischer's LSD test. Values in bold were statistically, significantly, different to the relevant control. Values in bold were statistically, significantly, different to the relevant control.

Table 3.9: Summary of resazurin accumulation assays challenging the Gram-negative pathogens with various phytochemicals at 0.5mg/ml concentrations.

Gram- negative pathogens average steady state resazurin accumulation (%)						
Phytochemical (0.5mg/ml)	<i>S. enterica</i>			<i>P. aeruginosa</i>		
	Normalised steady state fluorescence accumulation (Fluorescence Units)	SEM (\pm)	<i>p</i> value	Normalised steady state fluorescence accumulation (Fluorescence Units)	SEM (\pm)	<i>p</i> value
Solvent control	100	887.20	-	100	5517	-
Positive control	100	789.60	0.7690	370.21	4027	<0.0001
Prosur	76.99	9701	0.0007	318.34	3969	<0.0001
Eriodictyol	79.63	1133	0.0026	36.11	1192	<0.0001
Ferulic acid	59.64	11683	<0.0001	250.17	807.5	<0.0001
Quercetin	4.06	N/D	N/D	N/D	N/D	N/D
Caffeic acid	53.70	9890	<0.0001	107.66	1496	0.5869
Thymol	4.37	380.60	<0.0001	4.09	189.2	<0.0001
Kaempferol	51.63	1199	<0.0001	44.49	2722	<0.0001
Naringenin	88.52	2307	0.0867	74.02	1565	0.0668
Vanillin	75.64	6260	0.0003	171.61	3806	<0.0001

Data presented are the average values as percentages of the controls for the calculated steady state fluorescence accumulation (Fluorescence units/min) metric. Experiments were repeated with three biological replicates (five technical replicates each) over an incubation period of 16 hours, trimmed to an appropriate timescale where the accumulation curves begun to plateau. Values presented at 2 decimal places. Statistical analysis was performed using the GraphPad software v.8, using a 1-way repeated measures ANOVA Test with Fischer's LSD test. Values in bold were statistically, significantly, different to the relevant control.

Table 3.10: Summary of EtBr accumulation assays challenging the Gram-positive pathogens with various phytochemicals at 0.5mg/ml concentrations.

Gram-positive pathogens average steady state EtBr accumulation (%)						
Phytochemical (0.5mg/ml)	<i>S. aureus</i>			<i>L. monocytogenes</i>		
	Normalised steady state fluorescence accumulation (Fluorescence Units)	SEM (\pm)	<i>p</i> value	Normalised steady state fluorescence accumulation (Fluorescence Units)	SEM (\pm)	<i>p</i> value
Solvent Control	100	20488	-	100	2901	-
Positive Control	108.03	20032	0.5893	1024.55	23660	<0.0001
Prosur	106.33	9631	0.6704	809.83	15129	<0.0001
Eriodictyol	16.82	11308	<0.0001	128.89	2630	0.7475
Ferulic Acid	13.11	1894	<0.0001	71.58	769.6	0.7515
Quercetin	5.91	N/D	N/D	12.27	1095	N/D
Caffeic Acid	7.02	986.90	<0.0001	-1.51	1590	0.2588
Thymol	93.37	3219	0.6558	386.07	10075	0.0017
Kaempferol	31.46	3307	<0.0001	148.95	1307	0.5855
Naringenin	20.46	3114	<0.0001	59.46	1381	0.6515
Vanillin	0.77	155.50	<0.0001	11.02	330.20	0.3220

Data presented are the average values as percentages of the controls for the calculated steady state fluorescence accumulation (Fluorescence units/min) metric. Experiments were repeated with three biological replicates (five technical replicates each) over an incubation period of 16 hours, trimmed to an appropriate timescale where the accumulation curves begun to plateau. Values presented at 2 decimal places. Statistical analysis was performed using the GraphPad software v.8, using a 1-way repeated measures ANOVA Test with Fischer's LSD test. Values in bold were statistically, significantly, different to the relevant control.

3.3 Chapter Discussion

Although the antimicrobial activity of phytochemicals has been researched, with multiple studies published, there remains a great deal of variance in the active concentrations and spectra of activity reported. As this may be due to technical specifics (growth medium, inoculum density, pH etc.), a side-by-side baseline for a comparative activity analysis against the foodborne pathogens tested in this thesis was required. The data presented here shows the comparative activity of 14 compounds in the same controlled conditions, against a panel of foodborne pathogens. This allows the relative inherent antimicrobial activity, and the potential to act synergistically, of each compound to be measured. To identify the most potent phytochemicals from the panel (**Section 3.2.1**), semi-high throughput screening assays (**Sections 3.2.2-3.2.3**) were used.

Although other publications have used a variety of methods which make direct comparisons difficult, some similarities to the data generated here were seen. For example, cinnamic acid showed activity here against *S. enterica* and *P. aeruginosa* at 0.5mg/ml, similar to other studies with a range of 0.06-1mg/ml^[207, 208] although previously reported activity against *S. aureus* and *L. monocytogenes*^[207, 208] was not replicated here. The antimicrobial activity of eriodictyol has been observed previously, although within this thesis I present antimicrobial activity at a lower concentration of 0.125mg/ml against *S. aureus* than has been published in some studies (800µg/ml against *S. enterica* and *S. aureus*)^[209]. The antimicrobial activity of naringenin observed within this set of experiments (**Section 3.2.2**) is corroborated by the existing literature, with studies^[209-211] publishing MICs ranging from up to 400µg/ml against MRSA, although here I observed significant activity at as low a concentration as 0.125mg/ml against *S. aureus*; expanding the active range of this compound.

There were also some discrepancies between these data and the literature. Although thymol has extensively been described as having antimicrobial properties^[131, 212-214], these have usually detailed potent activity as being present at much lower concentrations than observed here, for example against *S. enterica* Typhimurium in the range of 55-150µg/ml and *S. aureus* at 225-400µg/ml^[131, 212].

The potential for some phytochemicals to potentiate the action of classic antibiotic compounds has also been reported^[153, 215-217]. Eriodictyol derivatives have been presented as displaying efflux pump inhibiting activities against multi-drug resistant *S. aureus* and MRSA^[218], supporting the results from the potentiation assays discussed here (**Section 3.2.3**). Ferulic and caffeic acids have also had synergistic interactions reported with streptomycin, lowering the MIC of this antibiotic against strains of *E. coli* and *P. aeruginosa*^[219].

In the growth curve experiments performed, caffeic acid displayed statistically significant inhibition against *S. aureus* and *L. monocytogenes*, inducing a reduced growth velocity and final CFU/ml for both micro-organisms at a 0.5mg/ml concentration (**Section 3.2.4**). This inhibitive capacity is similar to other work with *L. monocytogenes*^[220], reporting inhibition at a caffeic acid concentration of 1.5mg/ml^[221]. In this body of work caffeic acid exerted significant inhibitory activity against *S. aureus* and *L. monocytogenes* (**Section 3.2.4**); both Gram-positive micro-organisms which reflects a common pattern of phytochemicals tending to exert a more potent effect on Gram-positive than Gram-negative bacterial species^[141, 222-224]. There have been reports of caffeic acids inhibitive activity against *S. enterica* Typhimurium^[225] and other Gram-negative bacteria at 500µg/well concentrations^[226], which were not replicated here.

Multiple phytochemicals have been suggested to have the ability to potentiate antibiotics and synergise with other phytochemical compounds^[227-229] with membrane permeabilization a potential mechanism that explains this. Here, this was indirectly measured by determining accumulation of fluorescent substrates, resazurin or EtBr which are normally unable to accumulate within cells to a significant level (**Section 3.2.6**). Caffeic acid significantly increased the fluorescence accumulation velocity of *S. enterica* Typhimurium samples (**Section 3.2.6**), which is in agreement with the work of **(Hemaiswarya S. and Doble M. 2010)**^[230] who suggested that caffeic acid's mechanism of action was via membrane damage, which would consequently permeabilise this bacterial barrier. Synergy of caffeic acid with antibiotics has also been observed in time-kill curve experiments against *E. coli*, *P. aeruginosa* and *S. aureus*^[230-233] although no impact was seen here for the latter two species. Due to the significant potentiative activity exerted against *S. enterica* Typhimurium, and the trends observed across the other tested micro-organisms, caffeic acid was selected for further examination within this project.

Ferulic acid displayed no ability to significantly inhibit the growth of *S. enterica* Typhimurium, *S. aureus*, *P. aeruginosa* or *L. monocytogenes* in the growth curves (**Section 3.2.4**). Previous studies report contrasting results for ferulic acid's antimicrobial ability, while (**Pernin A. et al 2019**)^[234] found no inhibitive activity against *L. monocytogenes* with ferulic acid at a concentration of >30mmol/L, other studies have published activity against *E. coli* and *S. enterica* at 500µg/well^[226]. In terms of this hydroxycinnamic acid's potentiative capacity (**Section 3.2.6**), studies support the increased drug accumulation observed here with *S. enterica* and *P. aeruginosa* cultures exposed to ferulic acid^[230, 235]. A proposed mechanism for this activity is the ability of ferulic acid to reduce the cell surfaces' negative charge and to form pores, leading to irreversible membrane changes^[235].

The work here with quercetin (**Section 3.2.4**) demonstrating growth inhibition against Gram-positive species is supported by previous publications, (**Vaquero M.J.R. et al 2007**)^[220] showed *L. monocytogenes* growth inhibition using this flavonol, while methicillin-sensitive and resistant *S. aureus* strains have been significantly inhibited in a dose-dependent manner in growth curves challenged with quercetin^[236]. *P. aeruginosa* was not significantly inhibited by quercetin (**Section 3.2.4**); this observation is consistent with *P. aeruginosa* growth curves from (**Ouyang J. et al 2016**)^[237] but the data generated here contrasts publications that have reported quercetin significantly inhibiting the growth of *S. enterica* Typhimurium^[238, 239] and *S. enterica* Enteritidis^[240].

The flavonol kaempferol exerted significant inhibitive activity against *S. aureus* in the growth curves performed here (**Section 3.2.4**), which agrees with previous work^[241], although at a lower range of concentrations^[242]. However, other studies utilising growth curve assays found no significant antimicrobial activity against *S. aureus*^[243, 244], in contrast to the data gathered here. Similar to quercetin, kaempferol's highly pigmented nature made it unsuitable for the drug accumulation assay methodology chosen (**Section 3.2.6**).

In the growth curves used here (**Section 3.2.4**), naringenin displayed significant antimicrobial activity against all four pathogens tested. This inhibitive potential is supported by publications involving *S. aureus*^[245-247], *P. aeruginosa*^[246, 247], *S. enterica* species^[247] and *L. monocytogenes*. This antimicrobial activity has also been shown to

extend to other species including *E. coli*^[246, 247]. In terms of influencing the drug accumulation of foodborne pathogens (**Section 3.2.6**), naringenin significantly increased the fluorescence accumulation velocity of *S. enterica* Typhimurium but no other species. This finding supports a proposed membrane disruption mechanism of action for naringenin-derived compounds^[248]. There are some reports that conflict with the data gathered here however, concerning the membrane permeabilising potential of naringenin. Both **(Wang L.-H. et al 2017)**^[249] and **(Gao Y. et al 2021)**^[247] present the bioactivity of naringenin against cells of *S. aureus*, citing damage and disruption of the cytoplasmic membrane; the lack of fluorescence accumulation observed in the drug accumulation assays performed here may be due to a difference in methodology and concentrations used in these experiments.

The data from the vanillin growth curves are interesting. No pathogen was inhibited to a statistically significant level by vanillin at 0.5mg/ml (**Section 3.2.4**) however significant growth inhibition was displayed, to various degrees, against *S. aureus*, *P. aeruginosa* and *L. monocytogenes* at 0.05mg/ml (**Section 3.2.5**). Although dose-dependent effects are not a novel phenomenon surrounding the use of antimicrobial phytochemicals^[225] this negative correlation between compound concentration and bacterial inhibition is intriguing and not generally consistent with the pre-existing literature. Researchers have reported the inhibitive effects of vanillin against such micro-organisms as *B. cereus* in carrot broth at an equivalent concentration of 0.5mg/ml^[250]. While this activity could be explained by interactions between the compound and constituent components of the carrot broth raising the bioactive concentration, inhibitive activity has been presented by **(Karaosmanoglu H. et al 2010)**^[251] who observed a 73% reduction in the growth rate of *E. coli* strain O157:H7 at an equivalent 0.91mg/ml vanillin (6mM vanillin) in standard laboratory growth medium. Other studies have repeatedly presented the antimicrobial activity of vanillin within a range of 0.5-13mg/ml^[252], using various methodologies including growth curves using vanillin at a 1.5mg/ml (10mM) concentration^[253]. In parallel, some studies have supported the work within this project, reporting no significant antimicrobial activity from vanillin alone against *E. coli*, *S. aureus* and *P. aeruginosa*^[254]. In terms of vanillin's potentiative efficacy, the data from these drug accumulation assays (**Section 3.2.6**), and the literature agree better. **(Arya S.S. et al 2019)**^[255] utilised an EtBr - based assay to determine that vanillin-capped gold nanoparticles could block efflux pump systems of *P. aeruginosa* clinical isolates; supporting the significant increase in the steady

state fluorescence of *P. aeruginosa* cultures challenged with this compound in this project. Other studies report the potential for vanillin to permeabilise bacterial membranes via disruption of the phospholipid repair system and cell surface integrity of bacterial cells^[256-258]. Nevertheless, the lack of significantly increased, vanillin-induced drug accumulation against the other pathogens utilised within this project is at odds with studies^[259] who reported this activity against *E. coli* and *L. innocua* using a propidium iodide assay.

Eriodictyol was found to significantly inhibit the growth of *S. aureus* and *L. monocytogenes* (**Section 3.2.4**). This activity can be corroborated by the existing literature^[260] with a reported MIC of the compound at 512µg/ml against *S. aureus*^[261], eriodictyol derivatives 2,8-diprenyleriodictyol^[262] and 7-O-methyleriodictyol^[263] having also shown antimicrobial activity against *S. aureus*. Other micro-organisms inhibited in their growth by this flavanone include *E. coli*, *S. enterica*, *P. aeruginosa* and *P. putida* at concentrations ranging from 250-800µg/ml^[209], which was not replicated here with *S. enterica* Typhimurium or *P. aeruginosa*.

The Prosur NATPRE T-10+ mix was generally ineffective at inhibiting the growth of the tested pathogens within this project, only significantly affecting the final CFU/ml of *L. monocytogenes* cultures in the growth curve experiments (**Section 3.2.4**). As a commercial product there is very little in the published literature concerning its antimicrobial activity but its major constituents (eriodictyol, ferulic acid and naringenin) indicate that activity may have been expected. A potential reason for the Prosur NATPRE T-10+ mix's lack of inhibitive activity within this project may be due to the lower concentrations of each of these constituent phytochemicals, as opposed to the concentrations tested for the pure phytochemicals. In addition, the implementation of this phytochemical mixture in the food industry is recommended as including at least a heat treatment; this pre-treatment may act as a thermal catalyst to heighten its antimicrobial properties. The Prosur NATPRE T-10+ mix did display significant potential in increasing the drug accumulation by *S. enterica*, *P. aeruginosa* and *L. monocytogenes* (**Section 3.2.6**). Again, turning to the literature surrounding the constituent compounds may suggest supporting evidence for this commercial product's potentiative capacity, especially considering the synergy many phytochemicals display together. Ultimately, the Prosur NATPRE T-10+ mixture was selected for further experimentation in this project due to its potentiative performance

and for its use as a current industry standard for alternative, phytochemical-based food preservatives.

Exhibiting some of the most potent and consistent antimicrobial activity against the pathogen panel tested here, thymol exerted inhibitive effects against the growth of *S. enterica*, *S. aureus*, *P. aeruginosa* and *L. monocytogenes* (**Section 3.2.4**). This bioactivity has been repeated previously^[264-268] at a concentration range of 40-100mg/ml^[264]. In terms of the drug accumulation assays (**Section 3.2.6**), the rapid bactericidal effect of thymol makes measuring the accumulation difficult. Dead cells lack the ability to metabolize resazurin (see **Section 2.5.0**) resulting in low fluorescence readings which may under-report the amount of drug within the cell. Samples of the drug accumulation assays were plated after the completion of their fluorescence readings, confirming the absence of viable CFU in the sample wells after thymol exposure. Despite this, other studies have reported the capacity of thymol to permeabilise the bacterial membrane, using alternative methodologies. Implementing flow cytometry and fluorescent dye assays, (**Xu J. et al 2008**)^[269] found that thymol's antimicrobial effects were the result of the compound's ability to depolarise and permeabilise the cytoplasmic membrane of *E. coli*, at 0.2mg/ml. Membrane permeability assays based upon measurements of suspension conductivity, in combination with microscopy, have also revealed that thymol was able to disrupt the *S. aureus* membrane integrity^[270].

Conclusions drawn from this chapter are:

- Phytochemicals from the 14-compound panel displayed different degrees of inhibitory and potentiative activity. Non-glycosylated compounds generally presented more potent activity than their glycosylated structures (e.g.; quercetin vs. rutin, naringenin vs naringin).
- Selected phytochemicals (in particular thymol) demonstrated bactericidal activity against the tested pathogens.
- Some phytochemicals (caffeic acid, and the Prosur NATPRE T-10+ mix) exhibited a capacity to significantly increase the drug accumulation of the tested pathogens.

The data presented here shows the comparative activity of a range of compounds in the same controlled conditions against a panel of foodborne pathogens. This allows the relative inherent antimicrobial activity, and the potential to act synergistically, of each compound to be measured. Thymol was taken forward for mechanistic studies as the most directly antimicrobial

agent, as well as caffeic acid and the Prosur NATPRE T-10+ mix, due to their synergistic potentials. To understand mechanisms of action as well as potential resistance, the selection of resistant mutants to thymol, caffeic acid and the Prosur NATPRE T-10+ mix is described in the next chapter.

Chapter 4: Selection & characterisation of thymol-tolerant mutant strains

“Life, uh, finds a way.”- Dr. Ian Malcolm, Jurassic Park, 1993

4.1. Chapter introduction

The lifespan of an effective antimicrobial can be challenged by the emergence of mutant pathogenic strains resistant to its effects. This is evident with classic antibiotic compounds as their efficacy over time has diminished with the increasing rate of AMR^[111]. Few studies have focused upon the bacterial response and resistance to phytochemicals. After the comparative analysis and selection of three phytochemicals (thymol, caffeic acid and the Prosur NATPRE T-10+ mix) within **Chapter 3**, this chapter describes attempts at selecting mutant strains resistant to the antimicrobial actions of the three selected phytochemicals.

First, suitable concentrations of thymol, caffeic acid and the Prosur NATPRE T-10+ mix were identified (via microdilution broth methods) for use in selective agar plating experiments. The resulting putative mutant colonies were then collected, sequenced, and phenotypically assayed using (i) thymol microdilution agar MIC assays, (ii) antibiotic microdilution broth MIC assays, (iii) drug accumulation assays, (iv) growth curves, (v) crystal violet assays and (vi) congo red plating.

Hypotheses:

- 1.** The selected phytochemicals will select for resistant mutant strains of the tested foodborne pathogens.
- 2.** Sequencing of the selected mutant strains will identify mutations located in loci associated with classical AMR.
- 3.** Assaying of the selected mutant strains will reveal distinct phenotypes compared to the parental strains; superior growth in the presence of selective agents and cross-resistance to classic antibiotic compounds

4.2 Results

4.2.1 Identifying appropriate phytochemical concentrations for use in mutant selection experiments

Although previous experiments (see **Chapter 3**) have identified the bioactivity of the selected phytochemicals at various concentrations, for the generation of candidate mutant strains resistant to the inhibitive action of the three selected phytochemicals a much denser inoculum must be used. Due to this, the MICs of thymol, caffeic acid and the Prosur NATPRE T-10+ mix against a $\sim 10^7$ CFU/ml inoculum of *S. enterica*, *S. aureus*, *P. aeruginosa* and *L. monocytogenes* were determined. **Table 4.1** displays the results of the microdilution broth MIC assays (see **Section 2.6.1**) utilised to quantify these concentrations. The Prosur NATPRE T-10+ mix presented MICs in the range of 1-4mg/ml for *S. aureus*, *P. aeruginosa* and *L. monocytogenes*, however due to solubility issues a concentration of >4mg/ml for *S. enterica* cultures was impractical to test. Caffeic acid displayed MIC values ranging from 0.25-2mg/ml against *S. aureus*, *P. aeruginosa* and *L. monocytogenes*, however again due to solubility issues, a concentration of >4mg/ml was impractical to test for cultures of *S. enterica*. Thymol inhibited the growth of all four pathogens at concentrations ranging from 0.5-2mg/ml. Thus, to accommodate for the larger inocula used in the selection of candidate mutant strains, the phytochemical concentrations displayed in **Table 4.1** were utilised with one exception. Thymol at 0.5mg/ml failed to produce single candidate colonies of *S. aureus* (most likely due to variation between solid and liquid phase growth), however 0.25mg/ml was successful.

Table 4.1: Phytochemical MICs (mg/ml) for high density inocula of each tested pathogen.

High density inoculum phytochemical MICs (mg/ml) (n=2)			
Micro-organism	Phytochemical		
	Prosur NATPRE T-10+ Mix	Thymol	Caffeic acid
<i>S. enterica</i>	>4	0.5	>4
<i>S. aureus</i>	1	0.5	0.5
<i>P. aeruginosa</i>	4	2	2
<i>L. monocytogenes</i>	2	1	0.25

MICs (mg/ml) for thymol, caffeic acid and the Prosur NATPRE T-10+ mix against high density inocula ($\sim 10^7$ CFU) of the four tested pathogens within this body of work. Note that for the Prosur NATPRE T-10+ mix against *S. enterica*, a concentration of 4mg/ml was still not enough to inhibit bacterial growth. Experiments were repeated with one technical replicate for two biological replicates, MICs were observed as the phytochemical concentration that lacks culture turbidity.

4.2.2 Thymol retains capacity to select for candidate resistant mutants

To determine if the three selected phytochemicals could select for resistant mutant strains of the tested bacteria, mutant selection on phytochemical-laced agar experiments were used. The results of this set of experiments (see **Section 2.7.0**) are described as follows and are displayed in **Table 4.2**. At the concentrations described in **Table 4.1** of **Section 4.2.1**, caffeic acid and the Prosur NATPRE T-10+ mix did not select for single colonies, instead allowing for the complete growth of a bacterial lawn in all species. Considering the comparably weak antimicrobial activity previously displayed by this phytochemical and mixture, these compounds were subsequently dropped to focus on the most antimicrobial of the selected three compounds.

Thymol was successful at selecting single, candidate resistant mutant colonies of *S. enterica*, *S. aureus* and *P. aeruginosa*. The laced-agar plates containing *L. monocytogenes*, however, were not able to grow single colonies nor a bacterial lawn. Due to time constraints and the presence of colonies on agar plates of the other tested pathogens, *L. monocytogenes* was not pursued any further from this point on to determine if thymol could select for resistant strains of this micro-organism. Thymol at 0.5mg/ml selected for single colonies of *S. enterica* with a frequency of 6.84×10^{-9} . Eight colonies were randomly selected for further testing and sequencing. At 2mg/ml, thymol selected candidate mutant colonies of *P. aeruginosa* at a rate of 3.01×10^{-8} ; four were randomly selected for sequencing and phenotyping. As stated in **Section 4.2.1**, 0.5 mg/ml of thymol failed to produce single candidate colonies of *S. aureus* in this experiment, however a 0.25mg/ml concentration did select mutants at a frequency of 1.47×10^{-7} . Four colonies were again randomly selected for further experimentation and sequencing. The average mutation frequency across the three micro-organisms was calculated to be 3.77×10^{-8} . With a suitable number of candidate mutant strains selected against the antimicrobial actions of thymol, the MICs of these pathogens were subsequently quantified in microdilution agar MIC assays to confirm their apparent resistance.

Table 4.2: Mutation frequencies of the tested pathogens against the selected phytochemicals.

Mutation frequencies of tested pathogens (n=1)			
Micro-organism	Selecting phytochemical		
	Prosur NATPRE T-10+ Mix	Thymol	Caffeic acid
<i>S. enterica</i>	N/D	6.84×10^{-9}	N/D
<i>S. aureus</i>	N/D	$1.47 \times 10^{-7*}$	N/D
<i>P. aeruginosa</i>	N/D	3.01×10^{-8}	N/D
<i>L. monocytogenes</i>	N/D	N/D	N/D
Average mutation frequency	N/D	3.77×10^{-8}	N/D

Calculated mutation frequencies from the mutant selecting phytochemical laced agar plating experiments. Values are derived from the agar containing the MIC, as the 2xMIC agar plates failed to select for single colonies (barring for *P. aeruginosa*, although these were not investigated further due to the presence of colonies at the thymol MIC). N/D denotes an undetermined mutation frequency; in the cases of caffeic acid and the Prosur NATPR T-10+ mix this was due to the complete growth of a bacterial lawn. In the case of thymol against *L. monocytogenes* the mutation frequency was not determined due to a total lack of bacterial growth upon all agar plates. Experiments for each pathogen were repeated with three technical replicates for one biological replicate.

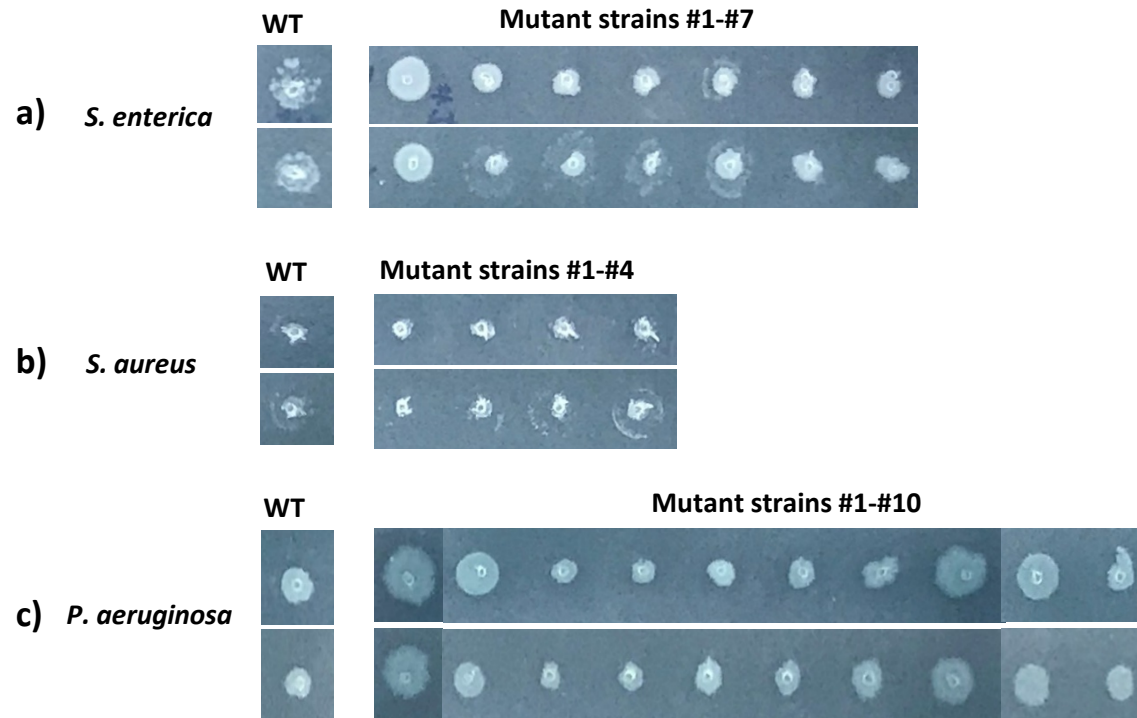
4.2.3 Thymol-selected candidate mutants display tolerant, not resistant, phenotypes

Once candidate, single colonies were selected (**Section 4.2.2**), their capacities to resist the antimicrobial actions of thymol were re-confirmed via microdilution agar MIC assays (**Section 2.6.2**) prior to sequencing (**Figure 4.1**). Thymol concentrations ranging from 0.03-8mg/ml were tested, with no visible colony growth observable for all *S. enterica* and *S. aureus* strains above the parental MICs (see **Section 4.2.1**). Parental and mutant strains of *P. aeruginosa* showed weak colony growth at a thymol concentration of 0.5mg/ml, though not at the thymol MIC identified for the higher inoculum (2mg/ml, see **Section 4.2.1**).

Although the mutants selected at the MIC did not show an elevated value, when grown on 0.25mg/ml thymol the mutant strains of *S. enterica*, *S. aureus*, and *P. aeruginosa* all exhibited larger colony morphologies than the parental strains (**Figure 4.1**). The lack of mutant strain growth above their respective MICs, along with the larger mutant colonies at 0.5x MIC, suggests that the candidate mutant strains display a tolerance, in contrast to resistance, phenotype to the actions of thymol.

Analysis of the growth of mutants compared to the parents supported the presence of a tolerant phenotype with small growth advantages seen in the presence of thymol compared to the parent strains. Sequencing of selected mutants was used to determine the presence and location of genetic mutations within the tested mutant strains.

Figure 4.1: Growth of the thymol-selected 'resistant' pathogenic strains compared to their parental strains on thymol-laced agar.



Panel a) colony growth of the parental, and seven randomly selected mutant, strains of *S. enterica*. b) colony growth of the parental, and four randomly selected mutant, strains of *S. aureus*. c) colony growth of the parental, and ten randomly selected mutant, strains of *P. aeruginosa*. Experiments were repeated with one technical replicate for two biological replicates, presented above one above the other. Statistical analysis not required.

4.2.4 Thymol-tolerant mutants across bacterial species carry SNPs within efflux pump operons

After determining that the thymol-selected mutants displayed a tolerance to the antimicrobial actions of this monoterpenoid phenol, the genetic elements responsible for this phenotype required elucidation. To this end, selected mutant strains of *S. enterica*, *S. aureus* and *P. aeruginosa* were sequenced (as described in **Section 2.10.1**); candidate SNPs with the potential to resist thymol are presented in **Table 4.3**. As can be seen, of the four *S. aureus* mutants sequenced only one SNP (in *S. aureus* mutant strain #4) was identified as differing from the parental reference genome. This SNP constituted a substitution of the adenine nucleotide base at position 478281 to a thymine base, resulting in the substitution of the positively charged lysine residue at position 236 to a hydrophobic isoleucine within the amino acid chain of the LacI family purine operon repressor PurR (**Table 4.3**). While this specific SNP has not been identified within the reviewed literature, research has correlated the mutation of this *S. aureus* gene with an increased resistance to cell wall targeting antimicrobials (daptomycin^[271], nisin^[272]). The PurR protein has also been shown to directly bind to the promoters of virulence factor genes^[273-275]. Altogether this may suggest a similar role is played in the tolerance shown within this work to the antimicrobial action of thymol.

Of the four *P. aeruginosa* mutant strains sequenced a total of 16 SNPs were identified, nine of which were shared between all sequenced mutant strains. Five of the seven unique SNPs (**Table 4.3**) were all possessed by the *P. aeruginosa* mutant strain #1, laying downstream of the PA14_10920 gene encoding a putative 2, 4'-dihydroxyacetophenone dioxygenase (the cleavage target of which studies suggest is an antimicrobial plant metabolite derived from coffee^[276]) and upstream of the AraC family transcriptional regulator *feaR* gene (**Table 4.3**). These SNPs may result in an altered efficiency of the *feaR* transcriptional promoter. The final SNP found within *P. aeruginosa* mutant strain #1 consisted of a cytosine to thymine nucleotide substitution at position 1922101 within the PA14_22080 gene; substituting the hydrophobic alanine amino acid residue to a polar uncharged threonine residue at position 199 within the translated amino acid chain of the resolvase protein product. The final unique SNP observed from the sequencing of the *P. aeruginosa* mutants was found in the mutant strain #4; a cytosine to thymine nucleotide substitution at position 2034984 within the *zbdP* gene encoding

a zinc-binding dehydrogenase. This results in the amino acid substitution of an arginine residue at position 266 for a cysteine residue within the ZbdP protein. Four SNPs within the *yejE* gene encoding a putative ABC transporter permease (**Table 4.3**) were also identified within the sequenced genomes of *P. aeruginosa* mutant strains #1 and #3.

From the eight *S. enterica* mutant strains sequenced, a total of four SNPs were identified (**Table 4.3**). *S. enterica* mutant strain #2 was found to harbour a unique nucleotide base substitution of cytosine to guanine at position 303172 within the putative class I SAM-dependant methyltransferase *yafS* gene. This provides a H107Q substitution within the amino acid chain of the translated protein (**Table 4.3**). The *yafS* gene, while identified within the literature^[277], has not been described in detail for *S. enterica*. Alongside this SNP, the *S. enterica* mutant strain #2 also possessed the unique base substitution of adenosine to cytosine at position 639279 within the *tetR/acrA* family transcriptional regulator *ramR*. This resulted in the substitution of the phenylalanine amino acid residue at position 48 of the RamR protein chain A to a cysteine residue (**Table 4.3**); a mutation not currently identified within the literature. *S. enterica* mutant strain #1 also possessed a *ramR* mutation, although at a different site. This was a known mutation of *ramR* (a cytosine to thymine substitution at position 639135) resulting in a G96D amino acid residue substitution (**Table 4.3**), a missense mutation^[278], in this repressor of efflux pump activity. **Figure 4.2** presents the 3D structure of the RamR protein, where the affected amino acid residues are highlighted. Mutants within *ramR* are well known to result in loss of RamA repression – a master regulator of multidrug resistance^[279].

One SNP identified within the *S. enterica* mutant strains #1, #5 and #6 was the insertion of a thymine base at position 3729980 upstream of the STM14_18795 (a putative cytoplasmic protein, GlpF homologue) gene and STM14_RS18790 gene encoding the putative DeoR family transcriptional regulator *glpR*. The putative product of the *glpR* gene has been described within *E. coli*^[280, 281] and *P. aeruginosa*^[282] as a repressor of the *glp* operon for sugar/carbohydrate transport and metabolization. Although this gene has not had a function described to it in *S. enterica*, it may be assumed that it serves a similar function and that the insertional mutation observed here may constitute a disabling of the gene's promoter region.

As SNPs were found multiple times and across species related to efflux-associated genes (*ramR*, *yejE*), it was hypothesised that at least part of these mutants mechanism of resistance

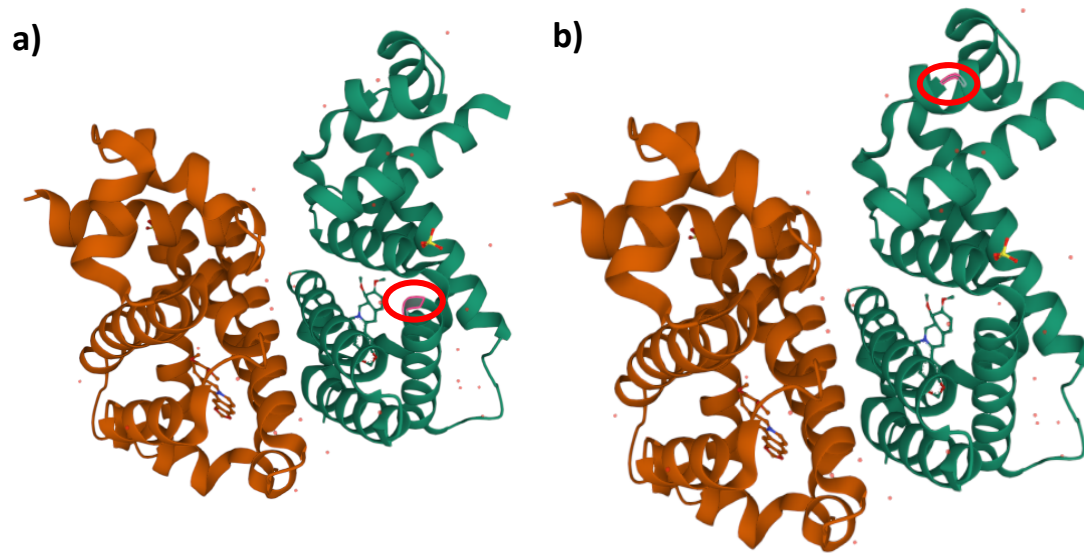
to the inhibitory actions of thymol was due to an altered efflux phenotype. Thus, select mutant strains were phenotypically assayed to determine if this hypothesis could be supported.

Table 4.3 Unique SNPs found within the sequenced thymol-tolerant mutant strains.

Organism	No. of strains sequenced	Total SNPs identified	Unique SNPs of interest	SNP Position	SNP nucleotide base effect	Loci and product	Functional effect
<i>S. enterica</i>	8	4	3	303172	C - G	<i>yafS</i> , putative Class I SAM-dependant methyltransferase	H107Q substitution
				639135	C - T	<i>ramR</i> , TetR/AcrA family transcriptional regulator	G96D substitution
				639279	A - C	<i>ramR</i> , TetR/AcrA family transcriptional regulator	F48C substitution
<i>S. aureus</i>	4	1	1	478281	A - T	<i>purR</i> , purine operon repressor	K236I substitution
<i>P. aeruginosa</i>	4	16	5	945885	G - C	Upstream of <i>feaR</i> , AraC family transcriptional regulator	Alteration of promoter efficiency?
				945886	C - G		
945887	G - C						
945889	C - T						
945890	T - G						
			Shared*	3670537	T - C	<i>yejE</i> , putative permease of a peptidyl nucleoside antibiotic ABC transporter	F179F
				3670539	C - T		P180L
				3670540	T - G		P180P
				3670542	G - A		G181E
							substitutions

The number of sequenced mutant strains, the total number of SNPs identified and the number of which were unique to a single mutant strain are detailed above. The genomic numerical position, the nucleotide substitution and the described effects of such are also recorded.

Figure 4.2: 3D tertiary protein structure of the RamR protein and its two subunits.



Panel **a)** affected amino acid location from the novel amino residue F48C substitution resulting from the SNP possessed by the *S. enterica* mutant strain #2. **b)** affected amino acid location from the known amino residue G96D substitution resulting from the SNP possessed by the *S. enterica* mutant strain #1. Protein structure retrieved from the RCSB Protein Data Bank 3D molecular viewer, “Crystal Structure of The Berberine-bound Form of RamR (Transcriptional Regulator of TetR Family) from *Salmonella* Typhimurium”^[283].

4.2.5 Thymol-tolerant mutants present increased MICs for classically effluxed antibiotics

After sequencing of the thymol-selected mutant strains revealed the presence of SNPs within loci associated with efflux activity, microdilution broth MIC assays (see **Section 2.6.1**) were performed to determine the antibiotic sensitivity of the strains. Many bacterial AMR phenotypes are underpinned by altered efflux; with this in mind the MIC fold changes of the tested mutants, compared to the relevant parental strains, against a range of antibiotics are shown in **Table 4.4**. Kanamycin, included as a control due to the compound not being typically exported from the cell by efflux, did not exhibit an increased MIC across any of the thymol-selected mutant strains tested (although a slight decrease was present against *S. enterica* strain #2, **Table 4.4**).

The *S. enterica* mutants showed a 1.67-2.67x fold increase in the MICs of tetracycline, a 2.38-4.21x fold increase in the MICs of ampicillin, 1.67-3.42x fold increase in the MICs of chloramphenicol and, finally, a 2-4.17x fold increase in the MICs of nalidixic acid (**Table 4.4**). *S. enterica* strain #1 (containing a G96D amino acid substitution within the *ramR* efflux repressor gene) and strain #2, possessing an F48C amino acid substitution within the *ramR* locus, exhibited the highest MIC fold increases against the tested antibiotics.

There was no observable increase in the MICs of tetracycline against the thymol-selected *S. aureus* mutants and a 1.33-2x fold increase in the MICs of chloramphenicol. All *S. aureus* strains were resistant to the actions of ampicillin, piperacillin, nalidixic acid and ciprofloxacin up to 32µg/ml (**Table 4.4**). The mutant strains of *P. aeruginosa* exhibited a 2-4x fold increase in their tetracycline MICs, 1.33x fold increase in their ampicillin MICs, 3.33-4x fold increase in their chloramphenicol MICs and 1.33-2.67x fold increase in their nalidixic acid MICs (**Table 4.4**).

Overall, the MIC increases were consistent with an efflux phenotype for the relevant mutants (*S. enterica* mutant strains #1 and #2, *P. aeruginosa* mutant strains #1 and #3) with low-level increases to a panel of known efflux substrates.

Table 4.4: Antibiotic MIC fold changes for selected pathogenic strains.

Average MIC fold changes of mutant strains						
Micro-organism		Antibiotics				
		Kan	Tet	Amp/Pip*	Chlor	Nal/Cipro*
<i>S. enterica</i>	WT	1.00	1.00	1.00	1.00	1.00
	#1	1.00	2.67	4.21	3.42	4.17
	#2	0.83	2.67	4.21	3.42	4.17
	#6	1.00	1.67	2.38	1.67	2.00
<i>S. aureus</i>	WT	1.00	1.00	N/D	1.00	N/D
	#1	1.00	1.00	N/D	2.00	N/D
	#2	1.00	1.00	N/D	2.00	N/D
	#3	1.00	1.00	N/D	1.67	N/D
	#4	1.00	1.00	N/D	1.33	N/D
<i>P. aeruginosa</i>	WT	1.00	1.00	1	1.00	1.00
	#1	1.00	3.33	1.33	3.33	2.67
	#2	1.00	2.67	1.33	4.00	2.00
	#3	1.00	2.00	1	3.33	2.00
	#4	1.00	4.00	1	3.33	1.33

Kan denotes kanamycin. **Tet** denotes tetracycline. **Amp/Pip** denotes ampicillin for *S. enterica* and *P. aeruginosa*, piperacillin for *S. aureus*. **Chlor** denotes chloramphenicol. **Nal/Cipro** denotes nalidixic acid for *S. enterica* and *P. aeruginosa*, ciprofloxacin for *S. aureus*. **N/D** denotes an undetermined MIC fold change, as for the tested antibiotics against *S. aureus* the MIC was >34µg/ml. Values in **bold** represent increased MIC fold changes as compared to the parental strain. Experiments were repeated with three technical replicates for three biological replicates and average values presented at 2 decimal places.

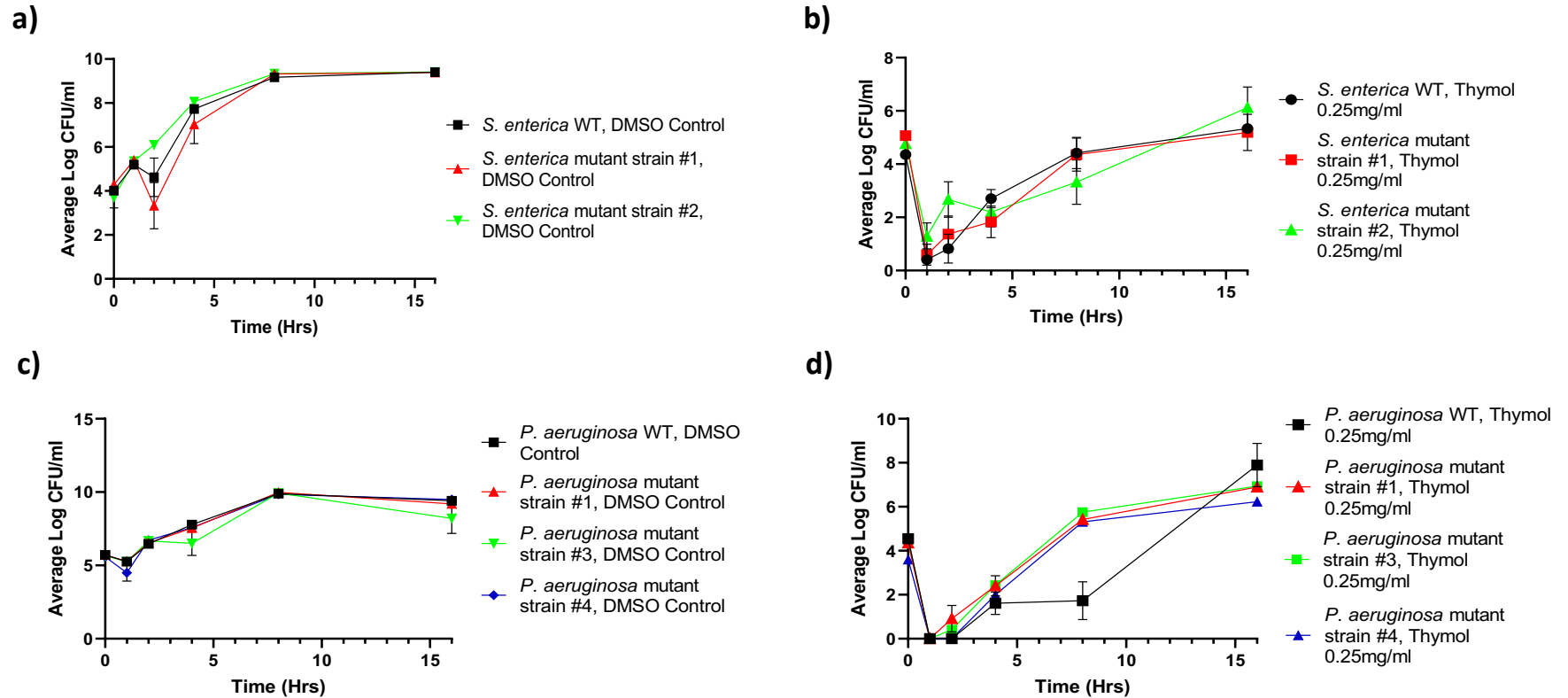
4.2.6 Thymol-tolerant mutants grow better under thymol stress

To further probe the phenotypes of the thymol-tolerant *S. enterica*, *S. aureus* and *P. aeruginosa* mutants CFU growth curves (**Section 2.4.0**) were used to investigate the growth kinetics of the selected mutants. **Figure 4.3** presents the growth curves of the tested *S. enterica* and *P. aeruginosa* mutants, both challenged with a solvent vehicle control and 0.25mg/ml thymol. Full tables and figures for these experiments can be found within the **Appendix, Section 9.4**. From **Figure 4.3** and the **Appendix, Section 9.4** the *S. enterica*, *S. aureus* and *P. aeruginosa* mutant strains grew at a similar rate to their comparable parental strains alongside the solvent vehicle. However, when challenged with 0.25mg/ml thymol the *S. enterica* mutant strains presented a slightly, yet not statistically significant, greater fitness in growth when compared to the parental strain (**Figure 4.3b**). This behaviour was also emulated with the *P. aeruginosa* mutant strains #1, #3 and #4 growing at a greater growth velocity (with statistically significant 98.79%, 174.78% and 121.12% respective increases) when compared to the parental strain (**Figure 4.3**), yet all tested *P. aeruginosa* strains concluded the experiment at a similar endpoint state CFU/ml (**Figure 4.3**).

Although the *S. aureus* thymol-tolerant mutant strains #3 and #4 grew at a similar rate to the parental *S. aureus* strain with the solvent vehicle, no mutant strain grew above the detection threshold of the enumeration method when challenged with 0.25mg/ml.

The growth curves (**Figures 4.3** and **Appendix, Section 9.4**), alongside the data collected from the complementary assays described elsewhere in this chapter, again show tolerant phenotypes observed for these thymol-selected *S. enterica*, *S. aureus* and *P. aeruginosa* mutant strains.

Figure 4.3: Thymol-tolerant mutant growth curves.

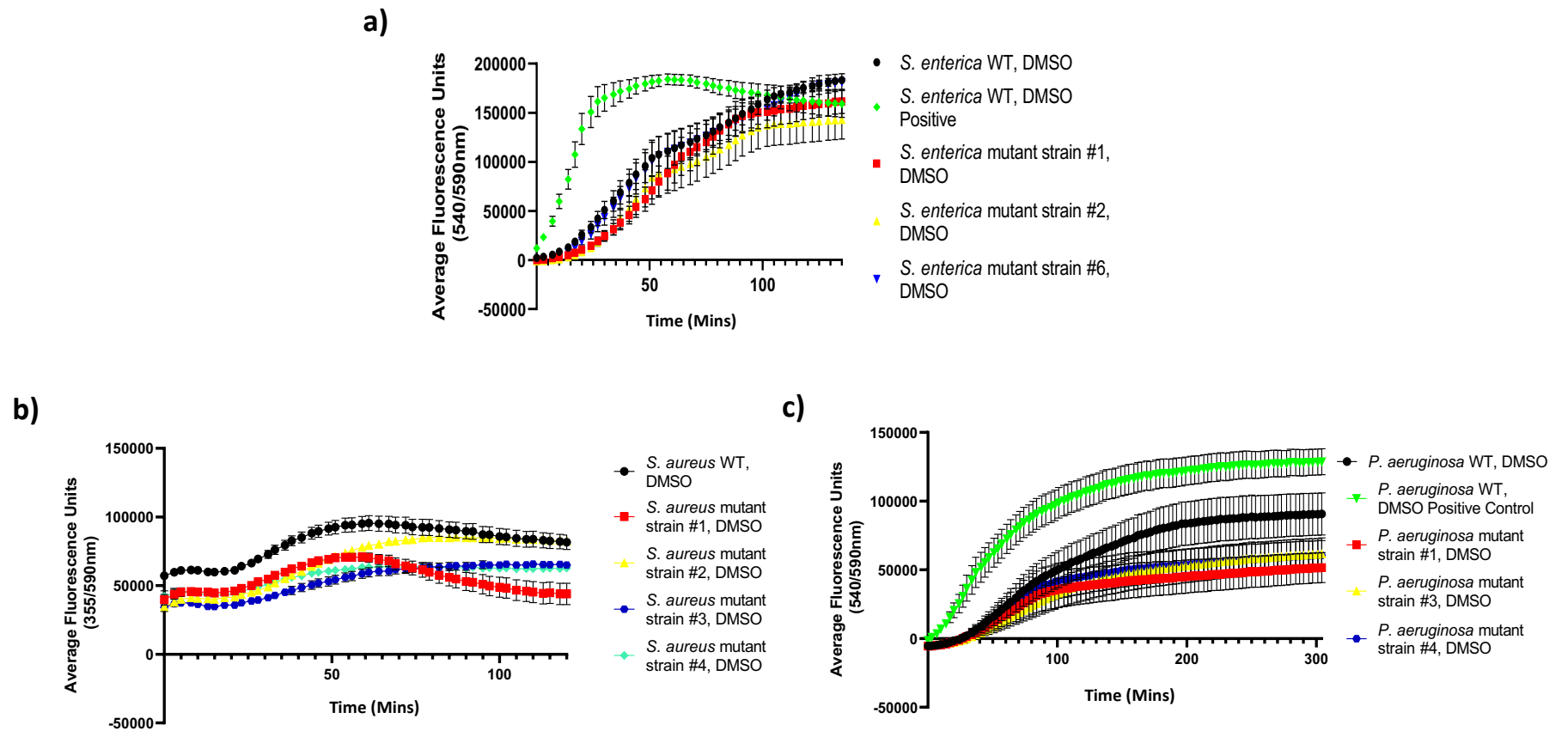


Panel a) *S. enterica* growth curves under solvent vehicle stress. b) *S. enterica* growth curves under thymol stress. c) *P. aeruginosa* growth curves under solvent vehicle stress. d) *P. aeruginosa* growth curves under thymol stress. Experiments were repeated with three technical replicates for three biological replicates. Error bars represent SEM. Statistical analysis was completed on the calculated growth kinetic metrics via the GraphPad software v.8, using a 1-way repeated measures ANOVA Test with Fischer's LSD test.

4.2.7 Thymol-tolerant mutants display a decreased drug accumulation

As part of the set of experiments phenotyping the thymol-selected *S. enterica*, *S. aureus* and *P. aeruginosa* mutants the accumulation of fluorescent efflux substrates was measured (see **Section 2.5.0**). **Figure 4.4** depicts the accumulation of drugs by selected *S. enterica*, *S. aureus* and *P. aeruginosa* mutants. *S. enterica* strain #2, *S. aureus* strain #1 and *P. aeruginosa* strain #1 exhibited significant decreases in their fluorescence accumulation velocities; of 20.36%, 82.85% and 40.48% respectively (**Appendix, Section 9.4**) as compared to their parental strains. Efflux mutants would be expected to exhibit a decreased fluorescence accumulation and some of the relevant thymol-selected mutants displayed such behaviour in these experiments (**Figure 4.4**).

Figure 4.4: Thymol-tolerant mutant drug accumulation assays.

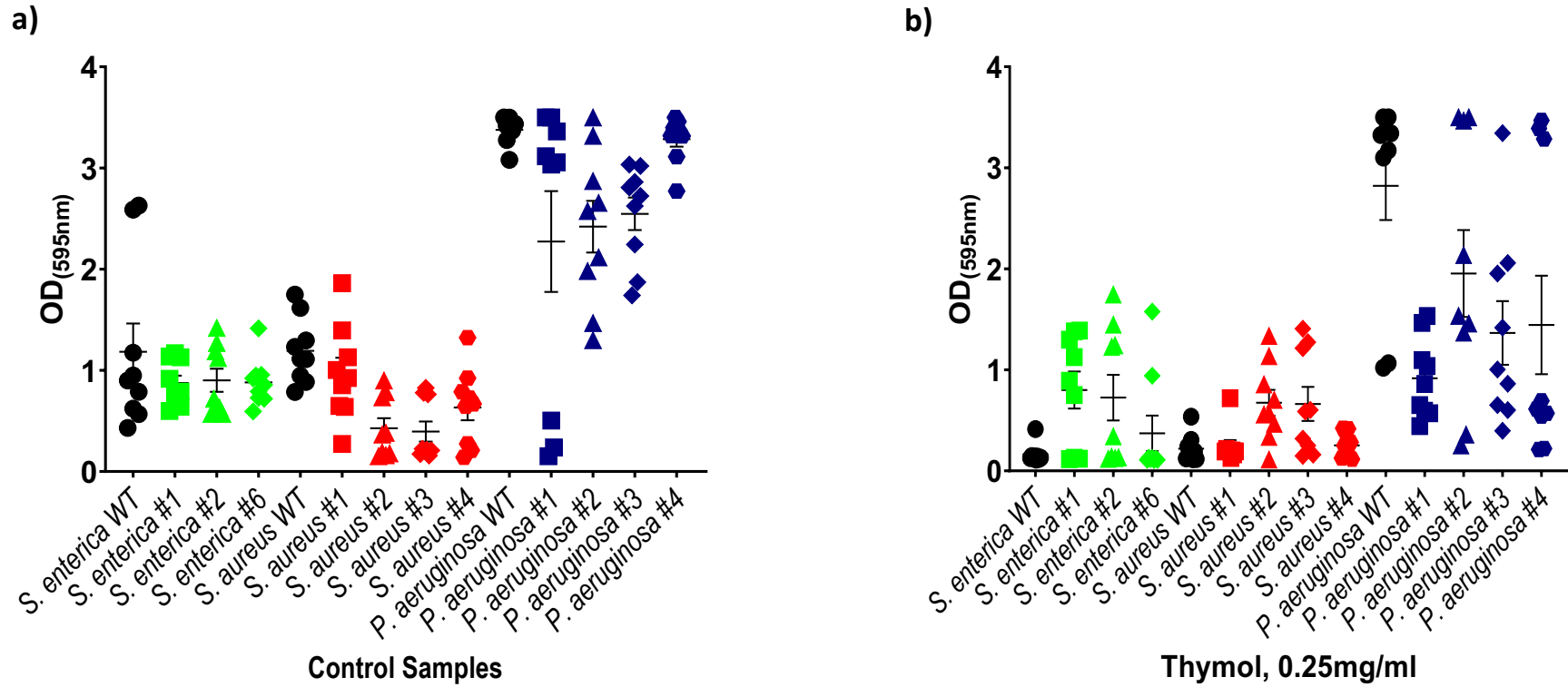


Panel **a)** *S. enterica* resazurin accumulation. **b)** *S. aureus* EtBr accumulation. **c)** *P. aeruginosa* resazurin accumulation. Experiments were repeated with five technical replicates for three biological replicates. Error bars represent SEM. Statistical analysis was completed on the calculated fluorescence accumulation metrics via the GraphPad software v.8, using a 1-way repeated measures ANOVA Test with Fischer's LSD test.

4.2.8 Thymol-tolerant mutants present reduced capacities to form biofilms

Alongside increased antibiotic MICs, another common aspect of efflux-dependant AMR phenotypes is a decreased capacity to produce a mature biofilm^[284]. With this in mind, crystal violet staining assays (see **Section 2.8.0**) were used to determine the thymol-tolerant mutants biofilm-forming potential. **Figure 4.5** presents the final OD_(590nm) measurements of these experiments while the statistically significant results discussed herein may be found within the **Appendix, Section 9.4**. The thymol-tolerant *S. enterica* mutants exhibited decreased biomass production based on OD_(590nm) measurements when compared to the parental strain. Similarly, the *S. aureus* mutants produced less biomass (**Figure 4.5a**). The data for the *P. aeruginosa* crystal violet assays, **Figure 4.5a**, displayed a greater variability than the two previous micro-organisms, however the general trend of lower OD_(590nm) measurements for the mutant strains compared to the parental strain continued. Biofilm formation was also measured in the presence of 0.25mg/ml thymol (**Figure 4.5b**)- parental *S. enterica* and *S. aureus* did not grow to make a biofilm whereas the mutants were able to produce biofilms in the presence of thymol. Surprisingly, the parental *P. aeruginosa* was able to make biofilm in the presence of 0.25mg/ml thymol.

Figure 4.5: Thymol-tolerant mutant crystal violet biofilm assays.



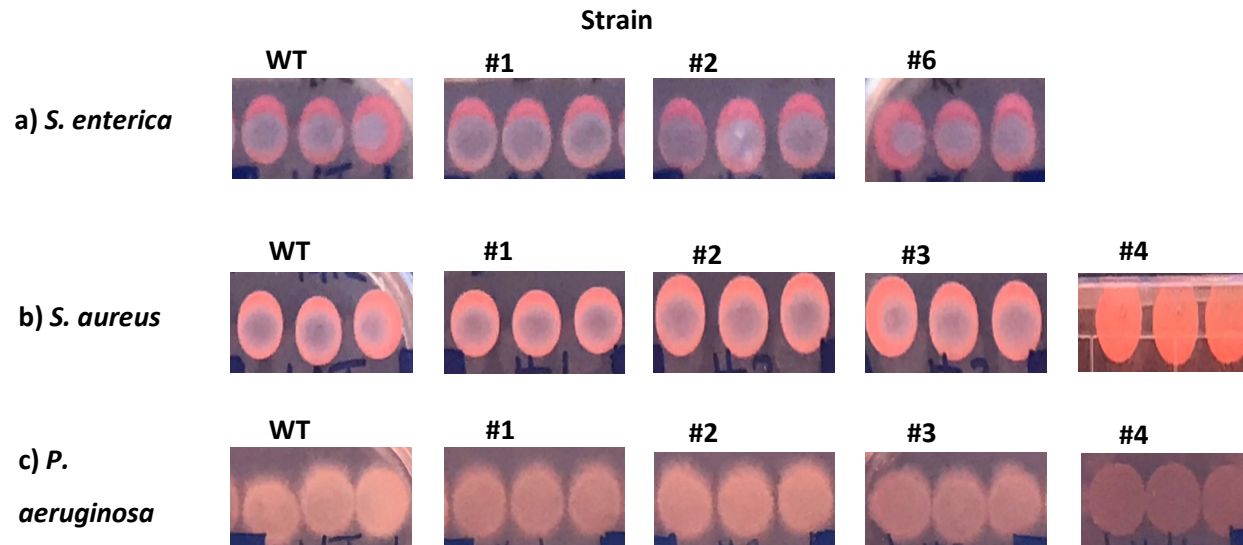
Panel **a)** Crystal violet assays under control conditions. **b)** Crystal violet assays under 0.25mg/ml thymol. Experiments were repeated with four technical replicates for three biological replicates. Error bars represent SEM, horizontal bars represent the mean for each data set. Statistical analysis was completed on the calculated growth kinetic metrics via the GraphPad software v.8, using a 1-way repeated measures ANOVA Test with Fischer’s LSD test.

4.2.9 Colony morphology of thymol-tolerant mutants

To complement the results of the crystal violet staining assays (Section 4.2.8), congo red plating (see Section 2.9.0) was used to assess any differing colony morphologies produced by the thymol-tolerant mutant and parental strains. Selected examples of these colony morphologies are presented in Figure 4.6. Congo red stains the extracellular component curli, in addition to other polysaccharides, of bacterial biofilm structures and thus the density of a biofilm can be inferred by the extent of light pink/red staining visible within a biofilm colony. As can be seen in Figure 4.6 the thymol-tolerant *S. enterica* strains #1 and #2 (possessing SNPs within the *ramR* efflux-associated locus) present a lesser degree of congo red staining than the parental strain, particularly on the lower half of each grown colony. *S. enterica* mutant strain #6, lacking an efflux-associated SNP, however displays an equal if not greater degree of congo red staining, supporting the altered efflux phenotypes of a number of the mutant strains investigated within this chapter.

In contrast, the biofilm morphologies of the *S. aureus* and *P. aeruginosa* mutant strains were less distinct; similar degrees of congo red staining were observable between the *S. aureus* parental and mutant strains #1, #2 and #3 (with *S. aureus* mutant strain #4 presenting a much greater degree of congo red staining) and a similar pattern was exhibited between the tested *P. aeruginosa* mutant and parental strains. As the congo red stain only interacts with a few biofilm constituents, additional components produced in these species may not be visible here.

Figure 4.6: Congo red staining of the parental and mutant strains.



Row **a)** *S. enterica* parental (WT), and three mutant strains. Mutant strains #1 and #2 possess SNPs within the efflux-associated *ramR* gene, while mutant strain #6 does not. **b)** *S. aureus* parental (WT), and four mutant strains. Only mutant strain #4 possessed a unique SNP, located within the *purR* locus. **c)** *P. aeruginosa* parental (WT), and four mutant strains. Numerous SNPs were found across these strains, including in the *yejE* and *zbdP* loci. Experiments were repeated with three technical replicates for one biological replicate.

4.3.0 Chapter Discussion

There is growing evidence that the selective pressure induced by exposure to non-antibiotic antimicrobials; biocides^[285], disinfectants^[286] and phytochemicals^[287] may promote cross-resistance to classical antibiotics. In light of this context and the serenity of literature surrounding the phenomenon of bacterial phytochemical resistance^[288], within this chapter I attempted to elucidate the rate at which three selected phytochemicals (caffeic acid, the Prosur NATPRE T-10+ mix and thymol) may select for resistant mutant strains of the four foodborne pathogens *S. enterica*, *S. aureus*, *P. aeruginosa* and *L. monocytogenes*.

Only the monoterpenoid phenol thymol successfully selected for single candidate mutant colonies at an average rate of 3.77×10^{-8} across *S. enterica*, *S. aureus* and *P. aeruginosa*. The elucidation of this mutation frequency is an important, novel finding for the application of thymol as an alternative antimicrobial and is akin to rates observed for antibiotics^[289-291]. This may reflect its potent antimicrobial effect inducing a greater selective pressure upon the challenged bacteria than the other two phytochemicals. This ability to select mutants suggests that while phytochemicals may be effective as alternative antimicrobials, a potential for resistance should be considered.

The mutant strains selected demonstrated a mild tolerant phenotype. There is minimal literature investigating the responses of bacteria to thymol exposure, although one study did select resistant *E. coli* strains^[292]. This work provides extra evidence, specifically in the case of *Salmonella* species that have yet to be studied for their resistance potential to thymol. Sequencing of selected, thymol-tolerant strains revealed various SNPs across the bacterial species. Of note were the *ramR* mutations within the *S. enterica* mutant strains #1 and #2, the SNP mutation upstream of the *glpR* loci of the *S. enterica* mutant strains #1, #5 and #6, the *purR* SNP within the *S. aureus* mutant strain #4 and the *yejE* SNPs located in the *P. aeruginosa* mutant strains #1 and #3 (**Section 4.2.4** and **Table 4.3**). The *glpR* and *purR* SNPs (associated respectively with repressor proteins of sugar metabolism and purine synthesis operons)^[271-275, 280-282] suggest an altered metabolism in the corresponding biological pathways of the thymol-tolerant mutants. An altered carbohydrate metabolism in response to phytochemical challenge has been previously reported by (Al-Kandari F. et al 2019)^[293] who published NMR data from the culture media of *E. coli* strain JM109, repeatedly exposed to sub-lethal concentrations of

thymol, containing increased lactate and lactic acid family amino acids. This data suggested a metabolic shift from aerobic respiration to fermentation^[293], and is further supported by **(Di Pasqua R. et al 2010)**^[294] who recorded an impaired citrate metabolic pathway in *S. enterica* serovar Thompson exposed to thymol. Additional studies have published data providing evidence for a shift in the transcriptome of *E. coli* exposed to thymol, upregulating genes associated with the oxidative stress response^[292, 295]. Perhaps more significant, the *ramR*-associated SNPs identified in the *S. enterica* thymol-tolerant mutants (specifically strains #1 and #2) indicate that a significant role is played by efflux in *Salmonella* thymol-resistance mechanisms. Altered efflux is a well-documented mechanism for AMR^[109, 296-299]. **(Al-Kandari F. et al 2019)**^[293] reported the generation of a stop codon within, and disabling of, the *acrR* efflux transcriptional repressor, enabling an increased level of efflux activity in thymol-treated *E. coli* JM109 cells. **(Fadli M. et al 2014)**^[287] has also reported the modified expression of the *acrAB* efflux pump genes in *E. coli* strains derived from exposure to thymol^[287]. These findings support the significance of the *ramR* SNPs identified within the *S. enterica* thymol-tolerant mutants generated in this body of work.

The drug accumulation assays (**Section 4.2.7, Figure 4.4**) support the efflux-dependant thymol-tolerance displayed by the selected mutants and the importance of efflux/decreased envelope permeability in bacterial AMR phenotypes is well understood^[300-302].

As classic efflux-dependant AMR phenotypes are often cross-resistant to multiple compounds^[108, 296, 303], the antibiotic MICs of the thymol-tolerant mutants generated within this project were determined and were consistent with an efflux phenotype (**Section 4.2.5, Table 4.4**). However, thymol-tolerant mutants lacking identified efflux-dependant SNPs also showed some increased MICs of tested antibiotics. This may suggest the non-efflux mutants SNPs also impact general drug sensitivity.

Further supporting the efflux-dependant mechanism of thymol-tolerance as presented within this work are the data generated from the crystal violet and congo red staining assays (**Section 4.2.8, Figure 4.5 and Section 4.2.9, Figure 4.6**). The generally reduced biomass measurements observed in the crystal violet staining assays, coupled with the lower degree of pigmentation observed in the photographed colonies, both suggest a decreased capacity in the efflux-dependant, thymol-tolerant mutant strains to produce a mature biofilm. This behaviour correlates with the existing literature on AMR bacterial strains as **(Kettles R.A. et al 2019)**^[304]

and (Alav I. et al 2018)^[305] demonstrated that the *E. coli* MarA efflux pump regulator also downregulated biofilm production, in addition to (Trampari E. et al 2021)^[284] who described *S. enterica* Typhimurium AMR also resulting in a reduced biofilm capacity. This appears to be a balanced trade-off between antimicrobial resistance and physiological fitness.

In the context of this chapters results, the conclusions detailed below may be drawn:

- Of three, only one phytochemical (thymol) selected for candidate resistant strains of *S. enterica*, *S. aureus* and *P. aeruginosa*. Caffeic acid and the Prosur NATPRE T-10+ mix's failure to do likewise is likely to be due to these compounds lesser degrees of direct antimicrobial activity.
- Sequencing of selected *S. enterica* (#1 and #2) and *P. aeruginosa* (#1 and #3) mutant strains showed efflux is important to thymol tolerance, with SNPs present within genetic loci previously associated with classic AMR phenotypes.
- Thymol-selected mutant strains only displayed a weak tolerance to thymol but many were multi-drug resistant.

The results of this chapter show that thymol, although a potent antimicrobial, retains the capacity to select for tolerant, resistant mutant strains of pathogenic bacteria, notably of *S. enterica* Typhimurium. This may pose a challenge for phytochemical application^[306]. This issue may be overcome via calculated use of these natural products as synergistic compounds in combinatorial therapies, an approach that has been previously suggested^[307-313]. This approach is already common within the food industry; where the addition of salts and organic acids combined with heat or desiccation treatments combine to form a robust hurdle technology to ensure the microbiological safety of food products^[314]. There may therefore still be opportunities for thymol (and other phytochemicals to be applied in practice).

In the next chapter (**Chapter 5**) I used an *S. enterica* TraDIS-Xpress library exposed to thymol as a starting point to highlight the most significantly influential genes in the bacterial survival of thymol challenge, in the hopes of defining a primary MOA for the monoterpenoid phenol thymol.

Chapter 5: A whole genome functional screen identifies various cell envelope genes in determining *S. enterica* sensitivity to thymol

"Push the envelope. Watch it bend."- Tool, *Lateralus*, 2001

5.1 Chapter introduction

The selection of thymol-tolerant *S. enterica* mutants identified potential resistance mechanisms for this pathogen (i.e.; altered efflux phenotypes, see **Chapter 4**). A further in-depth genetic analysis was used to identify genes involved in thymol sensitivity. Multiple inhibitory MOA have been suggested for phytochemical antimicrobial activity^[139, 141, 143, 206, 315], including envelope/membrane disruption, inhibition of DNA and protein synthesis in the case of thymol^[270, 306, 316]. Here, I used a TraDIS library to not only probe the genetic elements involved in the bacterial resistance/susceptibility towards thymol, but also to provide evidence supporting a primary inhibitory MOA for the monoterpenoid phenol.

First, concentrations of thymol were identified, via microdilution broth MIC assays, as suitable for the high CFU level inocula involved in the challenge of a *S. enterica* TraDIS-Xpress library. Once established, a pre-made *S. enterica* STM51 TraDIS-Xpress library (kindly provided by Dr. Emma Holden^[203]) was exposed to various concentrations of thymol with the surviving mutants being sequenced and the mutant abundance estimated through the AlbaTraDIS pipeline. This allowed the identification of specific genetic loci involved in the increased survival or vulnerability of the mutants to the inhibitory actions of this compound. Finally, transmission electron microscopy (TEM) was used to visualise thymol-bacterial interactions, providing supporting evidence of thymol's inhibitory MOA.

Hypotheses:

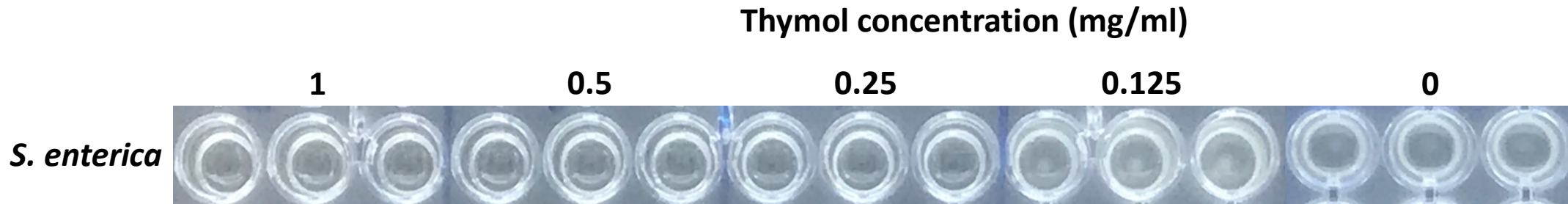
- 1.** Thymol challenge and sequencing of an *S. enterica* TraDIS-Xpress library will identify similar efflux-associated loci as were identified in **Chapter 4**.
- 2.** TraDIS-Xpress library mutants deficient in barrier function (synthesis, repair etc.) will be under-represented in the sequenced pool of surviving strains.

5.2 Results

5.2.1 Identifying appropriate thymol concentrations for use in *S. enterica* TraDIS-Xpress Library Challenge

Prior to challenging the *S. enterica* TraDIS-Xpress library with thymol, an appropriate concentration to be used against the high inoculum ($\sim 10^7$ CFU) used within the experiment was determined. **Figure 5.1** displays the turbidity of *S. enterica* cultures challenged with 0.125-1mg/ml thymol, photographed at the end of the performed microdilution broth MIC assays (**Section 2.6.1**). Due to the observable signs of growth at 0.125mg/ml thymol (and below), a range of 0.125-0.5mg/ml thymol was initially utilised in the *S. enterica* TraDIS-Xpress library challenge (**Section 2.11.0**).

Figure 5.1: Photographic evidence for culture turbidities of *S. enterica* exposed to a thymol concentration range.



Experiments were repeated with three technical replicates for one biological replicate, MICs were observed as the phytochemical concentration that lacked culture turbidity. Statistical analysis not required.

5.2.2 *S. enterica* mutants deficient in efflux and envelope-associated gene expression are more vulnerable to thymol challenge

In the thymol challenge of the *S. enterica* TraDIS-Xpress library (**Section 2.11.0**) at the concentration range previously identified (**Section 5.2.1**) too few mutants survived to be sequenced successfully. Thus, a lower concentration range was implemented. Challenged again with 0.03125mg/ml, 0.0625mg/ml and 0.125mg/ml of thymol sufficient mutants of the TraDIS-Xpress library survived the 0.03125-0.0625mg/ml range for Illumina sequencing (**Section 2.10.2**).

After sequencing, genetic alignment and analysis through the AlbaTraDIS bioinformatical pipeline, including a stringent filtering process (parameters of a q value ≤ 0.00001 and Log2FC value ± 2) identified 18 loci, many with negative average Log2FC values (-0.6 to -6.5). This implied a significant loss of these mutants after exposure to thymol in a 0.03125-0.0625mg/ml range, and by extension the importance of these loci in thymol challenge for *S. enterica*. **Table 5.1** displays the genomic loci identified as significant, although only the most likely candidate genes will be discussed herein. From the list described in **Table 5.1**, *acrAB* is one of the main efflux systems in *Salmonella*. The *acrA* gene product, a 42KDa membrane fusion protein that spans the inner and outer membranes, interacts with AcrB; an integral membrane protein anchored via 12 membrane-spanning α -helical domains. These two genes (particularly under-represented in the surviving sequenced mutants as suggested by the average Log2FC values of -5.9 and -6.5 at 0.0625mg/ml thymol, respectively) encode two thirds of the AcrAB-TolC tripartite efflux pump system^[317]. The outer membrane protein TolC (identified with a Log2FC value of -3 at 0.0625mg/ml thymol, **Table 5.1**) is essential for the selective transport of charged molecules across the bacterial membrane^[317] and associates with additional efflux systems such as AcrD, AcrEF, MdsAB, EmrAB and MacAB within *S. enterica* serovar Typhimurium^[318]. The significance of both the *acrAB* and *tolC* genes in bacterial-thymol interactions has already been inferred by the contents of this thesis **Chapter 4**, where mutants of *S. enterica* contained SNPs within the transcriptional regulator gene of this system, *ramR*. Another envelope-associated gene identified as significant in the sequencing and analysis of the thymol challenged TraDIS-Xpress library was *surA* (average Log2FC value of -2.7 at 0.0625mg/ml

thymol, **Table 5.1**). The protein product of this gene is a periplasmic chaperone, key in the biogenesis of β -barrel outer membrane proteins and previously linked to the virulence and biofilm formation of *E. coli* and *S. enterica* serovar Typhi strains^[319]. It may be hypothesised that the significance of this gene in the survival of *S. enterica* against thymol challenge may be in maintenance of bacterial envelope systems disrupted by the monoterpene phenol. Concerning β -barrel outer membrane proteins, the *ompA* gene encoding the highly conserved porin protein of the same name (responsible for the selective transport of charged molecules across the bacterial membrane^[320]) was also identified in the sequencing analysis of the surviving TraDIS-Xpress library mutants. The *ompA* gene was highlighted here as statistically significant, with an average Log2FC value of -2.7. Genes directly involved with the maintenance of the *S. enterica* outer membrane such as *rafG* (encoding a glucosyltransferase I enzyme involved in lipopolysaccharide (LPS) biosynthesis^[321]) and *yejM* (encoding an alkaline phosphatase superfamily hydrolase involved in outer membrane remodelling^[322]) were also significantly under-represented in the sequencing analysis, with average Log2FC values of -3.8 and -5, respectively, at 0.0625mg/ml thymol (**Table 5.1**). The *yej* operon was also highlighted within **Chapter 4** of this thesis as the thymol-selected *P. aeruginosa* mutant strains #1 and #3 possessed four SNPs within the *yejE* loci, encoding for a putative ABC transporter permease. Observing mutations within the *P. aeruginosa yejE*, alongside a lack of surviving *S. enterica* mutants with the TraDIS transposon construct in the *yejM* loci suggests a cross-species role for this operon in thymol-bacterial interactions. The significant changes in inserts between the thymol and control samples for the *acrAB-acrR* (**Figure 5.2**), *tolC* (**Figure 5.3**) and *ompA* (**Figure 5.4**) loci are clear.

Other loci identified in this statistical analysis included *rpoS* (an RNA polymerase sigma factor activated under stationary phase and general stress conditions^[323]), *galE* (an UDP-glucose-4-epimerase involved in the production of LPS^[324]) and *ycfF*. This latter gene, encoding the YcfF purine nucleoside phosphoramidase^[325, 326], is particularly intriguing considering a positive average Log2FC value (4.3, at 0.03125mg/ml thymol) was calculated, suggesting that mutants with the transposon construct located in this locus were over-represented in the surviving pool. Combined with the sequencing analysis of the generated *S. aureus* mutants described in **Chapter 4** of this thesis, where a SNP was identified within the *purR* purine operon repressor of *S. aureus* mutant strain #4, a role for purine nucleoside alterations may be played in the bacterial resistance mechanisms to thymol or this compounds' inhibitive MOA.

Overall, the statistical analysis of the sequenced, surviving *S. enterica* TraDIS-Xpress library mutants highlights multiple genes associated with efflux systems, OMPs and their localisation, in addition to the biogenesis of LPS. Altogether this suggests a significant role is played by the bacterial envelope in bacterial-thymol interactions, and as such further experiments were geared towards this hypothesis; that thymol's primary mechanism of inhibitory action is focused on interactions with the bacterial envelope.

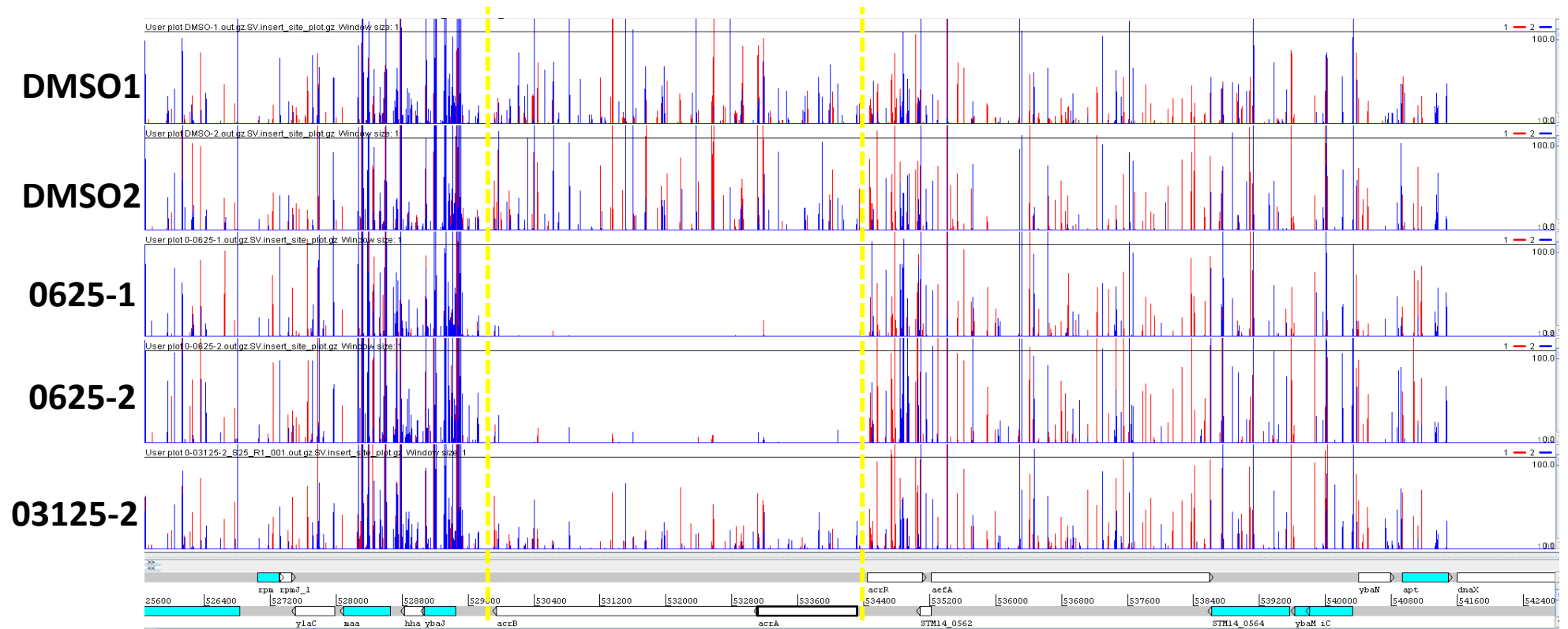
Table 5.1: Identified loci of the sequenced surviving mutants from the thymol challenged *S. enterica* TraDIS-Xpress Library.

Locus	Average Log ₂ FC (thymol mg/ml)		Product and function
	0.03125	0.0625	
<i>acrA</i>	-1.6	-5.9	AcrA, subunit of acridine RND family efflux pump
<i>acrB</i>	-2	-6.5	AcrB, subunit of acridine RND family efflux pump
<i>ompA</i>	-0.7	-2.7	OmpA, outer membrane protein A
<i>rfaG</i>	-1.8	-3.8	RfaG, putative glucosyltransferase I involved in LPS core biosynthesis
<i>surA</i>	-1.3	-2.7	Sur A, peptidyl-prolyl cis-trans isomerase; chaperone involved in the folding of extracytoplasmic proteins, OmpA in particular.
<i>tolC</i>	-1.8	-3	TolC, outer-membrane channel protein involved in efflux of hydrophobic/amphipathic molecules. Functions with a number of efflux systems
<i>yejM</i>	-5	-1.5	YejM, alkaline phosphatase superfamily hydrolase, utilised in remodelling the outer membrane
<i>galE</i>	-0.6	-3	GalE, UDP-galactose-4-epimerase, utilised in LPS production
<i>ycfF</i>	4.3	0	YcfF, purine nucleoside phosphoramidase
<i>rfbA</i>	-1	-2.6	RfbA, dTDP-glucose pyrophosphorylase; glucose-1-phosphate thymidyltransferase, utilised in LPS core production
<i>asmA</i>	-0.8	-2.1	AsmA, putative, outer membrane assembly protein
<i>yfhC</i>	2.4	0	YfhC, tRNA-specific adenosine deaminase; similar to <i>E. coli</i> putative deaminase (AAC75612.1)
<i>rpoS</i>	-1.2	-3.8	RpoS, RNA polymerase sigma factor, utilised during detection of external stress stimuli
<i>rfaI</i>	-1.9	-3.8	RfaI, lipopolysaccharide- α -1; 3-D-galactosyltransferase; UDP-D-galactose/glucosyl; lipopolysaccharide 1,3-galactosyltransferase. Utilised in
<i>rfaQ</i>	-1	-2.1	RfaQ, LPS core biosynthesis protein; similar to <i>E. coli</i> LPS core biosynthetic protein (AAC76656.1). Modifies the heptose region of the LPS core.
<i>wzxE</i>	-1.2	-2.4	WzxE, O-antigen translocase; similar to <i>E. coli</i> putative cytochrome (AAC76797.1); involved in LPS biosynthesis
<i>rfaH</i>	-1.6	-2.7	RfaH, transcriptional activator for

<i>dgkA</i>	-1.1	-3	DgkA, diacylglycerol kinase; similar to <i>E. coli</i> diacylglycerol kinase (AAC77012.1)
--------------------	------	----	---

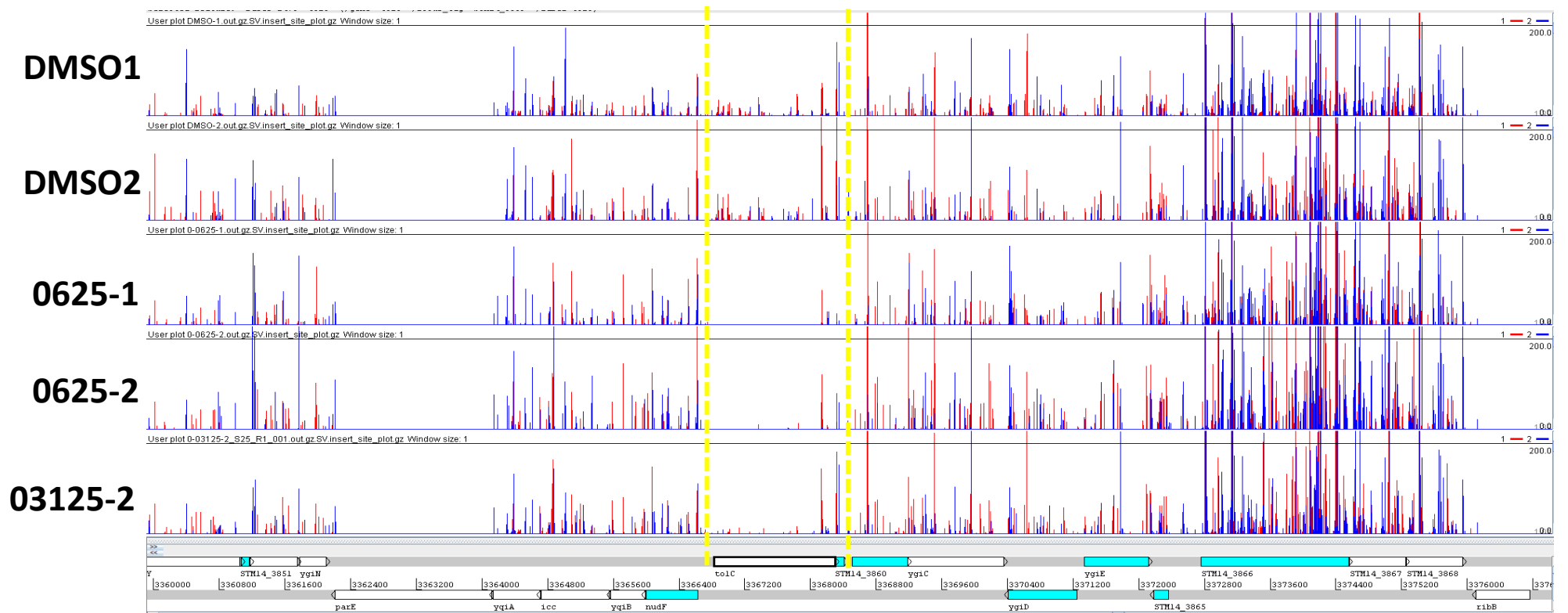
Loci filtered via a stringent q value (≤ 0.00001) and Log2FC value (± 2). Log2FC values are displayed to present a complementing suggestion of the loci's significance in the survival of *S. enterica* challenged with thymol. Original analysis performed by Dr. Keith Turner using the AlbaTraDIS bioinformatical pipeline, filtering performed by the author.

Figure 5.2: Artemis plots for the *S. enterica* TraDIS-Xpress library surrounding the *acrAB* operon on the 14028S reference genome.



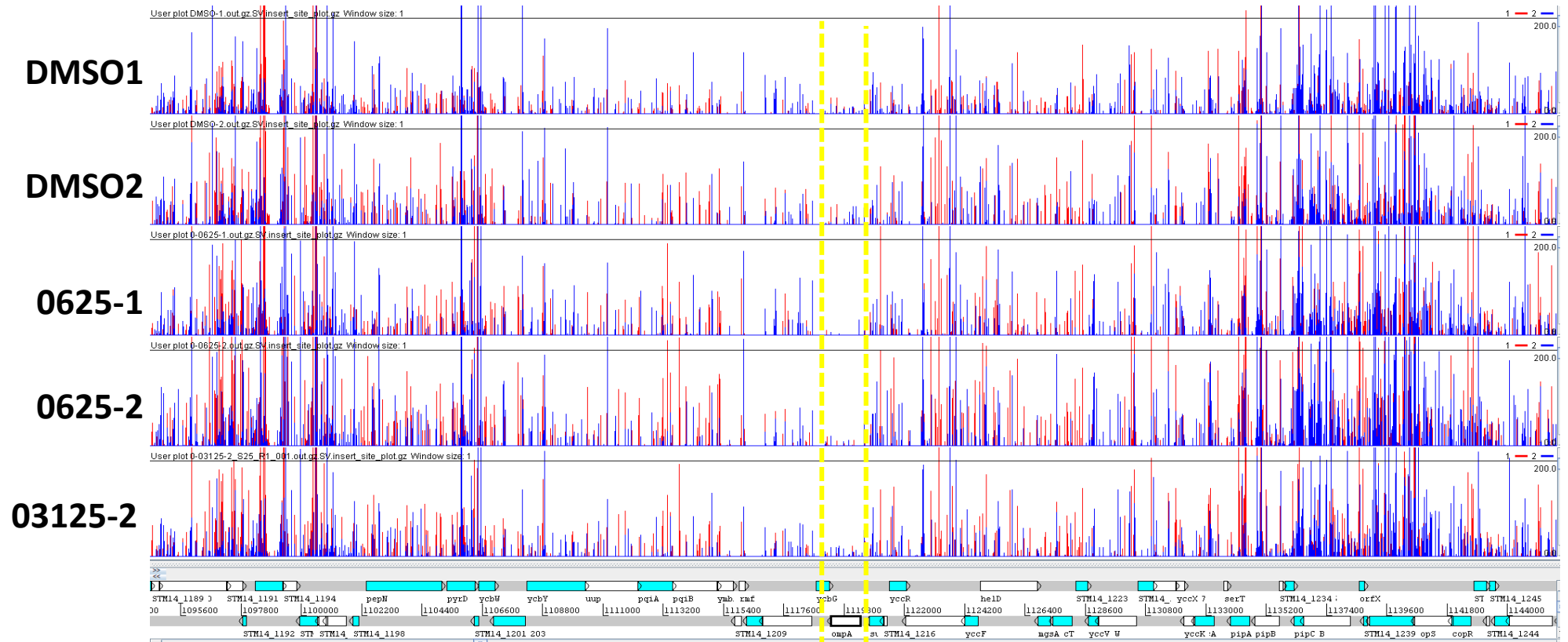
Note the significant lack of signals within the *acrAB* loci from the thymol-challenged samples compared to the solvent vehicle controls. Two biological replicates are displayed with the locus of focus highlighted by the yellow dashed lines. DMSO denotes a solvent control, 0625/03125 denote thymol concentrations, except for the 0.03125mg/ml thymol condition where the first biological replicate failed to provide sufficient DNA. Vertical lines indicate transposon inserts present with the height proportional to the number present. Blue lines indicate inserts oriented left to right as viewed, and red lines the opposite.

Figure 5.3: Artemis plots for the *S. enterica* TraDIS-Xpress library surrounding the *tolC* locus on the 14028S reference genome.



Note the significant lack of signals within the *tolC* locus from the thymol-challenged samples compared to the solvent vehicle controls. Two biological replicates are displayed with the locus of focus highlighted by the yellow dashed lines, DMSO denotes a solvent control, 0625/03125 denote thymol concentrations, except for the 0.03125mg/ml thymol condition where the first biological replicate failed to provide sufficient DNA. Vertical lines indicate transposon inserts present with the height proportional to the number present. Blue lines indicate inserts oriented left to right as viewed, and red lines the opposite.

Figure 5.4: Artemis plots for the *S. enterica* TraDIS-Xpress library surrounding the *ompA* locus on the 14028S reference genome.



Note the significant lack of signals within the *ompA* locus from the thymol-challenged samples compared to the solvent vehicle controls. Two biological replicates are displayed with the locus of focus highlighted by the yellow dashed lines, DMSO denotes a solvent control, 0625/03125 denote thymol concentrations, except for the 0.03125mg/ml thymol condition where the first biological replicate failed to provide sufficient DNA. Vertical lines indicate transposon inserts present with the height proportional to the number present. Blue lines indicate inserts oriented left to right as viewed, and red lines the opposite.

5.2.3 Thymol exhibits envelope-damaging effects

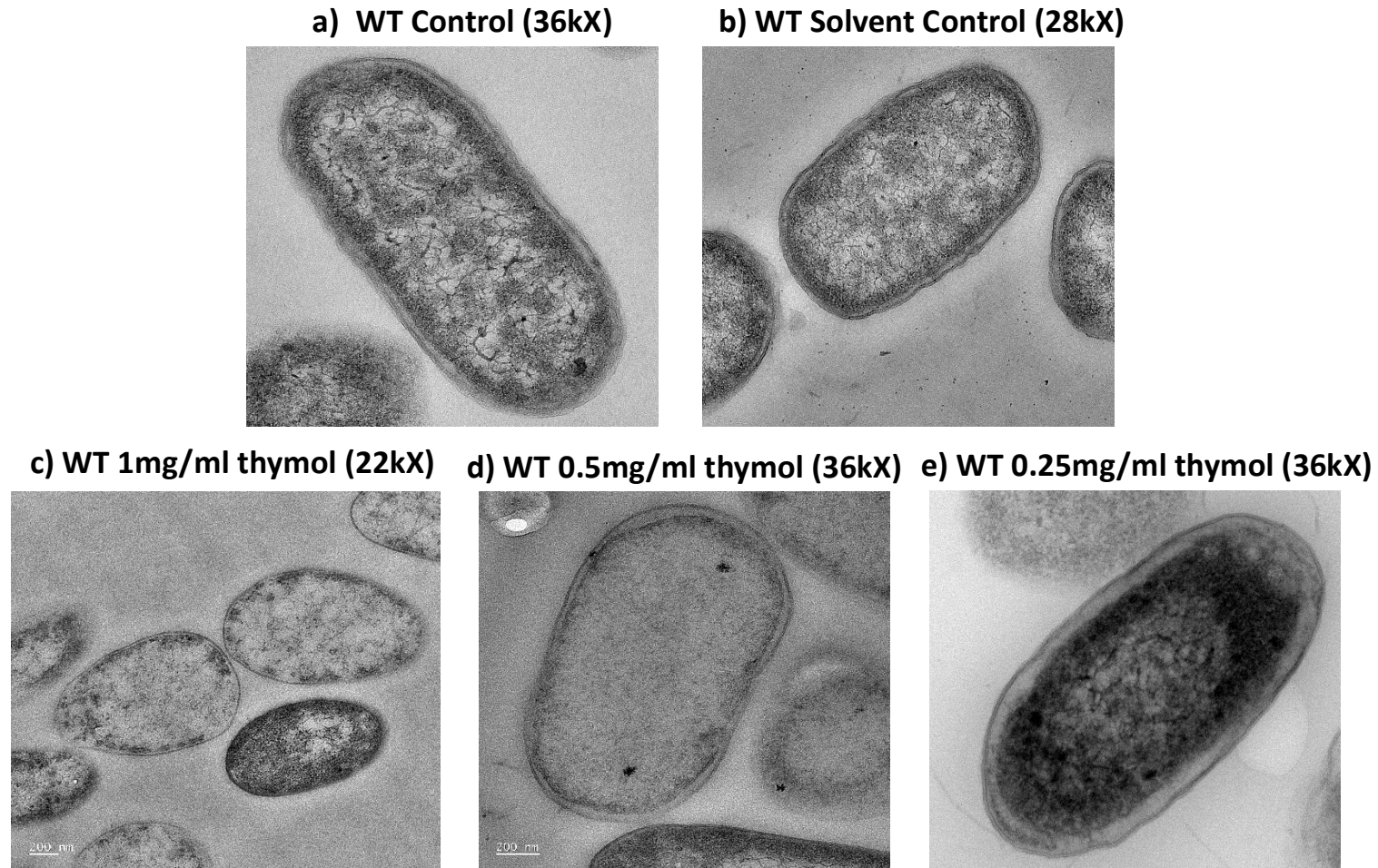
Due to the number of envelope-associated loci highlighted in the sequencing analysis of the thymol-challenged *S. enterica* TraDIS-Xpress library (**Section 5.2.2**) the experimental focus shifted towards observing bacterial surface physiology after thymol stress. TEM (see **Section 2.12.0**) was used to visually observe the results of thymol interactions between the *S. enterica* envelope and the cytoplasm of the bacterial cells. **Figure 5.5** presents TEM images captured from the exposure of the *S. enterica* parental strain to a 0.25-1mg/ml thymol concentration range. **Figure 5.6** depicts TEM images from the exposure of the *S. enterica* mutant strain #2 generated previously in **Chapter 4** to the same thymol range. **Table 5.2** presents a pair of analytical metrics calculated in the ImageJ software for the represented TEM images.

Focusing on **Figure 5.5**, the *S. enterica* parental strain presented a classic bacillary morphology and envelope appearance when exposed to both the PBS and solvent vehicle (DMSO) control. However, when exposed to various thymol concentrations for a period of two hours there were some drastic changes. Although no lysis or cellular debris was observed, the *S. enterica* parental strain presented a degraded rod shape, decreased cytoplasmic density, decreased envelope thickness and “fluffy” surface appearance with an increasing thymol concentration (**Figure 5.5**). The morphological rounding of the *S. enterica* parental strain was quantified with an increasing circularity value as the thymol concentration rose, although this was not found to be statistically significant (**Table 5.2**). Additionally, the average cytoplasmic density decreased with the thymol concentration (**Table 5.2**), with a statistically significant increase at 0.5mg/ml thymol when compared to the control condition.

Comparing the cellular morphologies of the *S. enterica* mutant strain #2 (possessing a unique SNP within the *ramR* locus, see **Chapter 4**) in **Figure 5.6** to the parental strain in **Figure 5.5**, some stark contrasts may be observed. Even within the PBS control conditions (**Figures 5.5-5.6, panels a**) the mutant strain displayed a unique morphology with a rounder form, thinner envelope, a less rigid, rougher surface and an increased periplasmic width/shrunken cytoplasm. This is reinforced by comparing the average circularity values of the parental (WT) and *S. enterica* #2 control conditions in **Table 5.2**, a difference of 0.1. Exposed to thymol, the mutant's morphology was more resistant to alteration than the parental *S. enterica* strain (**Figure 5.5**), maintaining a very similar appearance to the mutant and parental PBS controls. The average

cytoplasmic density values are significantly different for the mutant strain under thymol exposure (compared to the PBS control), although a lower numerical value infers a denser cytoplasm rather than lesser (**Table 5.2**), consistent with the visual evidence in **Figures 5.5-5.6**.

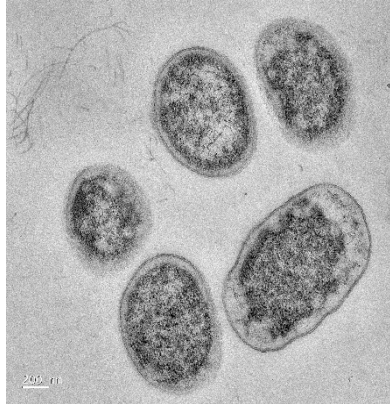
Figure 5.5: Exemplar TEM images of the *S. enterica* parental strain under various experimental conditions.



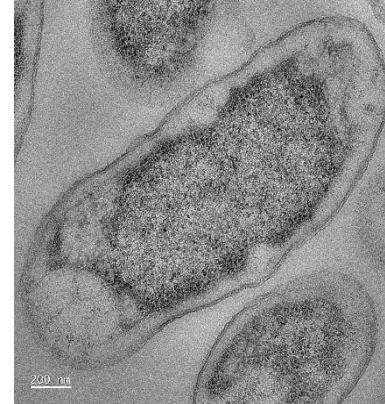
Panels depict the different experimental conditions that samples were exposed to for a period of two hours. Image magnifications are presented in parentheses within the given labels. Samples were tested in biological duplicate, fixed, stained and imaged by Ms. Kathryn Gotts and Dr. Catherine Booth.

Figure 5.6: Exemplar TEM images of the *S. enterica* mutant strain #2 under various experimental conditions.

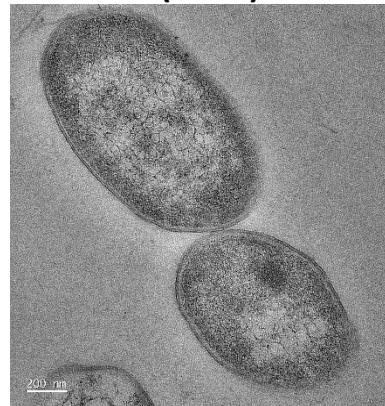
a) Mutant Control (22kX)



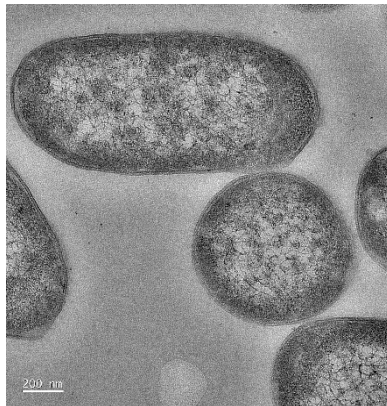
b) Mutant Solvent Control (36kX)



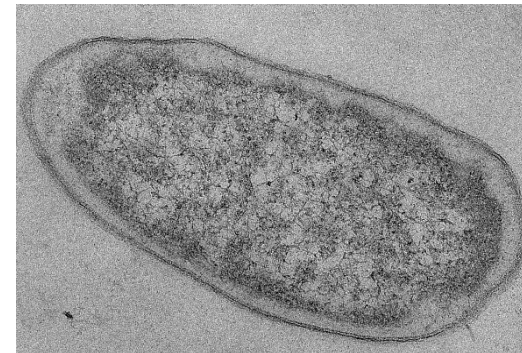
d) Mutant 0.5mg/ml thymol (36kX)



c) Mutant 1mg/ml thymol (36KX)



e) Mutant 0.25mg/ml thymol (36KX)



Panels depict the different experimental conditions that samples were exposed to for a period of two hours. Image magnifications are presented in parentheses within the given labels. Samples were tested in biological duplicate, fixed, stained and imaged by Ms. Kathryn Gotts and Dr. Catherine Booth.

Table 5.2: Analytical metrics generated from the Figures 5.5-5.6 TEM images.

<i>S. enterica</i> TEM ImageJ Analysis						
Sample	Average Cytoplasmic Density	SEM(\pm)	<i>p</i> value	Average Circularity value	SEM(\pm)	<i>p</i> value
WT Control	128.20	1.92	-	0.84	0.03	-
WT Solvent Control	98.59	8.66	0.0045	0.84	0.03	0.9668
WT 0.25mg/ml Thymol	98.49	5.70	0.0044	0.85	0.06	0.8028
WT 0.5mg/ml Thymol	152.50	8.19	0.0161	0.93	0.01	0.0723
WT 1mg/ml Thymol	140.49	5.96	0.1986	0.90	0.01	0.2060
<i>S. enterica</i> #2 Control	145.53	2.66	-	0.94	0.01	-
<i>S. enterica</i> #2 Solvent Control	139.79	1.90	0.0912	0.83	0.03	0.0078
<i>S. enterica</i> #2 0.25mg/ml Thymol	127.48	1.98	<0.0001	0.87	0.02	0.0880
<i>S. enterica</i> #2 0.5mg/ml Thymol	136.76	3.17	0.0134	0.94	0.01	0.9584
<i>S. enterica</i> #2 1mg/ml Thymol	128.51	1.26	<0.0001	0.86	0.04	0.0476

Quantitative values produced through analysis of five randomly selected cells across two TEM images are presented above. Average cytoplasmic density relates to mean gray values; the higher the value the less dense the cytoplasmic contents of the analysed cells. Circularity values quantify the degree to which the cells resemble a perfect circle; values closer to 1.0 indicate a perfect circle. Values presented at 2 decimal places. Statistical analysis was performed using the GraphPad software v.8, using a 1-way repeated measures ANOVA Test with Fischer's LSD test. Values in bold were statistically, significantly, different to the relevant control.

5.3 Chapter Discussion

Following from the sequencing of the thymol-tolerant mutants selected in **Chapter 4** of this thesis, a deeper genetic investigation into the bacterial mechanisms of thymol resistance was required which may also provide inferences for the primary inhibitory MOA of the monoterpenoid phenol. To this end an *S. enterica* TraDIS-Xpress library was exposed to a range of thymol concentrations and subsequently sequenced. Statistical analysis and filtering successfully highlighted several genetic loci significant to the survival of the library (see **Section 5.2.2**), evidenced by a lack of surviving mutants disrupted within these loci, associated with efflux and envelope linked functions. Overall, these data correlate and expand upon the results and conclusions drawn from this thesis' **Chapter 4** and include the genetic loci *acrAB*, *ompA*, *tolC*, *rfaG*, *surA*, and *yejM*.

Considering the functional overlap between the genomic loci highlighted in this chapter and the thymol-tolerant mutants from **Chapter 4**, efflux via AcrAB-TolC appears to be a key defence mechanism against thymol.

Also highlighted within the genomic sequencing of the surviving *S. enterica* TraDIS-Xpress library mutants was the *surA* locus. This gene encodes a chaperone protein responsible for the appropriate folding of extracellular proteins, particularly β -barrel proteins containing disulfide bonds and the OmpA protein^[327, 328]. The lack of a functioning *surA* gene may result in a deficit of properly folded extracellular proteins that slow, block or otherwise impede the antimicrobial interactions of thymol with the bacterial envelope, hence a significant lack of surviving mutants with the transposon construct in this genomic region after challenge (see **Section 5.2.2**). Studies have linked amino acid substitutions in the *Neisseria gonorrhoeae* SurA protein to a reduced susceptibility to broad range antibiotics due to a downstream effect of altered cell envelope proteins (e.g.; efflux pump activity)^[329]. Evidence has also suggested interactions between *surA* and AMR genes (e.g.; *acrA*) in *S. enterica* Typhi CT18^[330], while disruption of SurA function has been shown to restore antibiotic susceptibility to multidrug resistant *P. aeruginosa*^[331]. Altogether this suggests a link, if not a mechanism, for the involvement of the *surA* gene in the resistance to thymol's antimicrobial activity.

The bacterial envelope, consisting in Gram-negative species of the cytoplasmic membrane, peptidoglycan and outer membrane^[332] is a vital bacterial, morphological structure^[333]. Key functions of the bacterial envelope include the innate impermeability of the outer-membrane^[96] to antimicrobial xenobiotics, a function that can be partially traced to the properties of its component LPS^[334]. The *rfaG* gene highlighted in the sequencing of the TraDIS-Xpress library (**Section 5.2.2**), the *E. coli* homologue being referred to as *waaG*^[335], has been demonstrated to function as a core glucosyltransferase for phosphorylation in LPS synthesis^[335, 336] that, when disrupted, results in a destabilised outer-membrane^[336]. Hence, a *rfaG* lacking *S. enterica* mutant may present an increased susceptibility to thymol due to an increased envelope interaction with the molecule as the natural impermeability of this barrier is reduced.

Another locus observed to be significant in the sequencing of the challenged library is *yejM*. The translated product of this gene is an inner-membrane bound metalloenzyme hydrolase responsible for remodelling of the outer-membrane and envelope maintenance via directing proteolytic regulation^[322, 337-339]. *yeyM* (also referred to as *pbpA* in *Salmonella*) is essential for *E. coli* and *S. enterica* cell viability^[340], again underlining the importance of the bacterial envelope, and has also been found to provide resistance to antimicrobial peptides during cases of murine bacteraemia^[341]. Mutations in this locus may result in a knock-on effect that imbalances the lipid synthesis of the bacterial cell causing perturbations in the outer-membrane, a hypersensitivity to vancomycin, erythromycin^[338, 342] and an increased resistance to chloramphenicol antibiotics in some cases^[343]. Hence, a clear link between the *yeyM* locus and AMR can be seen, suggesting a role in thymol interactions with the bacterial cell is possible. The *ompA* locus was also identified as under-represented in the sequencing of the surviving library mutants; supported by studies that have presented the importance of this outer-membrane porin in AMR^[344-346] and thymol-resistance^[287, 292, 294] phenotypes.

In contrast to this evidence for the importance of the bacterial envelope, the sequencing of the thymol-challenged library also highlighted the loss of *ycfF* as important. Encoding a purine nucleoside phosphoramidase^[347] this locus was identified with a positive Log2FC value in the filtering process, suggesting a significant over-representation of mutants located in this locus after thymol challenge. This is an intriguing finding as the thymol-

tolerant *S. aureus* mutants generated in **Chapter 4** possessed a SNP within a purine operon repressor (*purR*). This observation that purine biosynthesis may hold an important role in thymol-tolerance in *Staphylococci* suggests a fundamental pathway of thymol-tolerance for multiple bacterial species, given that other studies have found altered metabolic pathways in thymol-adapted *E. coli* strains^[292-295]. Altogether the application of TraDIS has reinforced the small number of publications on the genetics underpinning bacterial phytochemical resistance.

Although a cross-species role for purine biosynthesis (demonstrated by the sequencing identification of the *S. enterica ycfF* locus here and the *S. aureus purR* gene in **Chapter 4**) in the bacterial interactions of thymol is suggested by the data gathered in this thesis; the bacterial envelope still remains a major, and primary site, of interaction for xenobiotics. Once the genetic elements underpinning the resistance of *S. enterica* to thymol had been established (i.e., generally focused upon the bacterial envelope) TEM was implemented to provide visual evidence for thymol's primary inhibitory MOA (**Section 5.2.3**). Overall, the images and quantitative values generated (**Figures 5.5-5.6** and **Table 5.2**) support the importance of the bacterial envelope in thymol interactions with *S. enterica*, with damage being observed to the standard morphology of the parental strain and less effect being observed on the efflux-dependant, tolerant mutant *S. enterica* strain #2. Scanning electron microscopy has observed membrane disruptions and complete loss of membrane integrity in cells of *S. enterica* Typhimurium exposed to thymol^[348, 349]. (**Eldien D.E. et al 2021**)^[350] also presented TEM images of *Salmonella* species displaying cell wall, membrane damage and degeneration of cytoplasmic constituents when exposed to thymol and associated essential oils^[350]. Other bacterial species, such as *E. coli*^[351] and *S. aureus*^[270], have also been presented with deformed cellular morphologies and damaged, wrinkled surfaces after thymol treatment.

In the context of this chapter's hypotheses and experiments, the conclusions detailed below may be drawn:

- Sequencing of a thymol-challenged TraDIS-Xpress library reinforced the data gathered in **Chapter 4** highlighting the importance of efflux-associated loci (*acrAB*, *ompA*, *surA* etc.) with efflux-deficient mutants significantly under-represented in the sequencing pool, while expanding the importance of other envelope-associated genes.

- TEM images did not present envelope blebbing or significant lysis of thymol-challenged parental *S. enterica* cells; though a distorted morphology and thinner envelope was clearly apparent when compared to unchallenged controls. A less dense cytoplasmic compartment was also observed, suggesting internal interactions with the antimicrobial phytochemical.
- TEM imaging of a thymol-selected, *ramR* mutant (the *S. enterica* strain #2, see **Chapter 4**) revealed a distinct morphology from the untreated parental strain, although this was maintained under thymol exposure unlike the drastic alterations seen with the parental *S. enterica* strain.

With evidence gathered for a primary inhibitory MOA of thymol, **Chapter 6** of this thesis will investigate the potential use of a phytochemical alternative food preservative; does the compound retain antimicrobial efficacy within an *in situ* vegetarian food model still remains a key question.

Chapter 6: Food challenge testing of thymol as a preservative

“Denn du bist, was du isst, Und ihr wisst, was es ist.”-

Rammstein, *Mein Teil*, 2004

6.1 Chapter introduction

The potent *in vitro* antimicrobial activity of thymol has been demonstrated throughout this body of work and is supported by the existing literature. However, the complex nutritional, physicochemical and microbiological environments that constitute food products may impede the inhibitive effects of alternative food preservatives^[352]. Fats and proteins found within foodstuffs, for example, have already been found to interact negatively with individual phytochemicals (essential oil components in particular)^[353]. Due to this fact, the concentration threshold for phytochemical *in situ* antimicrobial activity is generally higher than the *in vitro* activity described, however increasing phytochemical concentrations will likely alter the organoleptic qualities of the food product in question, potentially in a negative direction^[131, 354]. Thus, an *in situ* experiment to assess the potential for thymol as a preservative was established.

This chapter aims to investigate the *in situ* efficacy of thymol as an alternative food preservative within a vegetarian burger model along with a comparable, presently used industry standard, the Prosur NATPRE T-10+ mix.

Various growth conditions were tested to select an industrially and microbiologically appropriate incubation temperature, in addition to testing the CFU enumeration method within the food matrix to ensure an accurate and reliable count. Afterwards, a food challenge test (FCT) involving the incubation of a vegetarian burger model inoculated with *S. enterica* at 10°C for 30 days was implemented.

Hypothesis:

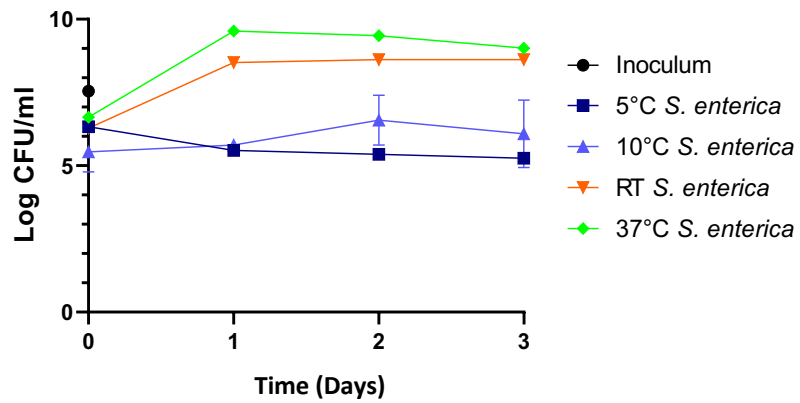
1. Thymol will induce a significant reduction in the CFU/g of inoculated *S. enterica* within an *in situ*, vegetarian burger model, when compared to the solvent vehicle control.
2. The Prosur NATPRE T-10+ mix will present no significant CFU/g reduction in the vegetarian burger model, when compared to the solvent vehicle control.

6.2 Results

6.2.1 Selection of 10°C as an appropriate chilled incubation temperature for *S. enterica*

For a realistic representation of the food production industry, a chilled temperature of 4°C would be used as the incubation temperature for the FCT (see **Sections 2.13.0** and **6.2.3**). However, the capacity for *S. enterica* to grow at this low a temperature required assessment to ensure the viable detection of bacteria present within the experiment. To this end, an optimisation experiment at various temperatures was performed (as described in **Section 2.13.1**), with the results displayed in **Figure 6.1**. The bacterial cultures placed at 37°C acted as a positive control within this experiment and displayed similar growth to the *S. enterica* cultures incubated at room temperature (RT, ~25°C). As can be seen in **Figure 6.1**, at 5°C there was no detectable growth across the three-day period, with in fact an average drop of 1.03 in the Log CFU/ml of the *S. enterica* cultures over time. However, there was a slight yet detectable increase in the Log CFU/ml of the bacterial cultures placed at 10°C over the course of the experiment (**Figure 6.1**). Due to the lack of detectable growth at 5°C, in contrast to the cultures placed at 10°C and the fact that this temperature is generally accepted as relevant to the food production chain from processing to packaging to transport; 10°C was selected as an incubation temperature for the FCT. This was agreed with the industrial partner of this project as a suitable condition.

Figure 6.1: *S. enterica* temperature optimisation growth curves.



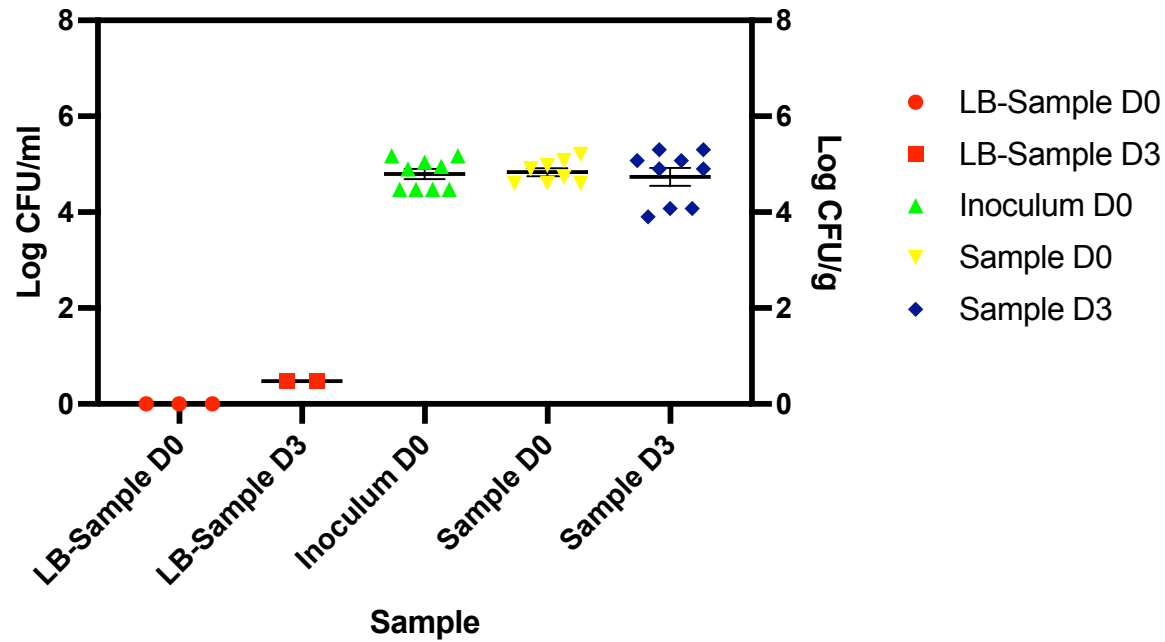
RT denotes Room Temperature; ~25°C. Experiments were repeated with three biological replicates (three technical replicates each) over an incubation period of 72 hours. Error bars represent the SEM(±).

6.2.2 Validation of CFU enumeration method in the food matrix model

Once an incubation temperature had been selected for the FCT (see **Sections 2.13.0** and **6.2.3**), the accuracy and reliability of the chosen enumeration method remained to be proven within the selected food model. A validation of the methodology outlined in **Section 2.13.0** was necessary before proceeding, via the protocol described in **Section 2.13.2**. **Figure 6.2** depicts the Log CFU/ml (for the inoculum) and the Log CFU/g calculated for these various food model samples, both on the day of inoculation and after 72 hours of incubation at 37°C. As can be seen, there are no significant differences between the Inoculum D0 and Sample D0 data sets; showing good recovery by the enumeration method selected for the FCT. There was little increase in the Log CFU/g between the Sample D0 and Sample D3 data sets, however this is most likely due to the use of a solid phase model unlike standard laboratory growth media optimised for bacterial growth in combination with the low incubation temperature. **Figure 6.3** presents an example XLD agar plate supplemented with fluconazole showing efficient identification of *S. enterica* colonies (pigmented black) and elimination of any contaminating background.

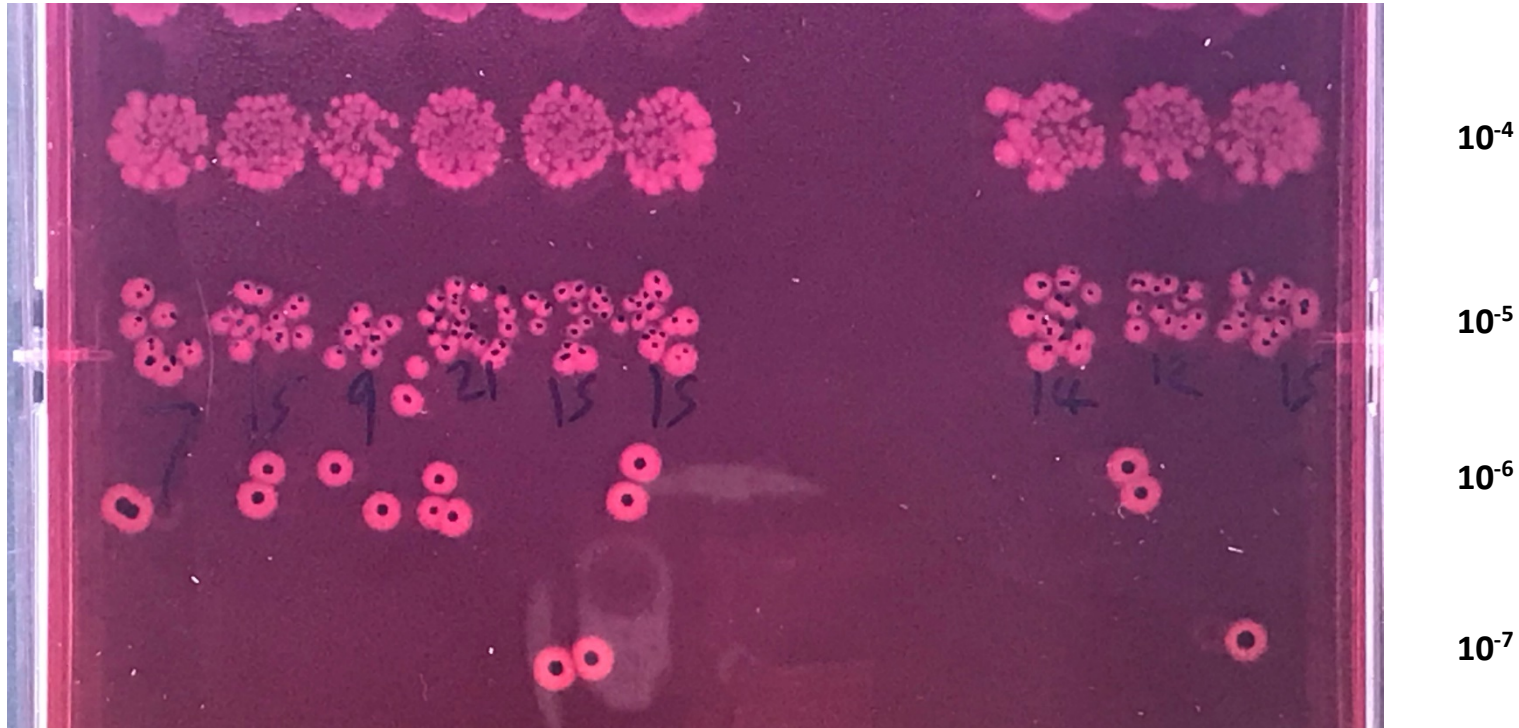
With a selected chilled incubation temperature of 10°C and confidence in the enumeration method, the FCT was implemented to determine the *in situ* efficacy of thymol as an alternative food preservative.

Figure 6.2: Recovery of *S. enterica* from the vegetarian burger model.



Left-hand y-axis denotes Log CFU/ml units for Inoculum D0, right-hand y-axis denotes Log CFU/g units for all other samples. D0 denotes sampling on the day of inoculation. D3 denotes sampling after 72 hours of incubation. Control samples consisted of one biological replicate, with three technical replicates. Experimental samples were repeated with three biological replicates (three technical replicates each), all over an incubation period of 72 hours.

Figure 6.3: *S. enterica* growth on XLD agar supplemented with fluconazole.



The use of XLD agar supplemented with fluconazole eliminated the growth of fungal contaminants from the vegetarian burger samples and allowed accurate enumeration of the *S. enterica* inoculum.

6.2.3 Thymol retains antimicrobial capacity in an *in situ* food model

After optimising for a suitable chilled incubation temperature and validating the chosen enumeration method (see **Sections 2.13.0, 6.2.1 and 6.2.2**), the FCT to determine the *in situ* efficacy of thymol as an alternative food preservative was implemented. An exemplar photograph of the preparation for the vegetarian food samples is displayed in **Figure 6.4**, which took place on one day over the course of 12 hours. The *S. enterica* enumeration results of the 30-day long experiment are presented in **Figure 6.5**, while the physical appearance of the vegetarian food samples throughout this time is displayed in **Figure 6.6**.

The uninoculated negative control samples showed no growth apart from the occasional, sporadic colony (**Figure 6.5b**), which may be expected given the preservative-free nature of the product. The positive control maintained a similar bacterial load to the solvent control until ~17 days of sampling (**Figure 6.5b**) when the Log CFU/g values dropped dramatically; this was unexpected and may be due to technical error while inoculating these samples. No significant difference was observed between the *S. enterica* bacterial load of the solvent control and the 1% Prosur NATPRE T-10+mix food samples (**Figure 6.5b-c**). Comparing the solvent control Log CFU/g values to the 1% thymol vegetarian food samples, a consistent decrease of approximately 5-10 fold in CFU/g was observed across the experiment (**Figure 6.5b**). This decrease was found to be statistically significant after utilising a 1-way repeated measures ANOVA with the addition of Fischers' LSD test (**Figure 6.5c**).

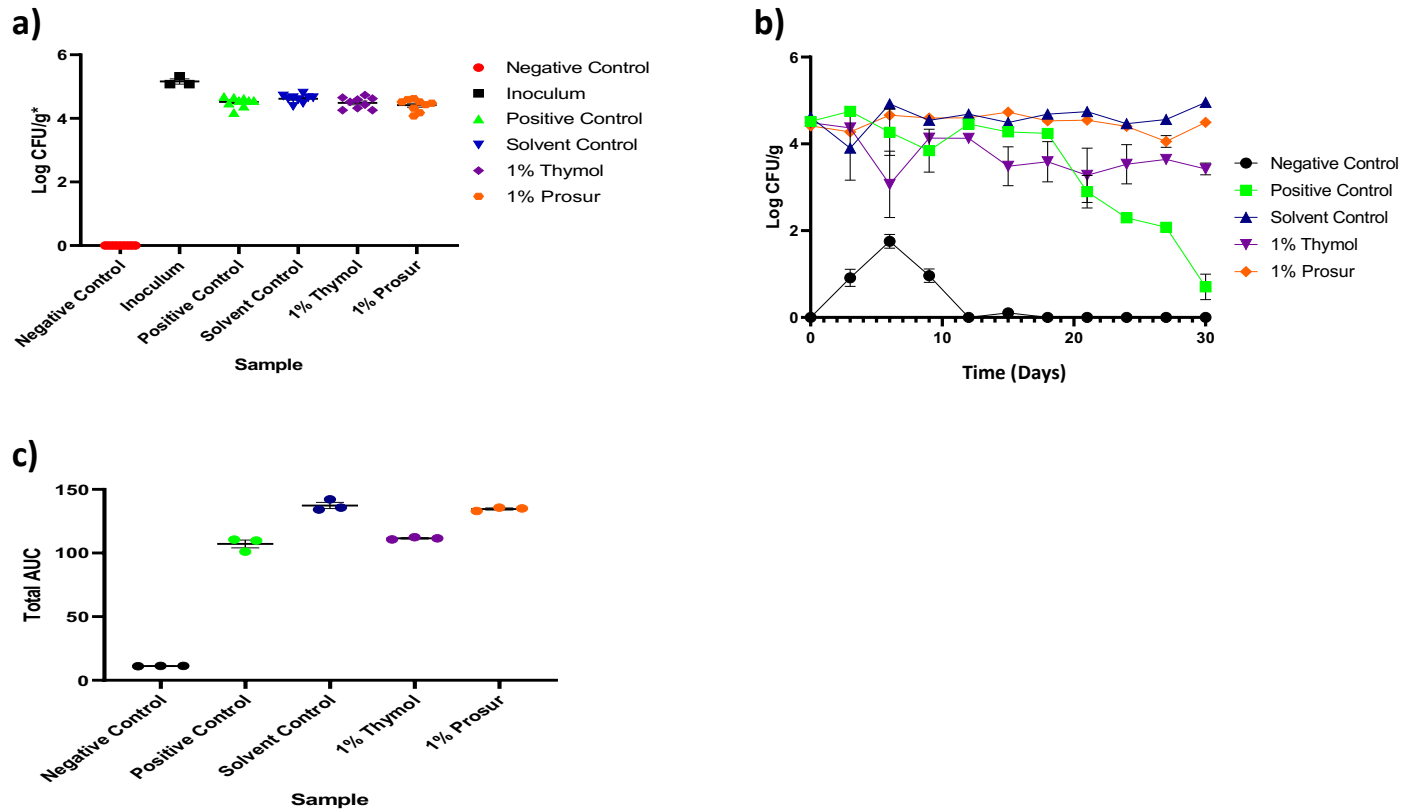
Daily photographs of random samples throughout the FCT (**Figure 6.6**) evidenced a visual deterioration in consistency and colour of the negative and positive controls throughout the 30-day experimental period. Gradually a mushy, yellow-brown and exudate-leaking appearance was observed within these experimental conditions while the solvent and phytochemical-laced vegetarian food samples maintained a more solid consistency and more of their original colour, developing a more granular appearance with far less apparent exudate (**Figure 6.6**). This pattern was seen for the 1% thymol, 1% Prosur NATPRE T-10+ mix and solvent control samples (**Figure 6.6**).

Figure 6.4: Preparation of vegetarian food model samples.



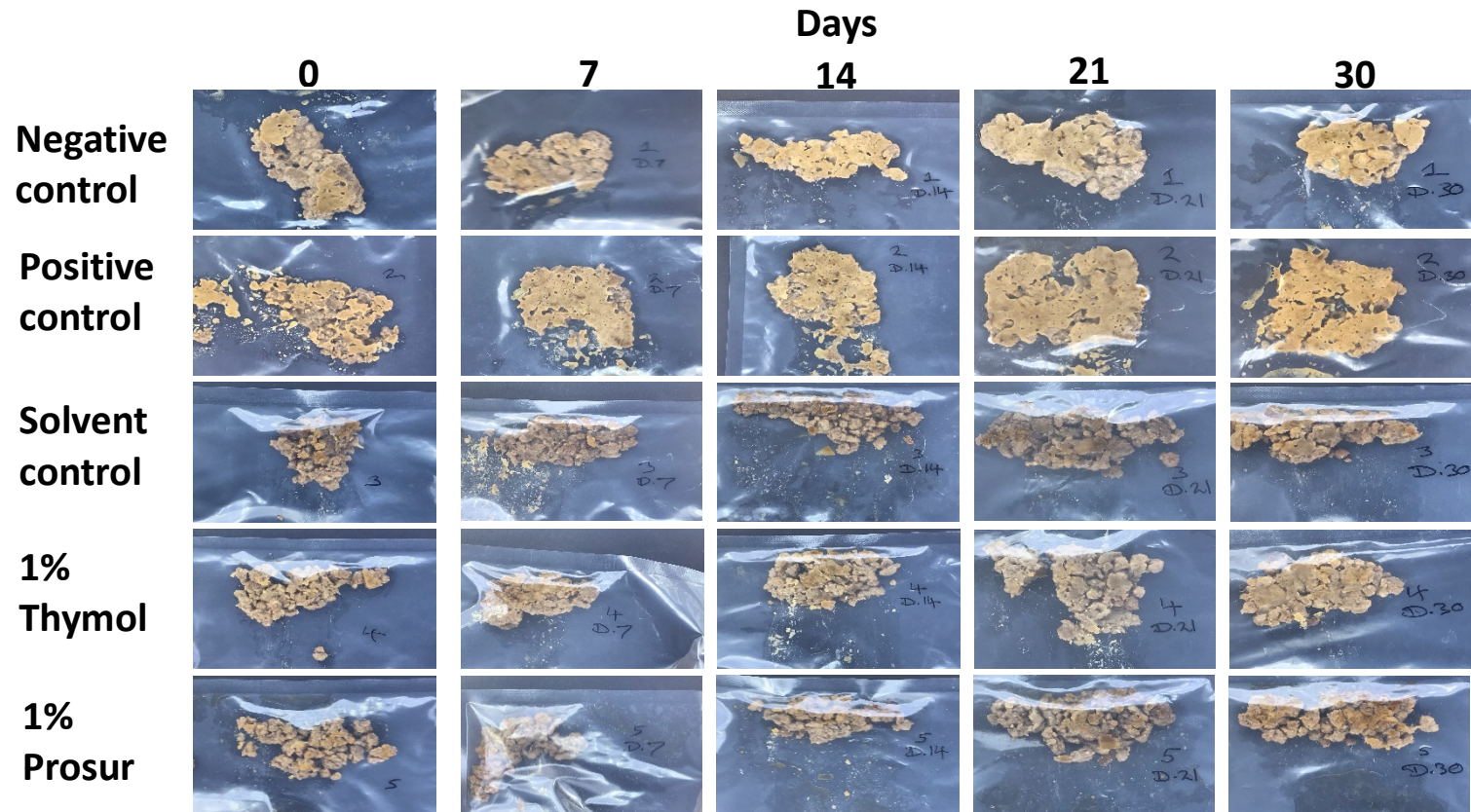
Vegetarian burger matter was supplemented with experimental solutions (PBS, DMSO or phytochemicals), thoroughly mixed by hand before 10g samples were spooned into vacuum packs and kept on ice until inoculation (also kept on ice, orange-capped centrifuge tube) with *S. enterica*. After inoculation, vegetarian food samples were placed back on ice before vacuum packaging and placement into a fridge at 10°C.

Figure 6.5: Results from the FCT.



Panel **a)** *S. enterica* enumerations recorded immediately after inoculation (D0) of the vegetarian food model. * denotes the units for the Inoculum were Log CFU/ml. **b)** enumeration of *S. enterica* inoculated vegetarian food model over the experimental period of 30 days. **c)** area under the curve (AUC) values for the whole ?? calculated from the growth curves in panel **b)**. A 1-way repeated measures ANOVA Test with Fischer's LSD test was performed on these values.

Figure 6.6: Physical appearances of the FCT vegetarian food samples.



All samples were inoculated with *S. enterica* (excluding the negative control) and incubated at 10°C for a 30-day period. The negative and positive controls lacked the addition of the vehicle solvent, thymol or the Prosur NATPRE T-10+ mix; note the gradual change to a mushy consistency and yellow-brown colour. The solvent vehicle and phytochemical samples retained their original consistency to a better degree, although only the addition of thymol reduced the bacterial load of the vegetarian food samples.

6.3 Chapter Discussion

Sodium nitrite, although used historically as a food preservative (particularly within cured/chilled meats) has been associated with an increased risk for the development of gastrointestinal cancers^[29, 31, 52, 53, 126, 127]. There is therefore a need for the food industry^[355] to identify alternative preservative compounds. Phytochemicals offer a promising source of chemical structures for this purpose with multiple advantages; recyclable from plant/fruit waste^[356], antimicrobial properties^[29, 123, 127, 132, 357-360] with many compounds already possessing a GRAS status^[129].

Within the FCT described in this chapter, the Prosur NATPRE T-10+ mix did not display antimicrobial activity within the *in situ* vegetarian food model (see **Section 6.2.3, Figure 6.5**). This lack of bacterial inhibition may have been predicted from the previous *in vitro* experiments performed within this thesis (**Chapters 3-4**) however, as this commercial product is presently used effectively in the preservation of food products, this discrepancy may be due to two combining factors. Firstly, the primary constituent phytochemicals comprising the Prosur NATPRE T-10+ mix (eriodictyol, ferulic acid and naringenin) may be at too low a concentration to enact an *in vitro* and *in situ* antimicrobial effect, even in a synergistic manner with each other, at present. Secondly, and perhaps most importantly, the production of foodstuffs typically comprises multiple additive and technical challenge hurdles (salts, nitrite, nisin, organic acids, heat treatments, desiccation etc.)^[357, 361-366] that may be required to “activate” the antimicrobial behaviour of the phytochemical mixture, hurdles that were not included in this work. This possibility is supported by the data presented within **Chapter 3 (Section 3.2.3 and Section 3.2.6)** of this thesis suggesting a potent capacity of the Prosur NATPRE T-10+ mix to synergise in combination with other compounds/hurdles.

The negative and positive control samples in the FCT visually decayed throughout the 30-day experimental time period (**Section 6.2.3, Figure 6.6**), as might be expected. The 1% thymol and Prosur NATPRE T-10+ mix conditions both maintained the samples visual appearance to a greater degree, however, so too did the solvent control. This suggests that this effect was not solely due to the added phytochemicals. The sensual profiles of these samples are beyond the scope of this FCT experiment, nevertheless the organoleptic qualities of foodstuffs (texture, colour, taste, smell etc.) are vital qualities to entice customer purchases^[132]. Sodium nitrite has been well recorded, alongside its antimicrobial usage, to impart and maintain the expected

colour/texture/flavour of chilled processed meats, partially as a result of this preservative's strong antioxidant activities^[31, 40, 48]. In substituting current chemical food preservatives, ideally phytochemicals would also act as functional replacements in the same vein. Promisingly, multiple phytochemicals have had potent antioxidant properties described for them within the literature^[132, 355, 367-369]. Thymol has presented potent antioxidant activity, both with *in vitro*^[138, 370, 371] and *in situ* experimental models^[372, 373]. In the specific case of thymol and the Prosur NATPRE T-10+ mix used within this FCT (**Section 6.2.3, Figure 6.6**), their potential in maintaining the organoleptic properties of the food samples largely remains unclear as the solvent vehicle controls used may have had an effect. The addition of DMSO to foodstuffs suitable for human or animal consumption is impractical but researchers have investigated alternative delivery systems for introducing phytochemicals to foodstuffs. These methods include nano-complexation of thymol and soy protein isolate (SPI) to improve the solubility and stability of the monoterpenoid phenol, while maintaining its antimicrobial activities^[374]. Thymol-encapsulated polylactic acid nanoparticles have also been investigated, exhibiting high stability during storage and an improved antimicrobial capacity compared to non-encapsulated thymol against *E. coli* inoculated apple slices^[375], in addition to other conjugated nano-encapsulated methods^[376]. Another alternative solution, the impregnation of food packaging films/wrappings etc., has also been probed with thymol-laced SPI-based composite films and pomegranate rind powder incorporated into polycaprolactone matrices that retained an effective degree of antimicrobial activity^[130, 266, 377, 378]. Biodegradable, composite films loaded with thymol (alone or in combination with carvacrol) have also been shown to maintain, and indeed extend, the antioxidant and antimicrobial activities of the active phytochemicals, enabling delivery of the independent or synergistic compounds into distilled water for up to six weeks^[378]. Altogether, this body of evidence reinforces the potential of novel phytochemical delivery systems that may overcome the compounds' innate low solubilities.

Thymol has been reported to provide antimicrobial activity within other food model systems^[374-377, 379]. (**Shah B. et al 2012**)^[380] presented antimicrobial activity against *L. monocytogenes* and *E. coli* O157:H7 from (free and nano-dispersed) thymol within apple cider and 2% reduced-fat milk^[380]. Free and nano-emulsified thymol at 600mg/kg were found to significantly decrease *E. coli* and *S. aureus* counts of inoculated sausage samples over a four week period^[381]. (**Mastromatteo M. et al 2010**)^[382] have also reported a dose-dependent antimicrobial effect with thymol loaded into the coating of ready to use peeled shrimps, particularly effective when combined with modified atmospheric packaging (MAP) in extending

the shelf-life of samples to approximately 14 days^[382]. The data from the experiments presented here add to this growing basis for the antimicrobial efficacy of phytochemicals, and thymol in particular, in food systems including vegetarian-based meat substitutes.

Conclusions may be drawn from the data in this chapter:

- Thymol induced a reduction in the CFU/g measurements of inoculated *S. enterica* within the novel vegetarian burger model. However, this effect was lower than *in vitro* experiments presented in **Chapter 3** of this work, suggesting a negative impact of the food matrix on the antimicrobial activity of this monoterpenoid phenol.
- The Prosur NATPRE T-10+ mix did not display any significant inhibition of the inoculated *S. enterica* throughout the experimental time period. This may be due to the experimental design of the FCT lacking any of the complementary challenge hurdles typically included in the formulation of food products.

The data produced here supports existing literature surrounding the antimicrobial efficacy of phytochemicals, and thymol specifically, within *in situ* food models. This extends the present research to include samples of vegetarian-based meat substitutes. Although further investigation is warranted to ensure safe and effective food, phytochemical and hurdle technology combinations, the results of this thesis FCT confirm the promise of these compounds as alternative food preservatives.

Chapter 7: Final discussion & acknowledgements

“Stay a while and listen.”- Deckard Cain, Diablo II, 2000

7.1.0 Final discussion

As has been described in **Chapter 1** there is an urgent need for novel, efficacious antimicrobial compounds in the clinic and food industry^[37, 40, 53, 54, 64, 156]. Produced by plant species for multiple secondary functions, including antimicrobial defence^[383-385], phytochemicals represent a novel source of potential candidates with varied, flexible chemical scaffolds^[62, 386]. Although phytochemicals have previously been shown to possess antimicrobial properties^[206, 387-390], there still remain key knowledge gaps before a successful application of these compounds in the food industry, the main focus of this body of work, can be implemented. These gaps include the frequency rate and mechanisms of potential bacterial phytochemical resistance, understanding of the primary inhibitory MOA of phytochemicals and the *in situ* efficacy of phytochemicals within a vegetarian burger model.

Given the conflicting literature regarding the activity of different phytochemicals a 14-compound panel was compared here under standardised conditions. The resulting data from these experiments showed a wide variation in activity as direct antimicrobials or as synergistic agents against the four tested pathogens. Thymol, caffeic acid and a commercial phytochemical mix (the Prosur NATPRE T-10+) were investigated further as examples with potent directly antimicrobial activity, potentiative capacity and present application in the food industry.

The potential for thymol, caffeic acid and the Prosur NATPRE T-10+ mix to select for resistant bacterial strains was investigated in **Chapter 4**, where thymol readily selected tolerant mutants. The mutation frequency rate of thymol for mutant strains of *S. enterica*, *S. aureus* and *P. aeruginosa* was comparable to that of classic antibiotic classes^[289-291]. This finding suggests that although thymol may be an effective antimicrobial, long-term use of this compound may be compromised by the selection of mutants. Furthermore, analysis of selected mutants showed a classic efflux-dependant, low level, multi-drug resistant phenotype mediated by mutations in efflux regulators.

Within **Chapter 5**, further genetic investigation was undertaken to investigate mechanisms of bacterial resistance to thymol, and to provide an inference towards the primary inhibitory MOA of this monoterpenoid phenol. To this end an *S. enterica* TraDIS-Xpress

library was applied to a phytochemical for the first time. The resulting sequencing analysis reinforced the role of efflux in thymol tolerance while also identifying a role for envelope-associated genes such as *ompA*, *surA*, *tolC* and *yejM*. Subsequent TEM revealed major structural alterations to the bacterial envelope and cytoplasmic density of thymol-exposed cells. This further points towards an envelope-targeting MOA for the antimicrobial activity of thymol. Multiple inhibitory MOA have been published for thymol however^[270, 306, 349], with evidence gathered here also suggesting a cross-species role for the altered regulation of nucleoside biosynthesis (i.e.; the *S. enterica ycfF* and *S. aureus purR* loci) in the bacterial mechanisms of thymol resistance. Nevertheless, the envelope is the first point of physical contact for the compound with the bacterial cell and thus may be considered a primary interaction to consider for inhibitive and resistance mechanisms. Ideally, further experiments utilising knock-out and complementation strains in efflux/permeability assays could reinforce this data, while DNA quantification and transcriptomic experiments may further elucidate the roles played by altered nucleoside biosynthesis. However, due to the global context at the time of research (i.e.; the COVID-19 pandemic), these experiments were curtailed to fit the modified timescale of this project.

Finally, in **Chapter 6** I investigated the antimicrobial efficacy of thymol and the Prosur NATPRE T-10+ mix in a novel vegetarian burger model. While the commercial Prosur NATPRE T-10+ mix failed to decrease the CFU/g enumerations of the inoculated *S. enterica*, due to reasons already discussed, thymol did exert an antimicrobial effect, albeit slightly dampened when compared to *in vitro* work. While this is promising, further research would be required to pin down the thymol-food matrix interactions underpinning the phytochemical's influences on the organoleptic qualities of the food model as this was beyond the scope of the present work. Previous research has suggested that this dynamic is a delicate combination of multiple factors^[353, 378, 391, 392].

In summary this thesis adds to the literature concerning phytochemicals, and thymol specifically, regarding their antimicrobial capacities while also expanding the existing knowledge base. I show potential for mutant selection, confirm efflux as a primary mechanism of resistance and the cell envelope as a (potentially main) target. The *in situ* efficacy of thymol within a vegetarian food model confirms promise as a preservative but more research is needed to ensure the safe and efficient application of phytochemicals within the food industry as alternative food preservatives.

7.2.0 Acknowledgements

I would like to extend my gratitude towards the previous members of the Peck group: Andrew Cartwright, Jason Brunt, Martin Webb, Sandra Stringer, Hannah Pye and, especially, Professor Mike Peck. Thank you for your support throughout my studies and for putting up with my moaning in the summer heat.

I would also like to thank the past and present members of the Webber group, not limited to but including: Emma Holden, Gregory Wickham, Eleftheria Trampari, and Professor Mark Webber. Thank you for taking me in as a warm and welcoming group, for all your support, advice and helping me plod on. I would also like to express my gratitude to Dr. Paul Kroon for the sensible advice received and for keeping me straight. To Keith Turner and Mohammed Yasir; a big thank you for all your help surrounding the TraDIS-Xpress work, for helping me make the most of my project timeframe. To the QIB Bioimaging department, and especially to Kathryn Gotts and Catherine Booth, a great many thanks for their help in implementing the TEM work within this project. To Nestlé and Stephen Grove for the support, advice, and funding that contributed to this work; thank you. To the students greatest friend and enemy, energy drinks, cigarettes and alcohol for numbing the pain, thank you but honestly, it was never going to work out between us. It's me, not you. A warm thank you to anyone else I may have forgotten to name directly here too; your aid was greatly appreciated even if my memory falters.

Words cannot adequately describe the gratitude and appreciation I have for my family; for their love, kindness and support throughout my life, without whom I would not be here let alone be the man I am today. Words cannot describe, but here lies an attempt.

To my mother Dorothy Dawn Sweet for raising me with determination, for the support, the weekly chats to uphold my spirits and humouring my nonsense... Thank you.

To my father Robert James Sweet for supporting me throughout the years, visiting me during my studies and for teaching me that you cannot take life too seriously... Thank you.

To my brothers, Jamie Sweet and Morgan William Sweet, for your support, brotherly love, and visits to help pull me out of my homesickness... Cheers lads. Sadly, you can't call me a lazy student anymore but the first round is on me.

This is for all of you.

Thank you.

Chapter 8: References

*“The more that you read, the more things you will know.
The more that you learn, the more places you’ll go.” – Dr.
Seuss, *I Can Read With My Eyes Shut!*, 1978*

1. Havelaar, A.H., et al., *World Health Organization Global Estimates and Regional Comparisons of the Burden of Foodborne Disease in 2010*. PLoS Med, 2015. **12**(12): p. e1001923.
2. Santosham, M., et al., *Progress and barriers for the control of diarrhoeal disease*. The Lancet, 2010. **376**(9734): p. 63-67.
3. Jemmi T., a.S.R., *Listeria monocytogenes Foodborne Pathogen and Hygiene Indicator*. Rev. Sci. Tech. Off. Int. Epiz. , 2006. **25**(2): p. 571-580.
4. Horlbog, J.A., et al., *Surviving host - and food relevant stresses: phenotype of L. monocytogenes strains isolated from food and clinical sources*. Scientific Reports, 2018. **8**(1): p. 12931.
5. Farber, J.M. and P.I. Peterkin, *Listeria monocytogenes, a food-borne pathogen*. Microbiological Reviews, 1991. **55**(3): p. 476.
6. Schuchat, A., B. Swaminathan, and C.V. Broome, *Epidemiology of human listeriosis*. Clinical Microbiology Reviews, 1991. **4**(2): p. 169.
7. Scallan, E., et al., *An assessment of the human health impact of seven leading foodborne pathogens in the United States using disability adjusted life years*. Epidemiology and Infection, 2015. **143**(13): p. 2795-2804.
8. Allerberger, F. and M. Wagner, *Listeriosis: a resurgent foodborne infection*. Clinical Microbiology and Infection, 2010. **16**(1): p. 16-23.
9. Dasti, J.I., et al., *Campylobacter jejuni: A brief overview on pathogenicity-associated factors and disease-mediating mechanisms*. International Journal of Medical Microbiology, 2010. **300**(4): p. 205-211.
10. Hsieh, Y.-H. and I.M. Sulaiman, *Chapter 5 - Campylobacteriosis: An Emerging Infectious Foodborne Disease*, in *Foodborne Diseases*, A.M. Holban and A.M. Grumezescu, Editors. 2018, Academic Press. p. 119-155.
11. Kisiela, D.I., et al., *Evolution of Salmonella enterica virulence via point mutations in the fimbrial adhesin*. PLoS pathogens, 2012. **8**(6): p. e1002733-e1002733.
12. Uzzau, S., et al., *Host adapted serotypes of Salmonella enterica*. Epidemiology and Infection, 2000. **125**(2): p. 229-255.
13. Chiu, C.-H., L.-H. Su, and C. Chu, *Salmonella enterica Serotype Choleraesuis: Epidemiology, Pathogenesis, Clinical Disease, and Treatment*. Clinical Microbiology Reviews, 2004. **17**(2): p. 311.
14. Fàbrega, A. and J. Vila, *Salmonella enterica serovar Typhimurium skills to succeed in the host: virulence and regulation*. Clinical microbiology reviews, 2013. **26**(2): p. 308-341.
15. Ehuwa, O., A.K. Jaiswal, and S. Jaiswal, *Salmonella, Food Safety and Food Handling Practices*. Foods, 2021. **10**(5): p. 907.
16. Rode, T.M., et al., *Different patterns of biofilm formation in Staphylococcus aureus under food-related stress conditions*. International Journal of Food Microbiology, 2007. **116**(3): p. 372-383.
17. Scallan, E., et al., *Foodborne illness acquired in the United States--major pathogens*. Emerging infectious diseases, 2011. **17**(1): p. 7-15.
18. Mead, P.S., et al., *Food-related illness and death in the United States*. Emerging infectious diseases, 1999. **5**(5): p. 607-625.
19. Sergelidis, D. and A.S. Angelidis, *Methicillin-resistant Staphylococcus aureus: a controversial food-borne pathogen*. Letters in Applied Microbiology, 2017. **64**(6): p. 409-418.
20. Hennekinne, J.-A., M.-L. De Buyser, and S. Dragacci, *Staphylococcus aureus and its food poisoning toxins: characterization and outbreak investigation*. FEMS Microbiology Reviews, 2012. **36**(4): p. 815-836.

21. Cosgrove, S.E., et al., *Comparison of Mortality Associated with Methicillin-Resistant and Methicillin-Susceptible Staphylococcus aureus Bacteremia: A Meta-analysis*. Clinical Infectious Diseases, 2003. **36**(1): p. 53-59.
22. Kadariya, J., T.C. Smith, and D. Thapaliya, *Staphylococcus aureus and Staphylococcal Food-Borne Disease: An Ongoing Challenge in Public Health*. BioMed Research International, 2014. **2014**: p. 827965.
23. Kang, C.-I., et al., *Pseudomonas aeruginosa Bacteremia: Risk Factors for Mortality and Influence of Delayed Receipt of Effective Antimicrobial Therapy on Clinical Outcome*. Clinical Infectious Diseases, 2003. **37**(6): p. 745-751.
24. Rossolini, G.M. and E. Mantengoli, *Treatment and control of severe infections caused by multiresistant Pseudomonas aeruginosa*. Clinical Microbiology and Infection, 2005. **11**: p. 17-32.
25. Bantawa, K., et al., *Food-borne bacterial pathogens in marketed raw meat of Dharan, eastern Nepal*. BMC Research Notes, 2018. **11**(1): p. 618.
26. Tambekar, D., et al., *Identification of microbiological hazards and safety of ready-to-eat food vended in streets of Amravati City, India*. Journal of Applied Biosciences, 2008. **7**(3): p. 195-201.
27. Sharif, M.K., K. Javed, and A. Nasir, *Chapter 15 - Foodborne Illness: Threats and Control*, in *Foodborne Diseases*, A.M. Holban and A.M. Grumezescu, Editors. 2018, Academic Press. p. 501-523.
28. Binkerd, E.F. and O.E. Kolari, *The history and use of nitrate and nitrite in the curing of meat*. Food and Cosmetics Toxicology, 1975. **13**(6): p. 655-661.
29. Sebranek, J.G. and J.N. Bacus, *Cured meat products without direct addition of nitrate or nitrite: what are the issues?* Meat Science, 2007. **77**(1): p. 136-147.
30. Cammack, R., et al., *Nitrite and nitrosyl compounds in food preservation*. Biochimica et Biophysica Acta (BBA) - Bioenergetics, 1999. **1411**(2): p. 475-488.
31. Pierson, M.D., L.A. Smoot, and M.C. Robach, *Nitrite, nitrite alternatives, and the control of clostridium botulinum in cured meats*. C R C Critical Reviews in Food Science and Nutrition, 1983. **17**(2): p. 141-187.
32. Gill, A.O. and R.A. Holley, *Interactive inhibition of meat spoilage and pathogenic bacteria by lysozyme, nisin and EDTA in the presence of nitrite and sodium chloride at 24 °C*. International Journal of Food Microbiology, 2003. **80**(3): p. 251-259.
33. Tompkin, R.B., *Antimicrobials in Food*. 3rd ed. 2005, USA: CRC Press, Technology & Engineering. 706.
34. Ávila, M., et al., *Inhibitory activity of reuterin, nisin, lysozyme and nitrite against vegetative cells and spores of dairy-related Clostridium species*. International Journal of Food Microbiology, 2014. **172**: p. 70-75.
35. Honikel, K.-O., *The use and control of nitrate and nitrite for the processing of meat products*. Meat Science, 2008. **78**(1): p. 68-76.
36. Zink, D.L., *The impact of consumer demands and trends on food processing*. Emerging infectious diseases, 1997. **3**(4): p. 467-469.
37. Joannou, C.L., et al., *The bacteriocidal effects of transition metal complexes containing the NO⁺ group on the food-spoilage bacterium Clostridium sporogenes*. FEMS Microbiology Letters, 1992. **98**(1-3): p. 67-70.
38. Cassens, R., et al., *Reactions of nitrite in meat*. Food Technology (USA), 1979.
39. Heck, D.E., *·NO, RSNO, ONOO⁻, NO⁺, ·NOO, NO_x-Dynamic Regulation of Oxidant Scavenging, Nitric Oxide Stores, and Cyclic GMP-Independent Cell Signaling*. Antioxidants & Redox Signaling, 2001. **3**(2): p. 249-260.
40. Grever, A.B. and A. Ruiter, *Prevention of Clostridium outgrowth in heated and hermetically sealed meat products by nitrite – a review*. European Food Research and Technology, 2001. **213**(3): p. 165-169.

41. Williams, D.L.H., *The Chemistry of S-Nitrosothiols*. Accounts of Chemical Research, 1999. **32**(10): p. 869-876.
42. Inoue, S. and S. Kawanishi, *Oxidative DNA damage induced by simultaneous generation of nitric oxide and superoxide*. FEBS Letters, 1995. **371**(1): p. 86-88.
43. Kroncke, K.D., et al., *Nitric Oxide Destroys Zinc-Sulfur Clusters Inducing Zinc Release from Metallothionein and Inhibition of the Zinc Finger-Type Yeast Transcription Activator LAC9*. Biochemical and Biophysical Research Communications, 1994. **200**(2): p. 1105-1110.
44. Woods, L.F.J., J.M. Wood, and P.A. Gibbs, *The involvement of nitric oxide in the inhibition of the phosphoroclastic system in Clostridium sporogenes by sodium nitrite*. Microbiology, 1981. **125**(2): p. 399-406.
45. Wolff, I.A. and A.E. Wasserman, *Nitrates, Nitrites, and Nitrosamines*. Science, 1972. **177**(4043): p. 15-19.
46. Warriss, P.D., E.A. Bevis, and P.J. Ekins, *The relationships between glycogen stores and muscle ultimate pH in commercially slaughtered pigs*. British Veterinary Journal, 1989. **145**(4): p. 378-383.
47. Igene, J.O., et al., *Mechanisms by which nitrite inhibits the development of warmed-over flavour (WOF) in cured meat*. Food Chemistry, 1985. **18**(1): p. 1-18.
48. Arendt, B., L.H. Skibsted, and H.J. Andersen, *Antioxidative activity of nitrite in metmyoglobin induced lipid peroxidation*. Zeitschrift für Lebensmitteluntersuchung und -Forschung A, 1997. **204**(1): p. 7-12.
49. Group, I.W., *IARC monographs on the evaluation of carcinogenic risks to humans. Ingested nitrate and nitrite, and cyanobacterial peptide toxins*. IARC monographs on the evaluation of carcinogenic risks to humans/World Health Organization, International Agency for Research on Cancer, 2010. **94**.
50. FSA, *Food Additives Legislation Guidance To Compliance, Food additives - Regulation 1333/2008*, F.S. Agency, Editor. 2015, UK Food Standards Agency: <https://www.food.gov.uk/.../food-additives-legislation-guidance-to-compliance.pdf>. p. 26-27.
51. Keeton, J.T., *History of nitrite and nitrate in food*, in *Nitrite and nitrate in human health and disease*. 2011, Springer. p. 69-84.
52. Magee, P.N. and J.M. Barnes, *The production of malignant primary hepatic tumours in the rat by feeding dimethylnitrosamine*. British journal of cancer, 1956. **10**(1): p. 114-122.
53. Magee, P. and J. Barnes, *Carcinogenic nitroso compounds*, in *Advances in cancer research*. 1967, Elsevier. p. 163-246.
54. Michail, N. *MEPs Urge Action On Nitrites and Nitrates*. 2016 [cited 2017 16th Feb.].
55. DeWitte, S.N. and J.W. Wood, *Selectivity of Black Death mortality with respect to preexisting health*. Proceedings of the National Academy of Sciences, 2008. **105**(5): p. 1436.
56. Kriss, T.C. and V.M. Kriss, *History of the Operating Microscope: From Magnifying Glass to Microneurosurgery*. Neurosurgery, 1998. **42**(4): p. 899-907.
57. Mohr, K.I., *History of Antibiotics Research*, in *How to Overcome the Antibiotic Crisis : Facts, Challenges, Technologies and Future Perspectives*, M. Stadler and P. Dersch, Editors. 2016, Springer International Publishing: Cham. p. 237-272.
58. Bentley, R., *The development of penicillin: genesis of a famous antibiotic*. Perspectives in biology and medicine, 2005. **48**(3): p. 444-452.
59. Yim, G., H. Huimi Wang, and J. Davies, *The truth about antibiotics*. International Journal of Medical Microbiology, 2006. **296**(2): p. 163-170.
60. Cirillo, V.J., *Two faces of death: fatalities from disease and combat in America's principal wars, 1775 to present*. Perspectives in biology and medicine, 2008. **51**(1): p. 121-133.
61. Eardley, W.G.P., et al., *Infection in conflict wounded*. Philosophical transactions of the Royal Society of London. Series B, Biological sciences, 2011. **366**(1562): p. 204-218.

62. Katz, L. and R.H. Baltz, *Natural product discovery: past, present, and future*. Journal of Industrial Microbiology & Biotechnology, 2016. **43**(2): p. 155-176.
63. Yazdankhah, S., et al., [*The history of antibiotics*]. Tidsskr Nor Laegeforen, 2013. **133**(23-24): p. 2502-7.
64. Luepke, K.H., et al., *Past, Present, and Future of Antibacterial Economics: Increasing Bacterial Resistance, Limited Antibiotic Pipeline, and Societal Implications*. Pharmacotherapy, 2017. **37**(1): p. 71-84.
65. Sadaka, C., et al., *Review on Abyssomicins: Inhibitors of the Chorismate Pathway and Folate Biosynthesis*. Molecules, 2018. **23**(6).
66. Wood, W.B., *STUDIES ON THE ANTIBACTERIAL ACTION OF THE SULFONAMIDE DRUGS*. The Journal of Experimental Medicine, 1942. **75**(4): p. 369.
67. Wu, Q., et al., *Interaction between typical sulfonamides and bacterial diversity in drinking water*. J Water Health, 2018. **16**(6): p. 914-920.
68. Tipper, D.J., *Mode of action of β -lactam antibiotics*. Pharmacology & Therapeutics, 1985. **27**(1): p. 1-35.
69. Bush, K. and P.A. Bradford, *β -Lactams and β -Lactamase Inhibitors: An Overview*. Cold Spring Harbor perspectives in medicine. **6**(8): p. a025247.
70. Wisseman, C.L., Jr., et al., *Mode of action of chloramphenicol. I. Action of chloramphenicol on assimilation of ammonia and on synthesis of proteins and nucleic acids in Escherichia coli*. Journal of bacteriology, 1954. **67**(6): p. 662-673.
71. Hahn, F.E., C.L. Wisseman, Jr., and H.E. Hopps, *Mode of action of chloramphenicol, II. Inhibition of bacterial D-polypeptide formation by an L-stereoisomer of chloramphenicol*. Journal of bacteriology, 1954. **67**(6): p. 674-679.
72. Schwarz, S., et al., *Lincosamides, Streptogramins, Phenicol, and Pleuromutilins: Mode of Action and Mechanisms of Resistance*. Cold Spring Harbor perspectives in medicine. **6**(11): p. a027037.
73. NCBI. *PubChem Compound Database*. 2019 [cited 2019 Jan. 9th]; Available from: <https://pubchem.ncbi.nlm.nih.gov/compound/5959>.
74. Chopra, I. and M. Roberts, *Tetracycline antibiotics: mode of action, applications, molecular biology, and epidemiology of bacterial resistance*. Microbiology and molecular biology reviews : MMBR, 2001. **65**(2): p. 232-260.
75. Hash J.N., W.M., and Miller P.A., , *On The Mode of Action of the Tetracycline Antibiotics in Staphylococcus aureus**. Journal of Biological Chemistry, 1964. **239**(6): p. 2070-2078.
76. Grossman, T.H., *Tetracycline antibiotics and resistance*. Cold Spring Harbor perspectives in medicine, 2016. **6**(4): p. a025387.
77. Hancock, R.E.W., *Aminoglycoside Uptake and Mode of Action- with Special Reference to Streptomycin and Gentamicin*. Journal of Antimicrobial Chemotherapy, 1981. **8**: p. 249-276.
78. Schroeder, R., C. Waldsich, and H. Wank, *Modulation of RNA function by aminoglycoside antibiotics*. The EMBO Journal, 2000. **19**(1): p. 1.
79. Jana, S. and J. Deb, *Molecular understanding of aminoglycoside action and resistance*. Applied microbiology and biotechnology, 2006. **70**(2): p. 140-150.
80. McKeating, K.S., et al., *High throughput LSPR and SERS analysis of aminoglycoside antibiotics*. Analyst, 2016. **141**(17): p. 5120-5126.
81. Mazzei, T., et al., *Chemistry and mode of action of macrolides*. Journal of Antimicrobial Chemotherapy, 1993. **31**(suppl_C): p. 1-9.
82. Kannan, K., et al., *The general mode of translation inhibition by macrolide antibiotics*. Proc Natl Acad Sci U S A, 2014. **111**(45): p. 15958-63.
83. Weisblum, B. and V. Demohn, *Erythromycin-inducible resistance in Staphylococcus aureus: survey of antibiotic classes involved*. Journal of Bacteriology, 1969. **98**(2): p. 447-452.

84. Arsic, B., et al., *16-membered macrolide antibiotics: A review*. International journal of antimicrobial agents, 2018. **51**(3): p. 283-298.
85. Hawkey, P.M., *Mechanisms of quinolone action and microbial response*. Journal of Antimicrobial Chemotherapy, 2003. **51**(suppl_1): p. 29-35.
86. Cheng, G., et al., *Antibacterial action of quinolones: From target to network*. European Journal of Medicinal Chemistry, 2013. **66**: p. 555-562.
87. Naeem, A., et al., *The current case of quinolones: synthetic approaches and antibacterial activity*. Molecules, 2016. **21**(4): p. 268.
88. Harms, J.M., et al., *Alterations at the peptidyl transferase centre of the ribosome induced by the synergistic action of the streptogramins dalfopristin and quinupristin*. BMC biology, 2004. **2**(1): p. 4.
89. Maisuria, V.B., Z. Hosseinidoust, and N. Tufenkji, *Polyphenolic Extract from Maple Syrup Potentiates Antibiotic Susceptibility and Reduces Biofilm Formation of Pathogenic Bacteria*. Applied and Environmental Microbiology, 2015. **81**(11): p. 3782.
90. Kommineni, S., et al., *Bacteriocin production augments niche competition by enterococci in the mammalian gastrointestinal tract*. Nature, 2015. **526**(7575): p. 719-22.
91. Patin, N.V., et al., *Competitive strategies differentiate closely related species of marine actinobacteria*. Isme j, 2016. **10**(2): p. 478-90.
92. Vaz Jauri, P., et al., *Subinhibitory antibiotic concentrations mediate nutrient use and competition among soil streptomyces*. PLoS One, 2013. **8**(12): p. e81064.
93. Lin, J., *Antimicrobial resistance: from basic science to translational innovation*. Anim Health Res Rev, 2017. **18**(2): p. 85-86.
94. Nobel Media, A.B. *Sir Alexander Fleming - Nobel Lecture*. 2018 [cited 2018 Nov. 26th]; Available from: <https://www.nobelprize.org/prizes/medicine/1945/fleming/lecture/>.
95. Alekshun, M.N. and S.B. Levy, *Molecular Mechanisms of Antibacterial Multidrug Resistance*. Cell, 2007. **128**(6): p. 1037-1050.
96. Giedraitienė, A., et al., *Antibiotic Resistance Mechanisms of Clinically Important Bacteria*. Medicina, 2011. **47**(3).
97. Blair, J.M.A., et al., *Molecular mechanisms of antibiotic resistance*. Nature Reviews Microbiology, 2014. **13**: p. 42.
98. Leclercq, R. and P. Courvalin, *Bacterial resistance to macrolide, lincosamide, and streptogramin antibiotics by target modification*. Antimicrobial agents and chemotherapy, 1991. **35**(7): p. 1267-1272.
99. Spratt, B.G., *Resistance to antibiotics mediated by target alterations*. Science, 1994. **264**(5157): p. 388.
100. Ruiz, J., *Mechanisms of resistance to quinolones: target alterations, decreased accumulation and DNA gyrase protection*. Journal of Antimicrobial Chemotherapy, 2003. **51**(5): p. 1109-1117.
101. Huang, L., et al., *Dihydropteroate synthase gene mutations in Pneumocystis and sulfa resistance*. Emerging infectious diseases, 2004. **10**(10): p. 1721-1728.
102. Hartman, B.J. and A. Tomasz, *Low-affinity penicillin-binding protein associated with beta-lactam resistance in Staphylococcus aureus*. Journal of Bacteriology, 1984. **158**(2): p. 513.
103. Shaikh, S., et al., *Antibiotic resistance and extended spectrum beta-lactamases: Types, epidemiology and treatment*. Saudi Journal of Biological Sciences, 2015. **22**(1): p. 90-101.
104. Yang, W., et al., *TetX is a flavin-dependent monooxygenase conferring resistance to tetracycline antibiotics*. Journal of Biological Chemistry, 2004. **279**(50): p. 52346-52352.
105. Vetting, M.W., et al., *A Bacterial Acetyltransferase Capable of Regioselective N-Acetylation of Antibiotics and Histones*. Chemistry & Biology, 2004. **11**(4): p. 565-573.
106. Matsuoka, M. and T. Sasaki, *Inactivation of macrolides by producers and pathogens*. Current Drug Targets-Infectious Disorders, 2004. **4**(3): p. 217-240.

107. Martinez, J.L., et al., *Functional role of bacterial multidrug efflux pumps in microbial natural ecosystems*. FEMS microbiology reviews, 2009. **33**(2): p. 430-449.
108. Marquez, B., *Bacterial efflux systems and efflux pumps inhibitors*. Biochimie, 2005. **87**(12): p. 1137-1147.
109. Piddock, L.J., *Clinically relevant chromosomally encoded multidrug resistance efflux pumps in bacteria*. Clinical microbiology reviews, 2006. **19**(2): p. 382-402.
110. Florez-Cuadrado, D., et al., *Antimicrobial resistance in the food chain in the European Union*. Advances in Food and Nutrition Research, 2018. **86**: p. 115-136.
111. Baker, S., et al., *Genomic insights into the emergence and spread of antimicrobial-resistant bacterial pathogens*. Science, 2018. **360**(6390): p. 733-738.
112. McDermott, P., et al., *The food safety perspective of antibiotic resistance*. Animal biotechnology, 2002. **13**(1): p. 71-84.
113. Pornsukarom, S. and S. Thakur, *Horizontal dissemination of antimicrobial resistance determinants in multiple Salmonella serotypes following isolation from the commercial swine operation environment after manure application*. Applied and environmental microbiology, 2017. **83**(20): p. e01503-17.
114. Kumar, P., et al., *Molecular insights into antimicrobial resistance traits of multidrug resistant enteric pathogens isolated from India*. Scientific reports, 2017. **7**(1): p. 1-12.
115. Schmidt, V.M., et al., *Routine antibiotic therapy in dogs increases the detection of antimicrobial-resistant faecal Escherichia coli*. Journal of Antimicrobial Chemotherapy, 2018. **73**(12): p. 3305-3316.
116. Algarni, S., et al., *The Dynamics of the Antimicrobial Resistance Mobilome of Salmonella enterica and Related Enteric Bacteria*. Frontiers in Microbiology, 2022. **13**.
117. Helms, M., et al., *Excess mortality associated with antimicrobial drug-resistant Salmonella Typhimurium*. Emerging infectious diseases, 2002. **8**(5): p. 490.
118. Carroll, L.M., et al., *Whole-Genome Sequencing of Drug-Resistant Salmonella enterica Isolates from Dairy Cattle and Humans in New York and Washington States Reveals Source and Geographic Associations*. Applied and Environmental Microbiology, 2017. **83**(12): p. e00140-17.
119. de Kraker, M.E., et al., *Clinical impact of antimicrobial resistance in European hospitals: excess mortality and length of hospital stay related to methicillin-resistant Staphylococcus aureus bloodstream infections*. Antimicrobial agents and chemotherapy, 2011. **55**(4): p. 1598-1605.
120. De Kraker, M., et al., *Burden of antimicrobial resistance in European hospitals: excess mortality and length of hospital stay associated with bloodstream infections due to Escherichia coli resistant to third-generation cephalosporins*. Journal of Antimicrobial Chemotherapy, 2011. **66**(2): p. 398-407.
121. Eliopoulos, G.M., S.E. Cosgrove, and Y. Carmeli, *The impact of antimicrobial resistance on health and economic outcomes*. Clinical infectious diseases, 2003. **36**(11): p. 1433-1437.
122. WHO, *Antimicrobial resistance global report on surveillance: 2014 summary*. 2014, World Health Organization.
123. Kurćubić, V.S., et al., *Antioxidant and antimicrobial activity of Kitaibelia vitifolia extract as alternative to the added nitrite in fermented dry sausage*. Meat science, 2014. **97**(4): p. 459-467.
124. Yu, X., H. Wu, and J. Zhang, *Effect of Monascus as a nitrite substitute on color, lipid oxidation, and proteolysis of fermented meat mince*. Food Science and Biotechnology, 2015. **24**(2): p. 575-581.
125. Malakar, P.K., et al., *Detection limit of Clostridium botulinum spores in dried mushroom samples sourced from China*. International journal of food microbiology, 2013. **166**(1): p. 72-76.

126. Sindelar, J.J. and A.L. Milkowski, *Human safety controversies surrounding nitrate and nitrite in the diet*. Nitric Oxide, 2012. **26**(4): p. 259-266.
127. Viuda-Martos, M., et al., *Effect of adding citrus waste water, thyme and oregano essential oil on the chemical, physical and sensory characteristics of a bologna sausage*. Innovative Food Science & Emerging Technologies, 2009. **10**(4): p. 655-660.
128. Attanzio, A., et al., *Fruit and vegetable derived waste as a sustainable alternative source of nutraceutical compounds*. 2018, Hindawi.
129. Gutiérrez-del-Río, I., J. Fernández, and F. Lombó, *Plant Nutraceuticals As Antimicrobial Agents in Food Preservation: Terpenoids, Polyphenols and Thiols*. International Journal of Antimicrobial Agents, 2018.
130. Khalid, S., et al., *Development and characterization of biodegradable antimicrobial packaging films based on polycaprolactone, starch and pomegranate rind hybrids*. Food Packaging and Shelf Life, 2018. **18**: p. 71-79.
131. Hyldgaard, M., T. Mygind, and R.L. Meyer, *Essential Oils In Food Preservation: Mode of Action, Synergies, and Interactions With Food Matrix Components*. Frontiers in Microbiology, 2012. **3**(12): p. 1-24.
132. Papuc, C., et al., *Plant Polyphenols as Antioxidant and Antibacterial Agents for Shelf-Life Extension of Meat and Meat Products: Classification, Structures, Sources, and Action Mechanisms*. Comprehensive Reviews in Food Science and Food Safety, 2017. **16**(6): p. 1243-1268.
133. Tomás-Menor, L., et al., *The promiscuous and synergic molecular interaction of polyphenols in bactericidal activity: An opportunity to improve the performance of antibiotics?* Phytotherapy Research, 2015. **29**(3): p. 466-473.
134. Wagner, H., *Synergy research: approaching a new generation of phytopharmaceuticals*. Fitoterapia, 2011. **82**(1): p. 34-37.
135. Koech, K., et al., *Antioxidant, antimicrobial and synergistic activities of tea polyphenols*. African Crop Science Journal, 2014. **22**: p. 837-846.
136. Sher, A., *Antimicrobial activity of natural products from medicinal plants*. Gomal Journal of Medical Sciences, 2009. **7**(1).
137. Omojate Godstime, C., et al., *Mechanisms of antimicrobial actions of phytochemicals against enteric pathogens—a review*. J Pharm Chem Biol Sci, 2014. **2**(2): p. 77-85.
138. Kumar, S. and A.K. Pandey, *Chemistry and Biological Activities of Flavonoids: An Overview*. Scientific World Journal, 2013: p. 1-16.
139. Gyawali, R. and S.A. Ibrahim, *Natural products as antimicrobial agents*. Food Control, 2014. **46**: p. 412-429.
140. Albuquerque, A.D.J.D.R., et al., *Polyphenols As a Source of Antimicrobial Agents Against Human Pathogens*. Plant Extracts: Role in Agriculture, Health Effects and Medical Applications. 2013. 275-294.
141. Górniak, I., R. Bartoszewski, and J. Króliczewski, *Comprehensive review of antimicrobial activities of plant flavonoids*. Phytochemistry Reviews, 2018.
142. Ahmad, A., et al., *Therapeutic Potential of Flavonoids and Their Mechanism of Action Against Microbial and Viral Infections- A Review*. Food Research International, 2015. **77**: p. 221-235.
143. Cowan, M.M., *Plant products as antimicrobial agents*. Clin Microbiol Rev, 1999. **12**(4): p. 564-82.
144. Cho, K.S., et al., *Terpenes from forests and human health*. Toxicological research, 2017. **33**(2): p. 97-106.
145. Clifford, M.N., *Miscellaneous phenols in foods and beverages – nature, occurrence and dietary burden*. Journal of the Science of Food and Agriculture, 2000. **80**(7): p. 1126-1137.

146. Rao, A., et al., *Mechanism of Antifungal Activity of Terpenoid Phenols Resembles Calcium Stress and Inhibition of the TOR Pathway*. *Antimicrobial Agents and Chemotherapy*, 2010. **54**(12): p. 5062.
147. Ait-Ouazzou, A., et al., *New Insights in Mechanisms of Bacterial Inactivation By Carvacrol* *Journal of Applied Microbiology*, 2012. **114**: p. 173-185.
148. Gaur, G., et al., *Plant-Derived Drug Molecules as Antibacterial Agents*, in *Functional Food and Human Health*, V. Rani and U.C.S. Yadav, Editors. 2018, Springer Singapore: Singapore. p. 143-171.
149. Gallucci, M.N., et al., *Antimicrobial combined action of terpenes against the food-borne microorganisms Escherichia coli, Staphylococcus aureus and Bacillus cereus*. *Flavour and Fragrance Journal*, 2009. **24**(6): p. 348-354.
150. Panche, A.N., A.D. Diwan, and S.R. Chandra, *Flavonoids: an overview*. *Journal of nutritional science*, 2016. **5**.
151. Mullen, W., et al., *Bioavailability and Metabolism of Orange Juice Flavanones in Humans: Impact of a Full-Fat Yogurt*. *Journal of Agricultural and Food Chemistry*, 2008. **56**(23): p. 11157-11164.
152. Tripoli, E., et al., *Citrus flavonoids: Molecular structure, biological activity and nutritional properties: A review*. *Food Chemistry*, 2007. **104**(2): p. 466-479.
153. Farhadi, F., et al., *Antibacterial activity of flavonoids and their structure–activity relationship: An update review*. *Phytotherapy Research*, 2019. **33**(1): p. 13-40.
154. Yi, S.-M., et al., *Tea polyphenols inhibit Pseudomonas aeruginosa through damage to the cell membrane*. *International journal of food microbiology*, 2010. **144**(1): p. 111-117.
155. Wu, T., et al., *A structure–activity relationship study of flavonoids as inhibitors of E. coli by membrane interaction effect*. *Biochimica et Biophysica Acta (BBA)-Biomembranes*, 2013. **1828**(11): p. 2751-2756.
156. Ultee, A., M. Bennik, and R. Moezelaar, *The phenolic hydroxyl group of carvacrol is essential for action against the food-borne pathogen Bacillus cereus*. *Applied and environmental microbiology*, 2002. **68**(4): p. 1561-1568.
157. Cushnie, T.T. and A.J. Lamb, *Recent advances in understanding the antibacterial properties of flavonoids*. *International journal of antimicrobial agents*, 2011. **38**(2): p. 99-107.
158. Fujita, M., et al., *Remarkable Synergies between Baicalein and Tetracycline, and Baicalein and β -Lactams against Methicillin-Resistant Staphylococcus aureus*. *Microbiology and Immunology*, 2005. **49**(4): p. 391-396.
159. Freitag, N.E., G.C. Port, and M.D. Miner, *Listeria monocytogenes—from saprophyte to intracellular pathogen*. *Nature Reviews Microbiology*, 2009. **7**(9): p. 623-628.
160. Kathariou, S., *Listeria monocytogenes virulence and pathogenicity, a food safety perspective*. *Journal of food protection*, 2002. **65**(11): p. 1811-1829.
161. Walker, S., P. Archer, and J.G. Banks, *Growth of Listeria monocytogenes at refrigeration temperatures*. *Journal of Applied Bacteriology*, 1990. **68**(2): p. 157-162.
162. Chan, Y.C. and M. Wiedmann, *Physiology and genetics of Listeria monocytogenes survival and growth at cold temperatures*. *Critical reviews in food science and nutrition*, 2008. **49**(3): p. 237-253.
163. Carpentier, B. and O. Cerf, *Persistence of Listeria monocytogenes in food industry equipment and premises*. *International journal of food microbiology*, 2011. **145**(1): p. 1-8.
164. Mørretrø, T. and S. Langsrud, *Listeria monocytogenes: biofilm formation and persistence in food-processing environments*. *Biofilms*, 2004. **1**(2): p. 107-121.
165. Pan, Y., F. Breidt Jr, and S. Kathariou, *Resistance of Listeria monocytogenes biofilms to sanitizing agents in a simulated food processing environment*. *Applied and environmental microbiology*, 2006. **72**(12): p. 7711-7717.
166. Pang, Z., et al., *Antibiotic resistance in Pseudomonas aeruginosa: mechanisms and alternative therapeutic strategies*. *Biotechnology advances*, 2019. **37**(1): p. 177-192.

167. Gales, A., et al., *Characterization of Pseudomonas aeruginosa isolates: occurrence rates, antimicrobial susceptibility patterns, and molecular typing in the global SENTRY Antimicrobial Surveillance Program, 1997–1999*. *Clinical Infectious Diseases*, 2001. **32**(Supplement_2): p. S146-S155.
168. O'Toole, G.A. and R. Kolter, *Flagellar and twitching motility are necessary for Pseudomonas aeruginosa biofilm development*. *Molecular microbiology*, 1998. **30**(2): p. 295-304.
169. Ingraham, J. and G. Bailey, *Comparative study of effect of temperature on metabolism of psychrophilic and mesophilic bacteria*. *Journal of bacteriology*, 1959. **77**(5): p. 609-613.
170. Kim, G., et al., *In vitro antibacterial and early stage biofilm inhibitory potential of an edible chitosan and its phenolic conjugates against Pseudomonas aeruginosa and Listeria monocytogenes*. *3 Biotech*, 2018. **8**(10): p. 1-8.
171. Cabezas-Pizarro, J., et al., *Antimicrobial activity of different sodium and potassium salts of carboxylic acid against some common foodborne pathogens and spoilage-associated bacteria*. *Revista argentina de microbiología*, 2018. **50**(1): p. 56-61.
172. Robillard, N.J. and A.L. Scarpa, *Genetic and physiological characterization of ciprofloxacin resistance in Pseudomonas aeruginosa PAO*. *Antimicrobial Agents and Chemotherapy*, 1988. **32**(4): p. 535-539.
173. Livermore, D.M., *Multiple Mechanisms of Antimicrobial Resistance in Pseudomonas aeruginosa: Our Worst Nightmare?* *Clinical Infectious Diseases*, 2002. **34**(5): p. 634-640.
174. Kumar, C.G. and S.K. Anand, *Significance of microbial biofilms in food industry: a review*. *International journal of food microbiology*, 1998. **42**(1-2): p. 9-27.
175. Jass, J. and H.M. Lappin-Scott, *The efficacy of antibiotics enhanced by electrical currents against Pseudomonas aeruginosa biofilms*. *Journal of Antimicrobial Chemotherapy*, 1996. **38**(6): p. 987-1000.
176. Taylor, P.K., A.T. Yeung, and R.E. Hancock, *Antibiotic resistance in Pseudomonas aeruginosa biofilms: towards the development of novel anti-biofilm therapies*. *Journal of biotechnology*, 2014. **191**: p. 121-130.
177. Raposo, A., et al., *Food spoilage by Pseudomonas spp.-an overview*. *Food borne pathogens and antibiotic resistance*, 2017: p. 41-58.
178. Shooter, R.A., et al., *Food and Medicaments As Possible Sources of Hospital Strains of Pseudomonas aeruginosa*. *The Lancet*, 1969. **293**(7608): p. 1227-1229.
179. Shooter, R.A., et al., *Isolation of Escherichia coli, Pseudomonas aeruginosa, and Klebsiella From Food In Hospitals, Canteens, and Schools*. *The Lancet*, 1971. **298**(7721): p. 390-392.
180. Arslan, S., A. Eyi, and F. Özdemir, *Spoilage potentials and antimicrobial resistance of Pseudomonas spp. isolated from cheeses*. *Journal of Dairy Science*, 2011. **94**(12): p. 5851-5856.
181. Shahrokhi, G.R., E. Rahimi, and A. Shakerian, *The Prevalence Rate, Pattern of Antibiotic Resistance, and Frequency of Virulence Factors of Pseudomonas aeruginosa Strains Isolated from Fish in Iran*. *Journal of Food Quality*, 2022. **2022**: p. 8990912.
182. Benie, C., et al., *Prevalence and Antibiotic Resistance of Pseudomonas aeruginosa Isolated from Bovine Meat, Fresh Fish and Smoked Fish*. *Archives of Clinical Microbiology*, 2017. **8**(3): p. 0-0.
183. Liu, X., et al., *Antibacterial activity and mechanism of linalool against Pseudomonas aeruginosa*. *Microbial Pathogenesis*, 2020. **141**: p. 103980.
184. Sharma, M. and S. Anand, *Biofilms evaluation as an essential component of HACCP for food/dairy processing industry—a case*. *Food control*, 2002. **13**(6-7): p. 469-477.
185. Simões, M., L.C. Simões, and M.J. Vieira, *A review of current and emergent biofilm control strategies*. *LWT-Food Science and Technology*, 2010. **43**(4): p. 573-583.
186. Andino, A. and I. Hanning, *Salmonella enterica: survival, colonization, and virulence differences among serovars*. *The Scientific World Journal*, 2015. **2015**.

187. Frye, J.G. and C.R. Jackson, *Genetic mechanisms of antimicrobial resistance identified in Salmonella enterica, Escherichia coli, and Enterococcus spp. isolated from US food animals*. *Frontiers in microbiology*, 2013. **4**: p. 135.
188. Randall, L., et al., *Antibiotic resistance genes, integrons and multiple antibiotic resistance in thirty-five serotypes of Salmonella enterica isolated from humans and animals in the UK*. *Journal of Antimicrobial Chemotherapy*, 2004. **53**(2): p. 208-216.
189. Gay, K., et al., *Plasmid-mediated quinolone resistance in non-Typhi serotypes of Salmonella enterica*. *Clinical Infectious Diseases*, 2006. **43**(3): p. 297-304.
190. Shi, X. and X. Zhu, *Biofilm formation and food safety in food industries*. *Trends in Food Science & Technology*, 2009. **20**(9): p. 407-413.
191. Wang, R., et al., *Biofilm formation, antimicrobial resistance, and sanitizer tolerance of Salmonella enterica strains isolated from beef trim*. *Foodborne pathogens and disease*, 2017. **14**(12): p. 687-695.
192. Srey, S., I.K. Jahid, and S.-D. Ha, *Biofilm formation in food industries: a food safety concern*. *Food control*, 2013. **31**(2): p. 572-585.
193. Corcoran, M., et al., *Commonly used disinfectants fail to eradicate Salmonella enterica biofilms from food contact surface materials*. *Applied and environmental microbiology*, 2014. **80**(4): p. 1507-1514.
194. Stepanović, S., et al., *Biofilm formation by Salmonella spp. and Listeria monocytogenes on plastic surface*. *Letters in applied microbiology*, 2004. **38**(5): p. 428-432.
195. Le Loir, Y., F. Baron, and M. Gautier, *[i] Staphylococcus aureus [/i] and food poisoning*. *Genetics and molecular research: GMR*, 2003. **2**(1): p. 63-76.
196. Labbé, R.G. and S. García, *Guide to foodborne pathogens*. 2013: John Wiley & Sons.
197. Lowy, F.D., *Staphylococcus aureus infections*. *New England journal of medicine*, 1998. **339**(8): p. 520-532.
198. Dinges, M.M., P.M. Orwin, and P.M. Schlievert, *Exotoxins of Staphylococcus aureus*. *Clinical microbiology reviews*, 2000. **13**(1): p. 16-34.
199. Zhao, Y., et al., *Staphylococcus aureus methicillin-resistance factor fmtA is regulated by the global regulator SarA*. 2012.
200. Chambers, H.F. and F.R. DeLeo, *Waves of resistance: Staphylococcus aureus in the antibiotic era*. *Nature Reviews Microbiology*, 2009. **7**(9): p. 629-641.
201. Jabra-Rizk, M., et al., *Effect of farnesol on Staphylococcus aureus biofilm formation and antimicrobial susceptibility*. *Antimicrobial agents and chemotherapy*, 2006. **50**(4): p. 1463-1469.
202. Carpentier, B. and O. Cerf, *Biofilms and their consequences, with particular reference to hygiene in the food industry*. *Journal of applied bacteriology*, 1993. **75**(6): p. 499-511.
203. Holden, E., *Massively parallel transposon mutagenesis to identify relationships between biofilm formation and efflux activity in Enterobacteriaceae*. 2021, University of East Anglia.
204. Elshikh, M., et al., *Resazurin-based 96-well plate microdilution method for the determination of minimum inhibitory concentration of biosurfactants*. *Biotechnology Letters*, 2016. **38**(6): p. 1015-1019.
205. Jones, C.J. and D.J. Wozniak, *Congo Red Stain Identifies Matrix Overproduction and Is an Indirect Measurement for c-di-GMP in Many Species of Bacteria*, in *c-di-GMP Signaling: Methods and Protocols*, K. Sauer, Editor. 2017, Springer New York: New York, NY. p. 147-156.
206. Govardhan Singh, R.S., P.S. Negi, and C. Radha, *Phenolic composition, antioxidant and antimicrobial activities of free and bound phenolic extracts of Moringa oleifera seed flour*. *Journal of Functional Foods*, 2013. **5**(4): p. 1883-1891.
207. Guzman, J.D., *Natural Cinnamic Acids, Synthetic Derivatives and Hybrids with Antimicrobial Activity*. *Molecules*, 2014. **19**(12): p. 19292-19349.

208. Schmidt, E., et al., *Antimicrobial Activities of Single Aroma Compounds*. Natural Product Communications, 2010. **5**(9): p. 1934578X1000500906.
209. Mandalari, G., et al., *Antimicrobial activity of flavonoids extracted from bergamot (Citrus bergamia Risso) peel, a byproduct of the essential oil industry*. Journal of applied microbiology, 2007. **103**(6): p. 2056-2064.
210. Tsuchiya, H., et al., *Comparative study on the antibacterial activity of phytochemical flavanones against methicillin-resistant Staphylococcus aureus*. Journal of Ethnopharmacology, 1996. **50**(1): p. 27-34.
211. Rauha, J.-P., et al., *Antimicrobial effects of Finnish plant extracts containing flavonoids and other phenolic compounds*. International Journal of Food Microbiology, 2000. **56**(1): p. 3-12.
212. Rúa, J., et al., *Combination of carvacrol and thymol: Antimicrobial activity against Staphylococcus aureus and antioxidant activity*. Foodborne pathogens and disease, 2019. **16**(9): p. 622-629.
213. Falcone, P., et al., *A study on the antimicrobial activity of thymol intended as a natural preservative*. Journal of food protection, 2005. **68**(8): p. 1664-1670.
214. Memar, M.Y., et al., *Carvacrol and thymol: strong antimicrobial agents against resistant isolates*. Reviews in Medical Microbiology, 2017. **28**(2): p. 63-68.
215. Mun, S.-H., et al., *Synergistic antibacterial effect of curcumin against methicillin-resistant Staphylococcus aureus*. Phytomedicine, 2013. **20**(8): p. 714-718.
216. Waditzer, M. and F. Bucar, *Flavonoids as Inhibitors of Bacterial Efflux Pumps*. Molecules, 2021. **26**(22): p. 6904.
217. Siritwong, S., et al., *The synergy and mode of action of quercetin plus amoxicillin against amoxicillin-resistant Staphylococcus epidermidis*. BMC Pharmacology and Toxicology, 2016. **17**(1): p. 39.
218. Johari, S.A., et al., *Efflux inhibitory activity of flavonoids from Chromolaena odorata against selected methicillin-resistant Staphylococcus aureus (MRSA) isolates*. African Journal of Microbiology Research, 2012. **6**(27): p. 5631-5635.
219. Saavedra, M.J., et al., *Antimicrobial Activity of Phenolics and Glucosinolate Hydrolysis Products and their Synergy with Streptomycin against Pathogenic Bacteria*. Medicinal Chemistry, 2010. **6**(3): p. 174-183.
220. Rodríguez Vaquero, M.J., M.R. Alberto, and M.C. Manca de Nadra, *Influence of phenolic compounds from wines on the growth of Listeria monocytogenes*. Food Control, 2007. **18**(5): p. 587-593.
221. Zhang, F., et al., *Synergistic Effect of Chlorogenic Acid and Caffeic Acid with Fosfomycin on Growth Inhibition of a Resistant Listeria monocytogenes Strain*. ACS Omega, 2020. **5**(13): p. 7537-7544.
222. Cushnie, T.P.T. and A.J. Lamb, *Antimicrobial activity of flavonoids*. International Journal of Antimicrobial Agents, 2005. **26**(5): p. 343-356.
223. Bobis, O., et al., *Influence of phytochemical profile on antibacterial activity of different medicinal plants against gram-positive and gram-negative bacteria*. Applied Biochemistry and Microbiology, 2015. **51**(1): p. 113-118.
224. Dahiya, P. and S. Purkayastha, *Phytochemical Screening and Antimicrobial Activity of Some Medicinal Plants Against Multi-drug Resistant Bacteria from Clinical Isolates*. Indian journal of pharmaceutical sciences, 2012. **74**(5): p. 443-450.
225. Wang, Y., et al., *Evaluation of physicochemical properties of Qinling Apis cerana honey and the antimicrobial activity of the extract against Salmonella Typhimurium LT2 in vitro and in vivo*. Food Chemistry, 2021. **337**: p. 127774.
226. Puupponen-Pimiä, R., et al., *Antimicrobial properties of phenolic compounds from berries*. Journal of Applied Microbiology, 2001. **90**(4): p. 494-507.

227. Barbieri, R., et al., *Phytochemicals for human disease: An update on plant-derived compounds antibacterial activity*. Microbiological Research, 2017. **196**: p. 44-68.
228. Sharma, G., et al., *Combinatorial antimicrobial effect of curcumin with selected phytochemicals on Staphylococcus epidermidis*. Journal of Asian Natural Products Research, 2014. **16**(5): p. 535-541.
229. Monte, J., et al., *Antimicrobial Activity of Selected Phytochemicals against Escherichia coli and Staphylococcus aureus and Their Biofilms*. Pathogens, 2014. **3**(2): p. 473-498.
230. Hemaiswarya, S. and M. Doble, *Synergistic interaction of phenylpropanoids with antibiotics against bacteria*. Journal of Medical Microbiology, 2010. **59**(12): p. 1469-1476.
231. Khan, F., et al., *Caffeic Acid and Its Derivatives: Antimicrobial Drugs toward Microbial Pathogens*. Journal of Agricultural and Food Chemistry, 2021. **69**(10): p. 2979-3004.
232. Seukep, A.J., et al., *Plant-derived secondary metabolites as the main source of efflux pump inhibitors and methods for identification*. Journal of Pharmaceutical Analysis, 2020. **10**(4): p. 277-290.
233. Perumal, S., R. Mahmud, and S. Ismail, *Mechanism of Action of Isolated Caffeic Acid and Epicatechin 3-gallate from Euphorbia hirta against Pseudomonas aeruginosa*. Pharmacognosy magazine, 2017. **13**(Suppl 2): p. S311-S315.
234. Pernin, A., et al., *Ferulic Acid and Eugenol Have Different Abilities to Maintain Their Inhibitory Activity Against Listeria monocytogenes in Emulsified Systems*. Frontiers in Microbiology, 2019. **10**.
235. Jubair, N., et al., *Review on the Antibacterial Mechanism of Plant-Derived Compounds against Multidrug-Resistant Bacteria (MDR)*. Evidence-Based Complementary and Alternative Medicine, 2021. **2021**: p. 3663315.
236. Hirai, I., et al., *Characterisation of anti-Staphylococcus aureus activity of quercetin*. International Journal of Food Science & Technology, 2010. **45**(6): p. 1250-1254.
237. Ouyang, J., et al., *Quercetin is an effective inhibitor of quorum sensing, biofilm formation and virulence factors in Pseudomonas aeruginosa*. Journal of Applied Microbiology, 2016. **120**(4): p. 966-974.
238. Espinosa-Muñoz, V., et al., *Ultrasonic-Assisted Extraction of Phenols, Flavonoids, and Biocompounds with Inhibitory Effect Against Salmonella Typhimurium and Staphylococcus Aureus from Cactus Pear*. Journal of Food Process Engineering, 2017. **40**(2): p. e12358.
239. Wang, S., et al., *Bacteriostatic Effect of Quercetin as an Antibiotic Alternative In Vivo and Its Antibacterial Mechanism In Vitro*. Journal of Food Protection, 2017. **81**(1): p. 68-78.
240. Shen, X., et al., *Antimicrobial effect of blueberry (Vaccinium corymbosum L.) extracts against the growth of Listeria monocytogenes and Salmonella Enteritidis*. Food Control, 2014. **35**(1): p. 159-165.
241. Gatadi, S., et al., *Promising antibacterial agents against multidrug resistant Staphylococcus aureus*. Bioorganic Chemistry, 2019. **92**: p. 103252.
242. Grecka, K. and P. Szweda, *Synergistic Effects of Propolis Combined with 2-Phenoxyethanol and Antipyretics on the Growth of Staphylococcus aureus*. Pharmaceutics, 2021. **13**(2): p. 215.
243. Ming, D., et al., *Kaempferol Inhibits the Primary Attachment Phase of Biofilm Formation in Staphylococcus aureus*. Frontiers in Microbiology, 2017. **8**.
244. Yin, N., et al., *Kaempferol inhibits the expression of α -hemolysin and protects mice from methicillin-resistant Staphylococcus aureus-induced lethal pneumonia*. Microbial Pathogenesis, 2022. **162**: p. 105336.
245. Kozłowska, J., et al., *Synthesis and Biological Activity of Novel O-Alkyl Derivatives of Naringenin and Their Oximes*. Molecules, 2017. **22**(9): p. 1485.
246. Mundlia, J., et al., *Improved antioxidant, antimicrobial and anticancer activity of naringenin on conjugation with pectin*. 3 Biotech, 2019. **9**(8): p. 312.

247. Gao, Y., et al., *Endophytic Fungi from Dalbergia odorifera T. Chen Producing Naringenin Inhibit the Growth of Staphylococcus aureus by Interfering with Cell Membrane, DNA, and Protein*. Journal of Medicinal Food, 2021. **24**(2): p. 116-123.
248. Lee, K.A., et al., *Antibacterial activity of a novel flavonoid, 7-O-butyl naringenin, against methicillin-resistant Staphylococcus aureus (MRSA)*. Food Science and Biotechnology, 2013. **22**(6): p. 1725-1728.
249. Wang, L.-H., et al., *Membrane and genomic DNA dual-targeting of citrus flavonoid naringenin against Staphylococcus aureus*. Integrative Biology, 2017. **9**(10): p. 820-829.
250. Valero, M. and M.J. Giner, *Effects of antimicrobial components of essential oils on growth of Bacillus cereus INRA L2104 in and the sensory qualities of carrot broth*. International Journal of Food Microbiology, 2006. **106**(1): p. 90-94.
251. Karaosmanoglu, H., et al., *Antimicrobial and Antioxidant Activities of Turkish Extra Virgin Olive Oils*. Journal of Agricultural and Food Chemistry, 2010. **58**(14): p. 8238-8245.
252. García-Ríos, E., et al., *Improved antimicrobial activity of immobilised essential oil components against representative spoilage wine microorganisms*. Food Control, 2018. **94**: p. 177-186.
253. Patrick, C.A., et al., *Proteomic Profiling, Transcription Factor Modeling, and Genomics of Evolved Tolerant Strains Elucidate Mechanisms of Vanillin Toxicity in Escherichia coli*. mSystems, 2019. **4**(4): p. e00163-19.
254. Bezerra, C.F., et al., *Vanillin selectively modulates the action of antibiotics against resistant bacteria*. Microbial Pathogenesis, 2017. **113**: p. 265-268.
255. Arya, S.S., et al., *Vanillin mediated green synthesis and application of gold nanoparticles for reversal of antimicrobial resistance in Pseudomonas aeruginosa clinical isolates*. Heliyon, 2019. **5**(7): p. e02021.
256. Nourbakhsh, F., et al., *From plants to antimicrobials: Natural products against bacterial membranes*. Phytotherapy Research, 2022. **36**(1): p. 33-52.
257. Sharma, S., et al., *Antimycobacterial mechanism of vanillin involves disruption of cell-surface integrity, virulence attributes, and iron homeostasis*. International Journal of Mycobacteriology, 2016. **5**(4): p. 460-468.
258. YEMİŞ, G.P., et al., *Effect of Vanillin, Ethyl Vanillin, and Vanillic Acid on the Growth and Heat Resistance of Cronobacter Species*. Journal of Food Protection, 2011. **74**(12): p. 2062-2069.
259. Fitzgerald, D.J., et al., *Mode of antimicrobial action of vanillin against Escherichia coli, Lactobacillus plantarum and Listeria innocua*. J Appl Microbiol, 2004. **97**(1): p. 104-113.
260. Toit, K.D., S. Buthelezi, and J. Bodenstein, *Anti-inflammatory and antibacterial profiles of selected compounds found in South African propolis : research letter*. South African Journal of Science, 2009. **105**(11): p. 470-472.
261. Xuewen, H., et al., *Eriodictyol protects against Staphylococcus aureus-induced lung cell injury by inhibiting alpha-hemolysin expression*. World Journal of Microbiology and Biotechnology, 2018. **34**(5): p. 64.
262. Paul Dzoyem, J., et al., *Antimicrobial action mechanism of flavonoids from Dorstenia species*. Drug Discoveries & Therapeutics, 2013. **7**(2): p. 66-72.
263. Echeverría, J., et al., *Structure-Activity and Lipophilicity Relationships of Selected Antibacterial Natural Flavones and Flavanones of Chilean Flora*. Molecules, 2017. **22**(608).
264. Siroli, L., et al., *Effects of sub-lethal concentrations of thyme and oregano essential oils, carvacrol, thymol, citral and trans-2-hexenal on membrane fatty acid composition and volatile molecule profile of Listeria monocytogenes, Escherichia coli and Salmonella enteritidis*. Food Chemistry, 2015. **182**: p. 185-192.
265. Gulin-Sarfraz, T., et al., *Inorganic Nanocarriers for Encapsulation of Natural Antimicrobial Compounds for Potential Food Packaging Application: A Comparative Study*. Nanomaterials, 2021. **11**(2): p. 379.

266. Chang, S., A. Mohammadi Nafchi, and H. Baghaie, *Development of an active packaging based on polyethylene containing linalool or thymol for mozzarella cheese*. Food Science & Nutrition, 2021. **9**(7): p. 3732-3739.
267. Ettayebi, K., J. El Yamani, and B.-D. Rossi-Hassani, *Synergistic effects of nisin and thymol on antimicrobial activities in Listeria monocytogenes and Bacillus subtilis*. FEMS Microbiology Letters, 2000. **183**(1): p. 191-195.
268. Cao, R., et al., *Preparation, investigation and storage application of thymol–chitooligosaccharide complex with enhanced antioxidant and antibacterial properties*. Journal of the Science of Food and Agriculture, 2022. **102**(4): p. 1561-1568.
269. Xu, J., et al., *The antibacterial mechanism of carvacrol and thymol against Escherichia coli*. Letters in Applied Microbiology, 2008. **47**(3): p. 174-179.
270. Wang, L.-H., et al., *Combination of microbiological, spectroscopic and molecular docking techniques to study the antibacterial mechanism of thymol against Staphylococcus aureus: membrane damage and genomic DNA binding*. Analytical and Bioanalytical Chemistry, 2017. **409**(6): p. 1615-1625.
271. Miller, C.R., et al., *Distinct subpopulations of intravalvular methicillin-resistant Staphylococcus aureus with variable susceptibility to daptomycin in tricuspid valve endocarditis*. Antimicrobial Agents and Chemotherapy, 2020. **64**(3): p. e01593-19.
272. Blake, K.L., C.P. Randall, and A.J. O'Neill, *In vitro studies indicate a high resistance potential for the lantibiotic nisin in Staphylococcus aureus and define a genetic basis for nisin resistance*. Antimicrobial agents and chemotherapy, 2011. **55**(5): p. 2362-2368.
273. Sause, W.E., et al., *The purine biosynthesis regulator PurR moonlights as a virulence regulator in Staphylococcus aureus*. Proceedings of the National Academy of Sciences, 2019. **116**(27): p. 13563-13572.
274. Goncheva, M.I., et al., *Stress-induced inactivation of the Staphylococcus aureus purine biosynthesis repressor leads to hypervirulence*. Nature communications, 2019. **10**(1): p. 1-14.
275. Alkam, D., et al., *The increased accumulation of Staphylococcus aureus virulence factors is maximized in a purR mutant by the increased production of SarA and decreased production of extracellular proteases*. Infection and Immunity, 2021. **89**(4): p. e00718-20.
276. Nishina, A., et al., *Antimicrobial substance, 3', 4'-dihydroxyacetophenone, in coffee residue*. Bioscience, biotechnology, and biochemistry, 1994. **58**(2): p. 293-296.
277. Bischofberger, A.M., et al., *Evolution of honey resistance in experimental populations of bacteria depends on the type of honey and has no major side effects for antibiotic susceptibility*. Evolutionary applications, 2021. **14**(5): p. 1314-1327.
278. Alcock, B.P., et al., *CARD 2020: antibiotic resistance surveillance with the comprehensive antibiotic resistance database*. Nucleic Acids Res, 2020. **48**(D1): p. D517-d525.
279. Shaheen, A., et al., *Transcriptional regulation of drug resistance mechanisms in Salmonella: where we stand and what we need to know*. World Journal of Microbiology and Biotechnology, 2020. **36**(6): p. 85.
280. Choi, Y.-L., et al., *Nucleotide sequence of the glpR gene encoding the repressor for the glycerol-3-phosphate regulon of Escherichia coli K12*. Nucleic acids research, 1988. **16**(15): p. 7732.
281. Yang, B. and T.J. Larson, *Multiple promoters are responsible for transcription of the glpEGR operon of Escherichia coli K-12*. Biochimica et Biophysica Acta (BBA)-Gene Structure and Expression, 1998. **1396**(1): p. 114-126.
282. Schweizer, H.P. and C. Po, *Regulation of glycerol metabolism in Pseudomonas aeruginosa: characterization of the glpR repressor gene*. Journal of bacteriology, 1996. **178**(17): p. 5215-5221.
283. Sehna, D., et al., *Mol* Viewer: modern web app for 3D visualization and analysis of large biomolecular structures*. Nucleic Acids Research, 2021. **49**(W1): p. W431-W437.

284. Trampari, E., et al., *Exposure of Salmonella biofilms to antibiotic concentrations rapidly selects resistance with collateral tradeoffs*. npj Biofilms and Microbiomes, 2021. **7**(1): p. 3.
285. Karatzas, K.A.G., et al., *Prolonged treatment of Salmonella enterica serovar Typhimurium with commercial disinfectants selects for multiple antibiotic resistance, increased efflux and reduced invasiveness*. Journal of Antimicrobial Chemotherapy, 2007. **60**(5): p. 947-955.
286. Deng, W., et al., *Antibiotic Resistance in Salmonella from Retail Foods of Animal Origin and Its Association with Disinfectant and Heavy Metal Resistance*. Microbial Drug Resistance, 2018. **24**(6): p. 782-791.
287. Fadli, M., et al., *Natural extracts stimulate membrane-associated mechanisms of resistance in Gram-negative bacteria*. Letters in Applied Microbiology, 2014. **58**(5): p. 472-477.
288. Borges, A., et al., *New Perspectives on the Use of Phytochemicals as an Emergent Strategy to Control Bacterial Infections Including Biofilms*. Molecules, 2016. **21**(7): p. 877.
289. Martinez, J.L. and F. Baquero, *Mutation Frequencies and Antibiotic Resistance*. Antimicrobial Agents and Chemotherapy, 2000. **44**(7): p. 1771-1777.
290. Lindgren, P.K., Å. Karlsson, and D. Hughes, *Mutation Rate and Evolution of Fluoroquinolone Resistance in Escherichia coli Isolates from Patients with Urinary Tract Infections*. Antimicrobial Agents and Chemotherapy, 2003. **47**(10): p. 3222-3232.
291. Long, H., et al., *Antibiotic treatment enhances the genome-wide mutation rate of target cells*. Proceedings of the National Academy of Sciences, 2016. **113**(18): p. E2498-E2505.
292. Yuan, W., et al., *Stress resistance development and genome-wide transcriptional response of Escherichia coli O157: H7 adapted to sublethal thymol, carvacrol, and trans-cinnamaldehyde*. Applied and environmental microbiology, 2018. **84**(22): p. e01616-18.
293. Al-Kandari, F., et al., *Thymol tolerance in Escherichia coli induces morphological, metabolic and genetic changes*. BMC Microbiology, 2019. **19**(1): p. 294.
294. Di Pasqua, R., et al., *Changes in the proteome of Salmonella enterica serovar Thompson as stress adaptation to sublethal concentrations of thymol*. PROTEOMICS, 2010. **10**(5): p. 1040-1049.
295. Barbosa, L.N., et al., *Proteomic analysis and antibacterial resistance mechanisms of Salmonella Enteritidis submitted to the inhibitory effect of Origanum vulgare essential oil, thymol and carvacrol*. Journal of Proteomics, 2020. **214**: p. 103625.
296. Okusu, H., D. Ma, and H. Nikaido, *AcrAB efflux pump plays a major role in the antibiotic resistance phenotype of Escherichia coli multiple-antibiotic-resistance (Mar) mutants*. Journal of Bacteriology, 1996. **178**(1): p. 306-308.
297. Webber, M.A. and L.J.V. Piddock, *The importance of efflux pumps in bacterial antibiotic resistance*. Journal of Antimicrobial Chemotherapy, 2003. **51**(1): p. 9-11.
298. Chen, S., et al., *Contribution of Target Gene Mutations and Efflux to Decreased Susceptibility of Salmonella enterica Serovar Typhimurium to Fluoroquinolones and Other Antimicrobials*. Antimicrobial Agents and Chemotherapy, 2007. **51**(2): p. 535-542.
299. Abouzeed, Y.M., S. Baucheron, and A. Cloeckaert, *ramR Mutations Involved in Efflux-Mediated Multidrug Resistance in Salmonella enterica Serovar Typhimurium*. Antimicrobial Agents and Chemotherapy, 2008. **52**(7): p. 2428-2434.
300. Kumar, A. and A. Kumar, *Antibiotic resistome of Salmonella typhi: molecular determinants for the emergence of drug resistance*. Frontiers of Medicine, 2021. **15**(5): p. 693-703.
301. Dam, S., J.-M. Pagès, and M. Masi, *Stress responses, outer membrane permeability control and antimicrobial resistance in Enterobacteriaceae*. Microbiology, 2018. **164**(3): p. 260-267.
302. Coldham, N.G., et al., *A 96-well plate fluorescence assay for assessment of cellular permeability and active efflux in Salmonella enterica serovar Typhimurium and Escherichia coli*. Journal of Antimicrobial Chemotherapy, 2010. **65**(8): p. 1655-1663.

303. Handzlik, J., A. Matys, and K. Kieć-Kononowicz, *Recent Advances in Multi-Drug Resistance (MDR) Efflux Pump Inhibitors of Gram-Positive Bacteria S. aureus*. *Antibiotics*, 2013. **2**(1): p. 28-45.
304. Kettles, R.A., et al., *The Escherichia coli MarA protein regulates the ycgZ-ymgABC operon to inhibit biofilm formation*. *Molecular Microbiology*, 2019. **112**(5): p. 1609-1625.
305. Alav, I., J.M. Sutton, and K.M. Rahman, *Role of bacterial efflux pumps in biofilm formation*. *Journal of Antimicrobial Chemotherapy*, 2018. **73**(8): p. 2003-2020.
306. Radulovic, N.S., et al., *Antimicrobial Plant Metabolites: Structural Diversity and Mechanism of Action*. *Current Medicinal Chemistry*, 2013. **20**(7): p. 932-952.
307. Jayaraman, P., et al., *Activity and interactions of antibiotic and phytochemical combinations against Pseudomonas aeruginosa in vitro*. *International journal of biological sciences*, 2010. **6**(6): p. 556-568.
308. Moo, C.-L., et al., *Mechanisms of Antimicrobial Resistance (AMR) and Alternative Approaches to Overcome AMR*. *Current Drug Discovery Technologies*, 2020. **17**(4): p. 430-447.
309. Aelenei, P., et al., *Coriander essential oil and linalool–interactions with antibiotics against Gram-positive and Gram-negative bacteria*. *Letters in applied microbiology*, 2019. **68**(2): p. 156-164.
310. Keça, M., et al., *Antimicrobial Potential of Caffeic Acid against Staphylococcus aureus Clinical Strains*. *BioMed Research International*, 2018. **2018**: p. 7413504.
311. Liu, M.-H., et al., *Synergistic Effect of Kaempferol Glycosides Purified from Laurus nobilis and Fluoroquinolones on Methicillin-Resistant Staphylococcus aureus*. *Biological and Pharmaceutical Bulletin*, 2009. **32**(3): p. 489-492.
312. Liu, Q., et al., *Synergy among thymol, eugenol, berberine, cinnamaldehyde and streptomycin against planktonic and biofilm-associated food-borne pathogens*. *Letters in Applied Microbiology*, 2015. **60**(5): p. 421-430.
313. Annunziato, G., *Strategies to Overcome Antimicrobial Resistance (AMR) Making Use of Non-Essential Target Inhibitors: A Review*. *International Journal of Molecular Sciences*, 2019. **20**(23): p. 5844.
314. Burt, S.A. and R.D. Reinders, *Antibacterial activity of selected plant essential oils against Escherichia coli O157: H7*. *Letters in applied microbiology*, 2003. **36**(3): p. 162-167.
315. Chibane, L., et al., *Plant antimicrobial polyphenols as potential natural food preservatives*. *Journal of the Science of Food and Agriculture*, 2019. **99**(4): p. 1457-1474.
316. Trombetta, D., et al., *Mechanisms of antibacterial action of three monoterpenes*. *Antimicrobial agents and chemotherapy*, 2005. **49**(6): p. 2474-2478.
317. Buckley, A.M., et al., *The AcrAB–TolC efflux system of Salmonella enterica serovar Typhimurium plays a role in pathogenesis*. *Cellular microbiology*, 2006. **8**(5): p. 847-856.
318. Horiyama, T., A. Yamaguchi, and K. Nishino, *TolC dependency of multidrug efflux systems in Salmonella enterica serovar Typhimurium*. *Journal of antimicrobial chemotherapy*, 2010. **65**(7): p. 1372-1376.
319. Lu, R., et al., *The Periplasmic Chaperone SurA Affects Motility and Biofilm Formation via the RcsCDB Pathway in Salmonella enterica Serovar Typhi*. *Journal of Nanoscience and Nanotechnology*, 2019. **19**(9): p. 5503-5509.
320. Chowdhury, A.R., et al., *Salmonella Typhimurium outer membrane protein A (OmpA) renders protection against nitrosative stress by promoting SCV stability in murine macrophages*. *bioRxiv*, 2021.
321. Kadam, S., A. Rehemtulla, and K. Sanderson, *Cloning of rfaG, B, I, and J genes for glycosyltransferase enzymes for synthesis of the lipopolysaccharide core of Salmonella typhimurium*. *Journal of bacteriology*, 1985. **161**(1): p. 277-284.
322. Gabale, U., et al., *The essential inner membrane protein YejM is a metalloenzyme*. *Scientific reports*, 2020. **10**(1): p. 1-14.

323. Dodd, C.E. and T.G. Aldsworth, *The importance of RpoS in the survival of bacteria through food processing*. International journal of food microbiology, 2002. **74**(3): p. 189-194.
324. Nnalue, N.A. and B. Stocker, *Some galE mutants of Salmonella choleraesuis retain virulence*. Infection and immunity, 1986. **54**(3): p. 635-640.
325. Sharma, D., et al., *Proteomic Analysis of the Colistin-resistant E. coli Clinical Isolate: Explorations of the Resistome*. Protein and Peptide Letters, 2022. **29**(2): p. 184-198.
326. Chou, T.-F., et al., *31P NMR and genetic analysis establish hinT as the only Escherichia coli purine nucleoside phosphoramidase and as essential for growth under high salt conditions*. Journal of Biological Chemistry, 2005. **280**(15): p. 15356-15361.
327. Mas, G., J. Thoma, and S. Hiller, *The periplasmic chaperones Skp and SurA*. Bacterial cell walls and membranes, 2019: p. 169-186.
328. Goemans, C., K. Denoncin, and J.-F. Collet, *Folding mechanisms of periplasmic proteins*. Biochimica et Biophysica Acta (BBA) - Molecular Cell Research, 2014. **1843**(8): p. 1517-1528.
329. Bodoev, I., et al., *Substitutions in SurA and BamA Lead to Reduced Susceptibility to Broad Range Antibiotics in Gonococci*. Genes, 2021. **12**(9): p. 1312.
330. Debroy, R., et al., *Gene interaction network studies to decipher the multi-drug resistance mechanism in Salmonella enterica serovar Typhi CT18 reveal potential drug targets*. Microbial Pathogenesis, 2020. **142**: p. 104096.
331. Klein, K., et al., *Deprivation of the Periplasmic Chaperone SurA Reduces Virulence and Restores Antibiotic Susceptibility of Multidrug-Resistant Pseudomonas aeruginosa*. Frontiers in Microbiology, 2019. **10**.
332. Dufresne, K. and C. Paradis-Bleau, *Biology and assembly of the bacterial envelope*. Prokaryotic systems biology, 2015: p. 41-76.
333. Shetty, D.M., *Role of the RpoE sigma factor and two-component Cpx systems, in biofilm formation of Salmonella enterica subspecies enterica serovar Enteritidis*. 2019, University of Saskatchewan.
334. Zhong, Z., et al., *Bacteriophage-Induced Lipopolysaccharide Mutations in Escherichia coli Lead to Hypersensitivity to Food Grade Surfactant Sodium Dodecyl Sulfate*. Antibiotics, 2020. **9**(9): p. 552.
335. Yethon, J.A., et al., *Mutation of the Lipopolysaccharide Core Glycosyltransferase Encoded by waaG Destabilizes the Outer Membrane of Escherichia coli by Interfering with Core Phosphorylation*. Journal of Bacteriology, 2000. **182**(19): p. 5620-5623.
336. Chang, V., et al., *The effect of lipopolysaccharide core structure defects on transformation efficiency in isogenic Escherichia coli BW25113 rfaG, rfaP, and rfaC mutants*. J. Exp. Microbiol. Immunol, 2010. **14**: p. 101-107.
337. Guest, R.L., et al., *YejM modulates activity of the YciM/FtsH protease complex to prevent lethal accumulation of lipopolysaccharide*. MBio, 2020. **11**(2): p. e00598-20.
338. Guest, R.L., S.T. Rutherford, and T.J. Silhavy, *Border Control: Regulating LPS Biogenesis*. Trends in Microbiology, 2021. **29**(4): p. 334-345.
339. Simpson, B.W., et al., *Restoring Balance to the Outer Membrane: YejM's Role in LPS Regulation*. mBio, 2020. **11**(6): p. e02624-20.
340. Dalebroux, Zachary D., et al., *Delivery of Cardiolipins to the Salmonella Outer Membrane Is Necessary for Survival within Host Tissues and Virulence*. Cell Host & Microbe, 2015. **17**(4): p. 441-451.
341. Cian, M.B., et al., *Salmonella enterica serovar Typhimurium uses PbgA/YejM to regulate lipopolysaccharide assembly during bacteremia*. Infection and immunity, 2019. **88**(1): p. e00758-19.
342. Nguyen, D., et al., *YejM Controls LpxC Levels by Regulating Protease Activity of the FtsH/YciM Complex of Escherichia coli*. Journal of Bacteriology, 2020. **202**(18): p. e00303-20.

343. Duo, M., S. Hou, and D. Ren, *Identifying Escherichia coli genes involved in intrinsic multidrug resistance*. Applied Microbiology and Biotechnology, 2008. **81**(4): p. 731-741.
344. Kwon, H.I., et al., *Outer membrane protein A contributes to antimicrobial resistance of Acinetobacter baumannii through the OmpA-like domain*. Journal of Antimicrobial Chemotherapy, 2017. **72**(11): p. 3012-3015.
345. Chowdhury, A.R., et al., *Outer membrane protein A (OmpA) deficient Salmonella Typhimurium displays enhanced susceptibility towards β -lactam antibiotics: third-generation cephalosporins (ceftazidime) and carbapenems (meropenem)*. bioRxiv, 2022.
346. Sultana, T., A.K. Mitra, and S. Das, *An in vitro approach to combat multidrug resistance in Salmonella typhi and human colon cancer with Excoecaria agallocha L. extract*. Bulletin of the National Research Centre, 2021. **45**(1): p. 210.
347. McCusker, M.P., et al., *Complete genome sequence of Salmonella enterica serovar Agona pulsed-field type SAGOXB. 0066, cause of a 2008 pan-European outbreak*. Genome Announcements, 2014. **2**(1): p. e01219-13.
348. Chauhan, A.K. and S.C. Kang, *Thymol disrupts the membrane integrity of Salmonella ser. typhimurium in vitro and recovers infected macrophages from oxidative stress in an ex vivo model*. Research in Microbiology, 2014. **165**(7): p. 559-565.
349. Miladi, H., et al., *Use of carvacrol, thymol, and eugenol for biofilm eradication and resistance modifying susceptibility of Salmonella enterica serovar Typhimurium strains to nalidixic acid*. Microbial Pathogenesis, 2017. **104**: p. 56-63.
350. Eldien, D.E., G.M.E. Moghazy, and H.N. Fahmy, *Studies on some plant extracts as antimicrobials and food preservatives*. Journal of Microbiology, Biotechnology and Food Sciences, 2021. **2021**: p. 790-798.
351. Elfaky, M.A., et al., *Innovative next-generation therapies in combating multi-drug-resistant and multi-virulent Escherichia coli isolates: insights from in vitro, in vivo, and molecular docking studies*. Applied Microbiology and Biotechnology, 2022. **106**(4): p. 1691-1703.
352. Sultanbawa, Y., *Plant antimicrobials in food applications: Minireview*. Science against microbial pathogens: Communicating current research and technological advances, 2011. **2**: p. 1084-99.
353. Kyung, K.H., *Antimicrobial properties of allium species*. Current opinion in biotechnology, 2012. **23**(2): p. 142-147.
354. Lv, F., et al., *In vitro antimicrobial effects and mechanism of action of selected plant essential oil combinations against four food-related microorganisms*. Food Research International, 2011. **44**(9): p. 3057-3064.
355. Beya, M.M., et al., *Plant-Based Phenolic Molecules as Natural Preservatives in Comminuted Meats: A Review*. Antioxidants, 2021. **10**(2): p. 263.
356. Osojnik Črnivec, I.G., et al., *Waste streams in onion production: Bioactive compounds, quercetin and use of antimicrobial and antioxidative properties*. Waste Management, 2021. **126**: p. 476-486.
357. Rodríguez Vaquero, M.J., et al., *Phenolic Compound Combinations on Escherichia coli Viability in a Meat System*. Journal of Agricultural and Food Chemistry, 2010. **58**(10): p. 6048-6052.
358. Rodríguez-Vaquero, M.J., P. Aredes Aredes-Fernández, and M.C. Manca de Nadra, *Phenolic compounds from wine as natural preservatives of fish meat*. Food technology and biotechnology, 2013. **51**(3): p. 376-382.
359. Stojković, D., et al., *In situ antioxidant and antimicrobial activities of naturally occurring caffeic acid, p-coumaric acid and rutin, using food systems*. Journal of the Science of Food and Agriculture, 2013. **93**(13): p. 3205-3208.
360. Albuquerque, B.R., et al., *Phenolic compounds: current industrial applications, limitations and future challenges*. Food & Function, 2021. **12**(1): p. 14-29.

361. Burt, S.A., et al., *Increase in activity of essential oil components carvacrol and thymol against Escherichia coli O157: H7 by addition of food stabilizers*. Journal of food protection, 2005. **68**(5): p. 919-926.
362. Maqsood, S. and S. Benjakul, *Preventive effect of tannic acid in combination with modified atmospheric packaging on the quality losses of the refrigerated ground beef*. Food Control, 2010. **21**(9): p. 1282-1290.
363. Zhao, S., et al., *Shelf life of fresh chilled pork as affected by antimicrobial intervention with nisin, tea polyphenols, chitosan, and their combination*. International Journal of Food Properties, 2019. **22**(1): p. 1047-1063.
364. Zhou, F., et al., *Synergistic Effect of Thymol and Carvacrol Combined with Chelators and Organic Acids against Salmonella Typhimurium*. Journal of Food Protection, 2007. **70**(7): p. 1704-1709.
365. Periago, P.M. and R. Moezelaar, *Combined effect of nisin and carvacrol at different pH and temperature levels on the viability of different strains of Bacillus cereus*. International journal of food microbiology, 2001. **68**(1-2): p. 141-148.
366. Tassou, C., E. Drosinos, and G. Nychas, *Effects of essential oil from mint (Mentha piperita) on Salmonella enteritidis and Listeria monocytogenes in model food systems at 4 and 10 C*. Journal of Applied Bacteriology, 1995. **78**(6): p. 593-600.
367. Carraro, L., et al., *Polyphenols from olive mill waste affect biofilm formation and motility in Escherichia coli K-12*. Microbial Biotechnology, 2014. **7**(3): p. 265-275.
368. Šarac, Z., et al., *Biological Activity of Pinus nigra terpenes- Evaluation of FtsZ Inhibition by Selected Compounds As Contribution To Their Antimicrobial Activity*. Computers in Biology and Medicine, 2014. **54**: p. 72-78.
369. de Camargo, A.C., et al., *Phenolic acids and flavonoids of peanut by-products: Antioxidant capacity and antimicrobial effects*. Food Chemistry, 2017. **237**: p. 538-544.
370. Aeschbach, R., et al., *Antioxidant actions of thymol, carvacrol, 6-gingerol, zingerone and hydroxytyrosol*. Food and Chemical Toxicology, 1994. **32**(1): p. 31-36.
371. Esmaeili, A. and A. Khodadadi, *Antioxidant activity of a solution of thymol in ethanol*. Zahedan Journal of Research in Medical Sciences, 2012. **14**(7): p. 14-18.
372. Yanishlieva, N.V., et al., *Antioxidant activity and mechanism of action of thymol and carvacrol in two lipid systems*. Food Chemistry, 1999. **64**(1): p. 59-66.
373. Rathod, N.B., et al., *Biological activity of plant-based carvacrol and thymol and their impact on human health and food quality*. Trends in Food Science & Technology, 2021. **116**: p. 733-748.
374. Chen, F.-p., et al., *Nanocomplexation between thymol and soy protein isolate and its improvements on stability and antibacterial properties of thymol*. Food Chemistry, 2021. **334**: p. 127594.
375. Marcet, I., et al., *Production and characterisation of biodegradable PLA nanoparticles loaded with thymol to improve its antimicrobial effect*. Journal of Food Engineering, 2018. **239**: p. 26-32.
376. Xue, J., P.M. Davidson, and Q. Zhong, *Thymol Nanoemulsified by Whey Protein-Maltodextrin Conjugates: The Enhanced Emulsifying Capacity and Antilisterial Properties in Milk by Propylene Glycol*. Journal of Agricultural and Food Chemistry, 2013. **61**(51): p. 12720-12726.
377. Wu, H., et al., *Development and characterization of antimicrobial protein films based on soybean protein isolate incorporating diatomite/thymol complex*. Food Hydrocolloids, 2021. **110**: p. 106138.
378. Lukic, I., J. Vulic, and J. Ivanovic, *Antioxidant activity of PLA/PCL films loaded with thymol and/or carvacrol using scCO₂ for active food packaging*. Food Packaging and Shelf Life, 2020. **26**: p. 100578.

379. de Oliveira, C.E.V., et al., *Inhibition of Staphylococcus aureus in broth and meat broth using synergies of phenolics and organic acids*. International Journal of Food Microbiology, 2010. **137**(2): p. 312-316.
380. Shah, B., P.M. Davidson, and Q. Zhong, *Nanocapsular Dispersion of Thymol for Enhanced Dispersibility and Increased Antimicrobial Effectiveness against Escherichia coli O157:H7 and Listeria monocytogenes in Model Food Systems*. Applied and Environmental Microbiology, 2012. **78**(23): p. 8448-8453.
381. Sepahvand, S., et al., *Antimicrobial Activity of Thymol and Thymol-Nanoemulsion Against Three Food-Borne Pathogens Inoculated in a Sausage Model*. Food and Bioprocess Technology, 2021. **14**(10): p. 1936-1945.
382. Mastromatteo, M., et al., *Shelf life of ready to use peeled shrimps as affected by thymol essential oil and modified atmosphere packaging*. International journal of food microbiology, 2010. **144**(2): p. 250-256.
383. Rajamanickam, K., J. Yang, and M.K. Sakharkar, *Phytochemicals as alternatives to antibiotics against major pathogens involved in bovine respiratory disease (BRD) and bovine mastitis (BM)*. Bioinformation, 2019. **15**(1): p. 32.
384. Septama, A.W., N. Simbak, and E.P. Rahmi, *Prospect of Plant-based Flavonoids to Overcome Antibacterial Resistance: A Mini-Review*. Walailak Journal of Science and Technology (WJST), 2019. **17**(5): p. 503-513.
385. Daglia, M., *Polyphenols as antimicrobial agents*. Current Opinion in Biotechnology, 2012. **23**(2): p. 174-181.
386. Singh, M., M. Kaur, and O. Silakari, *Flavones: An important scaffold for medicinal chemistry*. European Journal of Medicinal Chemistry, 2014. **84**: p. 206-239.
387. Končić, M.Z., et al., *Antioxidant and antimicrobial properties of Moltkia petraea (Tratt.) Griseb. flower, leaf and stem infusions*. Food and Chemical Toxicology, 2010. **48**(6): p. 1537-1542.
388. Aissani, N., et al., *Antioxidant potential and antimicrobial activity of Ailanthus altissima (Mill.) Swingle extracts against Pseudomonas aeruginosa*. Journal of Molecular Biology and Biotechnology, 2018. **3**(3).
389. De Zoysa, M.H.N., et al., *Determination of in vitro antimicrobial activity of five Sri Lankan medicinal plants against selected human pathogenic bacteria*. International journal of microbiology, 2019. **2019**.
390. Liu, Z., et al., *Chemical Composition Antimicrobial and Anti-Quorum Sensing Activities of Pummelo Peel Flavonoid Extract* Industrial Crops and Products, 2017. **109**: p. 862-868.
391. Kumar, Y., et al., *Improving Meat Safety Through Reformulation Strategies: Natural Antioxidants and Antimicrobials*, in *Reformulation as a Strategy for Developing Healthier Food Products: Challenges, Recent Developments and Future Prospects*, V. Raikos and V. Ranawana, Editors. 2019, Springer International Publishing: Cham. p. 251-289.
392. Negi, P.S., *Plant extracts for the control of bacterial growth: Efficacy, stability and safety issues for food application*. International Journal of Food Microbiology, 2012. **156**(1): p. 7-17.

Chapter 9: Appendix

*“Appendix usually means “small outgrowth from large intestine” but in this case it means “additional information accompanying main text.” Or are those really the same things?.”- Pseudonymous Bosch, *The Name of This Book Is Secret*, 2007*

9.1 Appendix

9.1.1 Chapter 3

Table 9.3.1: Summary of results of semi-high throughput inhibition assays against Gram-negative species.

Gram-Negative pathogen OD _(600nm) after phytochemical exposure as a percentage of solvent controls							
Phytochemical	Concentration (mg/ml)	<i>S. enterica</i>			<i>P. aeruginosa</i>		
		OD _(600nm)	SEM (±)	<i>p</i> value	OD _(600nm)	SEM (±)	<i>p</i> value
Prosur	0.5	103.01	0.03	0.3594	106.07	0.07	0.3583
	0.25	106.26	0.02	0.0004*	100.99	0.03	0.4665
	0.125	106.43	0.02	0.0002*	101.87	0.05	0.4057
Eriodictyol	0.5	103.48	0.03	0.2970	109.58	0.05	0.1476
	0.25	103.25	0.02	0.0571	102.22	0.01	0.1080
	0.125	104.92	0.02	0.0042*	103.09	0.03	0.1741
Naringin	0.5	101.28	0.03	0.7033	106.58	0.07	0.3198
	0.25	105.03	0.01	0.0038*	104.13	0.02	0.0037
	0.125	107.18	0.02	<0.0001*	103.91	0.04	0.0859
Ferulic acid	0.5	84.23	0.05	<0.0001	89.97	0.10	0.1301
	0.25	102.70	0.02	0.1101	102.18	0.02	0.1159
	0.125	106.65	0.02	0.0001*	104.52	0.04	0.0475
Hesperidin	0.5	98.03	0.07	0.5523	110.10	0.06	0.1279
	0.25	102.74	0.05	0.1072	103.04	0.02	0.0307
	0.125	104.30	0.05	0.0117*	103.18	0.04	0.1643
Rutin	0.5	97.74	0.02	0.4925	104.79	0.07	0.4648
	0.25	105.17	0.02	0.0030*	103.18	0.02	0.0240
	0.125	106.69	0.02	0.0001*	103.83	0.03	0.0917
Quercetin	0.5	21.07	-	-	48.83	-	-

	0.25	22.87	-	-	44.82	-	-
	0.125	23.64	-	-	45.37	-	-
Caffeic acid	0.5	96.19	0.04	0.3627	94.87	0.04	0.3005
	0.25	105.08	0.04	0.0107	104.81	0.02	0.0006
	0.125	106.07	0.03	0.0018	104.09	0.02	0.0165
Cinnamic acid	0.5	82.39	0.04	<0.0001	79.82	0.06	<0.0001
	0.25	103.48	0.04	0.0767	100.18	0.02	0.8788
	0.125	106.03	0.03	0.0019	102.22	0.02	0.1899
Thymol	0.5	51.18	0.09	<0.0001	57.41	0.07	<0.0001
	0.25	106.26	0.03	0.0018	103.27	0.02	0.0159
	0.125	108.42	0.03	<0.0001	104.57	0.03	0.0080
Kaempferol	0.5	83.69	-	-	86.34	-	-
	0.25	86.28	-	-	91.15	-	-
	0.125	85.42	-	-	90.78	-	-
Naringenin	0.5	101.25	0.04	0.7656	95.43	0.05	0.3555
	0.25	103.89	0.04	0.0490	101.50	0.03	0.2604
	0.125	106.25	0.03	0.0013	102.52	0.03	0.1333
Vanillin	0.5	79.20	0.05	<0.0001	72.19	0.08	<0.0001
	0.25	100	0.02	0.9953	98.37	0.02	0.2299
	0.125	102.17	0.03	0.2556	102.57	0.03	0.1279
Vanillic acid	0.5	91.25	0.03	0.0373	81.49	0.09	0.0003
	0.25	99.59	0.02	0.8344	102.27	0.02	0.0941
	0.125	102.17	0.02	0.2581	104.48	0.03	0.0088

Data show the average OD_(600nm) achieved, as a percentage of the comparable solvent vehicle control, after 16 hours by four biological replicates. Three technical replicates each. Values presented at 2 decimal places. Statistical analysis was performed using the GraphPad software v.8, using a 1-way repeated measures ANOVA Test with Fischer's LSD test. Values in bold were statistically, significantly, different to the relevant control.

Table 9.3.2: Summary of results of semi-high throughput inhibition assays against Gram-positive species.

Gram-Positive pathogen OD _(600nm) after phytochemical exposure as a percentage of solvent controls							
Phytochemical	Concentration (mg/ml)	<i>S. aureus</i>			<i>L. monocytogenes</i>		
		OD _(600nm)	SEM (±)	<i>p</i> value	OD _(600nm)	SEM (±)	<i>p</i> value
Prosur	0.5	93.20	0.07	0.0317	91.08	0.08	0.2676
	0.25	107.79	0.06	0.0628	104.97	0.06	0.3098
	0.125	108.47	0.02	0.0049	106.29	0.07	0.1934
Eriodictyol	0.5	13.13	0.03	<0.0001	87.84	0.12	0.1321
	0.25	24.16	0.04	<0.0001	93.38	0.13	0.1795
	0.125	41.59	0.09	<0.0001	87.69	0.10	0.0118
Naringin	0.5	97.97	0.06	0.5192	93.19	0.09	0.3982
	0.25	115.93	0.03	0.0002	103.20	0.06	0.5112
	0.125	108.61	0.02	0.0043	104.81	0.07	0.3160
Ferulic acid	0.5	102.80	0.02	0.3778	94.76	0.09	0.5139
	0.25	114.62	0.06	0.0007	108.89	0.08	0.0712
	0.125	110.07	0.04	0.0009	107.12	0.07	0.1405
Hesperidin	0.5	97.88	0.04	0.4930	89.35	0.18	0.1857
	0.25	112.91	0.03	0.0025	97.13	0.08	0.5583
	0.125	109.50	0.03	0.0017	94.05	0.13	0.2170
Rutin	0.5	96.67	0.05	0.2857	93.73	0.06	0.4368
	0.25	112.11	0.02	0.0043	107.50	0.08	0.1281
	0.125	108.01	0.02613	0.0077	105.23	0.07	0.2771
Quercetin	0.5	-4.57	-	-	10.19	-	-
	0.25	-17.87	-	-	28.36	-	-
	0.125	-15.60	-	-	35.90	-	-
Caffeic acid	0.5	97.20	0.1843	0.7960	88.86	0.09	0.2032
	0.25	107.29	0.05955	0.0645	96.17	0.05	0.4586
	0.125	105.24	0.03398	0.0088	97.12	0.06	0.5536
Cinnamic acid	0.5	120.28	0.03617	0.0641	101.14	0.11	0.8942
	0.25	115.33	0.04502	0.0002	104.13	0.08	0.4269

	0.125	108.90	0.02623	<0.0001	104.85	0.08	0.3181
Thymol	0.5	101.01	0.1631	0.9279	76.65	0.16	0.0088
	0.25	116.53	0.04039	<0.0001	102.53	0.06	0.6218
	0.125	110.21	0.03669	<0.0001	106.74	0.08	0.1673
Kaempferol	0.5	37.98	-	-	20.30	-	-
	0.25	48.16	-	-	33.36	-	-
	0.125	50.70	-	-	27.03	-	-
Naringenin	0.5	7.204	0.01476	<0.0001	118.59	0.14	0.0353
	0.25	10.47	0.01797	<0.0001	108.13	0.14	0.1184
	0.125	91.06	0.03105	<0.0001	103.90	0.11	0.4215
Vanillin	0.5	102.91	0.1753	0.7894	98.05	0.10	0.8256
	0.25	113.84	0.03674	0.0091	109.27	0.10	0.0765
	0.125	110.20	0.03132	0.0051	107.05	0.10	0.1485
Vanillic acid	0.5	104.49	0.02422	0.2035	113.57	0.10	0.1211
	0.25	113.84	0.01306	0.0106	112.73	0.10	0.0158
	0.125	110.20	0.02254	0.0242	108.60	0.10	0.0786

Data show the average OD_(600nm) achieved, as a percentage of the comparable solvent vehicle control, after 16 hours by four biological replicates. Three technical replicates each. Values presented at 2 decimal places. Statistical analysis was performed using the GraphPad software v.8, using a 1-way repeated measures ANOVA Test with Fischer's LSD test. Values in bold were statistically, significantly, different to the relevant control.

Table 9.3.3: Summary of results of semi-high throughput potentiation assays against Gram-negative species.

Percentage of final OD _(600nm) achieved by Gram-negative species in potentiation assays							
Phytochemical	Concentration (mg/ml)	<i>S. enterica</i>			<i>P. aeruginosa</i>		
		OD _(600nm)	SEM (±)	<i>p</i> value	OD _(600nm)	SEM (±)	<i>p</i> value
PAβN positive Control	0.512	13.95	0.02	<0.0001	18.74	0.01	<0.0001
prosur	0.5	103.57	0.04	0.3124	98.20	0.02	0.5309
	0.25	80.89	0.02	<0.0001	81.58	0.03	<0.0001
	0.125	77.62	0.02	<0.0001	77.16	0.03	<0.0001
Eriodictyol	0.5	98.64	0.01	0.6938	101.10	0.04	0.6932
	0.25	85.37	0.01	<0.0001	85.48	0.03	<0.0001
	0.125	83.91	0.01	<0.0001	81.64	0.02	<0.0001
Naringin	0.5	101.04	0.04	0.7756	94.27	0.04	0.0463
	0.25	80.06	0.02	<0.0001	81.08	0.04	<0.0001
	0.125	78.37	0.02	<0.0001	77.47	0.03	<0.0001
Ferulic acid	0.5	103.70	0.04	0.2932	99.68	0.03	0.9135
	0.25	81.53	0.02	<0.0001	81.17	0.03	<0.0001
	0.125	82.09	0.01	<0.0001	79.12	0.03	<0.0001
Hesperidin	0.5	100.45	0.07	0.8964	92.08	0.04	0.0062
	0.25	78.65	0.04	<0.0001	78.86	0.03	<0.0001
	0.125	76.91	0.03	<0.0001	77.51	0.04	<0.0001
Rutin	0.5	100.13	0.04	0.9658	96.20	0.02	0.1855
	0.25	79.24	0.03	<0.0001	79.17	0.04	<0.0001
	0.125	78.24	0.01	<0.0001	76.73	0.03	<0.0001
Quercetin	0.5	39.29	-	-	40.78	-	-
	0.25	20.45	-	-	21.57	-	-
	0.125	18.44	-	-	19.48	-	-
Caffeic acid	0.5	87.87	0.03	0.0002	86.92	0.04	0.0003
	0.25	78.28	0.02	<0.0001	81.13	0.03	<0.0001

	0.125	75.44	0.02	<0.0001	81.86	0.04	<0.0001
Cinnamic acid	0.5	80.42	0.04	<0.0001	86.98	0.03	0.0003
	0.25	75.22	0.02	<0.0001	82.71	0.01	<0.0001
	0.125	77.97	0.02	<0.0001	82.69	0.03	<0.0001
Thymol	0.5	50.82	0.07	<0.0001	42.20	0.07	<0.0001
	0.25	76.50	0.02	<0.0001	82.40	0.02	<0.0001
	0.125	75.62	0.02	<0.0001	82.86	0.03	<0.0001
Kaempferol	0.5	93.75	-	-	86.67	-	-
	0.25	71.56	-	-	80.58	-	-
	0.125	67.51	-	-	71.38	-	-
Naringenin	0.5	100.76	0.02	0.8085	97.59	0.03	0.4949
	0.25	86.47	0.01	<0.0001	85.39	0.04	<0.0001
	0.125	85.42	0.01	<0.0001	82.08	0.04	<0.0001
Vanillin	0.5	92.04	0.01	0.0117	91.73	0.02	0.0197
	0.25	77.50	0.02	<0.0001	79.45	0.03	<0.0001
	0.125	78.24	0.01	<0.0001	79.34	0.02	<0.0001
Vanillic acid	0.5	93.30	0.02	0.0329	92.97	0.03	0.0471
	0.25	78.33	0.01	<0.0001	83.76	0.03	<0.0001
	0.125	77.44	0.02	<0.0001	81.91	0.03	<0.0001

Data show the average OD_(600nm) achieved, as a percentage of the comparable solvent vehicle control, after 16 hours by four biological replicates. Three technical replicates each. Values presented at 2 decimal places. Statistical analysis was performed using the GraphPad software v.8, using a 1-way repeated measures ANOVA Test with Fischer's LSD test. Values in bold were statistically, significantly, different to the relevant control.

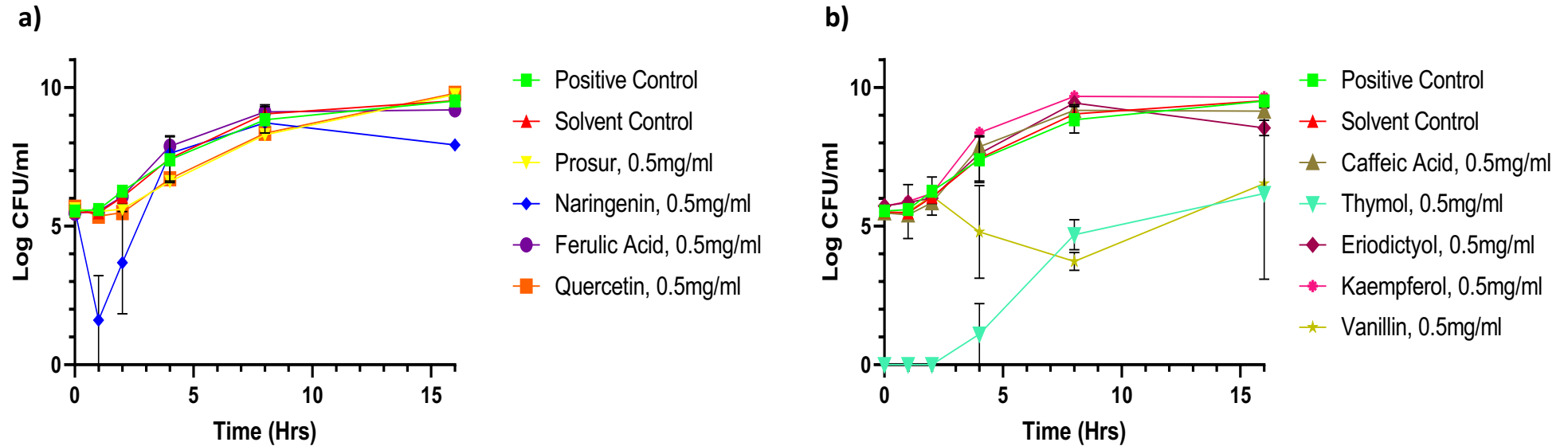
Table 9.3.4: Summary of results of semi-high throughput potentiation assays against Gram-positive species.

Percentage of final OD _(600nm) achieved by Gram-positive species in potentiation assays							
Phytochemical	Concentration (mg/ml)	<i>S. aureus</i>			<i>L. monocytogenes</i>		
		OD _(600nm)	SEM (±)	<i>p</i> value	OD _(600nm)	SEM (±)	<i>p</i> value
PAβN positive control	0.512	5.79	0.01	<0.0001	-8.33	0.10	<0.0001
Prosur	0.5	17.85	0.03	<0.0001	108.54	0.06	0.1263
	0.25	19.50	0.05	<0.0001	100.55	0.10	0.9260
	0.125	54.26	0.13	<0.0001	96.74	0.14	0.6431
Eriodictyol	0.5	10.41	0.01	<0.0001	90.54	0.07	0.0915
	0.25	9.41	0.01	<0.0001	90.48	0.07	0.1138
	0.125	13.81	0.06	<0.0001	89.55	0.11	0.1370
Naringin	0.5	116.92	0.12	0.1361	105.89	0.05	0.2878
	0.25	90.95	0.02	0.0187	102.91	0.11	0.6277
	0.125	82.82	0.02	<0.0001	97.69	0.15	0.7414
Ferulic acid	0.5	95.37	0.11	0.6795	109.95	0.05	0.0750
	0.25	86.93	0.06	0.0008	105.18	0.12	0.3870
	0.125	80.06	0.05	<0.0001	101.44	0.14	0.8388
Hesperidin	0.5	81.25	0.13	0.0980	106.38	0.10	0.2502
	0.25	86.38	0.04	0.0005	96.63	0.10	0.5751
	0.125	79.26	0.05	<0.0001	92.99	0.13	0.3179
Rutin	0.5	96.73	0.18	0.7700	111.89	0.08	0.0339
	0.25	84.22	0.05	<0.0001	105.69	0.13	0.3413
	0.125	74.53	0.06	<0.0001	100.68	0.16	0.9231
Quercetin	0.5	9.34	-	-	44.61	-	-
	0.25	-36.27	-	-	56.81	-	-
	0.125	-35.57	-	-	59.77	-	-
Caffeic acid	0.5	0.580	0.01	<0.0001	101.19	0.09	0.8888
	0.25	2.15	0.02	<0.0001	100.97	0.11	0.8795

	0.125	2.45	0.02	<0.0001	97.31	0.14	0.7074
Cinnamic acid	0.5	84.64	0.12	0.1805	101.78	0.13	0.8364
	0.25	90.60	0.05	0.1190	105.18	0.14	0.4193
	0.125	80.43	0.11	0.0184	101.25	0.16	0.8622
Thymol	0.5	32.05	0.13	<0.0001	86.49	0.20	0.1251
	0.25	80.55	0.10	0.0016	100.76	0.10	0.9069
	0.125	73.78	0.11	0.0018	97.77	0.16	0.7555
Kaempferol	0.5	26.20	-	-	32.62	-	-
	0.25	20.99	-	-	21.45	-	-
	0.125	21.12	-	-	16.51	-	-
Naringenin	0.5	4.41	0.01	<0.0001	108.43	0.10	0.3349
	0.25	22.71	0.13	<0.0001	103.16	0.10	0.6209
	0.125	44.14	0.24	<0.0001	100.57	0.12	0.9377
Vanillin	0.5	62.72	0.17	0.0015	106.49	0.10	0.4586
	0.25	81.56	0.09	0.0027	103.79	0.12	0.5505
	0.125	74.20	0.13	0.0022	99.47	0.15	0.9391
Vanillic acid	0.5	56.74	0.18	0.0003	111.51	0.10	0.1879
	0.25	81.31	0.07	0.0023	101.64	0.12	0.7967
	0.125	70.32	0.14	0.0005	96.89	0.15	0.6627

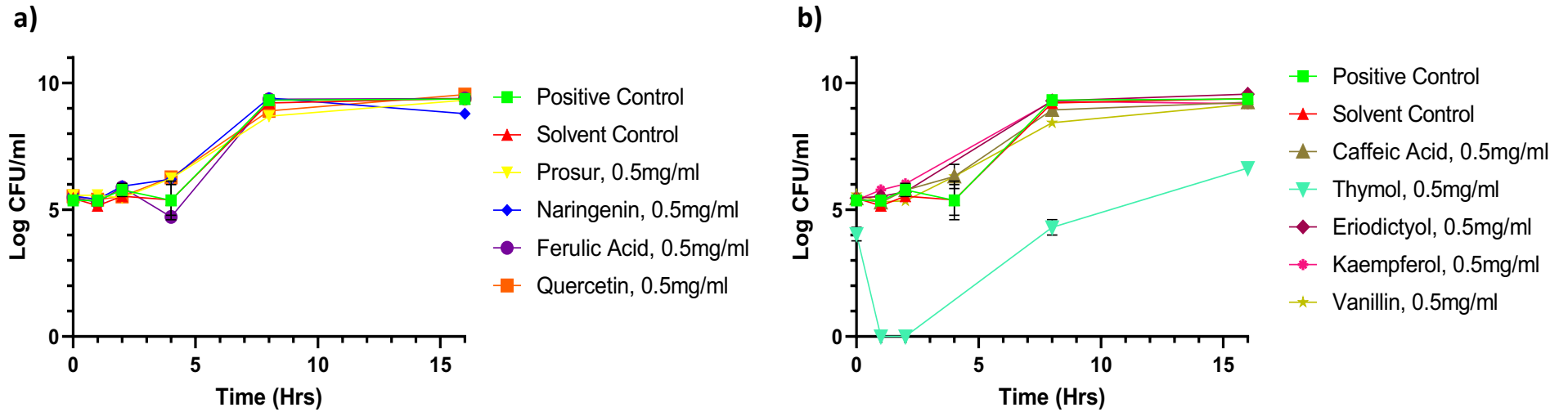
Data show the average OD_(600nm) achieved, as a percentage of the comparable solvent vehicle control, after 16 hours by four biological replicates. Three technical replicates each. Values presented at 2 decimal places. Statistical analysis was performed using the GraphPad software v.8, using a 1-way repeated measures ANOVA Test with Fischer's LSD test. Values in bold were statistically, significantly, different to the relevant control.

Figure 9.3.1: Growth curves for *S. enterica* challenged with 0.5mg/ml of various phytochemicals.



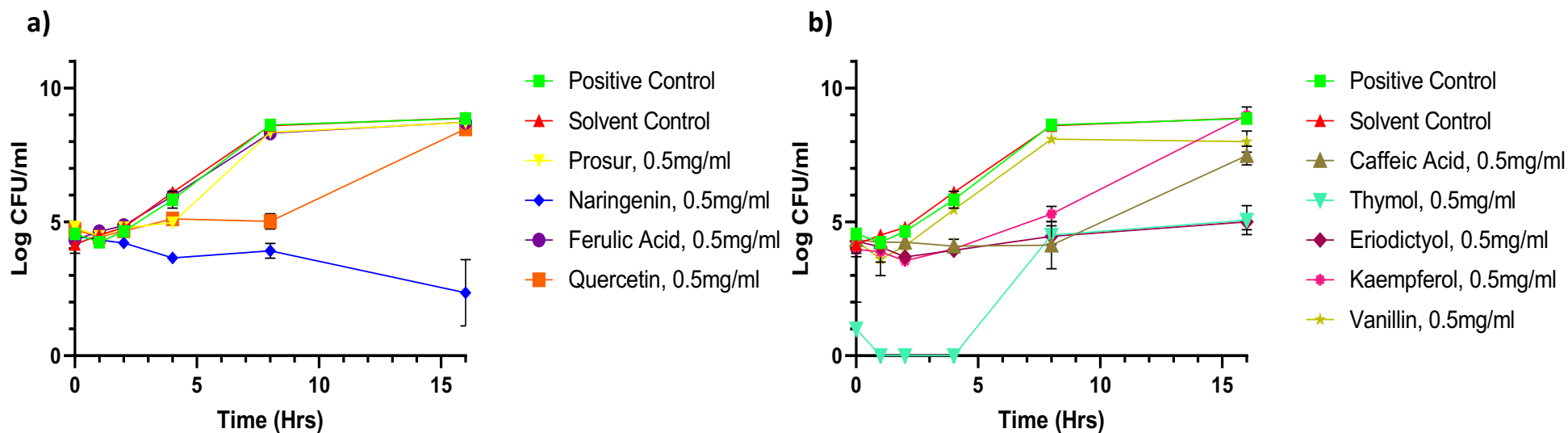
Panel **a)** *S. enterica* against the Prosur NATPRE T-10+ mix, naringenin, ferulic acid and quercetin, **b)** *S. enterica* against caffeic acid, thymol, eriodictyol, kaempferol and vanillin. Experiments were repeated with three biological replicates (three technical replicates each) over an incubation period of 16 hours. Points show the average value for each point and errors bars indicate the standard error of the mean.

Figure 9.3.2: Growth curves for *P. aeruginosa* challenged with 0.5mg/ml of various phytochemicals.



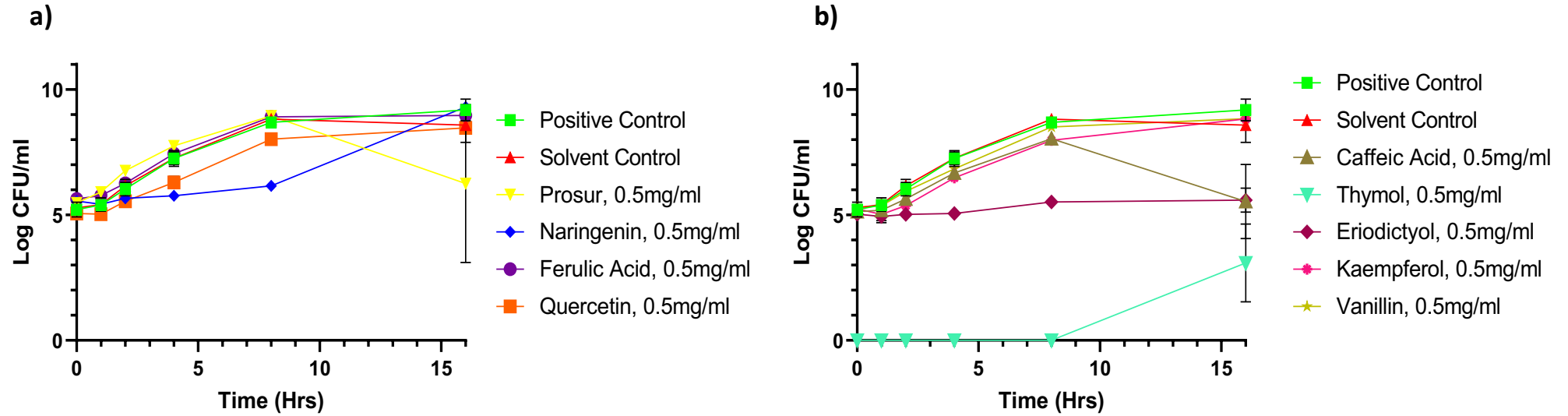
Panel **a)** *P. aeruginosa* against the Prosur NATPRE T-10+ mix, naringenin, ferulic acid and quercetin, **b)** *P. aeruginosa* against caffeic acid, thymol, eriodictyol, kaempferol and vanillin. Experiments were repeated with three biological replicates (three technical replicates each) over an incubation period of 16 hours. Points show the average value for each point and errors bars indicate the standard error of the mean.

Figure 9.3.3: Growth curves for *S. aureus* challenged with 0.5mg/ml of various phytochemicals.



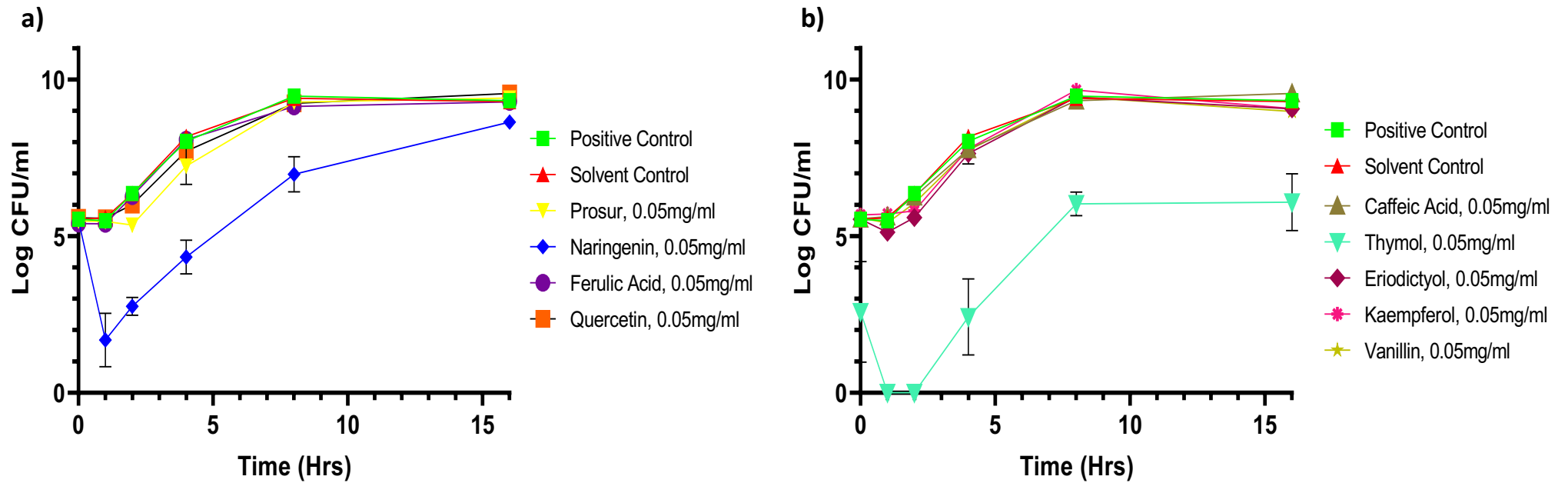
Panel **a)** *S. aureus* against the Prosur NATPRE T-10+ mix, naringenin, ferulic acid and quercetin, **b)** *S. aureus* against caffeic acid, thymol, eriodictyol, kaempferol and vanillin. Experiments were repeated with three biological replicates (three technical replicates each) over an incubation period of 16 hours. Points show the average value for each point and errors bars indicate the standard error of the mean.

Figure 9.3.4: Growth curves for *L. monocytogenes* challenged with 0.5mg/ml of various phytochemicals.



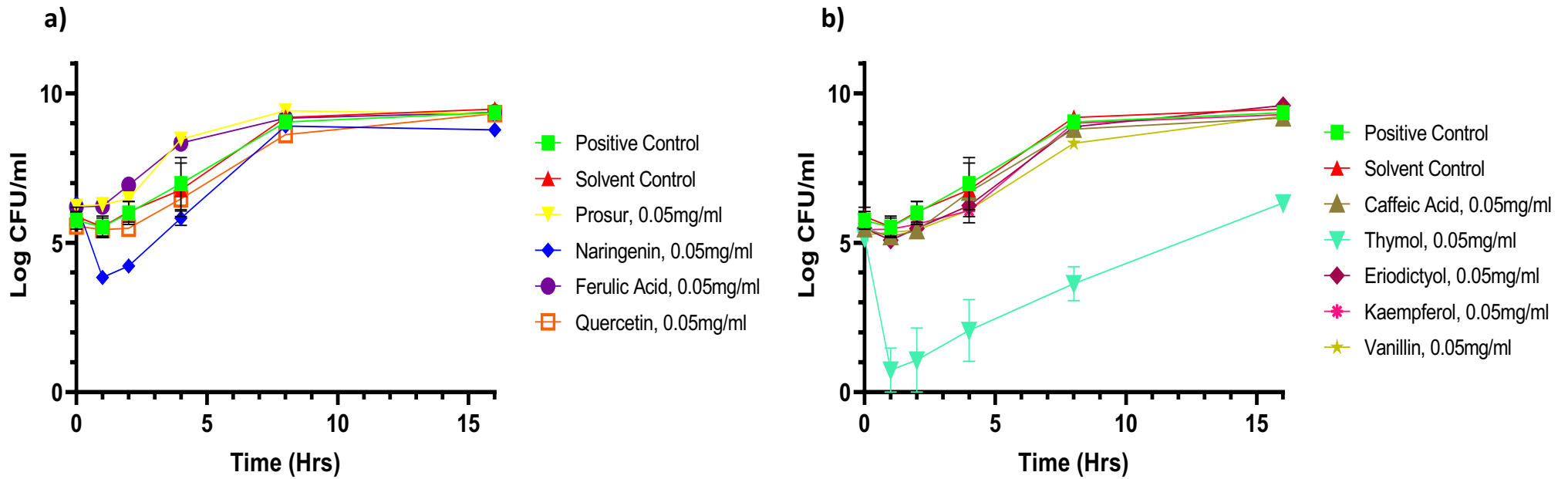
Panel **a)** *L. monocytogenes* against the Prosur NATPRE T-10+ mix, naringenin, ferulic acid and quercetin, **b)** *L. monocytogenes* against caffeic acid, thymol, eriodictyol, kaempferol and vanillin. Experiments were repeated with three biological replicates (three technical replicates each) over an incubation period of 16 hours. Points show the average value for each point and errors bars indicate the standard error of the mean.

Figure 9.3.5: Growth curves for *S. enterica* challenged with 0.05mg/ml of various phytochemicals.



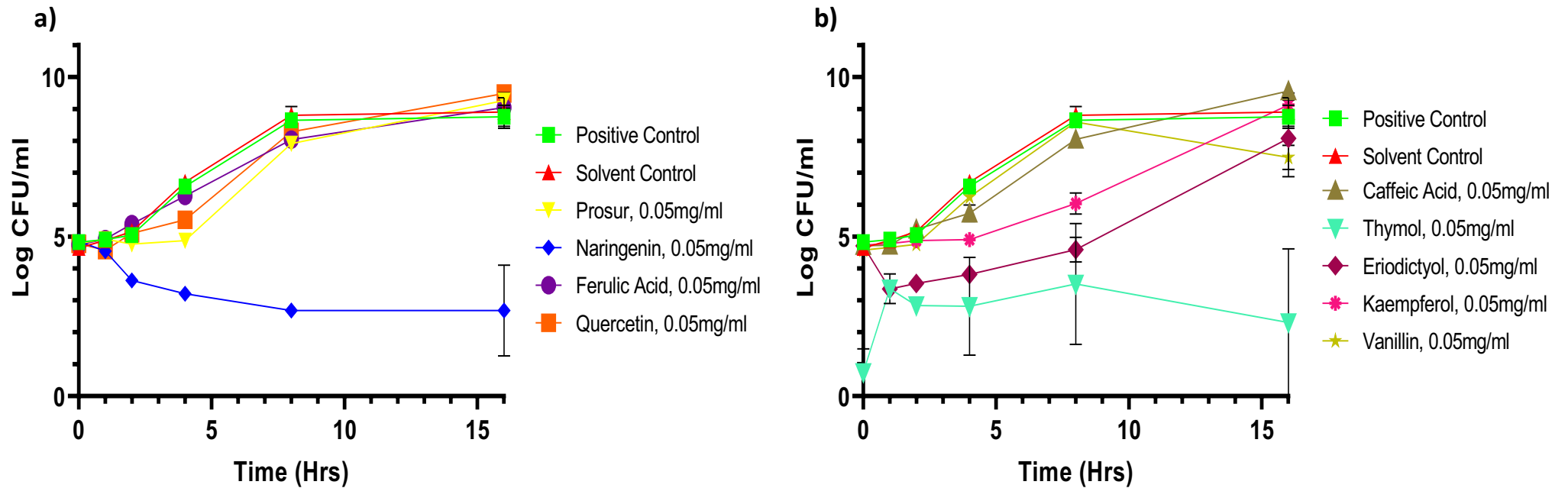
Panel **a)** *S. enterica* against the Prosur NATPRE T-10+ mix, naringenin, ferulic acid and quercetin, **b)** *S. enterica* against caffeic acid, thymol, eriodictyol, kaempferol and vanillin. Experiments were repeated with three biological replicates (three technical replicates each) over an incubation period of 16 hours. Points show the average value for each point and errors bars indicate the standard error of the mean.

Figure 9.3.6: Growth curves for *P. aeruginosa* challenged with 0.05mg/ml of various phytochemicals.



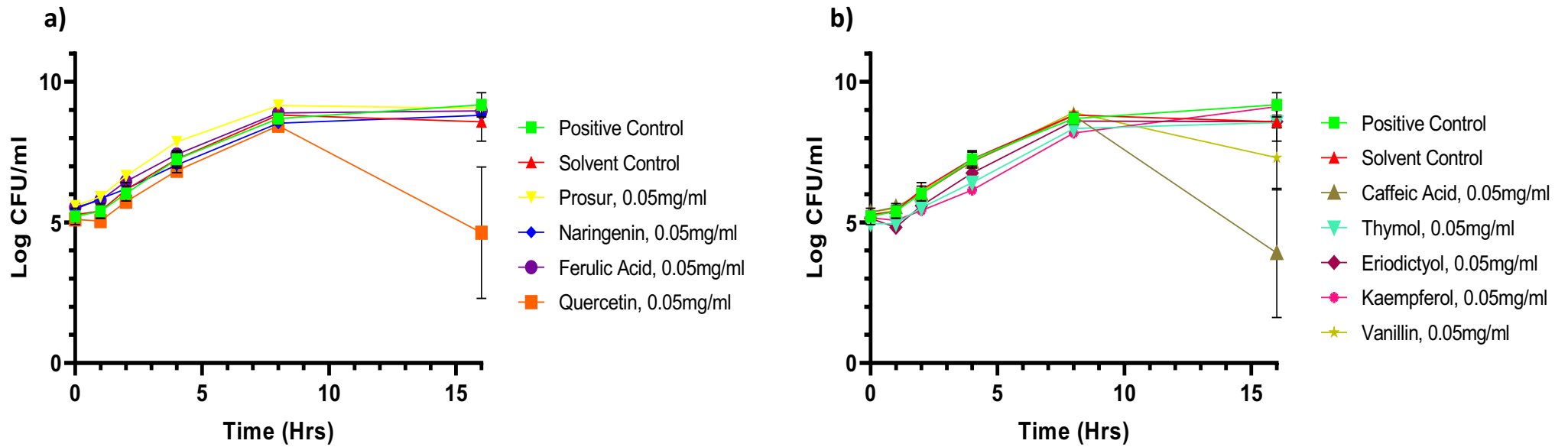
Panel a) *P. aeruginosa* against the Prosur NATPRE T-10+ mix, naringenin, ferulic acid and quercetin, b) *P. aeruginosa* against caffeic acid, thymol, eriodictyol, kaempferol and vanillin. Experiments were repeated with three biological replicates (three technical replicates each) over an incubation period of 16 hours. Points show the average value for each point and errors bars indicate the standard error of the mean.

Figure 9.3.7: Growth curves for *S. aureus* challenged with 0.05mg/ml of various phytochemicals.



Panel a) *S. aureus* against the Prosur NATPRE T-10+ mix, naringenin, ferulic acid and quercetin, b) *S. aureus* against caffeic acid, thymol, eriodictyol, kaempferol and vanillin. Experiments were repeated with three biological replicates (three technical replicates each) over an incubation period of 16 hours. Points show the average value for each point and errors bars indicate the standard error of the mean.

Figure 9.3.8: Growth curves for *L. monocytogenes* challenged with 0.05mg/ml of various phytochemicals.



Panel **a)** *L. monocytogenes* against the Prosur NATPRE T-10+ mix, naringenin, ferulic acid and quercetin, **b)** *L. monocytogenes* against caffeic acid, thymol, eriodictyol, kaempferol and vanillin. Experiments were repeated with three biological replicates (three technical replicates each) over an incubation period of 16 hours. Points show the average value for each point and errors bars indicate the standard error of the mean.

Table 9.3.5: Summary of growth velocity impacts after challenging the Gram-negative pathogens with various phytochemicals at 0.05mg/ml concentrations.

Gram-negative pathogens growth curve average growth velocities (%)						
Phytochemical (0.05mg/ml)	<i>S. enterica</i>			<i>P. aeruginosa</i>		
	Normalised Growth Velocity (vCFU/ml/min)	SEM (\pm)	<i>P</i> <i>value</i>	Normalised Growth Velocity (vCFU/ml/min)	SEM (\pm)	<i>P</i> <i>value</i>
<u>Solvent Control</u>	100	0.07292	-	100	0.07192	-
<u>Prosur</u>	98.37	0.08659	0.7166	103.12	0.05471	0.7387
<u>Eriodictyol</u>	100.63	0.07078	0.8908	94.99	0.05343	0.5918
<u>Ferulic Acid</u>	96.06	0.06133	0.3832	89.52	0.7296	0.2628
<u>Quercetin</u>	97.69	0.07514	0.6079	90.47	0.07136	0.3089
<u>Caffeic Acid</u>	99.37	0.03525	0.8875	93.99	0.02652	0.5202
<u>Thymol</u>	49.65	0.1787	<0.0001	1.74	0.1131	<0.0001
<u>Kaempferol</u>	104.40	0.05411	0.3301	96.97	0.02517	0.7454
<u>Naringenin</u>	51.77	0.6203	<0.0001	75.19	0.9282	0.0093
<u>Vanillin</u>	100.82	0.05544	0.8558	77.65	0.6381	0.0185

Data presented are the average values as percentages of the controls for the calculated growth velocity (CFU/ml/min) metric. Experiments were repeated with three biological replicates (three technical replicates each) over an incubation period of 16 hours. Values presented at 2 decimal places. Statistical analysis was performed using the GraphPad software v.8, using a 1-way repeated measures ANOVA Test with Fischer's LSD test. Values in bold were statistically, significantly, different to the relevant control.

Table 9.3.6: Summary of growth velocity impacts after challenging the Gram-positive pathogens with various phytochemicals at 0.05mg/ml concentrations.

Gram-positive pathogens growth curve average growth velocities (%)						
Phytochemical (0.05mg/ml)	<i>S. aureus</i>			<i>L. monocytogenes</i>		
	Normalised Growth Velocity (vCFU/ml/min)	SEM (\pm)	<i>P</i> <i>value</i>	Normalised Growth Velocity (vCFU/ml/min)	SEM (\pm)	<i>P</i> <i>value</i>
<u>Solvent Control</u>	100	0.1428	-	100	0.1031	-
<u>Prosur</u>	85.47	0.08735	0.1352	105.93	0.02640	0.4358
<u>Eriodictyol</u>	13.87	0.4234	<0.0001	96.66	0.1603	0.6595
<u>Ferulic Acid</u>	86.92	0.08134	0.1785	101.47	0.01958	0.8467
<u>Quercetin</u>	91.30	0.06980	0.3690	83.89	0.06767	0.0360
<u>Caffeic Acid</u>	78.73	0.6028	0.0301	99.80	0.03997	0.9793
<u>Thymol</u>	26.36	0.5854	<0.0001	71.97	0.06077	0.0004
<u>Kaempferol</u>	53.29	0.2100	<0.0001	90.01	0.06465	0.1903
<u>Naringenin</u>	0	0.000	<0.0001	84.77	0.06113	0.0473
<u>Vanillin</u>	74.83	0.8703	0.0107	101.92	0.03911	0.8023

Data presented are the average values as percentages of the controls for the calculated growth velocity (CFU/ml/min) metric. Experiments were repeated with three biological replicates (three technical replicates each) over an incubation period of 16 hours. Values presented at 2 decimal places. Statistical analysis was performed using the GraphPad software v.8, using a 1-way repeated measures ANOVA Test with Fischer's LSD test. Values in bold were statistically, significantly, different to the relevant control.

Table 9.3.7: Summary of impacts on final growth achieved after challenging Gram-negative pathogens with various phytochemicals.

Gram-negative pathogens growth curve average endpoint states (%)						
Phytochemical (0.05mg/ml)	<i>S. enterica</i>			<i>P. aeruginosa</i>		
	Normalised Endpoint State (vCFU/ml)	SEM (\pm)	<i>P value</i>	Normalised Endpoint State (vCFU/ml)	SEM (\pm)	<i>P value</i>
<u>Solvent Control</u>	100	0.05127	-	100	0.06594	-
<u>Prosur</u>	101.09	0.04625	0.8835	98.39	0.04914	0.8879
<u>Eriodictyol</u>	97.58	0.02548	0.7457	101.34	0.06071	0.9062
<u>Ferulic Acid</u>	99.75	0.05548	0.9744	99.02	0.06992	0.9311
<u>Quercetin</u>	102.64	0.05692	0.7230	77.35	1.382	0.0493
<u>Caffeic Acid</u>	102.62	0.06477	0.7255	86.14	1.020	0.2254
<u>Thymol</u>	65.26	0.4582	<0.0001	66.66	0.07566	0.0043
<u>Kaempferol</u>	97.60	0.03051	0.7477	87.61	1.036	0.2783
<u>Naringenin</u>	63.17	1.467	<0.0001	72.75	1.300	0.0187
<u>Vanillin</u>	96.44	0.05422	0.6337	97.31	0.08613	0.8135

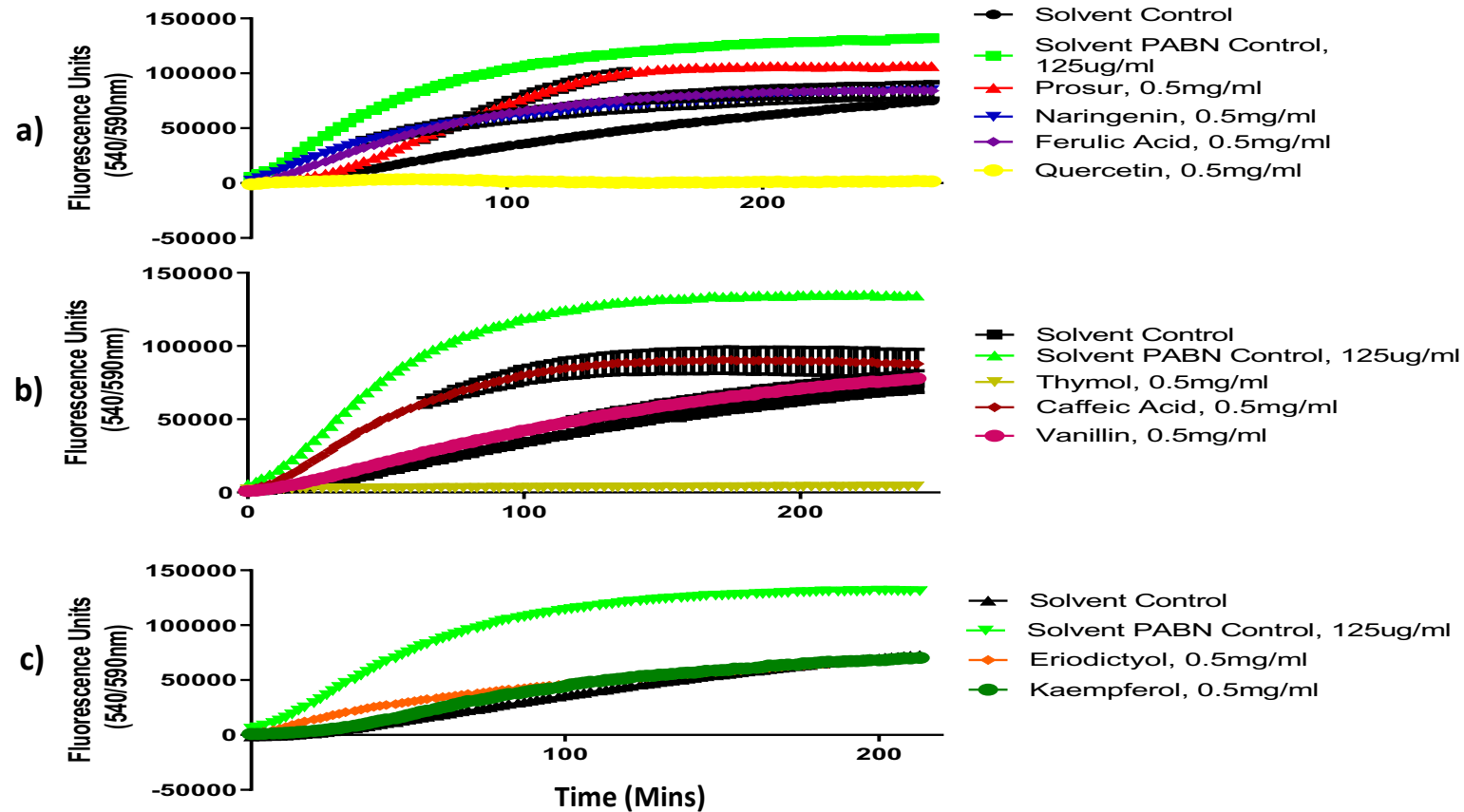
Data presented are the average values as percentages of the controls for the calculated endpoint state (CFU/ml) metric at the end of the 16 hour incubation period. Experiments were repeated with three biological replicates (three technical replicates each) over an incubation period of 16 hours. Values presented at 2 decimal places. Statistical analysis was performed using the GraphPad software v.8, using a 1-way repeated measures ANOVA Test with Fischer's LSD test. Values in bold were statistically, significantly, different to the relevant control.

Table 9.3.8: Summary of impacts on final growth achieved after challenging Gram-positive pathogens with various phytochemicals.

Gram-Positive Pathogens Growth Curve Endpoint States (%)						
Phytochemical (0.05mg/ml)	<i>S. aureus</i>			<i>L. monocytogenes</i>		
	Normalised Endpoint State (vCFU/ml)	SEM (\pm)	<i>P</i> value	Normalised Endpoint State (vCFU/ml)	SEM (\pm)	<i>P</i> value
<u>Solvent Control</u>	100	0.2246	-	100	0.1227	-
<u>Prosur</u>	103.83	0.1354	0.7205	105.73	0.03400	0.4484
<u>Eriodictyol</u>	68.26	1.292	0.0038	99.64	0.1421	0.9623
<u>Ferulic Acid</u>	101.26	0.08456	0.9069	104.34	0.06950	0.5657
<u>Quercetin</u>	106.52	0.03382	0.5427	54.06	1.166	<0.0001
<u>Caffeic Acid</u>	107.36	0.03069	0.4916	44.85	1.145	<0.0001
<u>Thymol</u>	25.86	1.150	<0.0001	99.63	0.05854	0.9601
<u>Kaempferol</u>	102.30	0.2061	0.8297	106.39	0.03835	0.3983
<u>Naringenin</u>	22.61	0.8032	<0.0001	102.74	0.03140	0.7159
<u>Vanillin</u>	75.59	0.8577	0.0246	84.58	0.5644	0.0435

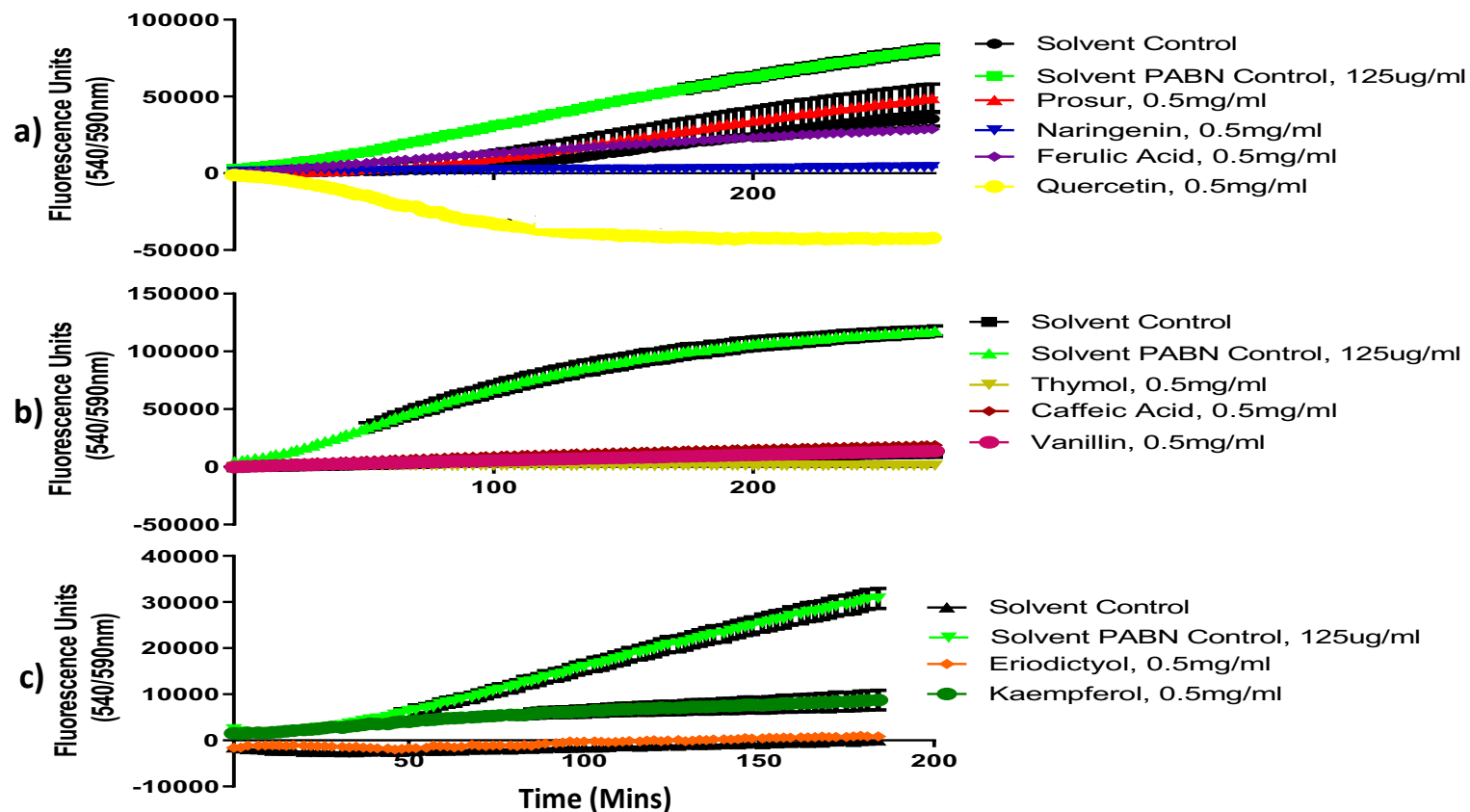
Data presented are the average values as percentages of the controls for the calculated endpoint state (CFU/ml) metric at the end of the 16 hour incubation period. Experiments were repeated with three biological replicates (three technical replicates each) over an incubation period of 16 hours. Values presented at 2 decimal places. Statistical analysis was performed using the GraphPad software v.8, using a 1-way repeated measures ANOVA Test with Fischer's LSD test. Values in bold were statistically, significantly, different to the relevant control.

Figure 9.3.9: Resazurin accumulation assays for *S. enterica* challenged with 0.5mg/ml of various phytochemicals.



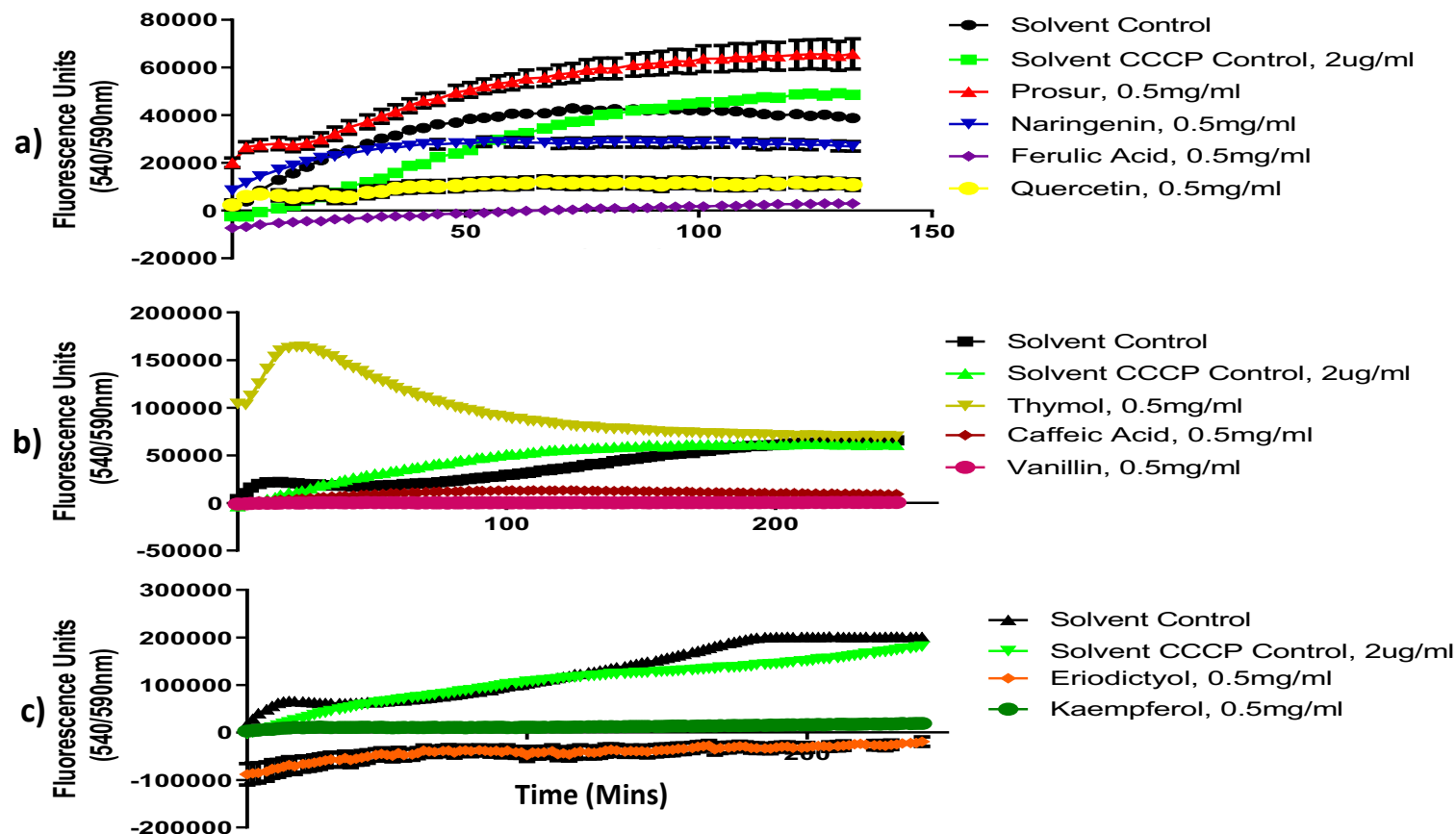
Panels a-c) *S. enterica* resazurin accumulation assays challenged with the various phytochemicals at 0.5mg/ml. The addition of Pa β N provides a positive control to ensure reliable measurements. Experiments were repeated with three biological replicates (five technical replicates each) over an incubation period of 16 hours, then trimmed to an appropriate timescale where the accumulation curves began to plateau.

Figure 9.3.10: Resazurin accumulation assays for *P. aeruginosa* challenged with 0.5mg/ml of various phytochemicals.



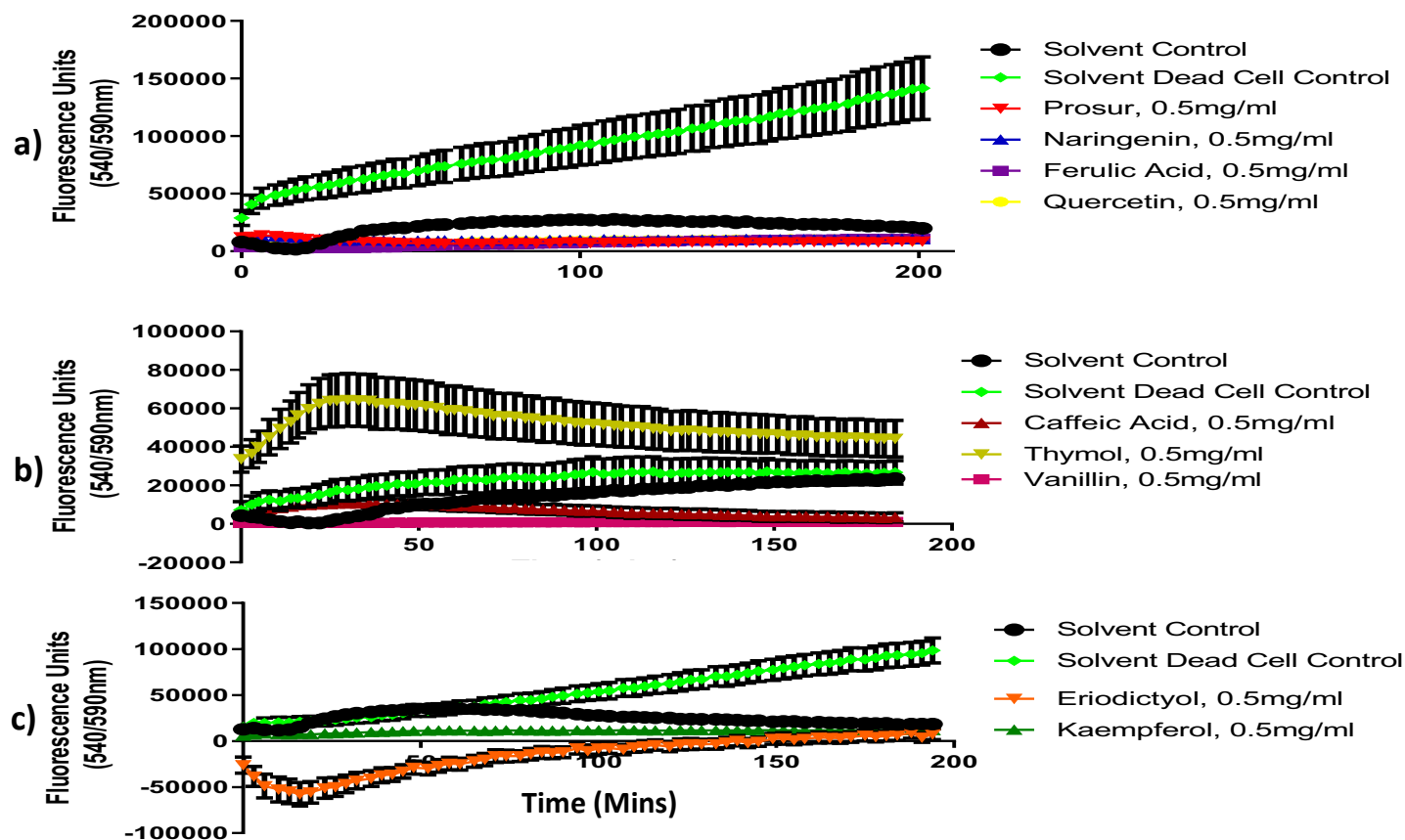
Panels a-c) *P. aeruginosa* resazurin accumulation assays challenged with the various phytochemicals at 0.5mg/ml. The addition of Pa β N provides a positive control to ensure reliable measurements. Experiments were repeated with three biological replicates (five technical replicates each) over an incubation period of 16 hours, then trimmed to an appropriate timescale where the accumulation curves began to plateau.

Figure 9.3.11: EtBr accumulation assays for *S. aureus* challenged with 0.5mg/ml of various phytochemicals.



Panels a-c) *S. aureus* EtBr accumulation assays challenged with the various phytochemicals at 0.5mg/ml. The addition of CCCP provides a positive control to ensure reliable measurements. Experiments were repeated with three biological replicates (five technical replicates each) over an incubation period of 16 hours, then trimmed to an appropriate timescale where the accumulation curves began to plateau.

Figure 9.3.12: EtBr accumulation assays for *L. monocytogenes* challenged with 0.5mg/ml of various phytochemicals.



Panels a-c) *L. monocytogenes* EtBr accumulation assays challenged with the various phytochemicals at 0.5mg/ml. The addition of CCCP provides a positive control to ensure reliable measurements. Experiments were repeated with three biological replicates (five technical replicates each) over an incubation period of 16 hours, then trimmed to an appropriate timescale where the accumulation curves began to plateau.

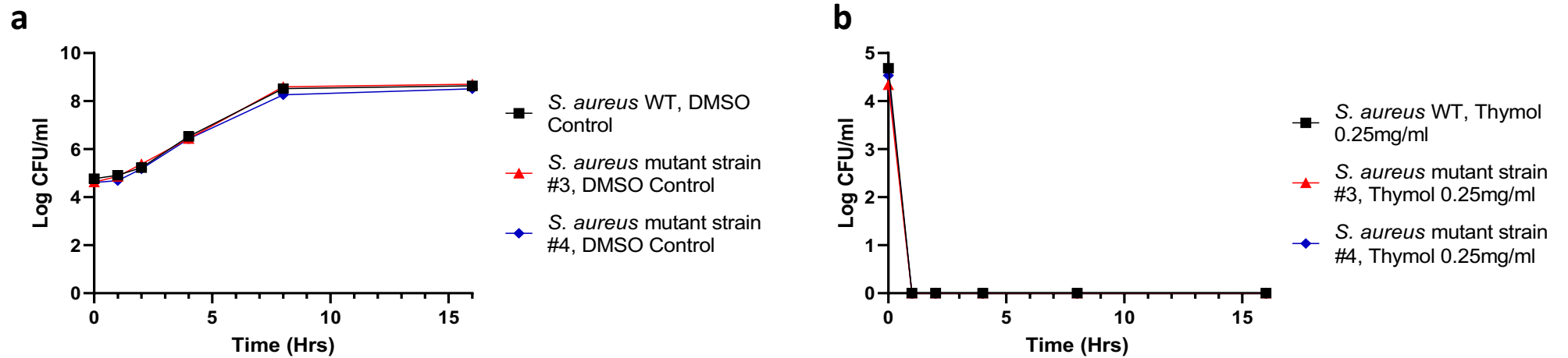
9.1.2 Chapter 4

Table 9.4.1: Antibiotic MIC changes for selected pathogenic strains.

Average MICs of Pathogens and Mutant Strains						
Micro-organism		Antibiotics				
		Kan	Tet	Amp/Pip*	Chlor	Nal/Cipro*
<i>S. enterica</i>	WT	2.67	1	6	3.33	4
	#1	2.67	2.67	16.67	11	16.67
	#2	2.33	2.67	16.67	11	16.67
	#6	2.67	1.67	11	5.33	8
<i>S. aureus</i>	WT	16	4	>34	8	>34
	#1	16	4	>34	16	>34
	#2	16	4	>34	16	>34
	#3	16	4	>34	13.33	>34
	#4	16	4	>34	10.67	>34
<i>P. aeruginosa</i>	WT	32	6.67	16	8	0.5
	#1	32	21.33	21.33	26.67	1.33
	#2	32	16	21.33	32	1
	#3	32	13.33	16	26.67	1
	#4	32	21.33	16	26.67	0.67

Kan denotes the use of kanamycin. **Tet** denotes the use of tetracycline. **Amp/Pip** denotes the use of ampicillin for *S. enterica* and *P. aeruginosa*, piperacillin for *S. aureus*. **Chlor** denotes the use of chloramphenicol. **Nal/Cipro** denotes the use of nalidixic acid for *S. enterica* and *P. aeruginosa*, ciprofloxacin for *S. aureus*. **N/D** denotes an undetermined MIC fold change, as for the tested antibiotics against *S. aureus* the MIC was >34 μ g/ml. Experiments were repeated with three technical replicates for three biological replicates. Values presented at 2 decimal places.

Figure 9.4.1: Growth curves for *S. aureus* parental and selected thymol-tolerant mutant strains challenged with 0.25mg/ml of thymol.



Panel a) *S. aureus* growth curves under solvent vehicle stress. b) *S. aureus* growth curves under thymol stress. Experiments were repeated with three technical replicates for three biological replicates. Error bars represent SEM. Statistical analysis was not performed due to the lack of data points present under thymol stress, and the similarity of the growth curves under the solvent vehicle control.

Table 9.4.2: Summary of growth velocity impacts after challenging the thymol-tolerant mutants with thymol at 0.25mg/ml concentrations.

Thymol-tolerant mutant growth curve average growth velocities (%)						
Strain	Solvent Control (5%)			Thymol (0.25mg/ml)		
	Normalised Growth Velocity (vCFU/ml/min)	SEM (\pm)	<i>P</i> value	Normalised Growth Velocity (vCFU/ml/min)	SEM (\pm)	<i>P</i> value
<i>S. enterica</i> WT	100	0.06141	-	100	0.4630	-
<i>S. enterica</i> #1	102.31	0.05416	0.1522	75.21	0.5355	0.5934
<i>S. enterica</i> #2	102.51	0.09345	0.1209	82.16	0.3724	0.7003
<i>S. aureus</i> WT	100	0.06456	-	100	-	-
<i>S. aureus</i> #3	101.32	0.05571	0.3700	N/D	-	-
<i>S. aureus</i> #4	95.56	0.05684	0.0049	N/D	-	-
<i>P. aeruginosa</i> WT	100	0.03305	-	100	0.4053	-
<i>P. aeruginosa</i> #1	101.22	0.02659	0.0329	298.79	0.3226	0.0002
<i>P. aeruginosa</i> #3	100.44	0.01179	0.4254	374.78	0.1175	<0.0001
<i>P. aeruginosa</i> #4	99.38	0.03407	0.2568	321.12	0.09879	<0.0001

Data presented are the average values as percentages of the parental strains (WT) for the calculated growth velocity (CFU/ml/min) metric. Experiments were repeated with three biological replicates (three technical replicates each) over an incubation period of 16 hours. Values presented at 2 decimal places. Statistical analysis was performed using the GraphPad software v.8, using a 1-way repeated measures ANOVA Test with Fischer's LSD test. Values in bold were statistically, significantly, different to the relevant control.

Table 9.4.3: Summary of impacts on final growth achieved after challenging the thymol-tolerant mutants with thymol at 0.25mg/ml concentrations.

Thymol-tolerant mutant growth curve average endpoint states (%)						
Strain	Solvent Control (5%)			Thymol (0.25mg/ml)		
	Normalised Endpoint State (vCFU/ml)	SEM (\pm)	<i>P</i> value	Normalised Endpoint State (vCFU/ml)	SEM (\pm)	<i>P</i> value
<i>S. enterica</i> WT	100	0.05909	-	100	0.1358	-
<i>S. enterica</i> #1	99.87	0.07221	0.8854	97.26	0.6780	0.8648
<i>S. enterica</i> #2	100.10	0.04101	0.9238	114.81	0.7743	0.3608
<i>S. aureus</i> WT	100	0.02549	-	100	-	-
<i>S. aureus</i> #3	100.76	0.03402	0.1467	N/D	-	-
<i>S. aureus</i> #4	98.56	0.03318	0.0098	N/D	-	-
<i>P. aeruginosa</i> WT	100	0.1126	-	100	0.9899	-
<i>P. aeruginosa</i> #1	97.74	0.07711	0.7770	87.30	0.08709	0.2714
<i>P. aeruginosa</i> #3	87.22	1.027	0.1144	87.84	0.06457	0.2917
<i>P. aeruginosa</i> #4	100.96	0.1490	0.9042	78.86	0.7842	0.0717

Data presented are the average values as percentages of the parental strains (WT) for the calculated endpoint state (CFU/ml) metric at the end of the 16 hour incubation period. Experiments were repeated with three biological replicates (three technical replicates each) over an incubation period of 16 hours. Values presented at 2 decimal places. Statistical analysis was performed using the GraphPad software v.8, using a 1-way repeated measures ANOVA Test with Fischer's LSD test. Values in bold were statistically, significantly, different to the relevant control.

Table 9.4.4: Summary of drug accumulation assays utilising thymol-tolerant mutant strains of *S. enterica*, *S. aureus* and *P. aeruginosa*.

Thymol mutants drug accumulation assay average fluorescence accumulation velocities (%)						
Strain	Solvent Control (5%)			Thymol (0.25mg/ml)		
	Normalised Accumulation Velocity (Fluorescence Units/min)	SEM (\pm)	<i>P</i> value	Normalised Accumulation Velocity (Fluorescence Units/min)	SEM (\pm)	<i>P</i> value
<i>S. enterica</i> WT	100	21.64	-	100	48.54	-
PABN Control	81.21	88.65	0.0165	74.57	38.16	0.6028
<i>S. enterica</i> #1	89.34	80.92	0.1712	187.79	67.81	0.0741
<i>S. enterica</i> #2	79.64	140.9	0.0096	297.66	129.7	<0.0001
<i>S. enterica</i> #6	100.52	55.77	0.9409	126.81	33.20	0.5832
<i>S. aureus</i> WT	100	46.97	-	100	28.08	<0.0001
Dead Cell Control	50.17	100.1	0.1343	-19.39	67.20	0.1483
<i>S. aureus</i> #1	17.15	68.36	0.0133	86.06	41.24	<0.0001
<i>S. aureus</i> #2	196.70	23.16	0.0040	30.01	19.30	<0.0001
<i>S. aureus</i> #3	126.56	5.195	0.4235	43.77	15.92	<0.0001
<i>S. aureus</i> #4	84.52	40.07	0.6415	37.18	19.63	<0.0001
<i>P. aeruginosa</i> WT	100	50.44	-	100	20.04	-
PABN Control	135.29	31.72	0.0357	89.84	20.36	0.7482
<i>P. aeruginosa</i> #1	59.52	35.95	0.0162	98.84	21.09	0.9705
<i>P. aeruginosa</i> #3	69.21	37.92	0.0665	75.90	12.24	0.4464
<i>P. aeruginosa</i> #4	68.61	35.25	0.0614	78.74	14.07	0.5016

Data presented are the average values as percentages of the parental strains (WT) for the calculated fluorescence accumulation velocity (Fluorescence units/min) metric. Experiments were repeated with three biological replicates (five technical replicates each) over an incubation period of 16 hours, trimmed to an appropriate timescale where the accumulation curves begun to plateau. Values presented at 2 decimal places. Statistical analysis was performed using the GraphPad software v.8, using a 1-way repeated measures ANOVA Test with Fischer's LSD test. Values in bold were statistically, significantly, different to the relevant control.

Table 9.4.5: Summary of drug accumulation assays utilising thymol-tolerant mutant strains of *S. enterica*, *S. aureus* and *P. aeruginosa*.

Thymol mutants drug accumulation assay average steady states (%)						
Strain	Solvent Control (5%)			Thymol (0.25mg/ml)		
	Log Steady State (Fluorescence Units/min)	SEM (\pm)	<i>P</i> value	Log Steady State (Fluorescence Units/min)	SEM (\pm)	<i>P</i> value
<i>S. enterica</i> WT	100	9230	-	100	7953	-
<i>S. enterica</i> #1	113.38	3994	0.4340	162.93	10916	0.0581
<i>S. enterica</i> #2	122.25	507.4	0.1943	208.53	24245	0.0013
<i>S. enterica</i> #6	112.71	7941	0.4571	120.69	7210	0.5304
<i>S. aureus</i> WT	100	19808	-	100	7075	0.0946
Dead Cell Control	90.99	27854	0.7649	426.86	21883	0.0003
<i>S. aureus</i> #1	60.16	12218	0.1873	126.71	12217	0.2160
<i>S. aureus</i> #2	105.57	6032	0.8533	259.30	5981	0.3503
<i>S. aureus</i> #3	172.50	15681	0.0170	229.18	6930	0.6593
<i>S. aureus</i> #4	96.21	6117	0.8999	200.53	3869	0.9768
<i>P. aeruginosa</i> WT	100	14137	-	100	15489	-
PABN Control	144.56	8780	0.0034	43.59	9413	0.0017
<i>P. aeruginosa</i> #1	84.73	7501	0.3101	89.69	9531	0.5605
<i>P. aeruginosa</i> #3	94.39	9370	0.7089	66.96	6009	0.0632
<i>P. aeruginosa</i> #4	89.63	8909	0.4902	94.29	11391	0.7471

Data presented are the average values as percentages of the parental strains (WT) for the calculated steady state fluorescence accumulation (Fluorescence units/min) metric. Experiments were repeated with three biological replicates (five technical replicates each) over an incubation period of 16 hours, trimmed to an appropriate timescale where the accumulation curves began to plateau. Values presented at 2 decimal places. Statistical analysis was performed using the GraphPad software v.8, using a 1-way repeated measures ANOVA Test with Fischer's LSD test. Values in bold were statistically, significantly, different to the relevant control.

Table 9.4.6: Summary of the OD_(595nm) measurements from the crystal violet assays using the thymol-tolerant mutant strains.

Thymol Mutants Crystal Violet Biofilm Assay Average OD _(595nm) (%)									
Strain	LB-NaCl Control			Solvent Control (5%)			Thymol (0.25mg/ml)		
	Normalised OD _(595nm)	SEM (±)	<i>P</i> value	Normalised OD _(595nm)	SEM (±)	<i>P</i> value	Normalised OD _(595nm)	SEM (±)	<i>P</i> value
<i>S. enterica</i> WT	100	0.2794	-	100	0.2024	-	17.97	0.03147	0.0011
<i>S. enterica</i> #1	73.88	0.07435	0.1651	69.84	0.08728	0.2136	88.09	0.1837	0.6215
<i>S. enterica</i> #2	76.21	0.1142	0.2057	81.18	0.1080	0.4359	79.80	0.2251	0.4032
<i>S. enterica</i> #6	74.47	0.07789	0.1748	80.77	0.1167	0.4259	40.84	0.1761	0.0164
<i>S. aureus</i> WT	100	0.1077	-	100	0.1201	-	24.10	0.04517	0.0011
<i>S. aureus</i> #1	81.26	0.1545	0.2505	94.25	0.1367	0.7987	27.04	0.05979	0.0017
<i>S. aureus</i> #2	35.81	0.09959	0.0001	58.39	0.1061	0.0680	74.16	0.1281	0.2541
<i>S. aureus</i> #3	33.08	0.09909	<0.0001	45.49	0.1048	0.0176	72.88	0.1686	0.2314
<i>S. aureus</i> #4	53.08	0.1261	0.0045	122.29	0.3187	0.3243	27.78	0.04270	0.0019
<i>P. aeruginosa</i> WT	100	0.04329	-	100	0.04147	-	85.43	0.3388	0.3320
<i>P. aeruginosa</i> #1	67.36	0.4982	0.0172	57.90	0.2636	0.0061	27.77	0.1316	<0.0001
<i>P. aeruginosa</i> #2	71.68	0.2556	0.0384	59.33	0.3134	0.0079	59.15	0.4299	0.0077
<i>P. aeruginosa</i> #3	75.44	0.1608	0.0719	68.17	0.4291	0.0362	41.34	0.3151	0.0002
<i>P. aeruginosa</i> #4	97.30	0.07385	0.8416	75.98	0.4573	0.1116	43.73	0.4876	0.0003

Data presented are the average OD_(595nm) values as percentages of the parental strains (WT) for the crystal violet assays. Experiments were repeated with four technical replicates for three biological replicates. Error bars represent SEM, horizontal bars represent the mean for each data set. Statistical analysis was completed on the calculated growth kinetic metrics via the GraphPad software v.8, using a 1-way repeated measures ANOVA Test with Fischer's LSD test. Values in bold were statistically, significantly, different to the relevant control.